EXTRAGALACTIC MOLECULES

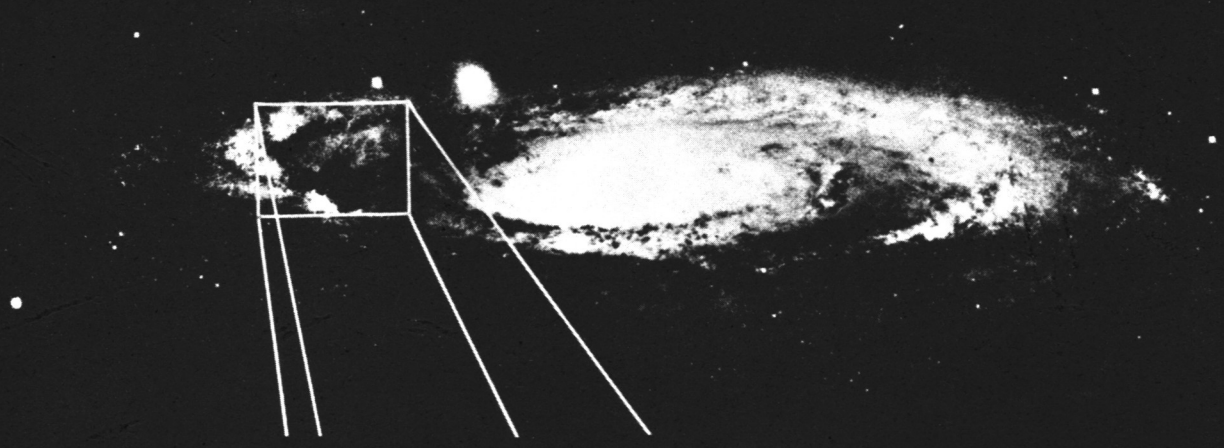

Proceedings of a workshop held at the
National Radio Astronomy Observatory
Green Bank, West Virginia
November 2-4, 1981

Edited by Leo Blitz and Marc Kutner

EXTRAGALACTIC MOLECULES

Proceedings of a Workshop held at the

National Radio Astronomy Observatory

Green Bank, West Virginia

November 2-4, 1981

Edited by Leo Blitz and by Marc L. Kutner

Distributed by:

Publications Division, NRAO

P.O. Box 2

Green Bank, West Virginia 24944

PREFACE

This workshop had its origin in the casual comment by one of us (MLK) to Mort Roberts that, though a wealth of data on extragalactic molecules existed, little of it was in the literature. This brought a response which went something like, "In that case, you should have a workshop at Green Bank." Having been at previous Green Bank workshops, we knew the idea was an excellent one. The isolation and friendly atmosphere allowed some 40 astronomers to gather for three days with little to do but talk about their work.

In preparing the program, the emphasis was on encouraging discussion. Within each three and a half hour session, no more than two hours of presentation time were scheduled. We are happy to say that this was one meeting in which the questioners at the end of each talk did not have to complain about being cut off. Some of the debate was quite lively, and carried over into the informal "lounge" sessions in the evenings. The informality was helped along by a power failure on the second afternoon of the meeting, which forced us to move from the conference room we were using to the residence hall lounge.

From the outset, we recognized that the study of extragalactic molecules is still in its infancy. Therefore, we viewed the conference as more of a progress report, to allow the participants to see what has been done and where things are going. However, it did give us a chance to see the trends that are emerging even at this early date, and to compare those with other studies of galaxies. To this end, the meeting was organized so that the extragalactic molecular observations were reported first, followed by observations of other species in galaxies. Then there was a comparison with work in our own galaxy, and finally, a session trying to tie things into some theoretical framework.

This volume is presented in the same spirit as the meeting, an informal progress report. The emphasis was placed on getting as much of the tabular and figure information as possible, so that readers can get a good idea of what has been done to date.

The success of the workshop was a result of the efforts of a number of people. Mort Roberts and Martha Haynes made the facilities at Green Bank available to us. Bob Havlen handled the major logistical arrangements, and Phyllis Jackson took care of a myriad of details, leaving us free to have the fun of planning the scientific program. Bob Moore and the support staff at Green Bank took care of the group's worldly cares, leaving them free to talk about the science. Wally Oref's masterful handling of lights and projectors allowed the sessions to flow along smoothly.

When it was all over, it seemed clear that, as is true in the Milky Way, an understanding of the molecular component of the gas is crucially important for understanding the structure and the star formation in spiral galaxies. But even at this early stage, a number of differences of opinion emerged that seem to insure that the study of extragalactic molecules will be a lively and exciting field. There seemed to be one word underlying all of the contributions which kept resounding throughout the workshop: resolution. We simply need more resolution than we've got. The meeting therefore focused attention on our need for a large aperture millimeter wave telescope at a time when the prospects for the 25-m telescope seemed at their lowest. In that sense, this volume is dedicated to our redoubled efforts to obtain that telescope.

Leo Blitz
College Park, MD

Marc L. Kutner
Troy, NY

March 1982

List of Attendees

Name	Institution
Bally, John	Bell Laboratories
Bash, Frank	University of Texas
Blitz, Leo	University of Maryland
Bosma, Albert	Columbia University
Cohen, Richard	Institute for Space Studies
Combes, Francoise	Meudon Observatory
Dame, Thomas	Columbia University
de Graauw, Thijs	ESTEC
Dickey, John	NRAO
Giovanelli, Riccardo	NRAO
Gordon, Mark	NRAO
Harper, Doyal	Yerkes Observatory
Havlen, Robert	NRAO
Haynes, Martha	NRAO
Ho, Paul	University of California, Berkeley
Jog, Chanda	State University of New York, Stony Brook
Kerr, Frank	University of Maryland
Kutner, Marc	Rensselaer Polytechnic Institute
Linke, Richard	Bell Laboratories
Lo, Fred	California Inst. of Technology
Lockman, Jay	NRAO
Lord, Stephen	University of Massachusetts
Martin, Robert	Max-Planck-Institut fur Radioastronomie
Mathieu, Robert	University of California, Berkeley
Mead, Kathryn	Rensselaer Polytechnic Institute
Peters, William	University of Texas
Prendergast, Kevin	Columbia University
Rickard, Lee J	Howard University
Roberts, Morton	NRAO
Sancisi, Renzo	NRAO & Kapteyn Labs
Sanders, David	University of Massachusetts
Scoville, Nicholas	University of Massachusetts
Seaquist, Ernest	NRAO & University of Toronto
Smith, James	University of Chicago
Solomon, Philip	State University of New York, Stony Brook
Stark, Anthony	Bell Laboratories
Tacconi, Linda	University of Massachusetts
Thonnard, Norbert	Department of Terrestrial Magnetism
Turner, Barry	NRAO
Verter, Frances	Princeton University
Vietri, Mario	Princeton University
Young, Judith	University of Massachusetts

A G E N D A

Green Bank Workshop

on *"Extragalactic Molecules"*

November 2

SESSION I. OBSERVATIONS OF MOLECULES IN THE NUCLEI AND CENTRAL PORTIONS OF EXTERNAL GALAXIES
Morning
Chairman: Marc Kutner

15m	1.	*K. Y. Lo*	Anomalous CO Emission from M82 and NGC 253
30m	2.	*P. Ho*	Ammonia in IC 342
5m	3.	*M. Gordon*	Negative Results on Clumpy Irregulars
15m	4.	*R. Mathieu*	CO in Seyfert Galaxies
10m	5.	*L. J Rickard*	New Observations of Central CO Sources
10m	6.	*M. Vietri*	Detection of Three Galaxies in the Virgo Cluster
15m	7.	*B. Turner*	Extragalactic OH Observations

SESSION II. OBSERVATIONS OF MOLECULES IN THE DISKS OF EXTERNAL GALAXIES
Afternoon
Chairman: Frank Bash

10m	1.	*L. Blitz*	GMCs in M31
20m	2.	*R. Linke*	CO Observations of M31
20m	3.	*A. Stark*	CO Observations of M82
20m	4.	*J. Young*	CO Mapping of IC 342 and NGC 6946
5m	5.	*L. Tacconi*	CO Observations of NGC 3628
20m	6.	*N. Scoville*	CO Mapping of M51
20m	7.	*P. Solomon*	CO Observations of M101 and NGC 891

EVENING SESSION. A SUMMARY OF THE DAYS' CONTRIBUTIONS AND A PERSPECTIVE ON EXTRAGALACTIC MOLECULES
Lee J Rickard

November 3

SESSION III. RELATED OBSERVATIONS AND MORE MOLECULES
Morning *Chairman: Martha Haynes*

15m	1.	*Th. de Graauw*	CO (2→1) Observations in the Magellanic Clouds
15m	2.	*F. Combes*	Can Spiral Arms Form GMCs?
15m	3.	*J. Smith*	IR Observations of M51
15m	4.	*D. Harper*	Extragalactic IR Observations
15m	5.	*L. J Rickard*	Extragalactic IR and Recombination Line Observations
15m	6.	*E. Seaquist*	VLA Detection of H110α in M82
10m	7.	*F. Verter*	CO Survey: Comparison with Morphological Type
15m	8.	*R. Martin*	Ammonia in M31

SESSION IV. COMPARISONS WITH THE MILKY WAY GALAXY
Afternoon *Chairman: Morton Roberts*

10m	1.	*F. J. Lockman*	25 kpc^3 of HI
10m	2.	*J. Dickey*	Underestimate of HI in the Inner Galaxy
10m	3.	*K. Mead*	Large-Scale CO Distribution in the Outer Galaxy
15m	4.	*M. Kutner*	Properties of the Outer Galaxy Molecular Clouds
10m	5.	*W. Peters*	CO (2→1) in the Galactic Survey
20m	6.	*D. Sanders*	The Milky Way in CO as Seen from Afar
25m	7.	*R. Cohen*	CO in the Milky Way
10m	8.	*B. Turner*	Diffuse 1720 MHz OH Emission: A Tracer of Spiral Arms?

EVENING SESSION: OVERVIEW ON THE COMPARISONS WITH THE MILKY WAY
Frank Kerr

November 4

SESSION V. THEORY AND RELATIONSHIPS TO OTHER GALACTIC COMPONENTS
Morning *Chairman: Mark Gordon*

15m	1.	*F. Bash*	Triggering Star Formation in Molecular Clouds
15m	2.	*C. Jog*	Two-Fluid Gravitational Instabilities in the Galaxy
15m	3.	*A. Bosma*	HI Kinematics in Disk Galaxies
20m	4.	*K. Prendergast*	Global Star Formation
15m	5.	*R. Giovanelli*	The HI Content and Size of Galaxies
15m	6.	*N. Thonnard*	Comparison of Molecular Gas with Other Tracers
10m	7.	*P. Ho*	Formation of OB Clusters
45m	8.	*K. Prendergast*	CONCLUDING CONTRIBUTION. MEETING SUMMARY AND PERSPECTIVES

**
****
**

Contributions

I. EXTRAGALACTIC MOLECULAR SOURCES

A. Carbon Monoxide

REVIEW OF CURRENT STATE OF OBSERVATIONS OF EXTRAGALACTIC MOLECULES

L. J Rickard (Howard University)

This workshop comes roughly at the 10th anniversary of Weliachew's first report of an extragalactic molecule (OH), so it seems an appropriate opportunity to reflect on the achievements and ambitions of the field Ambitions are easy to list in the form of the questions we are trying to answer How common are molecular components in galaxies? Is their presence somehow linked to the morphological type? What forms characterize the radial variations of the total mass of interstellar matter and the fraction of that mass in molecular form? Does the structure of the molecular component reflect specific details of the structure of the galaxy (such as inner Lindblad resonances, bars, spiral arms, etc.)? Is there any correlation between the presence of molecular components and activity in galaxies (such as central starbursts)? Can we sensibly relate the results of these inquiries to such pressing questions as the lifetimes of molecular clouds, the efficiency of star formation, the need for external triggers of star formation, etc?

On the side of the achievements, we may note the detection of nine molecular species in the interstellar gas of other galaxies, and the recognition of the widespread appearance of two of them - CO and OH - at last count detected in 35 and 12 galaxies, respectively CO has proven to be a useful probe of, at least, the extent of the molecular component in nearly a dozen galaxies Indeed, CO appears to be the tool of choice in this field, as

illustrated by the fact that papers on CO in this workshop outnumbered those on all other molecules by a factor of 6. This emphasis remains in this paper

It is, of course, a pleasure to be able to view at last the molecular components from a position not hopelessly immersed within them. Unfortunately, most of the basic problems of the interpretation of Galactic CO data have not been avoided by this shift in vantage. Depressingly familiar arguments about the characteristic sizes and velocity widths of GMCs and the conversion from $\int T_A^*(^{12}CO)dV$ to σ_{H_2} seem to be unavoidable.

Several specific areas of active work were not represented at the workshop For example, observations of OH and H_2O masers have revealed both the normal variety and "supermasers", the latter exceeding by an order of magnitude the strongest Galactic masers Current theoretical work suggests a combination of strong background radiation with inversions produced by a far-infrared pump and a systematic velocity field, all occurring in the central regions of the galaxy Also, the near-infrared H_2 lines detected in NGC 1068 seem to be generated by conditions akin to the shocked gas in Orion, but representing the equivalent of a million such sources Each of these peculiar phenomena seems to indicate the interaction of nuclear activity with a surrounding normal molecular component, and draws our attention to possible links between the two.

If we concentrate on questions of concern within this workshop, we find two general categories: the frequency of occurrence of molecular components, and the structure of those components I shall deal with these in turn.

CO surveys seem to have been the basic method of searching for molecular components. This is unfortunate. The searches are dominated by various selection effects: a tendency to search only towards nuclei, the greater ease of detecting face-on galaxies (where the line is enhanced by velocity crowding), the preference to observe many different galaxies rather than accumulate lots of time on a few sources (attributable to the short length of most observing runs), etc. Thus, while I have personally searched $\sim$80 galaxies, with 10 detections, another 10 of my negative results have subsequently been reported as detections, indicating their low statistical significance. We need a statistically-meaningful sample searched at a constant sensitivity, with a limit well below $T_A^* = 0.1$ K, before sensible remarks can be made Having said that, I will proceed to remark that one can only say at present that detections of central sources depend on Hubble type only in the general failure to detect ellipticals The current paucity of detected Magellanic-type irregulars may simply reflect the absence of an obvious place to look Correlations of CO luminosity with far-IR and nonthermal radio continuum luminosities persist

Absorption-line searches (e.g., OH seen against compact central continuum sources) provide another method of producing a statistically-significant sample. They have the benefit that, given a flux and optical-depth limit, they are distance independent, unlike emission line searches. Current data suggest that just about every spiral galaxy will show OH absorption if the central compact continuum source is strong enough. If the presence of the molecular source is not linked to that of the continuum source, then molecular components must be fairly common.

In the context of questions about the structures of individual molecular components, we can isolate the same three problems listed in my review for the U. Md. IAU symposium: (1) Is there a distinct central source? (2) What is the form of the axisymmetric component? (3) Are there spiral patterns?

The first question should be more properly phrased: is the central emission peak in the CO maps dominated by a central source that is distinct, in its physical and dynamic characteristics, from the disk? The principal evidence supporting this is the large velocity spread often seen in central sources, either in CO or OH. Other support, from far-IR temperature differences and observations of cloud "discriminants" ($^{13}CO/^{12}CO$, HCO^+/HCN, etc.), must be considered tentative.

The argument that the axisymmetric molecular component is an exponential distribution mimicking that of the optical luminosity has been

advanced in several papers at this workshop. Although I have tended to consider the CO disks to be more or less flat out to the edges of the molecular component, I feel that I disagree less with the exponential interpretation than with the confidence with which it is promoted. Figure 1 shows a typical CO disk, in this case for NGC 6946 (where the beam size corresponds to $\sim$3 kpc). The contour separation (2 K km s^{-1}) corresponds to a level of about 3σ in the data. Thus, the fluctuations in the disk, with sizes as small as that of the beam, are real features in the molecular component.

Table 1 shows the values of the summed reduced residuals for fits of various axisymmetric models to this source. Given the number of degrees of freedom, the F-test demands that the ratio of these sums exceed about 2 before one model can be preferred over the other at the 95% confidence level. Incredibly, even the pure uniform disk, which neglects the obvious central peak, can only be marginally rejected The problem is that the fluctuations in the disk have an amplitude comparable to the mean value of the overall disk emission. Trying to fit a model to such data is like trying to find a weak line in the presence of baseline ripple.

The relative dominance of H_2 over HI and the form of the total proton distribution are hostages to the poorly known CO-to-H_2 conversion. I tend to use $\sigma_{H_2}(M_\odot\ pc^{-2})/\int T_A^*(^{12}CO)dV\ (K\ km\ s^{-1}) \sim 2$; values as high as 8 have been quoted in this workshop. My own estimate of the

probable errors suggests that one shouldn't trust these numbers to be better than an order of magnitude. Figure 2 shows the significance of this problem For NGC 6946, my numbers lead to a crossover of $\sigma_{H_2} \sim \sigma_{HI}$ at $\sim$5 kpc, and a fairly flat σ_{tot} in the outer disk. A mere factor of two increase in the inferred σ_{H_2} would shift the crossover to 10 kpc, and make σ_{tot} more steeply declining.

The final question of the presence of spiral arms is also obscured by the considerable fluctuating structure of the sources. Furthermore, the indication from other species is that arm contrasts may vary in counter-productive ways; for example, Shane's HI map of M51 shows that the arm/interarm contrast is only large (>3) outside the region of detectable CO emission. In addition, the beam sizes are generally no better than comparable to the separation of arms. Figure 3 shows the beautiful spiral pattern of M51 as it would appear to the 36-foot telescope. One is reduced to an analysis of model fits, such as shown in figure 4 for M51. The best fit contrast is $\sim$4, but the F-test allows much larger values to be considered viable. In sum, the only evidence for the presence of spiral structure so far is in the one well-resolved case, M31; unfortunately, by its lack of a central CO source and low H_2/HI in the disk, M31 is clearly different from most of the galaxies with molecular components.

TABLE 1: Summed squared reduced residuals for model fits to CO in NGC 6946

$$S = \sum_i (\text{data}_i - \text{model}_i)^2 / \sigma_i^2$$

Model	S
Uniform disk	2289
Exponential disk	1687
Uniform disk + Gaussian center	1248
Exponential disk + Gaussian center	1256

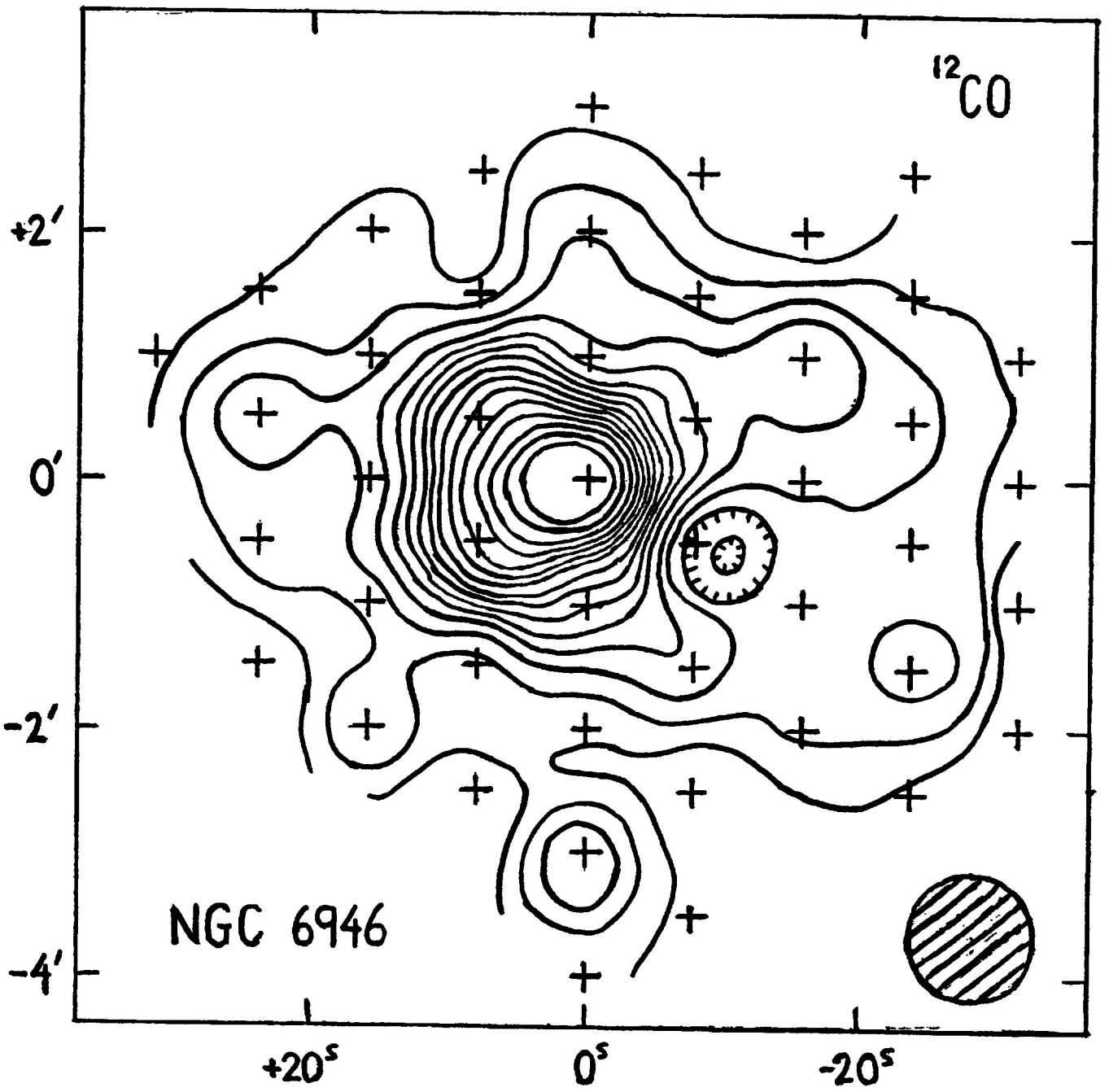

Figure 1

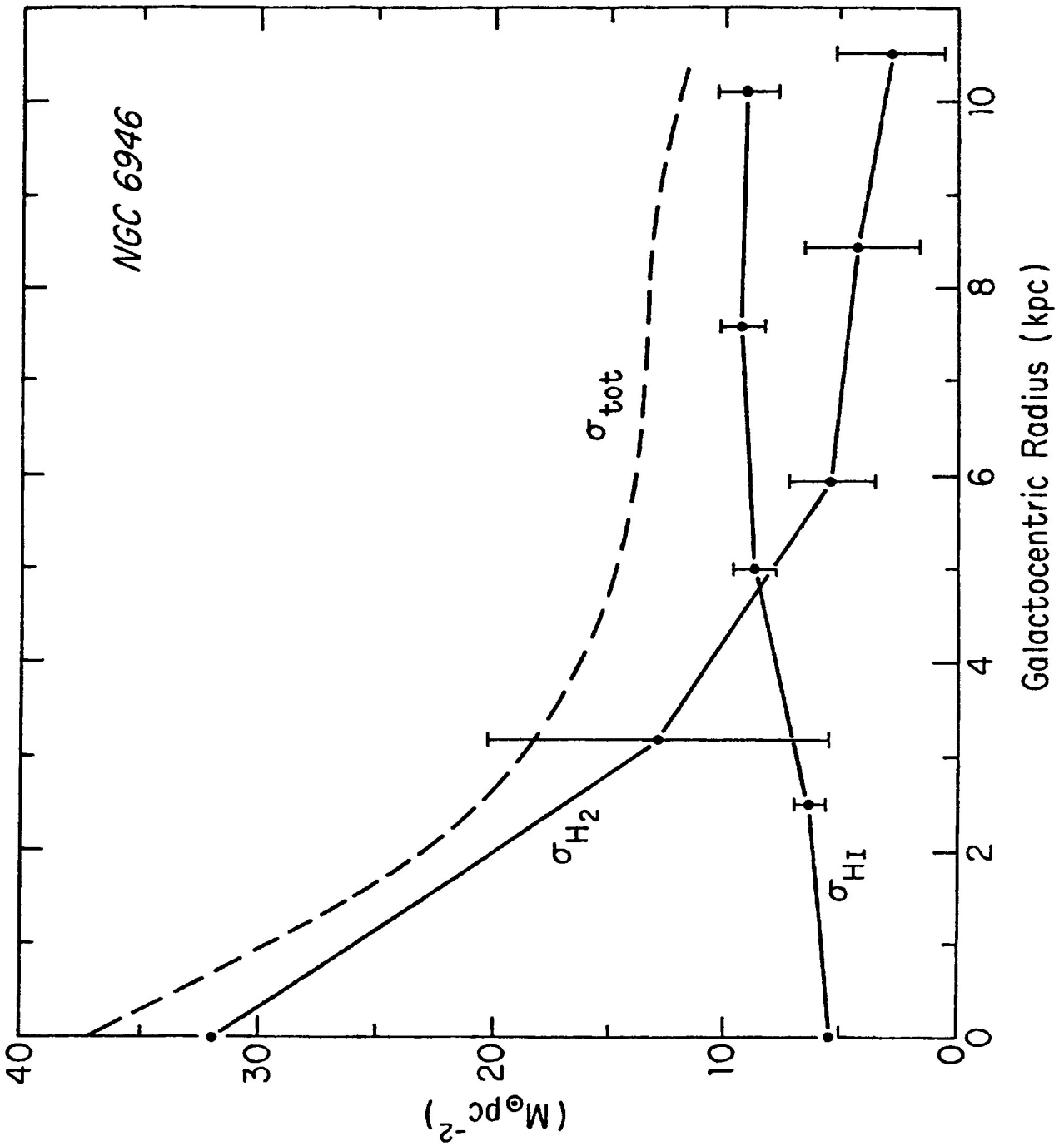
NGC 6946
σ_{tot}
σ_{H_2}
σ_{HI}
$(M_\odot pc^{-2})$
Galactocentric Radius (kpc)
0
10
20
30
40
0
2
4
6
8
10

Figure 2

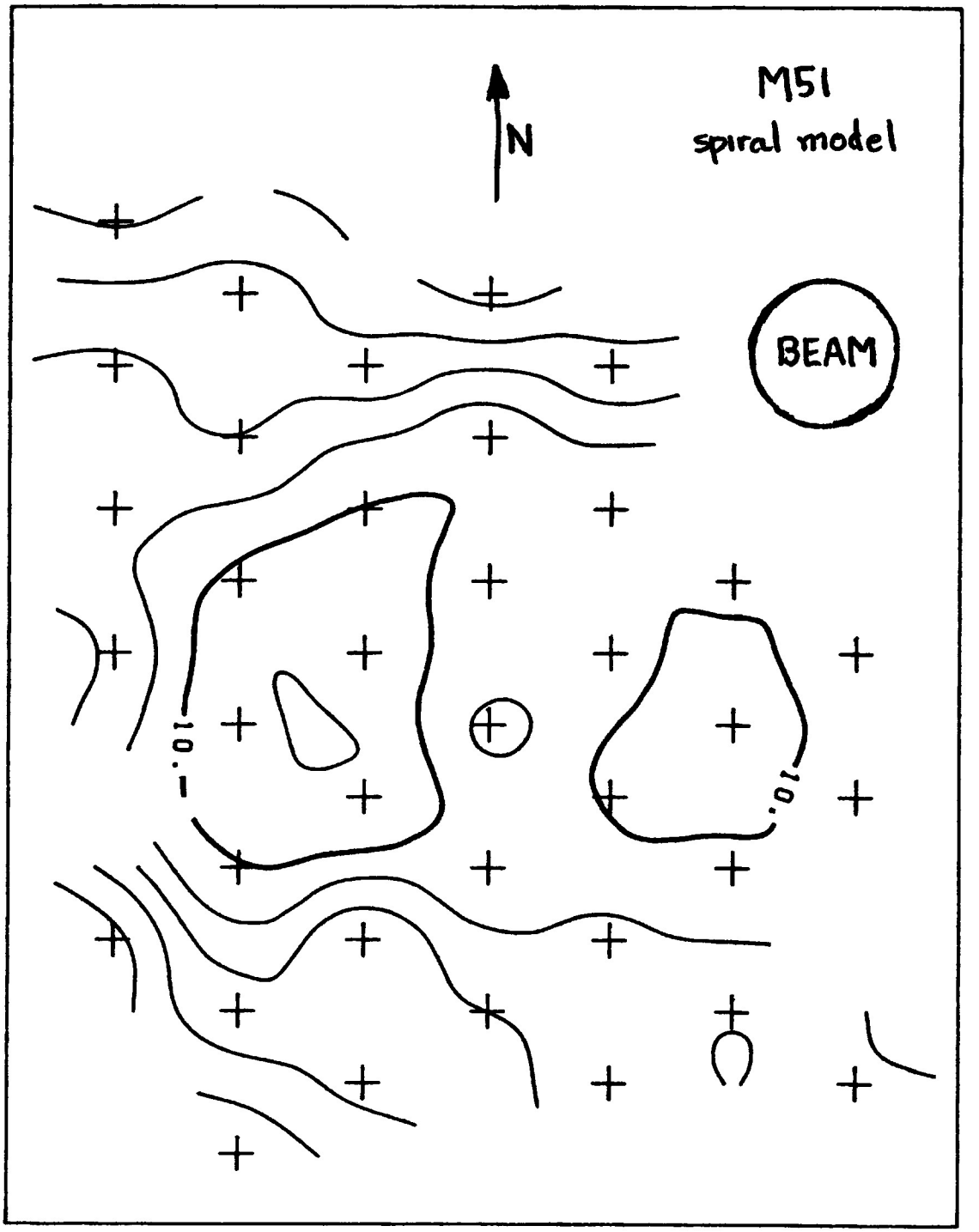

Figure 3

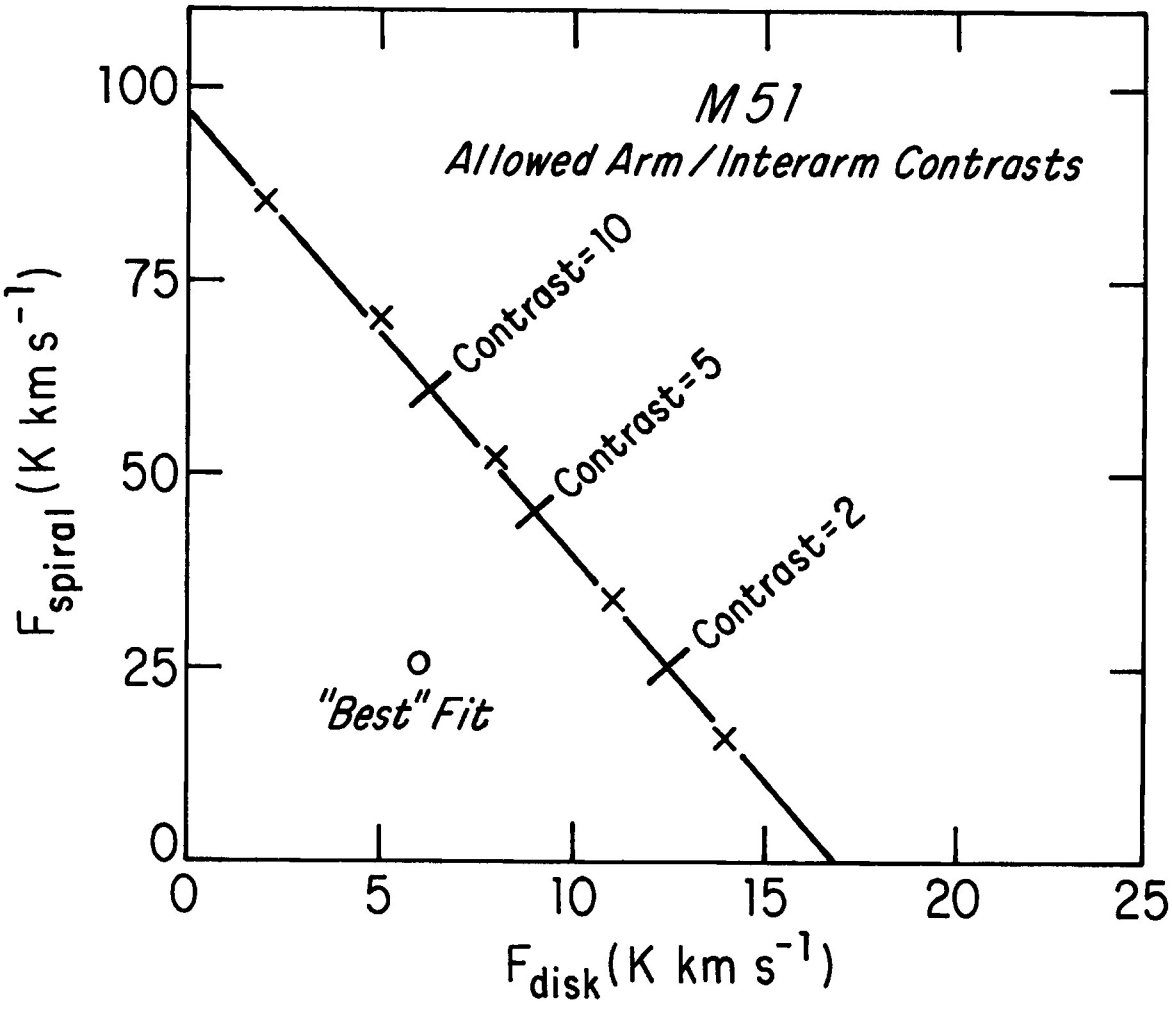
M51
Allowed Arm/Interarm Contrasts
Contrast=10
Contrast=5
Contrast=2
"Best" Fit
100
75
50
25
0
0
5
10
15
20
25
F_{spiral} (K km s^{-1})
F_{disk} (K km s^{-1})

FIGURE 4

CO in Seyferts

R. D. Mathieu (Berkeley)

Because of their large infra-red excesses and luminous active nuclei, Seyfert galaxies represent prime candidates for the detection of CO emission. One of the first galaxies detected in CO was in fact the Seyfert NGC 1068 (Rickard et al. 1977). Since then, three additional detections and one possible detection have been made: NGC4051, NGC 3227 (Bieging et al. 1980); NGC 6814, MKN 231 (?) (Blitz and Mathieu 1982). Many sensitive upper limits have also been set, essentially exhausting the sample of local Seyferts. A summary of this data is given in Table I.

The spectra are typical of extra-galactic sources, broad (several hundred km/sec in width) and featureless. The line centers and shapes agree well with HI data, with the notable exception of NGC 3227 where a single horn present in the HI data (possibly due to tidal distortion from NGC 3226) is not present in the CO spectrum. The line widths, however, are significantly different, with the CO/HI line width ratio being in the four cases: NGC 1068, 1.0; NGC 3227, 0.8; NGC 4051, 0.7; NGC 6814, 0.5. These line width differences can be explained by the smaller CO beam sampling emitting regions on the rising portion of the rotation curve. In the case of NGC 6814, this explanation requires a rather extended rise in the rotation curve. Such a rotation curve is unusual but has been observed (Rubin, Burstein and Thonnard 1980). An alternative possibility is that the rotation curve has the more common rapid rise in the inner regions and that the CO itself is centrally confined in a region smaller than the beam size. Observations are presently being made to distinguish between these two possibilities.

Correlations between CO luminosities[1] and other gas/dust tracers have

[1] It has been common for CO observers to attempt to estimate the H_2 masses from CO observations. Such estimates are notoriously difficult to make because of the very uncertain conditions in the CO emitting regions and are at best valid only to an order of magnitude. A more useful standard of comparison is simply the observed quantity itself, in particular, the CO luminosity in units of integrated CO line strength multiplied by the area subtended by the beam. The CO luminosity thus defined is a measure of the absolute signal strength of unresolved sources, independent of the observing instrument.

been searched for. There is no correlation whatsoever with HI mass. There may, however, be a correlation with 10μ luminosity (Fig. 1), although this is based largely on one point, NGC 1068, as MKN 231 is a marginal detection in CO and the upper limits are not generally sufficiently sensitive to be interesting. NGC 4151 is a notable anomaly, however. Given the association of dust and CO in the Galaxy, a 10μ/CO correlation would certainly be reasonable. Similarly, a 100μ/CO correlation would also be expected, so comparison with the new 100u data will be interesting. (As a tangential note, Blitz and Mathieu observed NGC 4736 on the basis of its strong 100μ emission (Harper, private communication) and detected a weak CO source.)

Bieging, J.H., Blitz, L., Lada, C.J., and Stark, A.A. 1981, Ap. J., 247, 443.

Blitz, L. and Mathieu, R.D. 1982, in preparation.

Rickard, L.J., Palmer, P.,Morris, M., Turner, B.E., and Zuckerman, B. 1977, Ap. J., 213, 673.

Table I

Summary of CO Emmisivities

Galaxies	Summary Beam Size (arcmin)	$\Sigma T_A^* \Delta V$ (K km s^{-1})	Distance (MPC)	Beam AREA (kpc^2)	CO Luminosity (K km s^{-1} kpc^2)	Total Area (kpc^2)	Total CO Luminosity (K km s^{-1} kpc^2)
		Seyfert Galaxies					
NGC 1068	1.1	51	15.5	2.0	1000		
NGC 1275	1.1	< 9	72	410	< 3700		
NGC 2782	1.1	< 4	34	93	< 370		
NGC 2992	1.1	< 3(5)	25	49	< 150(5)		
NGC 3227	1.7	4.0	13.4	34	140		
NGC 4051	1.7	3.5	10.0	19	70		
NGC 4151	1.1	< 3	13.7	15	< 45		
NGC 4939	1.1	< 9	40	130	< 1100		
NGC 5506	1.1	< 3(5)	23	41	< 125(5)		
NGC 6764	1.1	< 7	36	100	< 730		
NGC 6814	1.1	2.2	23	42	90		
MK 3	1.1	< 10	56	250	< 2500		
MK 231	1.1	(2)	167	2250	(4500)		
MK 348	1.1	< 2	63	323	< 650		
		non Seyferts (centers)				(integrated over disk)	
M 51(1)	1.1	23	9.6	7.4	170	49	370
M 82(2)	1.1	105	8.9	0.85	89	11.9	490
NGC 4736(M94)	1.1	4.6	4.4(3)	4.6	7.0	--	--
IC 342(1)	1.1	28	4.5	1.6	4.6	60	390
NGC 253(2)	1.1	89	3.4	0.93	83	> 9.3	> 590
NGC 6946	1.1	32	10.1	8.1	260	275	1990

(1) Data from Rickard and Palmer (1981).
(2) Data from Rickard et al. (1977).
(3) Distance from Sandage and Tammann modified for Ho = 75 km s^{-1} Mpc^{-1}.
(4) Upper limits based on HI line width.
(5) HI line width of 300 km s^{-1} assumed.

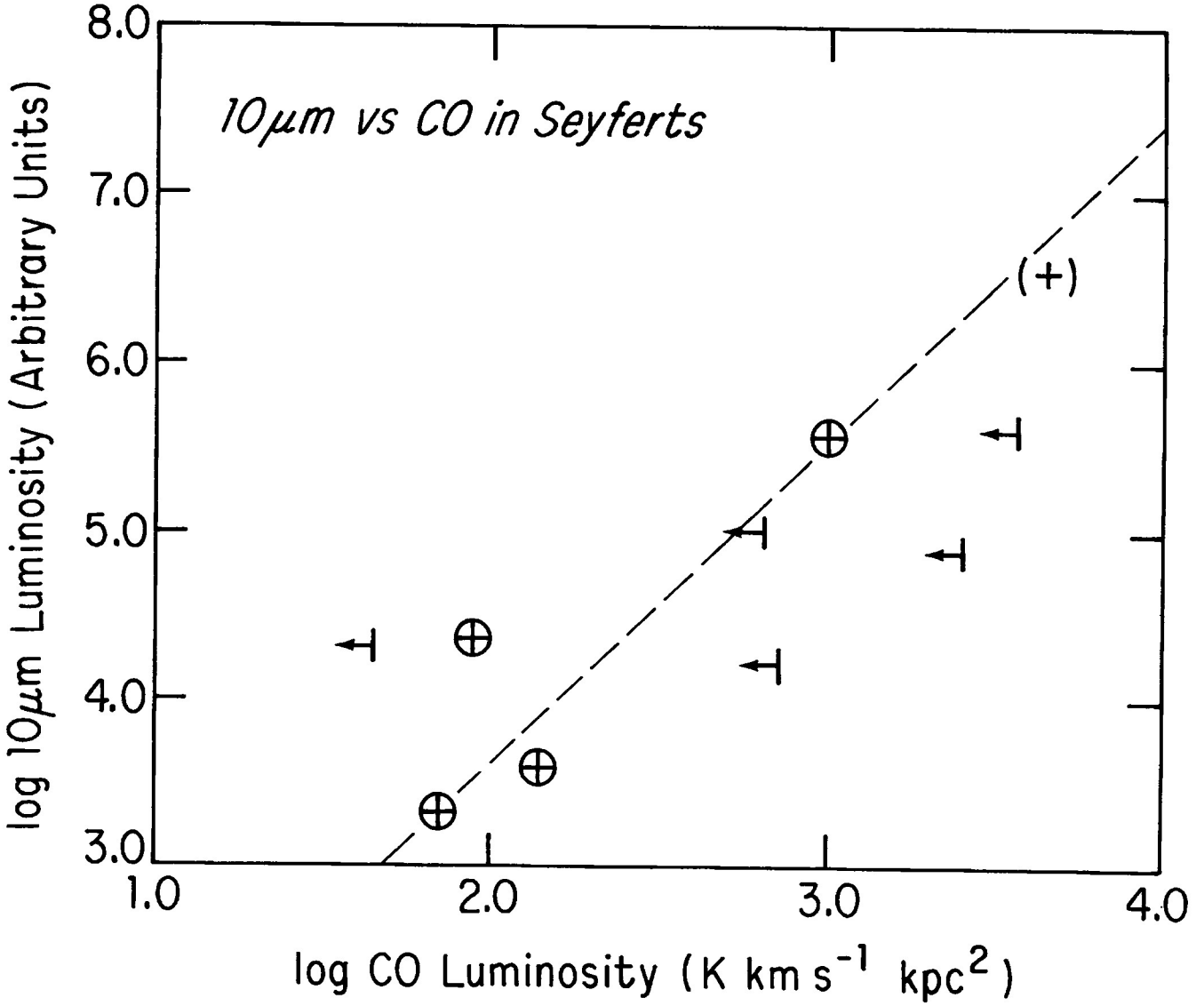

FIGURE 1 Equivalent to beam corrected flux density-integrated emission comparison. IR from Rieke (1978), (+) = MK 231. Dashed line is least squares fit to detections.

A SEARCH FOR CARBON MONOXIDE IN CLUMPY IRREGULAR GALAXIES*

M. A. GORDON

National Radio Astronomy Observatory

J. HEIDMANN

Observatoire de Paris, France

and

EUGENE E. EPSTEIN

The Aerospace Corporation

The failure to detect the 115-GHz line of CO in the galaxies Ma 7, Ma 8, Ma 296, Ma 297, Ma 325, Ma 432, and VV 523 leads to limits on the column density and mass of carbon monoxide. The upper limits to the masses of CO in each of these galaxies, relative to the masses of atomic hydrogen, and of the entire galaxies, tend to be comparable to or less than what is observed for our galaxy. If all spectra are averaged together to give a limit for a composite galaxy, the mass of CO relative to that of atomic hydrogen is about 8 times less than observed for our galaxy.

*To appear in P.A.S.P.

CO Radial Distributions in IC 342 and NGC 6946

Judy Young

Five College Radio Astronomy Observatory

University of Massachusetts, Amherst

The CO emission in two Scd galaxies, IC 342 and NGC 6946, has been mapped using the 14-m FCRAO telescope (HPBW = 50") in collaboration with Nick Scoville. Observations were made along two perpendicular axes in each galaxy at 45" spacing, with sufficient sensitivity to yield accurate radial distributions for comparison with that in our own Galaxy. Spectra at 33 positions in IC 342 and 23 positions in NGC 6946 were obtained; for distances of 4.5 and 10.1 Mpc for IC 342 and NGC 6946 the 14-m resolution corresponds to 1.1 and 2.4 kpc respectively. Figure 1 shows the spectra north of the nucleus of IC 342. In both galaxies the spectra exhibit velocity and intensity changes which correlate well with galactic location. The highest intensities are observed in the nuclei, with smooth falloffs at larger galactic radii. The mean velocities vary regularly across both galaxies in the sense expected from galactic rotation. Figure 2 shows the spatial-velocity map along the N-S axis in IC 342. We have derived CO rotation curves for these two galaxies assuming the same inclination, distance, systemic velocity, and position angle of the major axis as Rogstad and Shostak (1972), and find good agreement with HI rotation curves (Figure 3). Optical rotation curves are not available for either of these galaxies.

The CO radial distribution for NGC 6946 is shown in Figure 4; also plotted are the integrated intensities expected for our own Galaxy, viewed at the same resolution, inclination, and positions as NGC 6946. Although our effective resolution is clearly adequate, there is no evidence for a "hole" in

either external galaxy like that at R = 1-4 kpc between the nucleus and molecular cloud annulus in our Galaxy.

We have compared the CO radial distributions with the B luminosity profiles observed for these galaxies (Ables 1971) in Figure 5, and find the striking result that the CO distributions follow the luminosity profiles in both galaxies. The well-known exponential nature of the luminosity profiles is evident as a straight line in Figure 5. The observed CO radial distributions in both Scd galaxies are also well fit by exponential distributions in radius, $I(R) = I_o e^{-R/R_o}$, and the CO scale lengths R_o are in good agreement with those found by Ables for the optical light. Other functional forms were fit to the data (excluding the nuclei) as well: in IC 342 both an exponential and R^{-1} power law give equally good fits at the 85% confidence level, while in NGC 6946 an exponential and $R^{-1.4}$ power law give equally good fits at the 75% confidence level. Both galaxies were fit poorly (< 1% confidence level) with gaussian and flat (R°) distributions. The particular functional form used to describe the distribution is not critical since the important point is that the CO follows the light distribution.

Most of the optical luminosity measured in the B band probably arises from young stars, $< 2 \times 10^9$ years old, and reflects recent star formation rates at different radii. The close correlation of the luminosity and H_2 distributions may be understood if the star formation rate varies approximately linearly with mean density and mass of H_2, that is, the star formation rate per nucleon of H_2 is constant.

We have derived a conversion from CO line flux to H_2 column density based on analysis of CO emission in our Galaxy (see the contribution in these proceedings entitled "Relating CO Line Flux to H_2 Column Density", Young and

Scoville; also Appendix I of Young and Scoville 1981). Using the empirical relation $N_{H_2} = 4 \times 10^{20} I_{CO}$, in both IC 342 and NGC 6946 we find that H_2 dominates HI in the inner regions, that is H_2 increases exponentially while HI decreases in toward the center, so that the total gas density is a strong function of radius. Figure 6 shows the H_2 and HI surface densities as a function of radius for NGC 6946. The H_2 mass in IC 342 out to 8 kpc is 4×10^9 $M_\odot$ compared with 10^{10} $M_\odot$ out to 12 kpc in NGC 6946.

The discrepancy between the H_2 distributions in our Galaxy and in IC 342 and NGC 6946 is that in our Galaxy at 1-4 kpc there is a deficiency of gas. The occurrence of this gap in the CO distribution in our Galaxy but in neither of the external galaxies suggests a possible link between the lack of gas and the inner Lindblad resonance (ILR) which is expected in this zone of the Milky Way. The two external galaxies undergo nearly rigid rotation inside 5 kpc, as shown in Figure 7, and therefore have no ILR's. The effect of this resonance could be to remove any interstellar gas which may have existed originally at R = 2-4 kpc in our Galaxy to either larger or smaller radii. That is, as the gas from this zone executes large radial oscillations it would collide with gas clouds at larger and smaller radii. As a result the gas originally in the ILR zone would no longer return to the equilibrium radius from which it started but would be preferentially at larger or smaller radii depending upon whether it collided with gas on the exterior or interior portion of its epicyclic motion. Further association of the molecular gap with the ILR is provided by CO observations at 7 positions in NGC 4321, the largest Sc in Virgo. The rotation curve of this galaxy has an inner bump at 1 kpc (Rubin et al. 1980), and the CO distribution appears like that in our own Galaxy with coarser resolution.

The degree of clumping on the scale of our resolution (1 to 2 kpc) can be estimated from the fractional discrepancies of the observed intensities from the exponential distribution. Several positions with strong CO relative to the exponential are on optical arms, but not all arms are associated with strong CO emission. A global spiral structure is not evident from the molecular data.

References

Ables, H.D. 1971, Publ. U.S. Naval Obs. Sec. Ser., Vol. XX, Part IV, Washington, D.C.

Morris, M. and Lo, K.Y. 1978, Ap.J., 223, 803.

Rogstad, D.H. and Shostak, G.S. 1972, Ap.J., 176, 315.

Rubin, V.C., Ford, W.K., and Thonnard, N. 1980, Ap.J., 238, 471.

Young, J.S. and Scoville, N.Z. 1982, Ap.J., submitted.

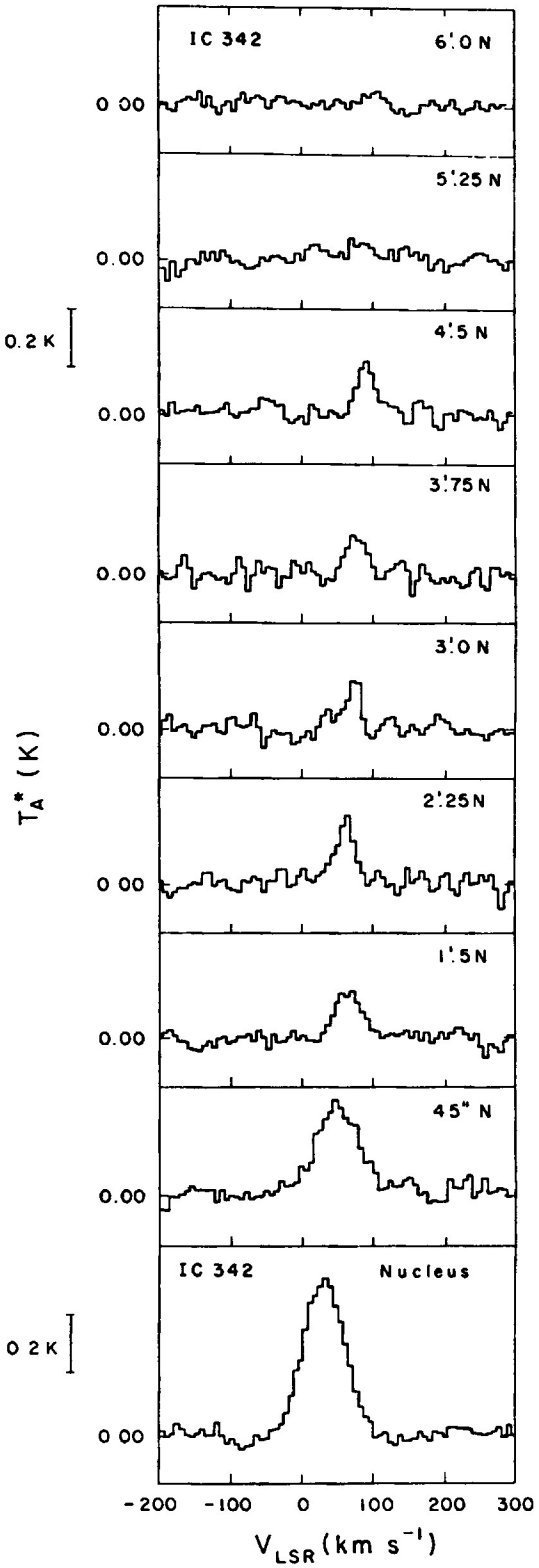

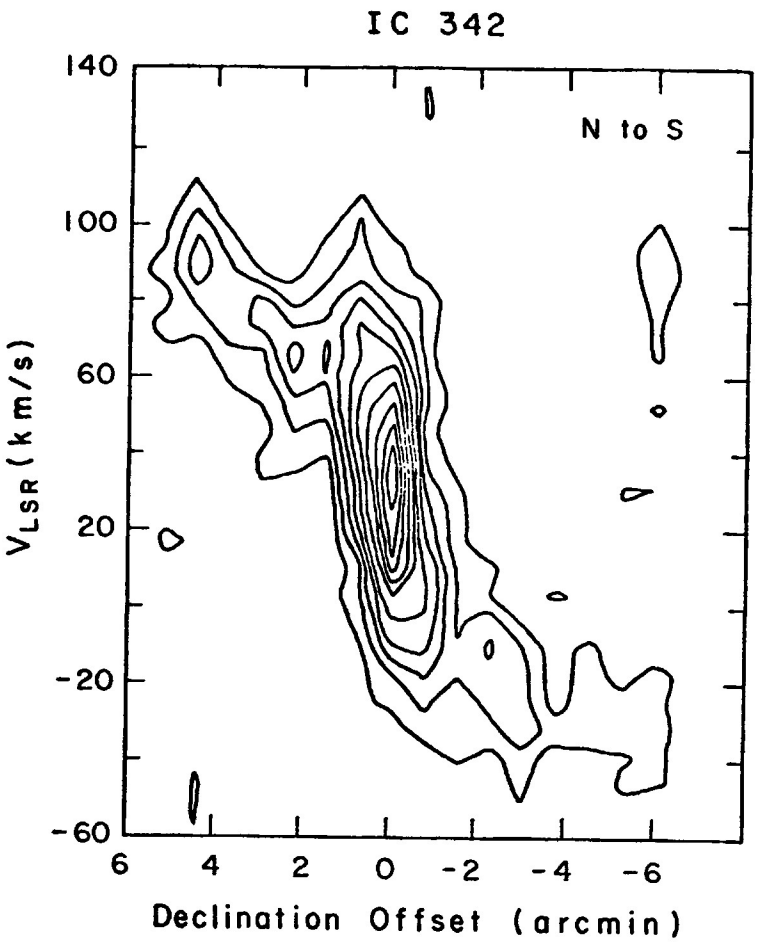

Figure 2. Spatial-velocity map along the north-south axis in IC 342 showing observed CO rotational velocities on the sky. Contours are in intervals of 0.05 K.

Figure 1. Spectra of IC 342 north of the nucleus. At a distance of 4.5 Mpc the 50" resolution corresponds to 1.1 kpc. Intensities fall off smoothly away from the nucleus, and velocities shift in the sense expected from galactic rotation.

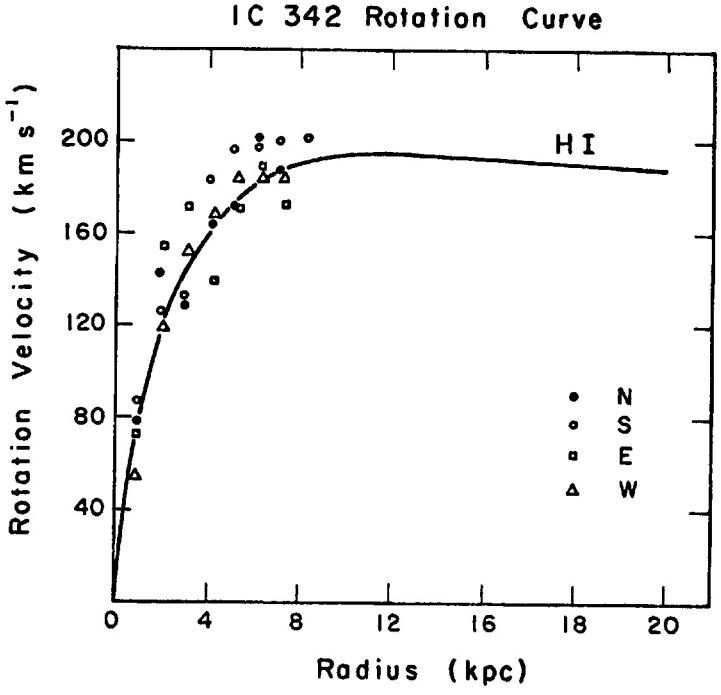

Figure 3. CO rotation curve for IC 342. The HI rotation curve is from Rogstad and Shostak (1972) with 2' resolution. The agreement between CO and HI velocities is equally good for NGC 6946.

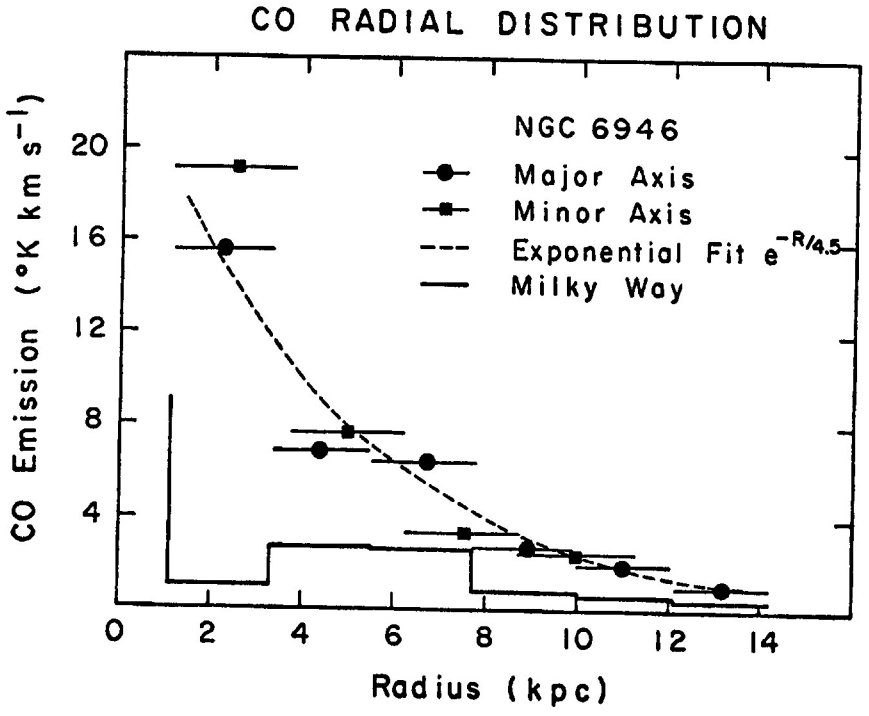

Figure 4. CO radial distribution in NGC 6946. The horizontal bars through the data points indicate the beamsize on the galaxy (2.4 kpc). The solid lir represents the CO distribution for the Milky Way, viewed at the same distance and inclination as NGC 6946. The dashed line is the best exponential fit to the data. The nuclear emission is off scale at 46 K km s^{-1}.

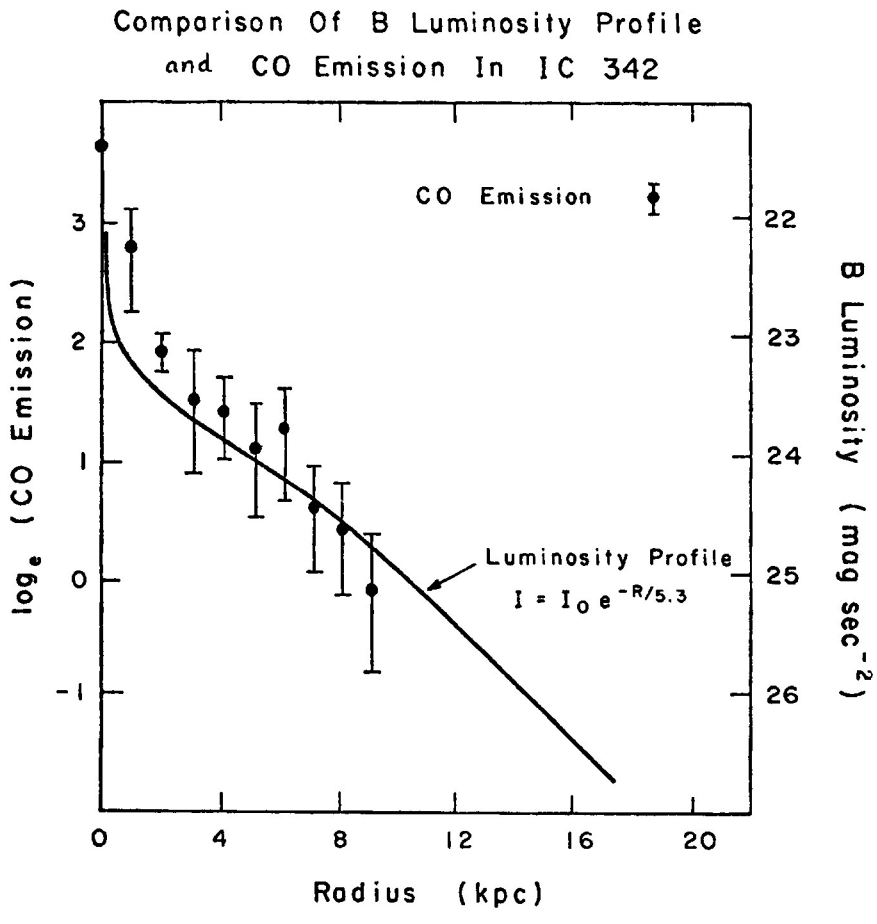

(a)

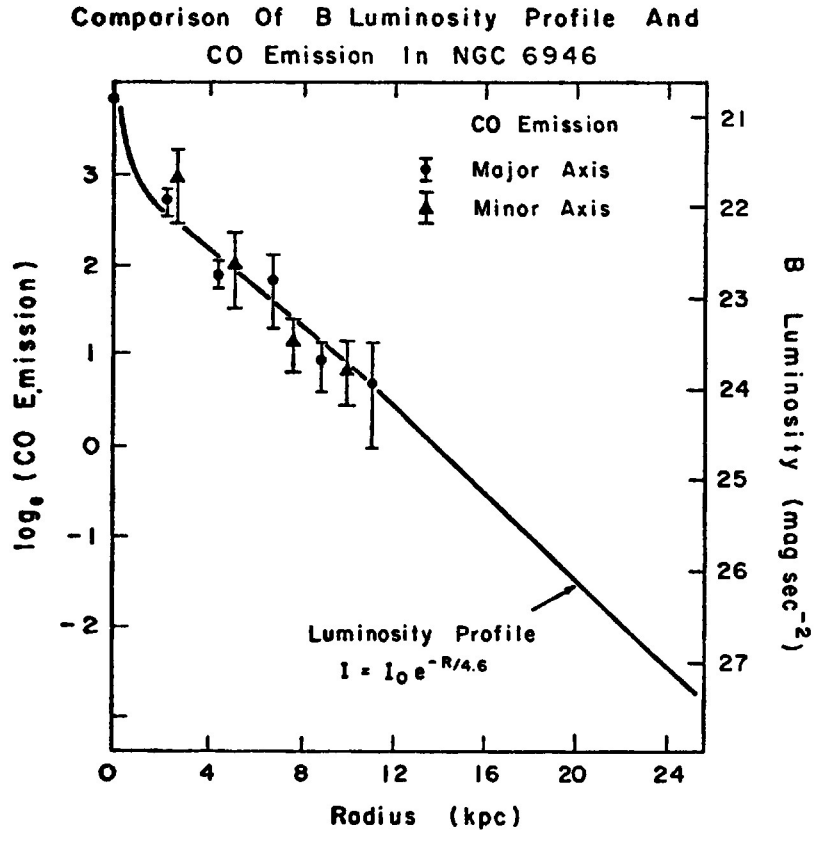

(b)

Figure 5. Comparison of the CO distribution (on a log scale) with Ables' (1971) B luminosity profile for (a) IC 342 and (b) NGC 6946. The close agreement between the CO and optical light distributions is striking. The exponential nature of the luminosity profiles is evident on these semi-log plots as straight lines.

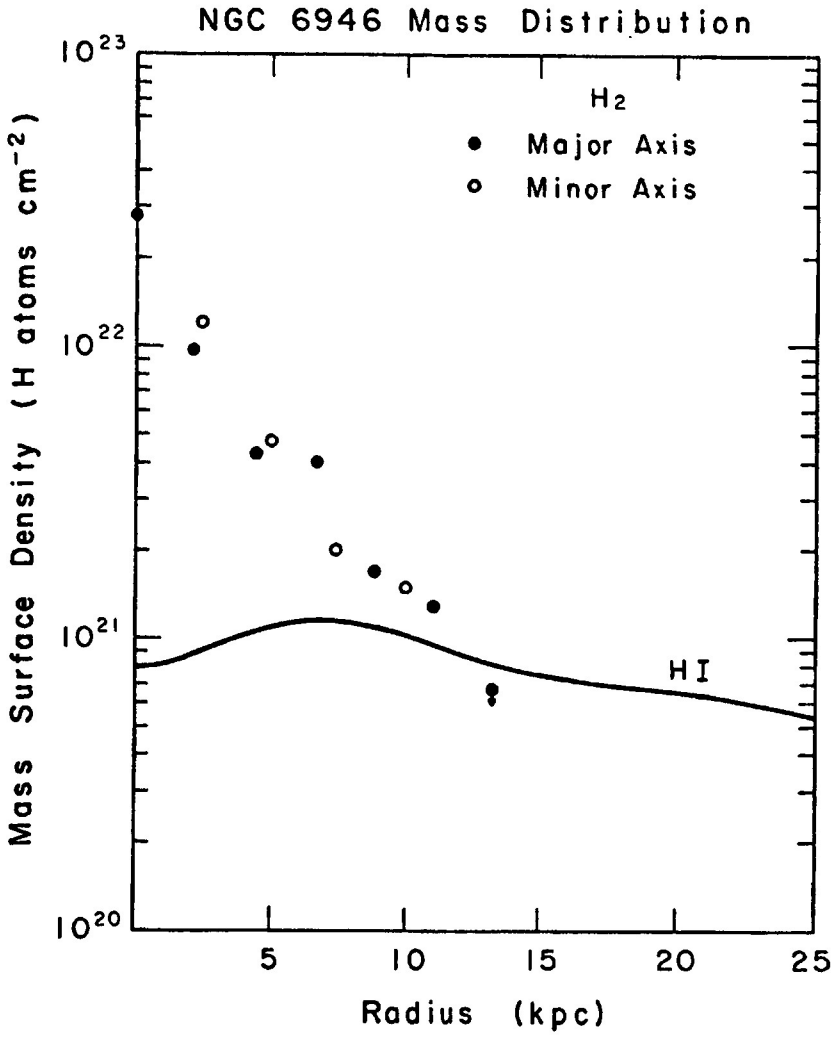

Figure 6. Mass surface densities in NGC 6946. The H_2 values are derived assuming a linear relationship between CO flux and H_2 column density. The solid curve represents the HI mass surface density from Rogstad and Shostak (1972). H_2 dominates HI over the interior of the galaxy; a similar result is found for IC 342.

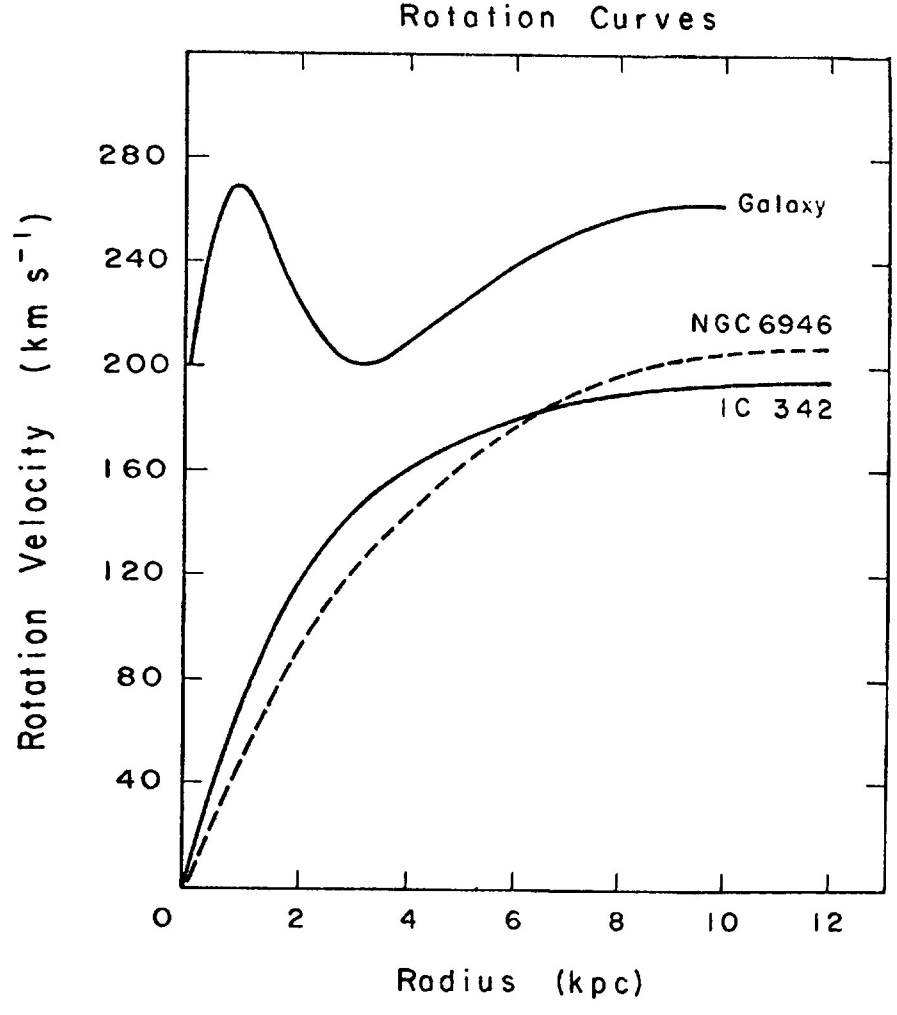

Figure 7. Rotation curves of IC 342 and NGC 6946 (Rogstad and Shostak 1972) compared with that for the Milky Way. In IC 342 and NGC 6946 the roughly solid body rotation extends to 5 kpc while in our Galaxy the solid body rotation occurs only for the inner 1 kpc.

CO OBSERVATIONS OF GALAXIES IN THE VIRGO CLUSTER

MARIO VIETRI

Princeton University Observatory

Preliminary results are reported of a project begun by A. A. Stark, J. Bally, J. Knapp and myself with the Bell Labs 7-m antenna. The aim of the project is the detection of an homogeneous sample of galaxies in the $1 \rightarrow 0$ transition of CO. To this aim, a number of galaxies, all of them within the Virgo Cluster, has been selected, according to the criteria: (1) previous H I detections existed, (2) the galaxy has a diameter (as deduced from Uppsala catalog), larger than our beam (= 100"). The preliminary observations reported here were made in order to check the feasibility of this study. No constraints were set on the inclination of the galaxies.

To date, 12 galaxies have been observed. Eight non-detections are listed in Table I together with the total observing time for each. Also, a typical spectrum for a non-detection (NGC4032) is shown in Fig. 1. In this Figure, a linear baseline has been removed, and the data smoothed to a resolution of 4 MHz. The peak at $\sim$ 1400 km s^{-1} is due to a "bad" channel.

Two galaxies have definitely been detected: NGC4254 and NGC4303. Spectra for the (optical) central positions for these galaxies are shown in Fig. 2 and Fig. 3, and appropriate data are given in Table II. The difference between the ease of detection of these two galaxies and the previously mentioned ones cannot be attributed to baseline problems or lack of sensitivity, but rather to the fact that NGC4254 and 4303 happen to be the brightest galaxies in our sample, in both the optical and H I, and also the only face-on ones.

H I spectra for NGC4254 and NGC4303 from Davies and Lewis (1973) are shown in Fig. 4. They both appear to be typical H I spectra for galaxies. Both centroids and line shapes and widths in CO and H I are in agreement, thus revealing no strong concentration of CO with respect to H I, at least not with respect to length scales over which the rotation curve reaches its asymptotic

value. For NGC 4303, marginal evidence of a CO distribution anomaly at the red end of the line exists.

More information is available for NGC4254. Figures 5-8 display spectra taken at RA and Dec offsets of ± 1.5 arcmin, which corresponds to our beam width, and, at the Virgo Cluster distance of d = 14.5 Mpc, to a linear size of 7 kpc. The spectra taken with $\Delta RA = -1.5$, $\Delta Dec = 0$ and $\Delta RA = 0$, $\Delta Dec = -1.5$ are consistent with the hypothesis that the beam is just collecting signal from the center. In fact, the blue end of the central spectrum (Fig. 2) is basically equivalent to either one of Figs. 5 and 6. Figure 7 displays a point which lies at $\Delta Dec = +1.5$ from the center. This corresponds to a region sitting on one of the two prominent spiral arms of NGC4254 (see for instance, the Hubble Atlas), but along the minor axis of the nucleus. The most interesting feature can be seen in Fig. 8, where a strong peak at ~ 2500 km s^{-1} can be seen, outside the range of velocities seen for the spectrum at the center of the galaxy. In fact, this high-velocity peak contains a significant (~20-30%) amount of the total emission of the galaxy; from the Hubble Atlas picture, though, it is not obvious what this peak might be associated with.

Thus Figs. 5-8 support the conclusion that, while most of the detected CO is confined within ~ 7 kpc, there is at least one direction in which evidence is found for the existence of a strong concentration of CO at a few kpc from the center, evidence which seems inconsistent with the idea of an exponential disk.

Computation of the total H_2 mass content is done under the assumption that all of the emission is due to giant molecular clouds, whose properties are similar to those of the clouds in our galaxy. In this case, the parameter on which the total emission depends, and which contains the properties of the clouds in our galaxy is (Knapp 1981) $F_c \equiv \frac{M_c}{T_c \Delta V_c r_c^2}$, a most

uncertain quality. The value of F_c is 7, somewhat intermediate between those of Morris & Lo, (F_c = 3), and Bieging et al. (1981) (F_c = 30). The values obtained for our galaxies are in Table II; for both of them, only the central region (i.e., within our beam, which is ~ 7 Kpc at their distance) has been included. For NGC4254, assuming that our previous discussion is correct, a correction of ~ 20% is necessary in order to take into account the off center source. Total H I masses as derived by Davis & Lewis, are ~ 7 10^9 $M_\odot$ for both galaxies. These are total mass contents, that is, obtained with a beam much larger (17' x 13', Mark I) than the galaxy size. Nonetheless, since it is apparent from both these observations of NGC4254 and our knowledge of the galaxy that the total H_2 content outside a radius of ~ 7 Kpc is but a fraction of the total content, it appears that the discrepancy of a factor of 4 in the HI and H_2 mass content is real, even though one should be reminded that the quantity F_c by means of which the content was derived might be wrong by a factor of 3 on either side; thus our conclusion is that M(HI) > M(H_2) but the exact amount by which HI dominates H_2 is not clear. This stands in clear contrast with data for our galaxy, where M(HI) ≃ M(H_2), but agrees with data for M31 (Linke and Stark, private communication).

There is, eventually, the possible detection of NGC4527, whose data are shown in Table II, and whose raw spectrum, obtained in 2 hours, is in Fig. 9. Two more galaxies, NGC4651 and NGC3976, may have been detected at a lower level (1σ). For these two galaxies, though, base line problems which make the interpretation of the data rather ambiguous have been found. For them, as for NGC4527, confirmation will have to wait a better signal-to-noise ratio observation.

ACKNOWLEDGEMENTS

I would like to thank Jill Knapp, Arno Penzias and Tony Stark for all sorts of advice and encouragement, and the Bell Labs' staff for use of their observational and computational facilities.

REFErences

Davies, R.D. and Lewis, B.M. 1973, M.N.R.A.S., 165, 231.

Knapp, J.R. 1981, preprint.

Bieging et al., 1981, preprint.

Morris, M. and Lo, K.Y., 1978, Ap.J., 223, 803.

Table I

NGC	Observing Time (on source)
3976	4^h15^m
4032	3^h20^m
4178	1^h45^m
4216	1^h
4517	2^h
4579	1^h40^m
4651	3^h
4654	2^h20^{20}

Table II

	NGC4254	NGC4303	NGC4527
Classification	Sc	Sb/SBc	Sb
Magnitude	$10^m.2$	10.9	11.3
Color	$(B-V)^\circ_T = 0^m.48$	.51	.74
Rec. velocity (helioc)	2400 km s^{-1}	1599	1730
Uppsala Inclination	1	1	3
Total Obs. Time (on source)	2^h30^m	4^h	2^h
Ch. to Ch. rms noise at 10 km s^{-1} res	$\lesssim$ 0.01°K	$\lesssim$ 0.01°K	$\lesssim$ 0.01°K
Peak Temperature	90 m K	90 m K	--
FWHM	200 km s^{-1}	140 km s^{-1}	--
Vel. Centroid (LSR)	2395 km s^{-1}	1562 km s^{-1}	--
Int. Emission	13°K km s^{-1}	10°K km s^{-1}	--
Total mass content in H_2	1.6×10^9 $M_\odot$	1.3×10^9 $M_\odot$	--

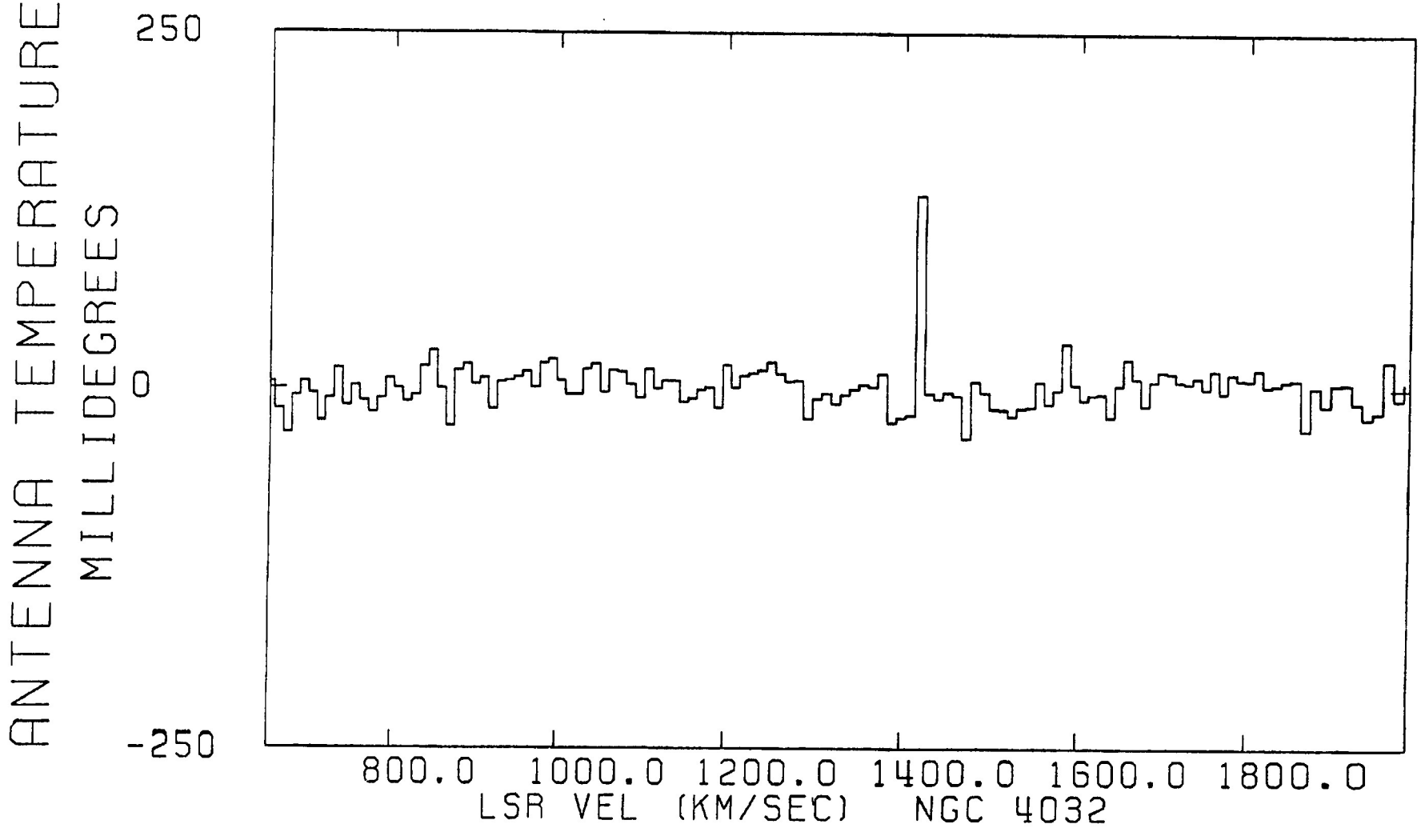
ANTENNA TEMPERATURE
MILLIDEGREES
250
0
-250
800.0
1000.0
1200.0
1400.0
1600.0
1800.0
LSR VEL (KM/SEC)
NGC 4032

Figure 1

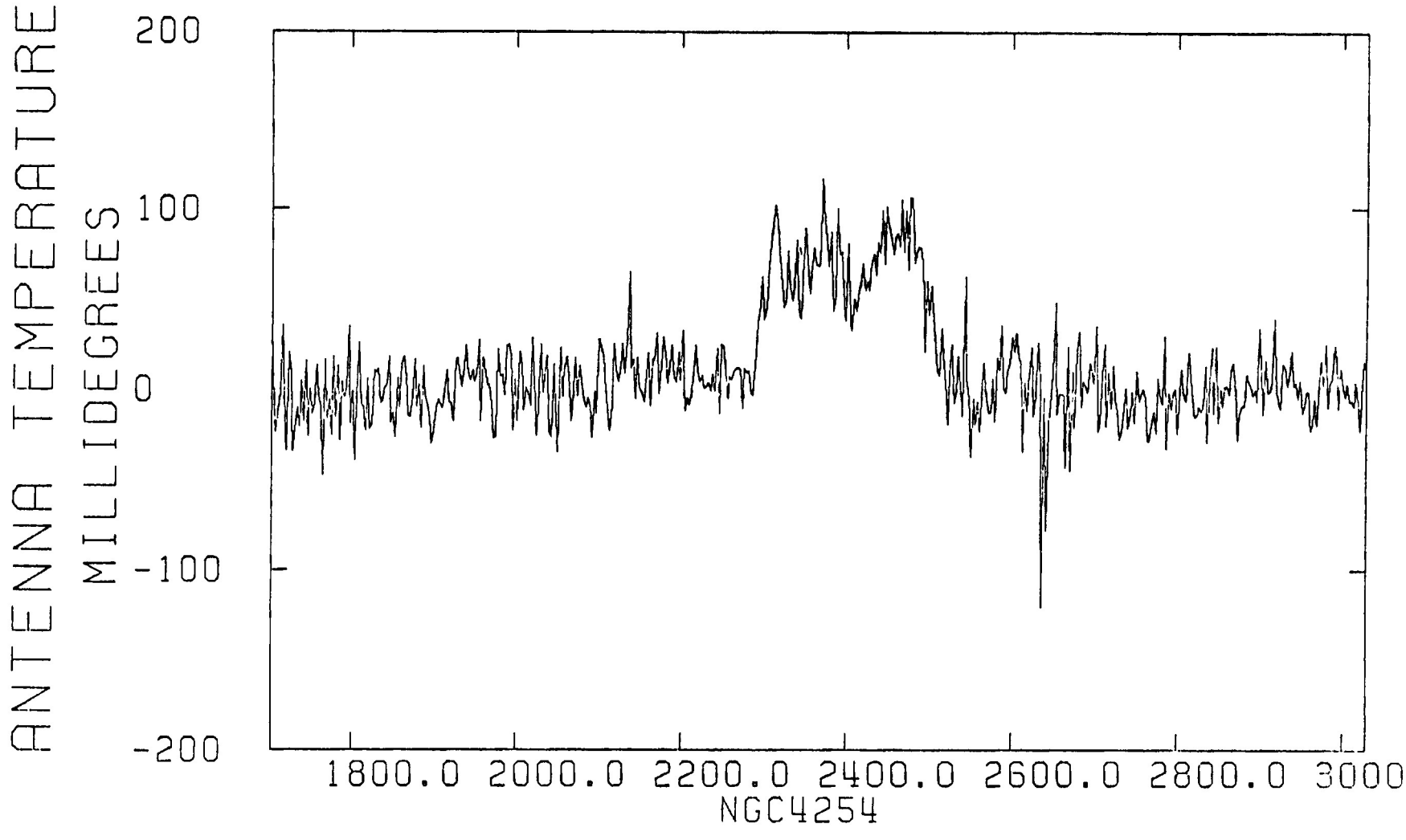
ANTENNA TEMPERATURE
MILLIDEGREES
200
100
0
-100
-200
1800.0
2000.0
2200.0
2400.0
2600.0
2800.0
3000
NGC4254

Figure 2

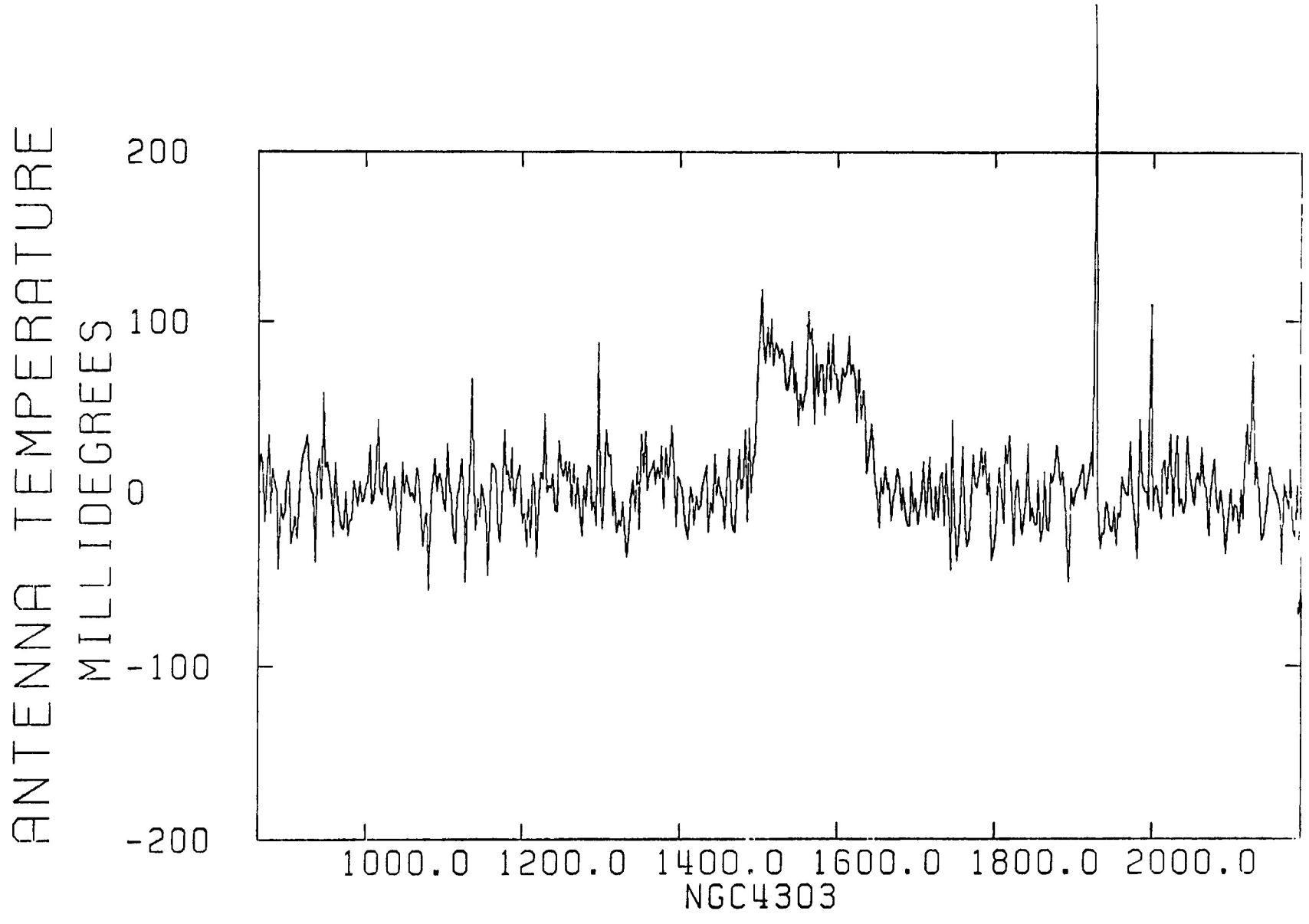
ANTENNA TEMPERATURE
MILLIDEGREES
200
100
0
-100
-200
1000.0
1200.0
1400.0
1600.0
1800.0
2000.0
NGC4303

Figure 3

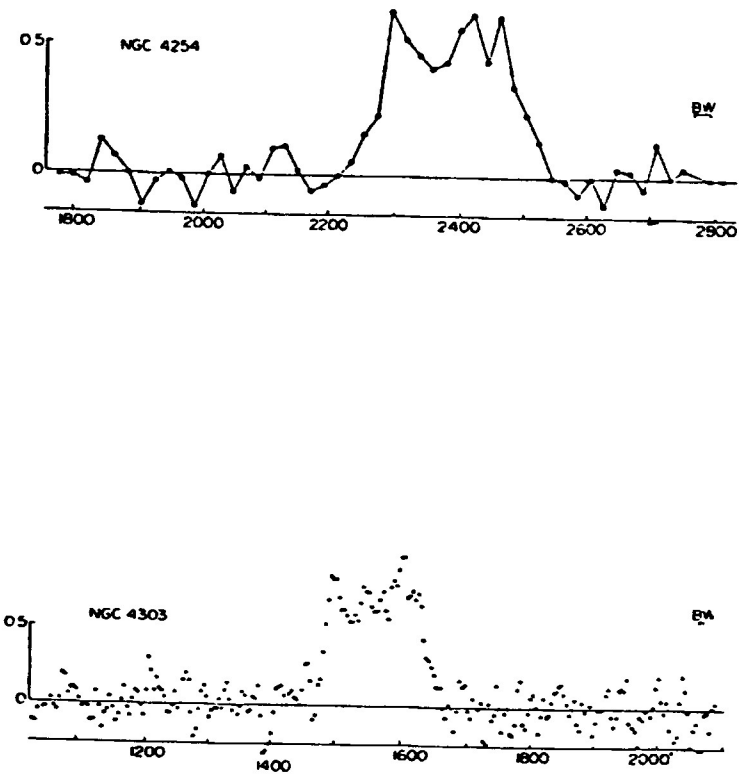
0.5
NGC 4254
BW
0
1800
2000
2200
2400
2600
2900
0.5
NGC 4303
BW
0
1200
1400
1600
1800
2000

Figure 4

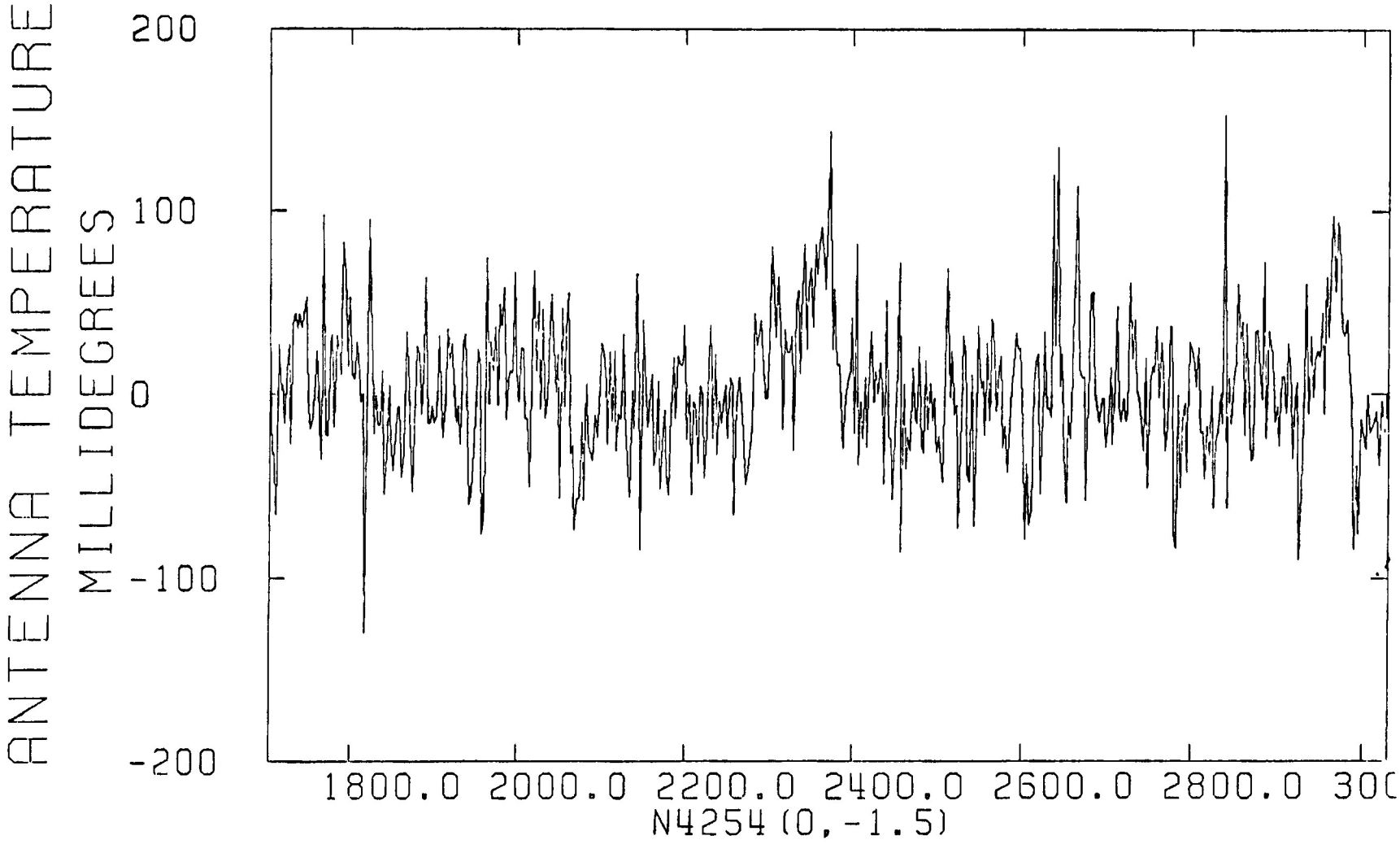
ANTENNA TEMPERATURE
MILLIDEGREES
200
100
0
-100
-200
1800.0
2000.0
2200.0
2400.0
2600.0
2800.0
N4254 (0,-1.5)

Figure 5

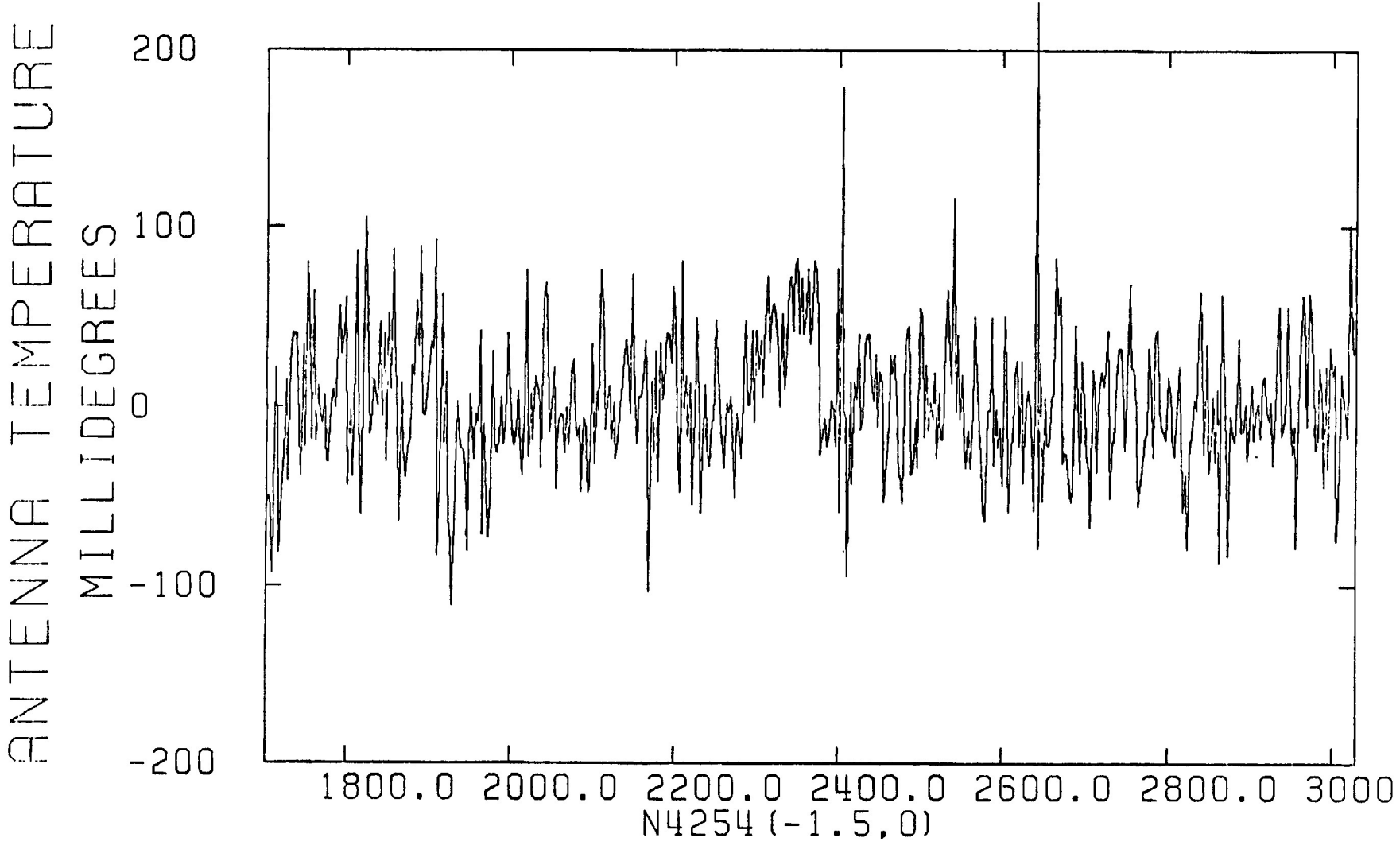
ANTENNA TEMPERATURE
MILLIDEGREES
200
100
0
-100
-200
1800.0
2000.0
2200.0
2400.0
2600.0
2800.0
3000
N4254 (-1.5,0)

Figure 6

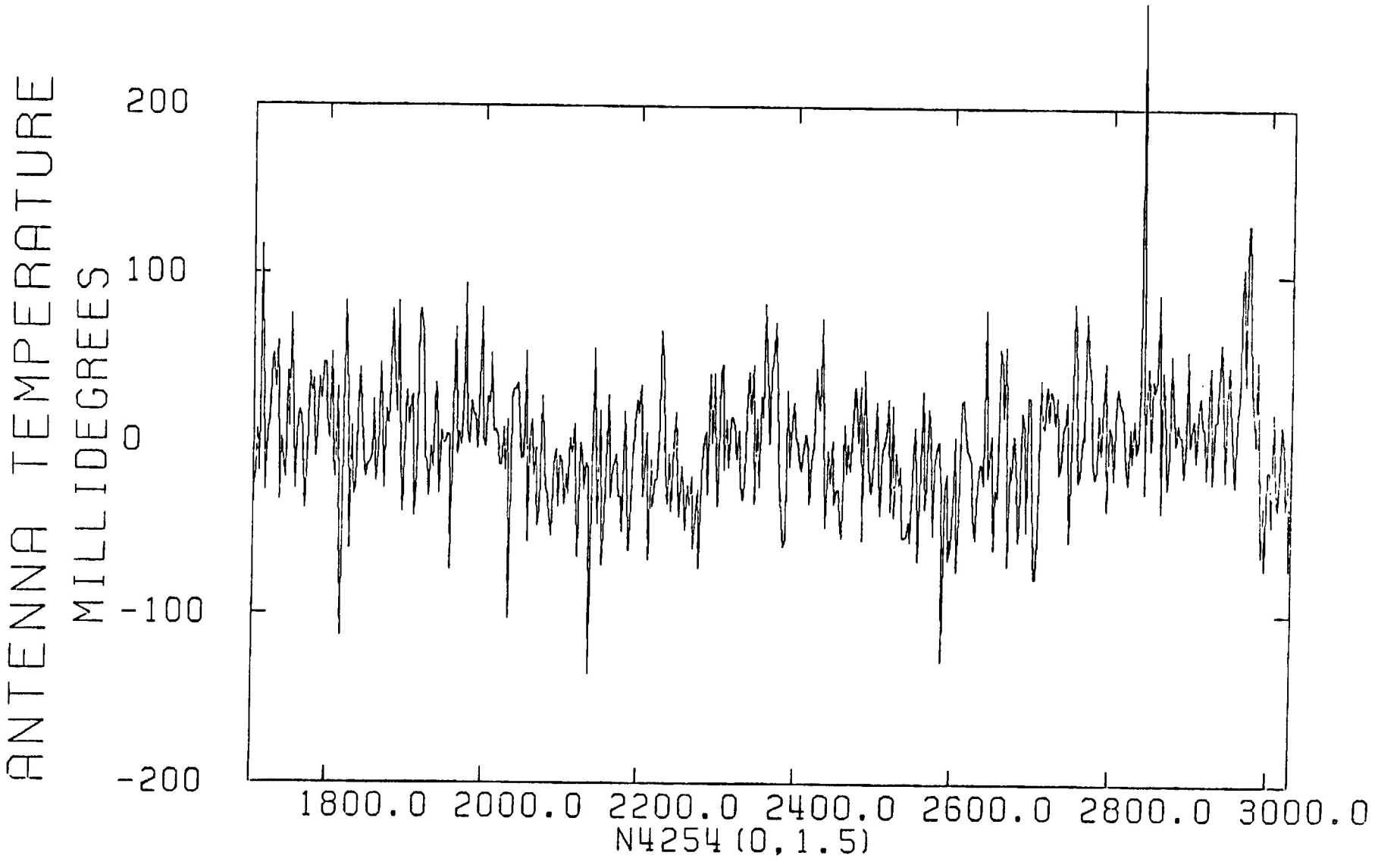
ANTENNA TEMPERATURE
MILLIDEGREES
200
100
0
-100
-200
1800.0
2000.0
2200.0
2400.0
2600.0
2800.0
3000.0
N4254 (0, 1.5)

Figure 7

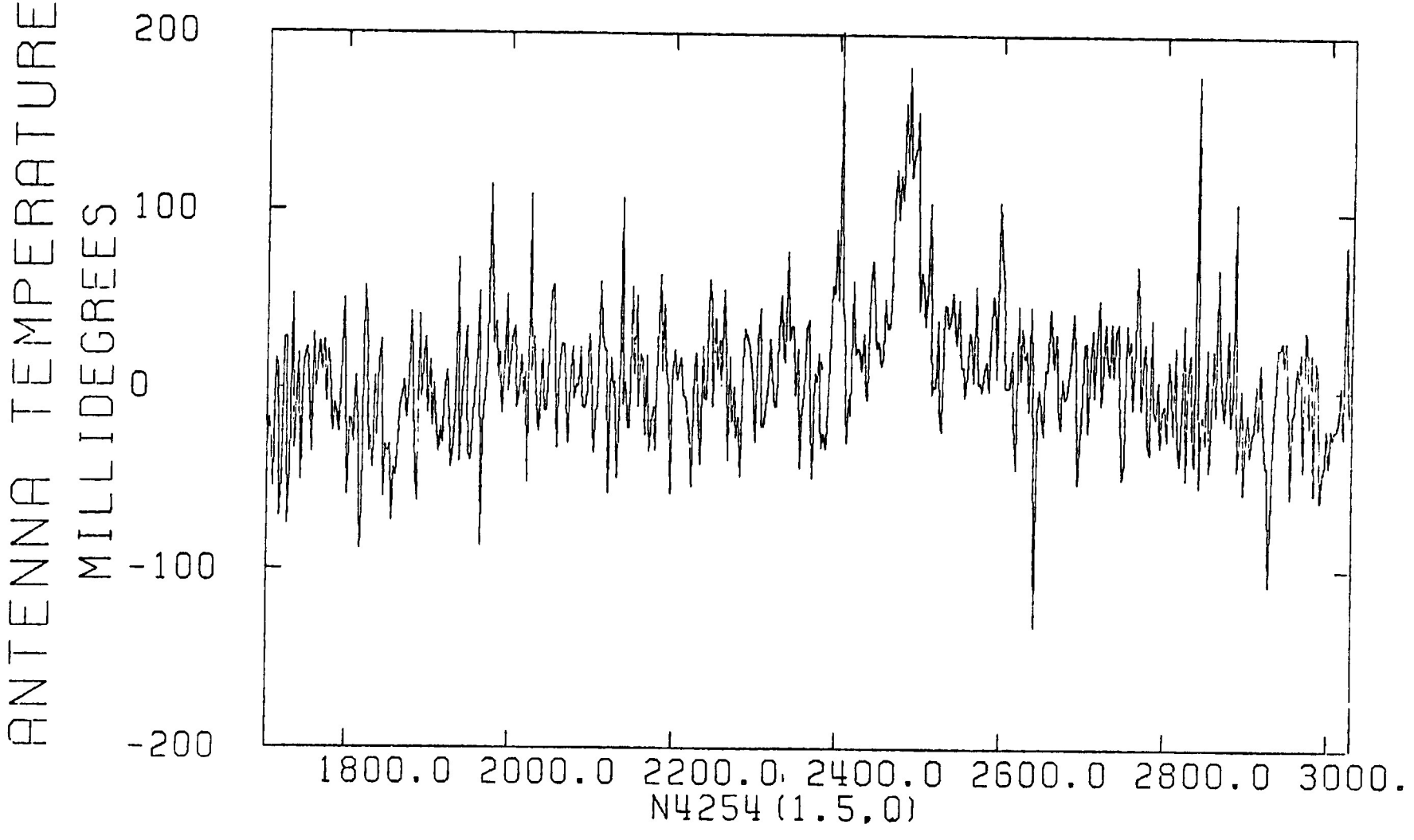
ANTENNA TEMPERATURE
MILLIDEGREES
200
100
0
-100
-200
1800.0
2000.0
2200.0
2400.0
2600.0
2800.0
3000.
N4254 (1.5,0)

Figure 8

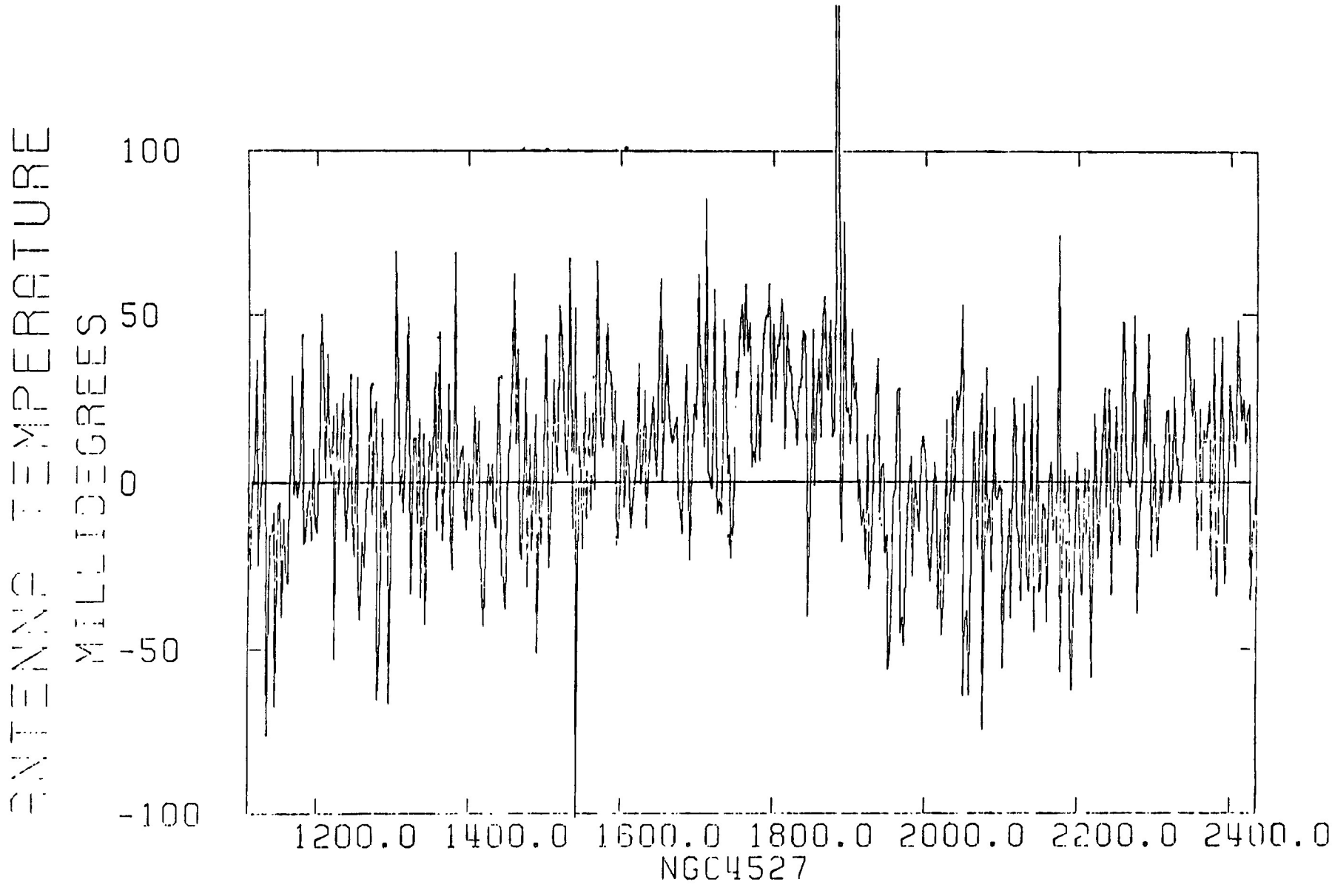
ANTENNA TEMPERATURE
MILLIDEGREES
100
50
0
-50
-100
1200.0
1400.0
1600.0
1800.0
2000.0
2200.0
2400.0
NGC4527

Figure 9

THE MOLECULAR CLOUD DISTRIBUTION IN N891 BETWEEN 3 and 15 Kpc

P. M. Solomon
Astronomy Program
SUNY, Stony Brook, N.Y. 11794

NGC 891 is an edge on ($i = 88^{o}$) SbI galaxy with a large angular extent of 13!5 along the major axis. It has an optical appearance very much like our Galaxy (Osterbrock and Sharpless 1952, Code and Houck 1955) as can be seen in the photograph in figure 4. In this paper† we present observations of CO emission at 2.6 mm along the major axis of NGC 891 carried out with the FCRAO 14m antenna. We compare the distribution of molecular clouds with that of HI and nonthermal radio continuum within NGC 891 (Sancisi and Allen, 1979; Allen et'al. 1978) and with the distribution of molecular clouds in our galaxy. The initial CO survey of our Galaxy (Scoville and Solomon 1975) showed that molecular clouds, unlike HI, had their strongest concentration in the inner galaxy. This has since been confirmed by several more extensive surveys (Gordon and Burton 1976, Cohen and Thaddeus 1977, Solomon et al. 1979, 1980). In particular therefore we wish to answer the question: Does NGC 891 have its molecular ISM concentrated to the inner galaxy?

Although an edge on galaxy does not offer the opportunity to measure the nonaxisymmetric structure such as the degree of concentration of molecular clouds into spiral arms, the large line of sight through the disk enables the observer to determine the radial distribution of emission from relatively strong signals by assuming an axisymmetric disk. The angular resolution of 45" offered by the FCRAO 14m antenna corresponds to 3 kpc at D = 14 Mpc for this galaxy. The average CO emission as a function of radius from the galaxy, NGC 891, can thus be determined out to 15 Kpc by 11 observations spaced every 0!75 along the major

†A more complete description of this work is being submitted to the Ap.J. by P. Solomon, J. Barrett, D. Sanders and R. deZafra.

axis. In N891 the beam takes in the entire z height of the plane (found for HI by Sancisi and Allen 1979). These CO observations are approximately analgous to observing our Galaxy with a very small (~ 1 cm) antenna or just a feed horn.

Figure 1 shows the 11 CO spectra, obtained every 45" along the major axis, with a velocity resolution of 10 km/s. The sharp rise in the rotation curve of the galaxy in the inner 1!5 is readily apparent as is the decrease in integrated intensity with increasing distance from the center beyond 0!75. The spatial velocity diagram in figure 2 depicts the CO emission and 1 contour of the HI emission. The difference between the shape of the CO and HI contours is very striking. The CO emission along each line of sight is stronger at the higher velocities (w.r.t. the systemic v = 530 Km/s) which correspond to emission from smaller R. Thus the different spatial distribution of molecular clouds and HI is apparent in the velocity distribution of their emission. Figure 3 is a schematic representation of the spatial velocity diagrams showing the rotation curve, the axis of peak CO emission and axis of peak HI emission. The rotation rises steeply to a flat velocity law about 1!5 from the center of the galaxy The axis of peak CO emission intersects the flat rotation curve at about 2!2 from the center while the HI intersects at 4' from the center, again demonstrating the different spatial distributions of HI and H_2 as traced by CO. The HI ring in this galaxy extends well beyond the region of strong CO emission although weak CO emission is present out to the last point observed. The difference between the HI and H_2 distribution in this galaxy is perhaps best seen in Figure 4 which depicts the integrated intensity of CO, HI and nonthermal radio continuum as a function of distance along the major axis. The <u>half power projected radius of the CO emission is only 2!5 corresponding to less than half of the size of the optical disk</u> while the HI extends out to 4!5 to its half power points The CO emission

has a half power size close to that of the nonthermal radio continuum. Strong Population I indicated by molecular clouds and the nonthermal continuum is thus concentrated in the inner galaxy.

In figure 5 the radial distribution of equivalent CO surface integrated intensity, I, is presented for N891 and the Galaxy. The N891 distribution was determined assuming complete axial symmetry from the 11 observations through the disk. No value is given for the center since self shielding by foreground clouds due to the small velocity gradient is apparent. The central dip in figure 4 in HI and CO is probably effected by overlapping clouds along the line of site. Figure 5 clearly shows a strong monotonic decrease in CO surface emission as a function of R, declining by a factor of at least 7 between 3 and 15 Kpc. Since the point at 3 Kpc may be somewhat reduced by self shielding (it falls on the linear part of the rotation law) the factor of 7 is probably a lower limit. A comparison with our galaxy shows N891 to be richer in molecular clouds with no inner edge to the distribution at 3 Kpc. However assuming a closer distance, for N891, of 10 Mpc would shrink the N891 I(R) curve to smaller R bringing it in line with the galaxy at 6 Kpc.

The total mass of molecular hydrogen, H_2, in N891 inferred from the total integrated intensity across the disk is

$$M_{H_2} = 7 \times 10^9 \, M_\odot \, (D/14 \text{ Mpc})^2 \, ,$$

using the conversion factor employed in our paper on M101 (this volume). Sancisi and Allen (1979) find for total atomic H mass

$$M_{HI} = 8 \times 10^9 \, M_\odot \, (D/14 \text{ Mpc})^2 \quad .$$

Thus approximately one half of all ISM in N891 is in the form of H_2 but the two components have completely different radial distributions. The inner half of N891 has an ISM dominated by H_2 and the outer half dominated by HI.

Recent observations of the outer part of our galaxy have led Kutner and Meade (1981) to claim that the total CO surface emission at R ~ 15 Kpc is much greater than expected or found by previous surveys. They ascribe this to warping of the outer plane and increased scale height. It is interesting to note that in NGC 891 where these observations cover the complete plane out to 15 Kpc there is a continuous monotonic decrease in the total CO emission as would be expected from extrapolating the data from the inner 10 or 12 Kpc. Indeed the surprise is that the CO emission from the strong dust lanes in the outer part of the optical disk is very weak. Molecular clouds exist out at large radii but there are less of them, particularly in comparison with HI.

References

Allen, R. J., Baldwin, J. E., Sancisi, R., 1978, A & A 62, 397.

Code, A. D., and Houck, T. E., 1955, Ap.J. 121, 533.

Cohen, R. S. and Thaddeus, P. 1977, Ap.J. Letters 217, 155.

Gordon, M. A. and Burton, W. B. 1976, Ap.J. 208, 346.

Kutner, M. and Meade K., 1981 Preprint submitted to Ap. J.

Osterbrock, D. and Sharpless, S., 1952, Ap. J. 115, 140

Sancisi, R. and Allen, R. J., 1979, A & A 74, 73.

Scoville, N. Z. and Solomon, P. M., 1975, Ap. J. 199, L105.

Solomon, P. M., Sanders, D. B., Scoville, N. Z. 1979, IAU Symposium No. 84, "Large Scale Characteristics of the Galaxy" ed. B. Burton, p. 35.

Solomon, P. M. and Sanders, D. B., 1980, "Giant Molecular Clouds in the Galaxy" eds. P. Solomon and M. Edmunds, Pergamon Press.

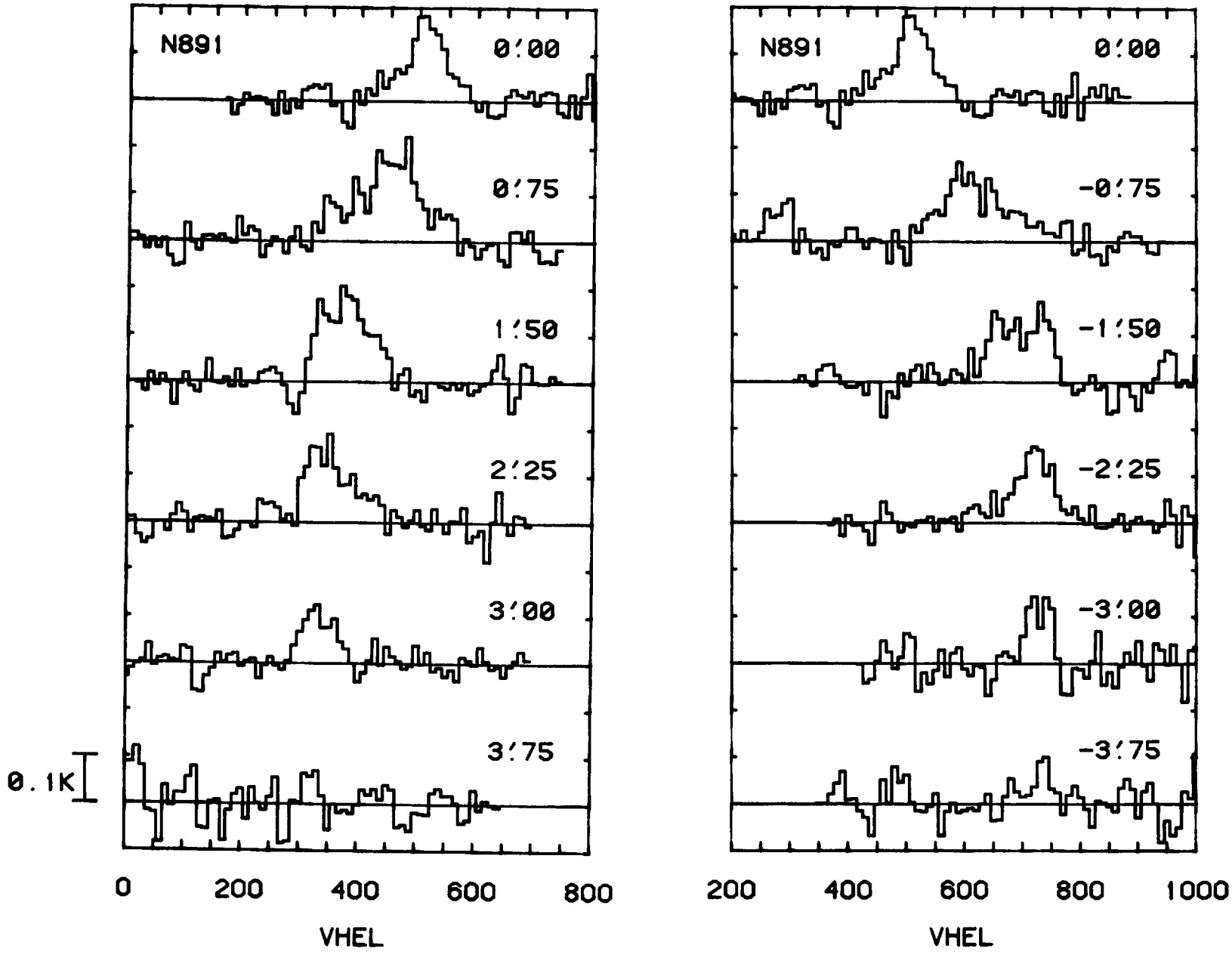

Figure 1. Spectra of CO emission, from NGC 891 along the major axis, obtained with the FCRAO 14 m antenna (HPBW = 50"). Intensities are corrected antenna temperatures T_A^* calibrated with respect to standard sources (e.g. Orion, T_A^* = 60 K).

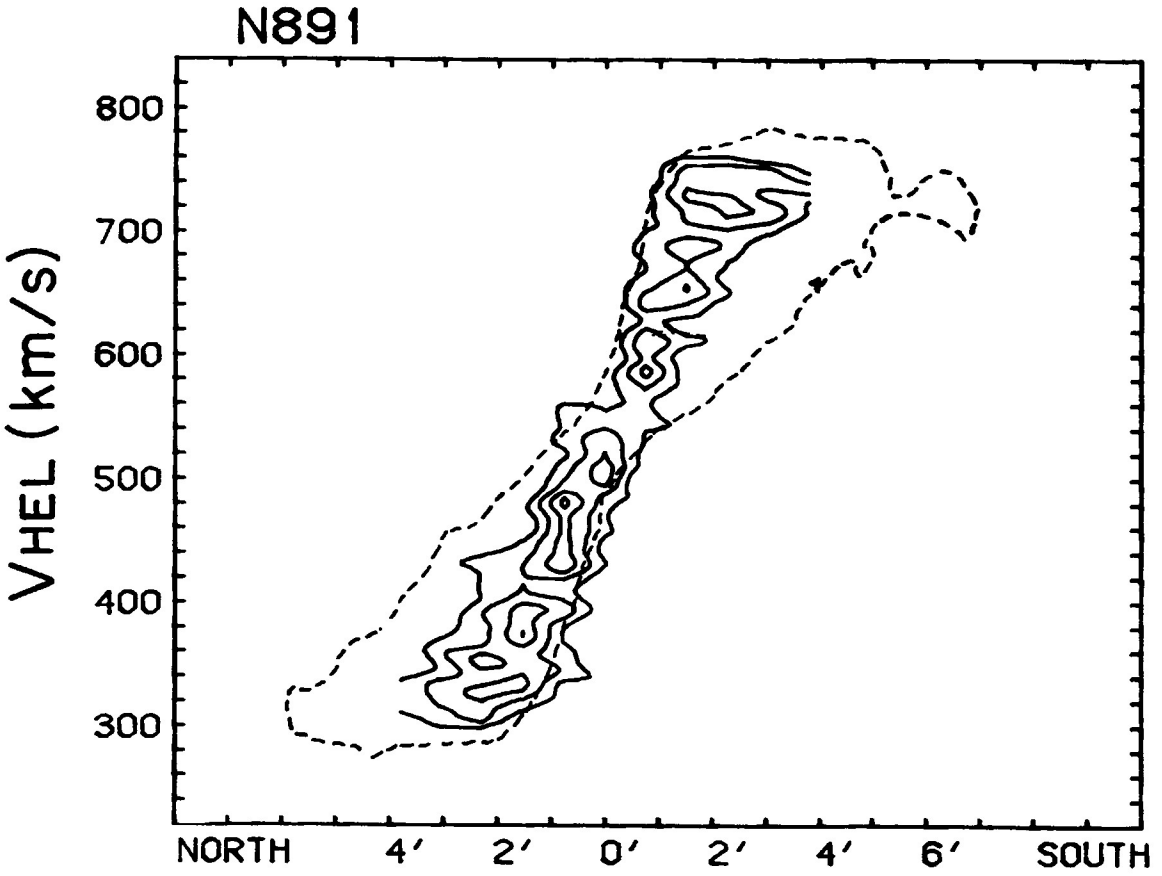

Figure 2. Spatial Velocity Diagram of CO and HI emission in NGC 891. Solid lines are CO emission with contours spaced every .05 K in units of T_A^*. The dashed curve is the HI emission contour at T_b = 8.5 K from Sancisi and Allen (1979). The asymmetry of the CO, compared to the HI, with stronger emission at higher velocity in the South and lower velocity in the North is due to the concentration of molecular clouds in the inner part of the galaxy. The stronger CO emission at each line of sight appears at the radial velocities corresponding to the inner galaxy while the HI is more widely distributed.

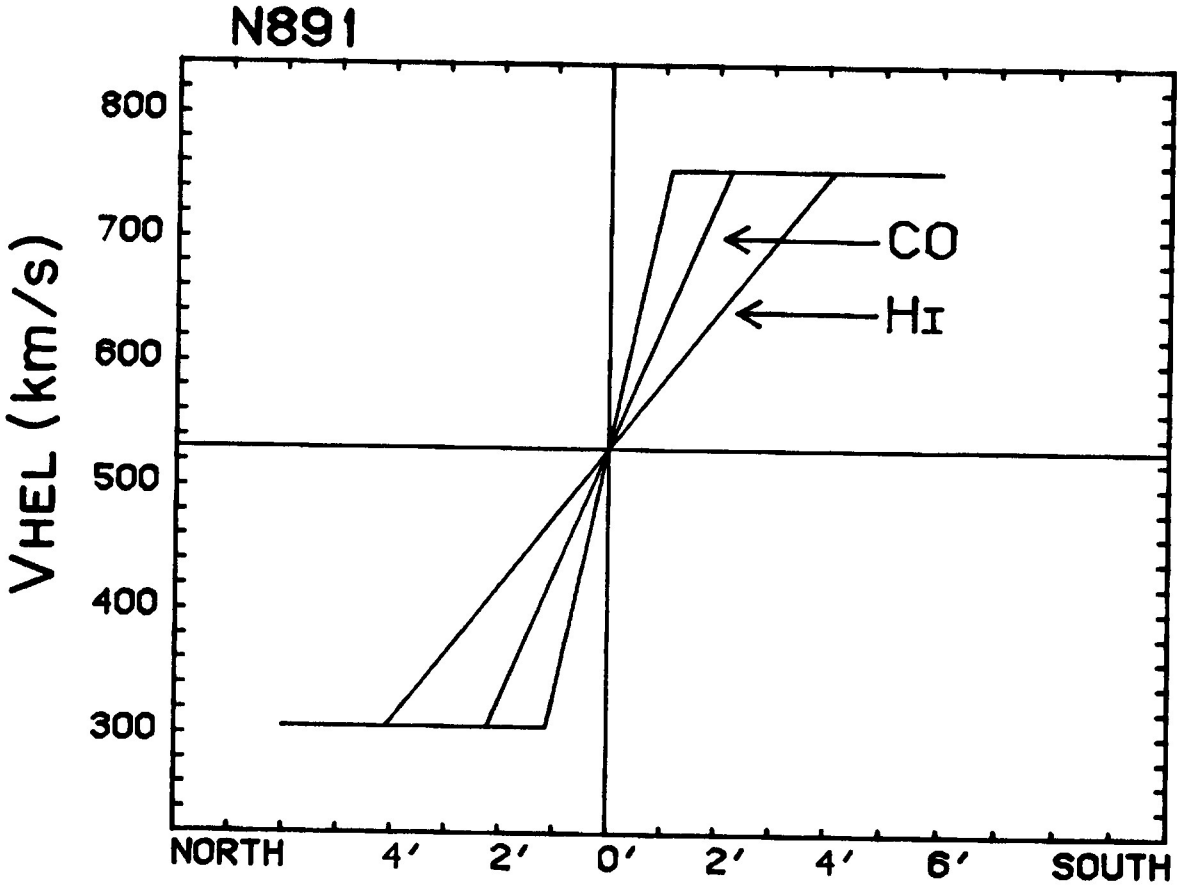

Figure 3. A schematic representation of the velocity along the major axis corresponding to the rotation curve of N891, (see Sancisi and Allen, 1979, for HI data) the axis of peak CO emission and the axis of peak HI emission. The peak CO emission intersects the flat part of the rotation curve at a distance of 2' from the center while the peak HI emission intersects at 4'.

Figure 4. The distribution of CO emission, HI emission and nonthermal radio continuum emission along the major axis of NGC 891. The half power width of the CO is much closer to that of the nonthermal continuum than the HI. Strong population I as indicated by the molecular clouds, nonthermal continuum and far infrared (see Harper, this volume) is thus concentrated in the inner galaxy of N891. Note that the strong CO emission does not continue out to the strong dust lanes in the outer part of the galaxy although weak emission is clearly present. The photograph is from a KPNO 4 meter print.

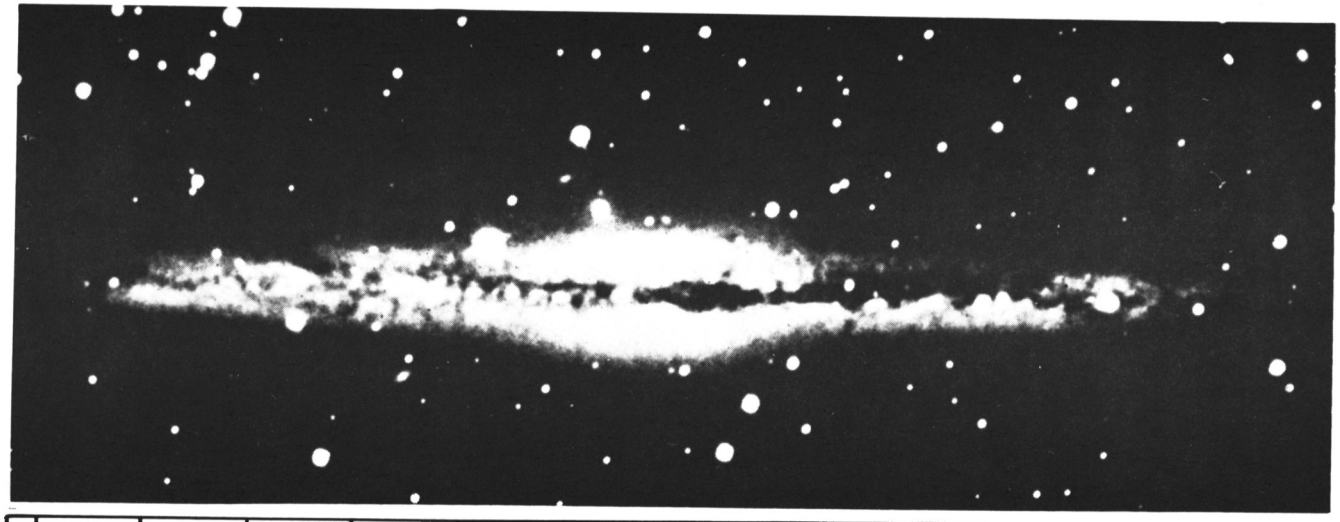

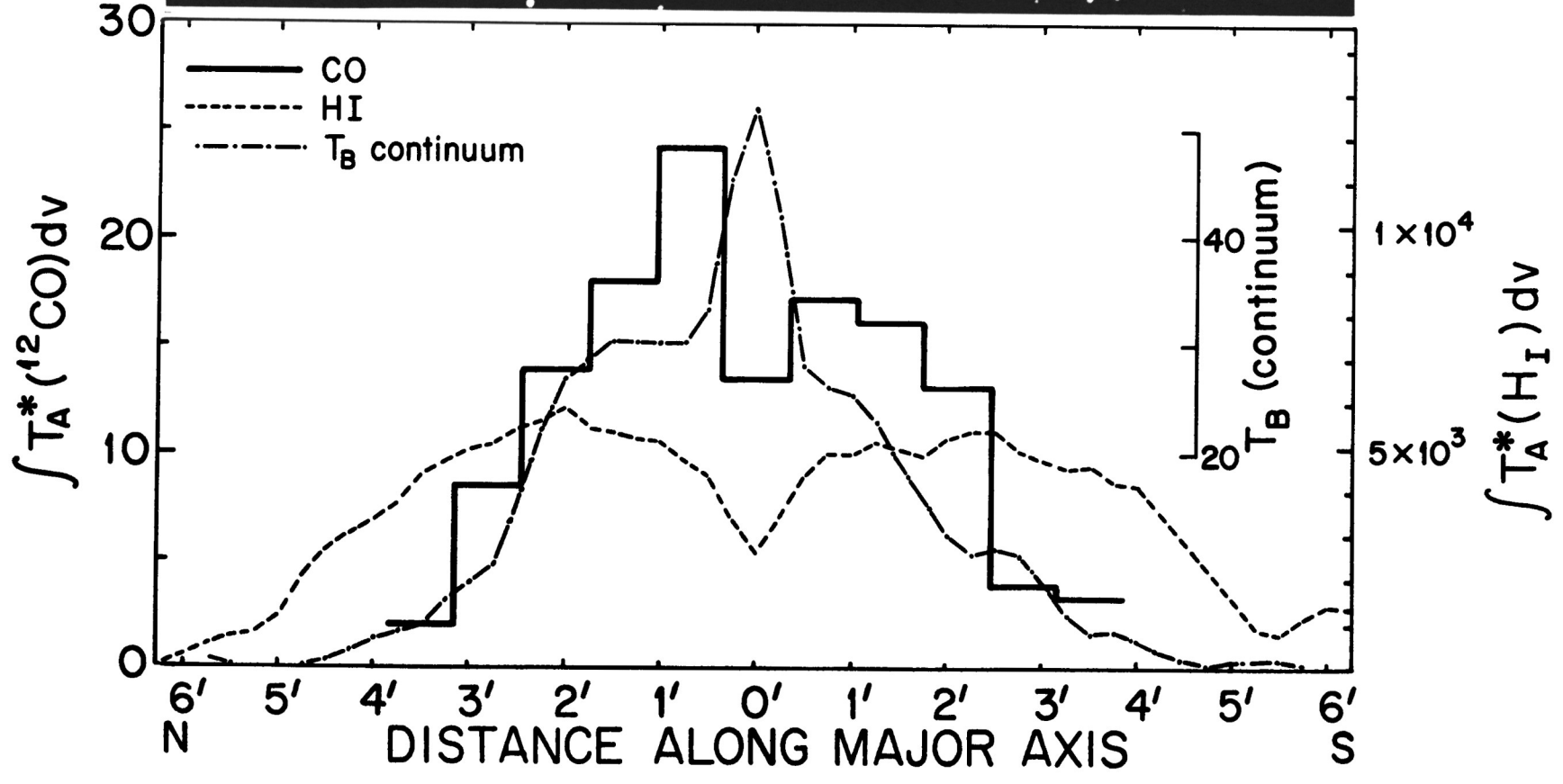
30
20
10
0
CO
HI
T_B continuum
$\int T_A^*(^{12}CO)dv$
40
20
T_B (continuum)
1×10^4
5×10^3
$\int T_A^*(H_I)dv$
6′ 5′ 4′ 3′ 2′ 1′ 0′ 1′ 2′ 3′ 4′ 5′ 6′
N
DISTANCE ALONG MAJOR AXIS
S

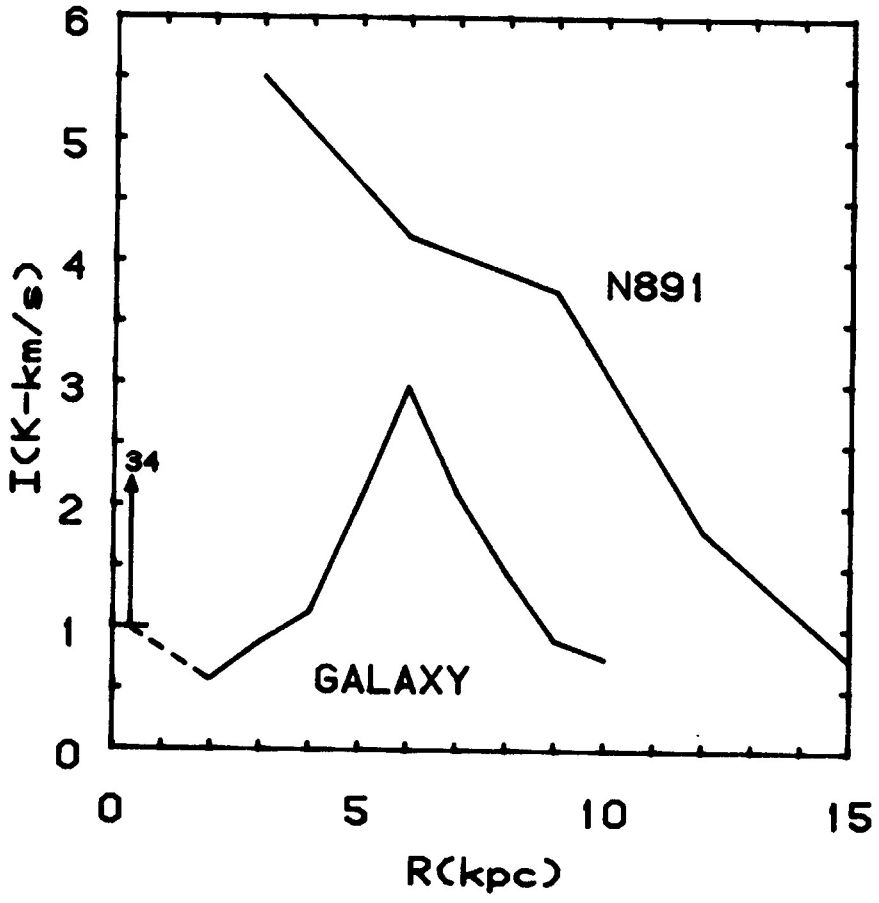

Figure 5. Radial distribution of CO equivalent face on integrated intensity I for N891 and for our Galaxy (see text). The assumed distance for N891 is 14 Mpc, corresponding to H = 50 km/s/Mpc; if a smaller distance is adopted the N891 curve shrinks to smaller radii and the values for I at a given R will more closely match those of the galaxy, although there is no dip at 3 Kpc.

The Molecular Distribution in M51

Nick Scoville

University of Massachusetts, Amherst

CO emission has been mapped (by Judy Young, Steve Lord, and myself) along four strips in M51 using the 14 m FCRAO telescope (HPBW = 50") in order to sample the radial distribution of molecular gas. Sample spectra along the north-south strip (10° from the major axis) are shown in Figure 1. They indicate the overall quality of the data in addition to showing the velocity shifts and systematic intensity decrease with distance away from the nucleus.

The radial variaton of the CO emission is shown in Figure 2 where the integrated intensities observed at each position (▲'s) are plotted as a function of radius. The boxes indicate the mean integrated intensities at each radius. The monotonic falloff in the CO emission with radius is strongly reminiscent of the CO morphology in the in two Scd galaxies IC 342 and NGC 6946 (Young and Scoville 1981 and Young - this symposium). It is markedly different from the distribution in the Milky Way where the CO emissivity is clearly bimodal in radius: here, peaks occur in a ring at R = 4-8 kpc and in the galactic center at R < 400 pc with a deep trough in between (Scoville and Solomon 1975; Burton and Gordon 1978). The significant difference in the molecular distributions of the Milky Way and the two Scd galaxies is the absence of CO emission at R = 1-4 kpc in the former. All three galaxies show similar exponential falloffs at R > 4 kpc and all three show the greatest emission in the nucleus.

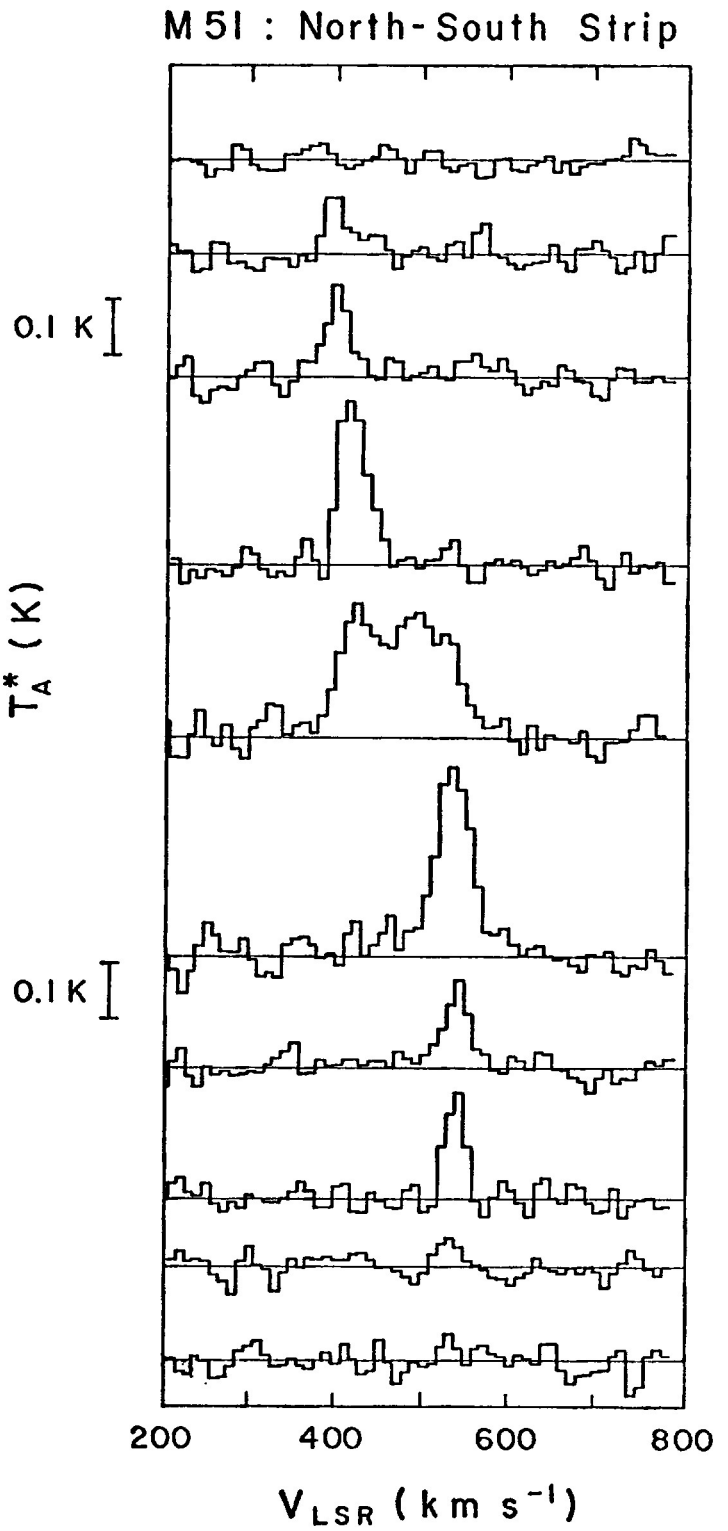

Fig. 1 - Spectra of ^{12}CO J = 1 → 0 taken along the N-S strip crossing the nucleus smoothed to the 10 km s^{-1} resolution. This strip runs within 10° of the major axis. Note the velocity gradient due to galactic rotation and the systematic falloff in intensity with increasing galactic radius.

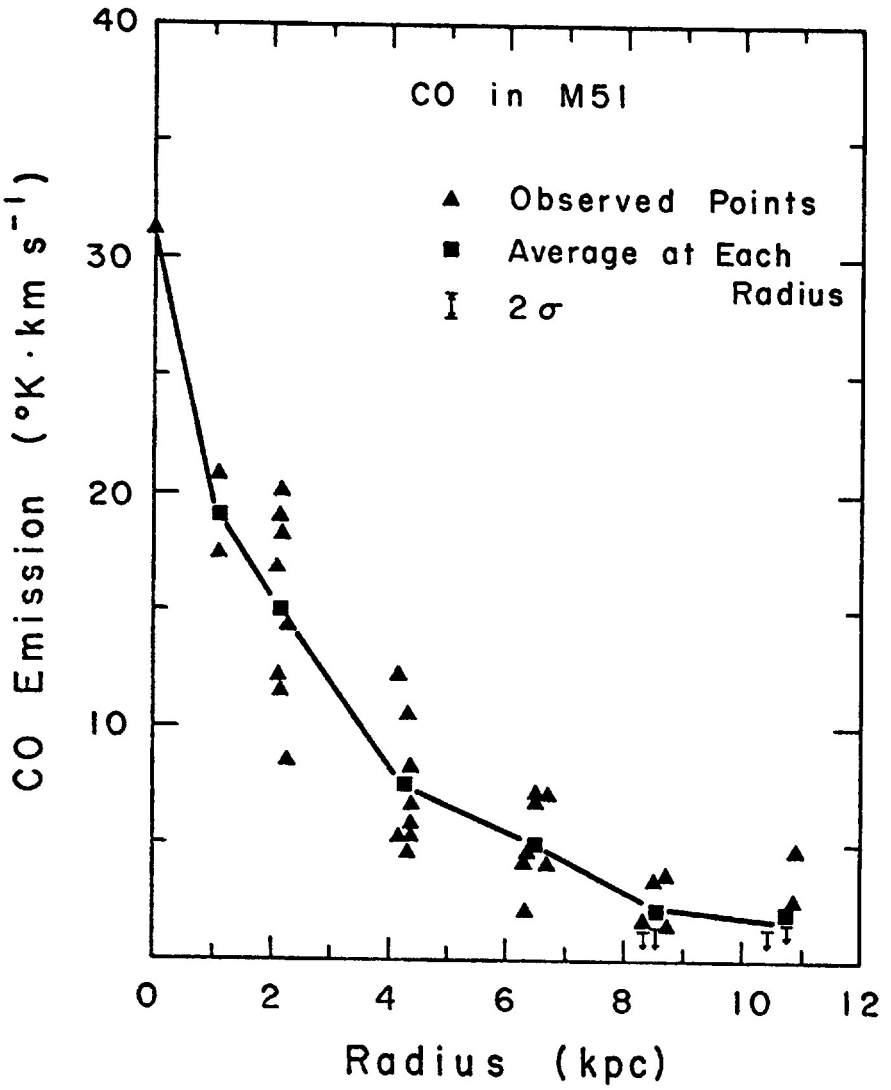

Fig. 2 - The CO integrated line intensities (▲) are plotted as a function of galactic radius at the beam center of the observation. Also shown are the mean intensities (■) for each radial bin and the line connects these mean values.

In deriving H_2 abundances from the CO observations we follow the same procedures employed by Young and Scoville (1981) in analyzing IC 342 and NGC 6946. We assumed a linear relationship exists between the CO line integral and the H_2 column density averaged over the antenna beam. The constant of proportionality in this relationship is estimated from observations of nearby dark nebula (Dickman 1978 and Frerking, Langer, and Wilson 1981) and giant molecular clouds sampled in an unbiased fashion in the inner galactic plane of our own galaxy (Solomon, Sanders, and Scoville 1982). The column densities in those clouds were obtained by three techniques: extinction measurements, ^{13}CO column density measurements, and Virial Theorem analysis. The adopted empirical relation for the column density and mass surface density is $N_{H_2} = 4 \times 10^{20} I \cos i \; H_2 \; cm^{-2}$ where I is the CO intensity integral ($T_A^* \Delta V$) and i is the inclination (20° for M51). The abundance of H_2 (assuming $H_2 \; \alpha$ CO emission) is such that over the entire disk out to R = 10 kpc, 3/4 of the ISM nucleons are in H_2 rather than HI. The radial falloff of H_2 mass surface density (shown in Figure 3) closely follows the disk light distribution (Schweizer 1976), the FIR luminosity (Smith 1981), and the non-thermal radio emission (Mathewson et al. 1972). The form of this falloff is approximately exponential with scale length 4 kpc from R = 1 to 10 kpc. (The radial distribution of HI is flat with a hole in the center of the galaxy). The kinematics of the CO (and Hα) are consistent with a total mass distribution (stars and gas) in the disk of M51 which follows the derived H_2 and optical light "exponential" falloff.

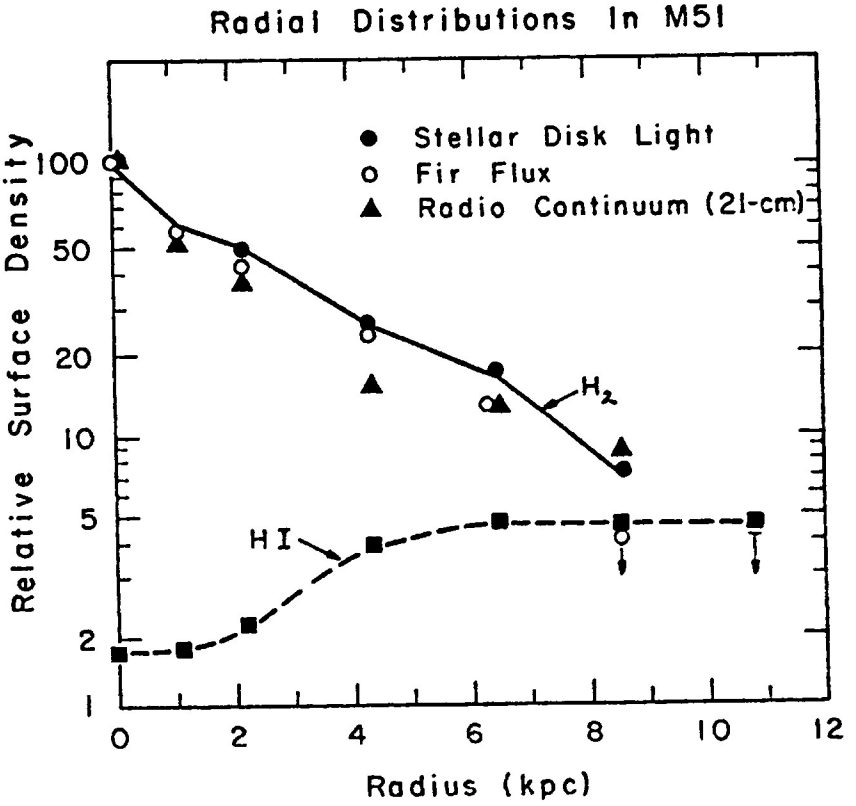

Fig. 3 - The radial distributions of H_2 derived from the CO observations and HI observations of Weliachew and Gottesman (1973) are compared with the disk light distribution (Schweizer 1976) and FIR flux (Smith 1981).

References

Burton, W.B., and Gordon, M.A. 1978, Astr.Ap., 63, 7.

Dickman, R.L. 1978, Ap.J.Suppl., 37, 107.

Frerking, M., Langer, W.L., and Wilson, R.W. 1981 (preprint).

Mathewson, D.S., van der Kruit, P.C., and Brouw, W.N. 1972, Astr.Ap., 17, 468.

Scoville, N.Z., and Solomon, P.M. 1975, Ap.J.(Letters), 199, L105.

Schweizer, F. 1977, Ap.J., 211, 324.

Smith, J. 1981, preprint.

Solomon, P.M., Sanders, D.B., and Scoville, N. 1982, (in preparation).

Young, J., and Scoville, N. 1981, submitted to Ap.J.

CO Observations of NGC 3628

Linda Tacconi and Judy Young
University of Massachusetts, Amherst

CO emission was mapped in the edge-on Sb/Sc galaxy NGC 3628 with the 14-m antenna of the FCRAO (HPBW = 50"). This galaxy is a member of the Leo Triplet, which also includes NGC 3623 (Sa) and NGC 3627 (Sb). Optical and HI observations indicate the presence of a plume extending 100 kpc from the eastern tip of NGC 3628 (Kormendy and Bahcall 1974; Rots 1978; Haynes, Giovanelli and Roberts 1979) which is believed to have been caused by the close passage of NGC 3627 to NGC 3628 (Toomre and Toomre 1972; Rots 1978).

The spectra observed at 9 positions in NGC 3628 are shown in Figure 1; the observations are spaced by 45" which corresponds to 1.5 kpc at a distance of 6.7 Mpc. The CO intensities and kinematics are asymmetric with respect to the nucleus, where the emission is strongest. The average CO radial distribution falls off smoothly with radius (Figure 2) to where it is undetectable 6 kpc from the nucleus. We have modeled the emission from the Milky Way viewed edge-on at a distance of 6.7 Mpc, which is plotted in Figure 2 for comparison. The CO distribution in NGC 3628 is distinctly different from a molecular ring like that in our Galaxy viewed edge-on.

HI observations of NGC 3628 with 3' resolution (Haynes et al. 1979) indicate the rotation curve with 6 kpc resolution out to 18 kpc; our CO observations fill in the inner 5 kpc of the HI rotation curve, as shown in Figure 3. Asymmetries with respect to the systemic velocity are present in both CO and HI. Another comparison of CO and HI velocities has been made by adding up all of the CO observations and comparing this total profile with Rots' HI pro-

file for the entire galaxy. The CO and HI velocity widths are identical (see Figure 4), indicating that the CO extends out to where the rotation curve becomes flat; the shapes differ greatly, indicating that the CO is centrally peaked while the HI extends out to larger radii. Using the CO to H_2 conversion derived by Young and Scoville (1981, and in this symposium), $N_{H_2} = 4 \times 10^{20} I_{CO}$ where I_{CO} is the CO intensity integral, we find that the surface density of H_2 is 10 times higher than HI towards the center of the galaxy. The lower limit to the mass in H_2 observed out to a radius of 4 kpc is $10^9 M_\odot$.

We have also mapped NGC 3623 in 6 positions and NGC 3627 in 7 positions.

References

Haynes, M.P., Giovanelli, R., and Roberts, M.S. 1979, Ap.J., 229, 83.

Kormendy, J. and Bahcall, J.N. 1974, A.J., 79, 671.

Rots, A.H. 1978, A.J., 83, 219.

Toomre, A. and Toomre, J. 1972, Ap.J., 178, 623.

Young, J.S. and Scoville, N.Z. 1981, Ap.J., submitted.

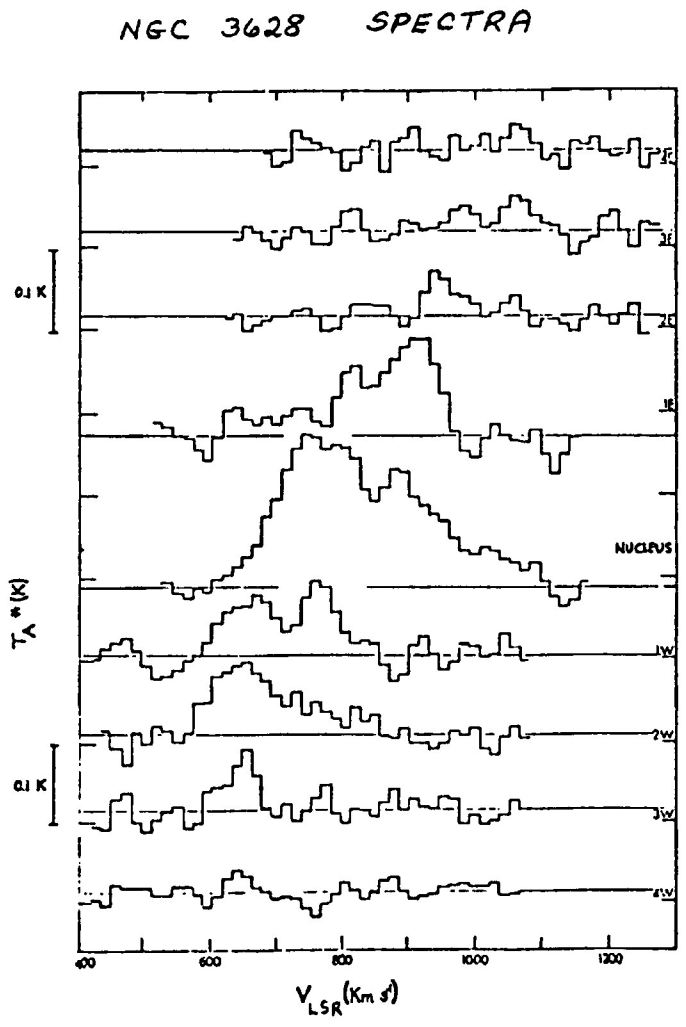

Figure 1. Spectra at nine positions in NGC 3628 smoothed to 20 km/s. At a distance of 6.7 Mpc each observation corresponds to 1.5 kpc on the galaxy. Velocities and intensities are asymmetric with respect to the nucleus.

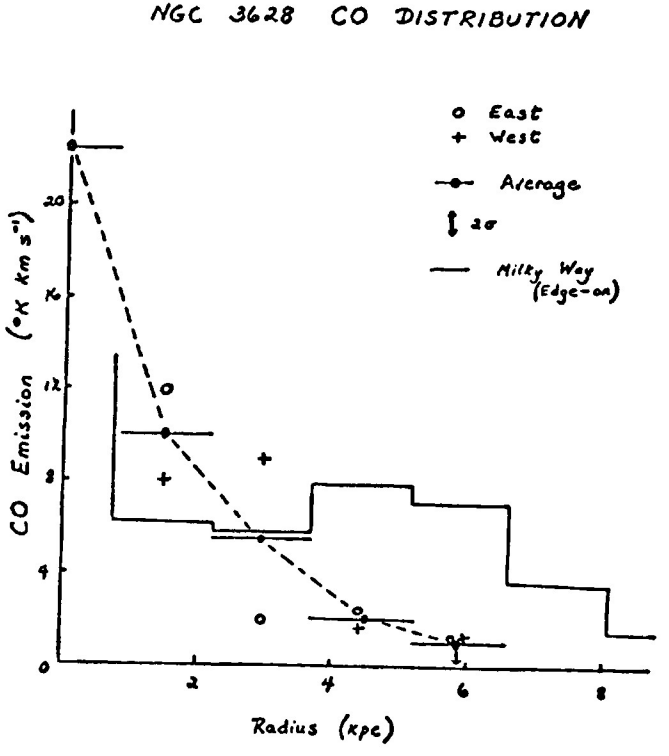

Figure 2. CO radial distribution in NGC 3628. The average intensity (dashed line) falls off smoothly with radius, while the Milky Way viewed edge-on (solid line) would appear distinctly different.

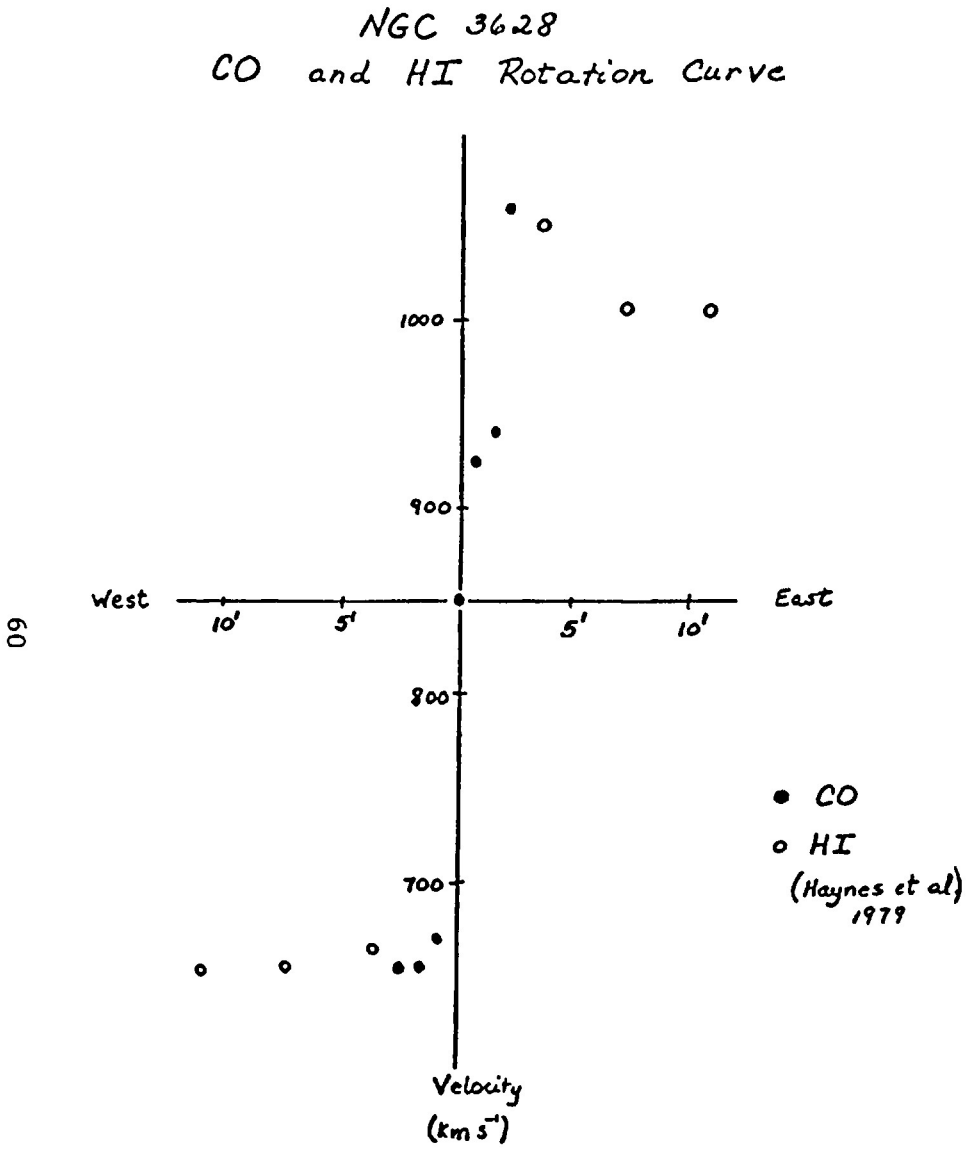

Figure 3. Rotation curve. The CO observations with 50" resolution out to 5 kpc in radius fill in the inner portion of the HI rotation curve (Haynes et al. 1979) with 3' resolution. HI and CO velocities are asymmetric with respect to nucleus.

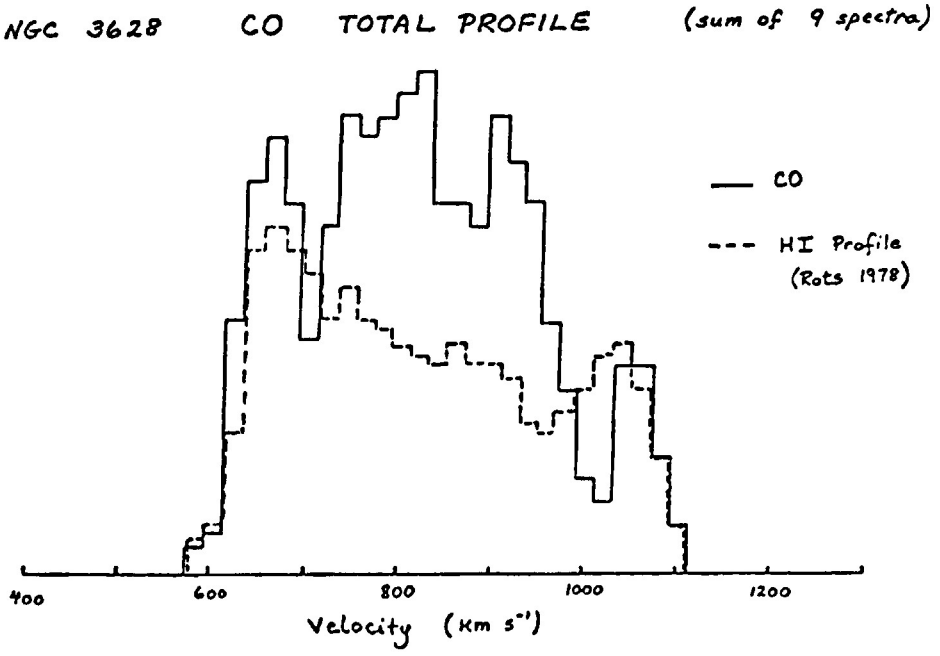

Figure 4. Sum of all CO spectra compared with HI (Rots 1978) smoothed to 20 km/s. The similar widths indicate that the CO extends out to where the rotation curve is flat. The different profile shapes result from the different beamsizes and the differences in the CO and HI distributions: the CO is centrally peaked while the HI extends out to larger radii.

CO Emission and the Optical Disk in the Giant Sc Galaxy M101

P. M. Solomon
Astronomy Program, SUNY Stony Brook, N.Y. 11794

The giant SC I galaxy M101 is one of the largest and nearest face on late type spirals. The distribution of HI emission (Allen and Goss 1979 and references therein) and optical surface brightness (Okamura et al. 1976, Schweizer 1976) in the disk of M101 have been thoroughly observed. The HI emission is found to be strongest and approximately constant at galactocentric radii from 6 to 19 kpc with a sharp dip in the inner 6 kpc to 1/3 of the peak and a long tail out to 50 kpc. The central 6 kpc are clearly deficient in atomic hydrogen. The deficiency of atomic hydrogen in the M101 inner disk can be interpreted as indicating a true gas deficiency or a region of the galaxy where most of the gas is in molecular form. The optical surface brightness of the disk has a standard exponential falloff with radius, characteristic of Freeman disks, with a larger than average scale length of 5.4 kpc (D = 7.2 Mpc).

In this paper* we present observations of emission from 40 locations in M101 and compare the radial dependence of CO surface emission with the optical light and the HI deduced from 21 cm. We find that the CO emission and hence the interstellar molecular clouds follow the optical surface brightness of the disk in marked contrast to the atomic hydrogen. The dense star forming molecular clouds have a radial distribution which fits an exponential disk

*A full report of this work has been submitted to the Ap.J. by P. Solomon, J. Barrett, D. Sanders and R. deZafra.

determined from optical surface brightness.

Observations

The CO data was obtained primarily at the NRAO 36 foot antenna in 4 observing sessions in late 1979 and 1980. All intensities are calibrated with reference to standard sources (Ulich and Haas 1976). Figure 1 shows some sample spectra from positions in M101 near the major axis. M101 is a moderate CO emitter with the central integrated intensity about 1/3 that of M51. The inner 4' in radius (R ~ 8 kpc) of the galaxy was mapped with 1 arc minute spacing over 2/3 of the disk and 5 observations were made between R = 9 and 12 kpc. Figure 2 shows a spatial velocity map near the major axis.

Figure 3 shows the CO integrated intensity I as a function of galactocentric radius in M101. All of the strongest emission was from the central 6 kpc although weak emission was found in one of the points at 12 kpc. The general trend of increasing I with decreasing R is obvious; however there is a great deal of realscatter which shows a contrast as high as a factor of 3 between points at the same R. Of the 40 positions observed 25 have definite signals. Blitz et al. (1981) have reported detection of CO from 1 out of 5 locations centered in H II regions in the outer galaxy and argued that the 1 location at R ~ 9 kpc with a detection is an outstanding giant molecular cloud complex. The integrated intensity found by Blitz et al. in the 1 detected H II region of the outer galaxy is only about 1 K·km s^{-1}, significantly lower than 21 positions we have observed and five times weaker than the strongest point in figure 3. Clearly the outer galaxy in M101 is weak in CO emission and an attempt to determine the molecular content of a galaxy by concentrating observations in the outer parts is completely misleading.

Comparison of Molecular Cloud Distribution with the Optical Disk

In figure 4 we present the average CO integrated intensity as a function of radius on a semi-log plot. All 40 observations have been employed in determining the radial distribution. While there is widespread scatter amongst individual points, the mean I shows a clear decrease with radius declining about a factor of 8 from the innermost point at the center to 12 kiloparsecs. The solid line is the optical surface brightness of the disk at Blue wavelength; the optical surface brightness at longer wavelength shows a very similar dependence on R. There is clearly a very strong correlation between the CO emission and the exponential fall off of the optical disk. The scale length of the CO emission is the same as the optical light to within the errors of the determination of $\pm$ 1 kpc. While the CO data alone does not cover a sufficient range of R to rule out a power law or other form for the radial dependence of I, the close correspondence with the optical exponential disk strongly points to an exponential fall off for the CO emission.

Comparison of CO emission with HI and with the Galaxy

Figure 5 shows the average CO integrated intensity in M101 compared with that of the Galaxy, which has been determined (using the Stony Brook-Massachusetts survey of the galaxy, see Sanders 1981) from mean CO emissivity at the peak of the Z distribution and scale height as a function of R. The curve in figure 5 labeled Galaxy thus shows what the galactic radial dependence of CO emission would look like if observed face on from the outside. The mean CO surface brightness indicated by I is similar to M101 at

about R ~ 5 kpc but the shape of the distribution is clearly different. There is no inner edge at 3 or 4 kpc to the molecular cloud distribution in the disk of M101 and the center of the galaxy at a resolution of 1 kpc in radius is stronger than M101.

The surface density of molecular hydrogen has been determined from the CO surface brightness using a conversion factor of (see Sanders 1981)

$$N_{H_2} = 3.6 \times 10^{20} \int T_A^* \, dv \quad (cm^{-2})$$

Figure 6 shows a comparison between the HI and H_2 surface density. It is clear that in the inner galaxy (R < 6 kpc) the interstellar medium is predominantly in the form of molecular hydrogen; this will remain true even if the conversion factor above is decreased by a factor of 2 or more. There is no deficiency of interstellar matter in the inner disk as found from HI measurements.

The close correspondence between the optical surface brightness and the CO surface brightness is perhaps the most interesting result of these observations. The U-B, B-V colors of the M101 disk indicate that the light is primarily from A to F stars. These have ages of the order of $1\text{-}2 \times 10^9$ years. Thus the similarity between the radial dependence of the light and CO emission could be understood if the average star formation rate on this timescale is proportional to the first power of the <u>average</u> molecular density. HI by itself is thus a very poor indicator of the true distribution of the ISM in a galaxy and models of galactic evolution need to be reconsidered in light of the molecular interstellar medium.

References

Allen, R. J. and Goss, W. M., 1979 A. and A. Suppl. 36, 136.

Blitz, L., Israel, F. F., Neugeabuer, G., Gatly. I., Lee, T. J., Beattie, D. H. 1981, Ap.J. 249, 76.

Okamura, S., Kanazawa, T., Kudaira, K., 1976, PASJ 28, 329.

Sanders, D. B. 1981, Ph.D. thesis SUNY, Stony Brook.

Schweizer, F., 1976 Ap. J. Suppl. 31, 313.

Ulich, B. L., and Haas, R. W. 1976 Ap. J. Suppl. 30 247.

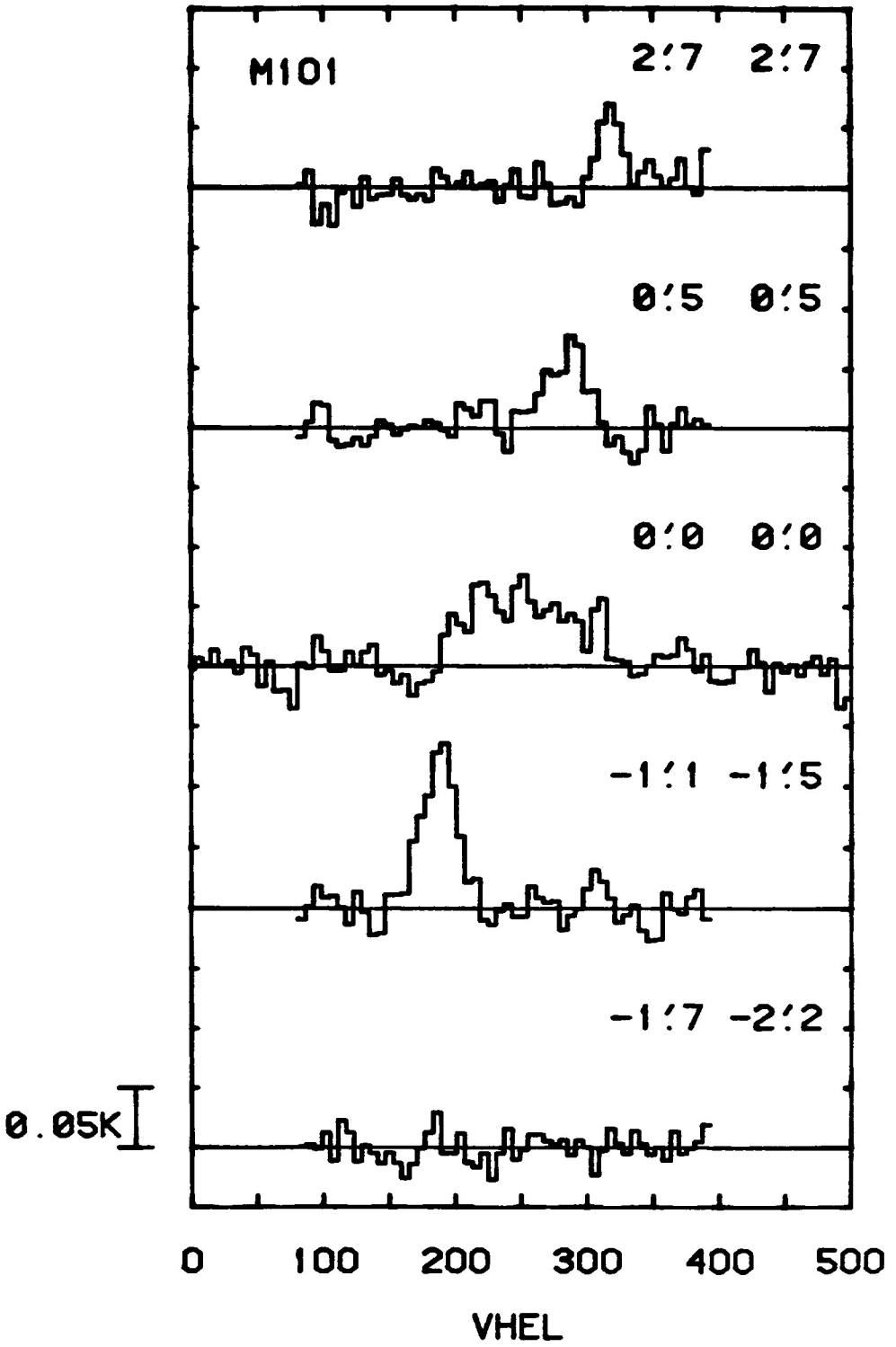

Figure 1. Sample CO emission spectra from positions near the major axis. Intensities are antenna temperature T_A^* with the NRAO 36 foot antenna. Calibration is with respect to standard CO sources (e.g. Orion, $T_A^* = 60$ K). Spectra were smoothed to a resolution of 8 km s^{-1} and replotted every 6 km s^{-1}. Although the highest integrated intensity is from the center of the galaxy, there are several locations including -1!1, -1!5 with stronger peak emission and with only slightly lower integrated intensity.

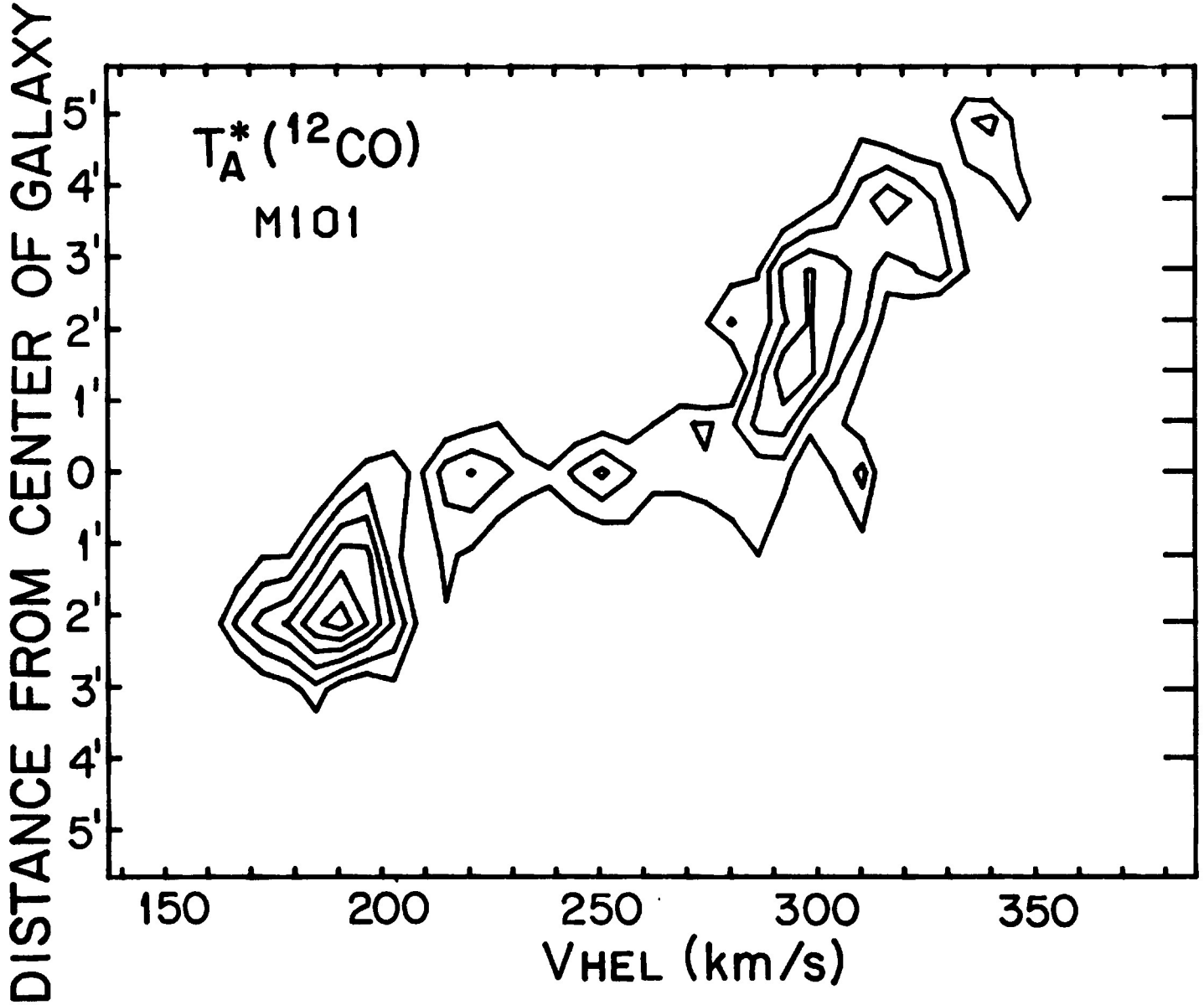

Figure 2. Spatial velocity diagram of CO emission along a position angle of 38^{o} close to the major axis. Contour levels spaced equally in T_A^* every 25 millikelvin.

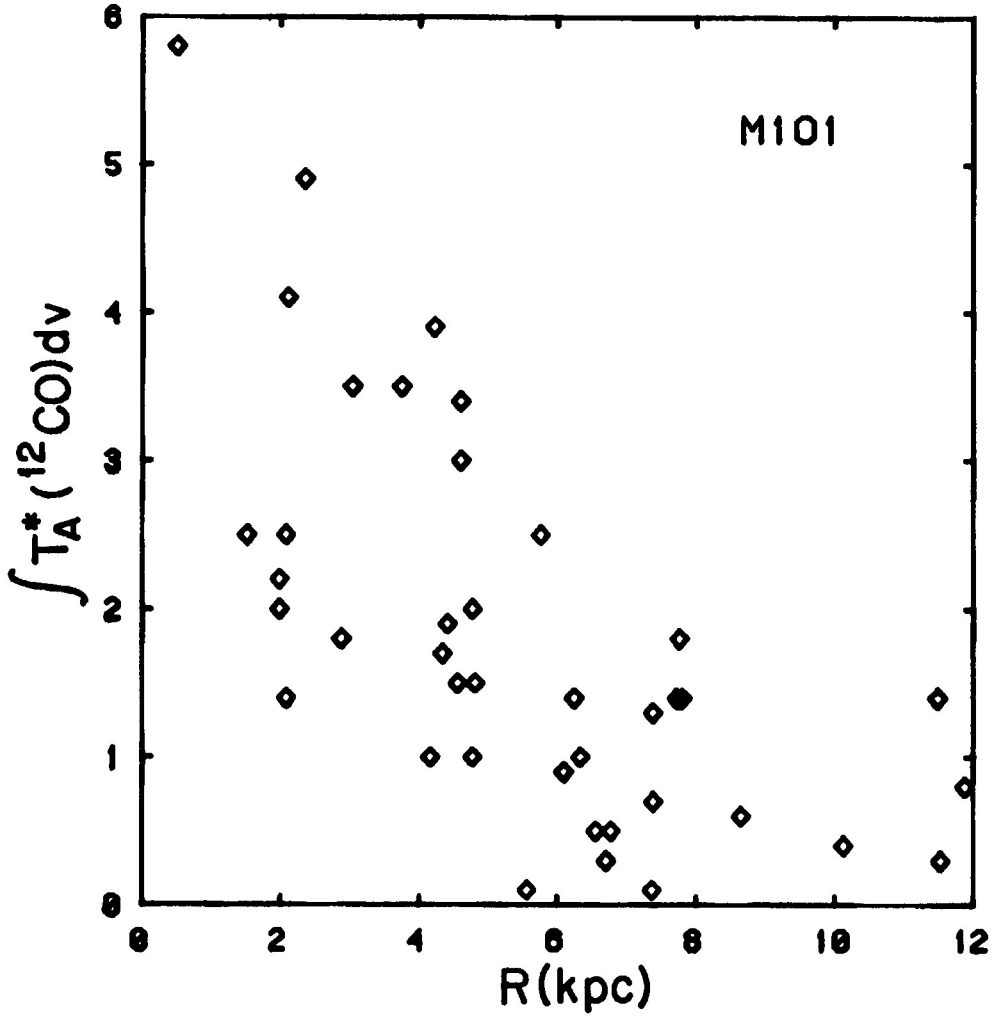

Figure 3. Integrated intensity as a function of galactocentric distance (D = 7.2 Mpc) for 40 locations in M101. The noise level in individual points varies but is generally around $\pm$ 0.5 K·km s^{-1}. Note the large scatter at fixed R which is above the noise and is due to non-axisymmetric structure. In all cases the velocity range for measuring $\int T_A^*$ dv was determined from HI data.

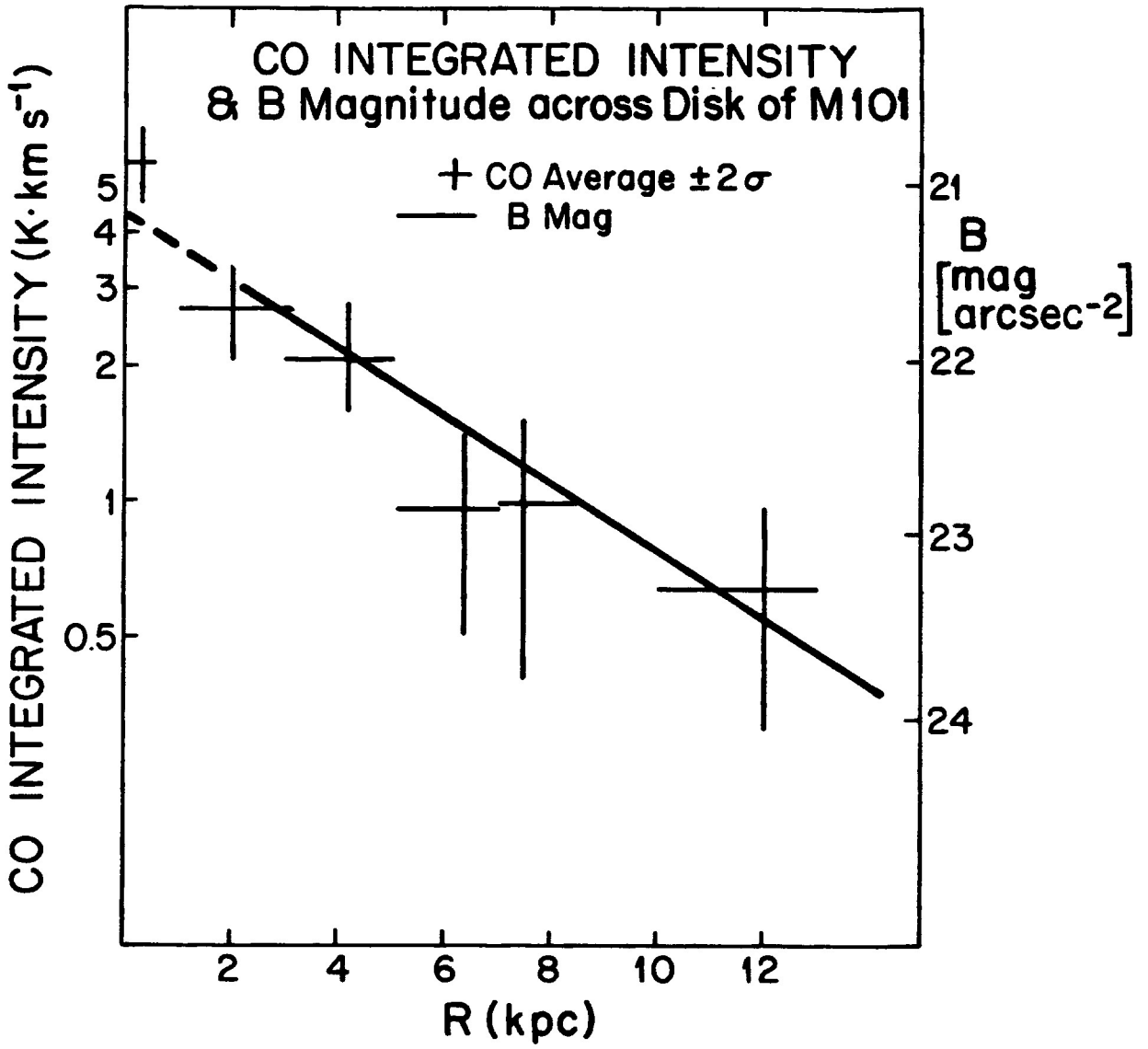

Figure 4. Comparison of CO surface brightness and optical surface brightness for M101 as a function of galactocentric distance. The optical brightness includes disk + arms but is primarily disk light (Schweizer 1976). The data have been normalized at R = 4 kpc. The dashed line is the disk component of the light extrapolated into the center.

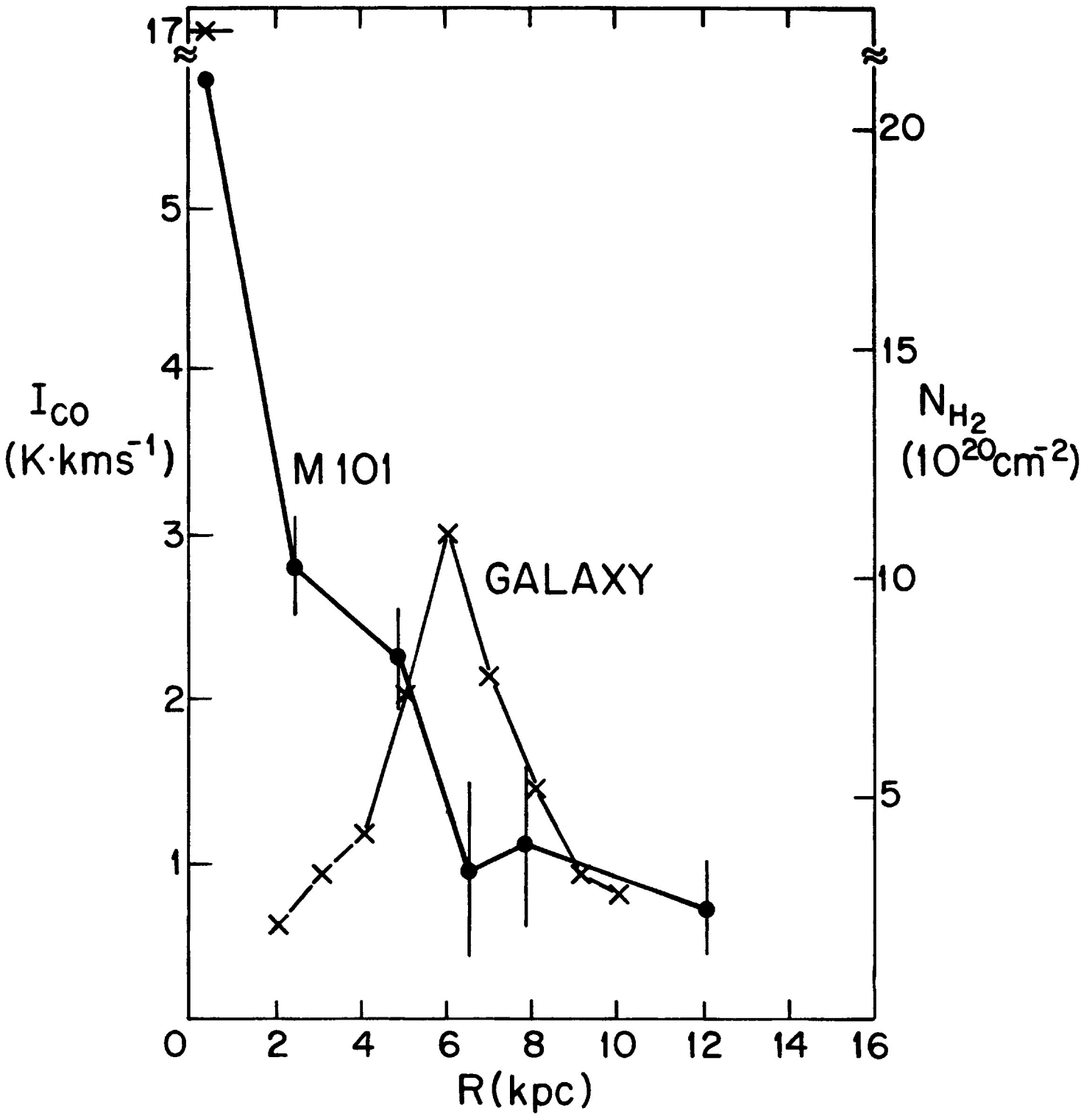

Figure 5. Radial averaged CO integrated intensity I, in M101 compared with that of the galaxy if viewed face on. The error bars represent two standard deviations of the mean; the true dispersion can be seen from figure 3. The innermost point in M101 is plotted at the effective radius of the 1 arc minute beam and is uncertain by about 1 K·km s^{-1}due to the broad shallow line and baseline uncertainty. The equivalent face on intensity for the Galaxy is obtained from the Stony Brook-Massachusetts galactic CO survey.

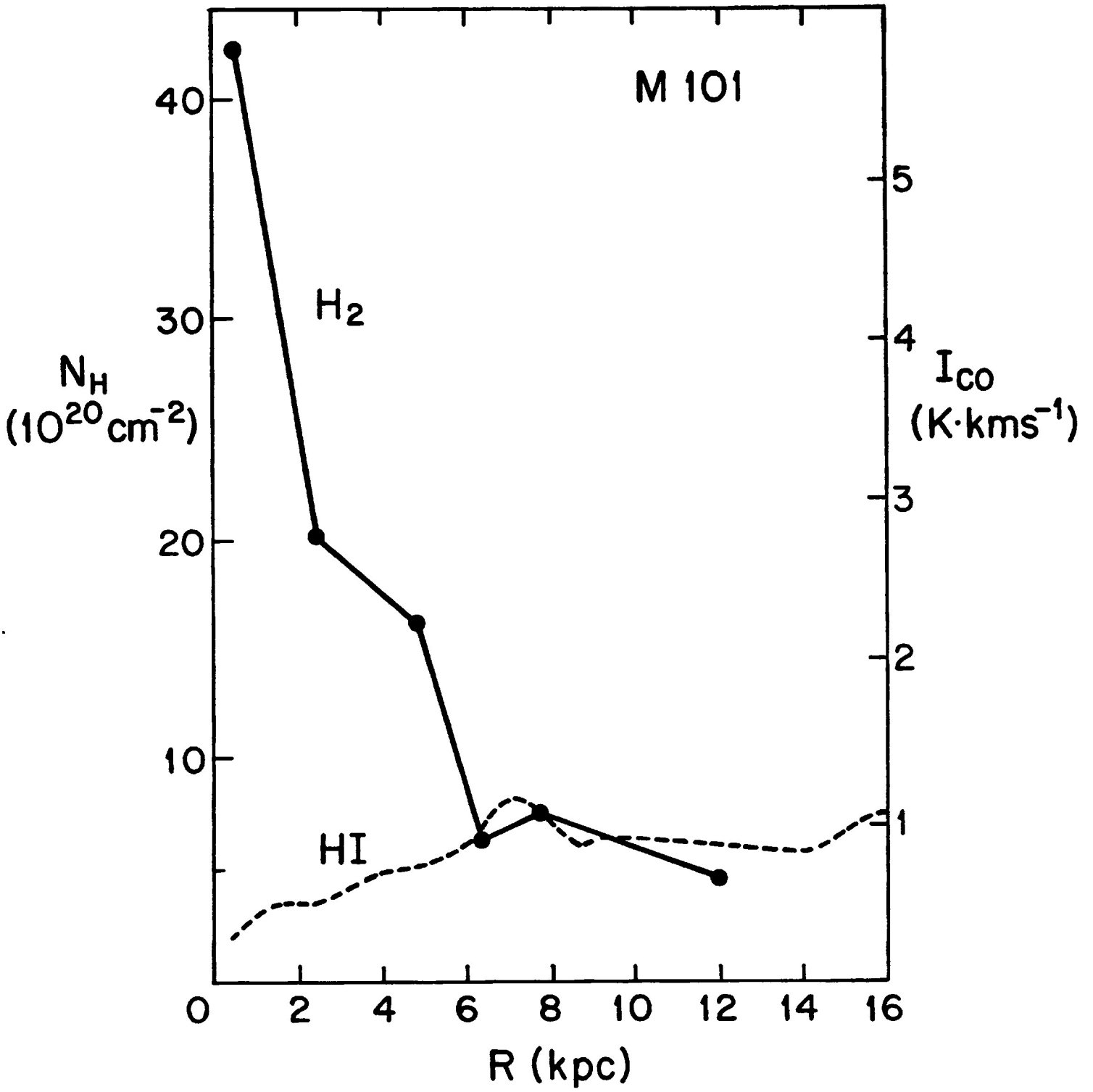

Figure 6. The surface density of interstellar hydrogen in units of equivalent atoms per cm^2 in the form of HI and H_2. The HI surface density is from the Westerbork survey and the H_2 is from these 40 observations scaled as discussed in the text. Inside of R = 6 kpc the interstellar medium is predominantly H_2.

NEW OBSERVATIONS OF CO IN CENTRAL SOURCES

L. J Rickard (Howard University), Patrick Palmer (Univ. Chicago), and
B E. Turner (NRAO)

We report four hitherto unpublished detections of CO emission seen toward the central regions of the late-type galaxies NGC 660, 3504, 3628, and 4303. Details of these results are being prepared for publication. Spectra follow (figures 1a-d).

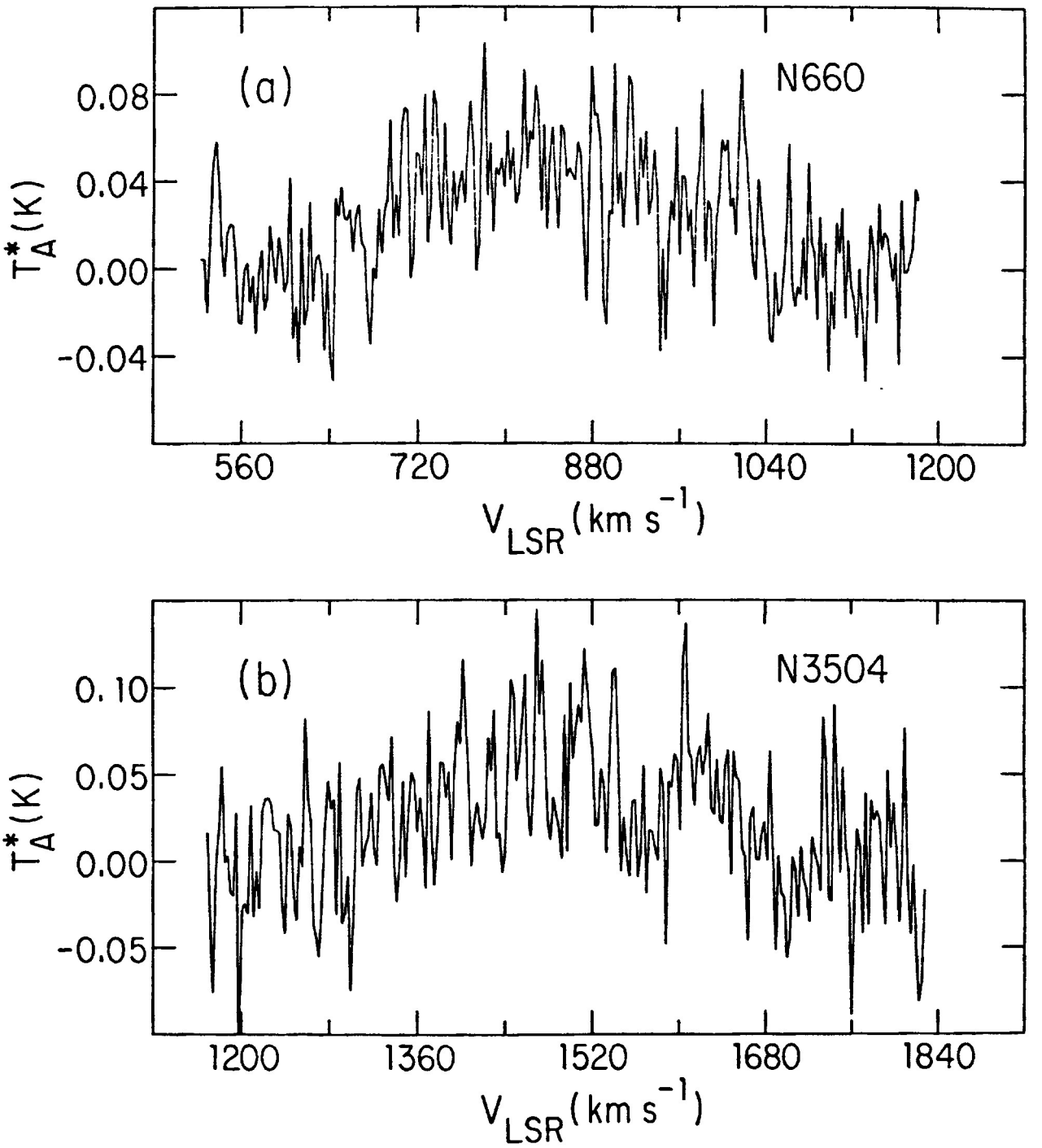
(a)
N660
0.08
0.04
0.00
-0.04
$T_A^*(K)$
560
720
880
1040
1200
$V_{LSR}(km\ s^{-1})$
(b)
N3504
0.10
0.05
0.00
-0.05
$T_A^*(K)$
1200
1360
1520
1680
1840
$V_{LSR}(km\ s^{-1})$

Figure 1

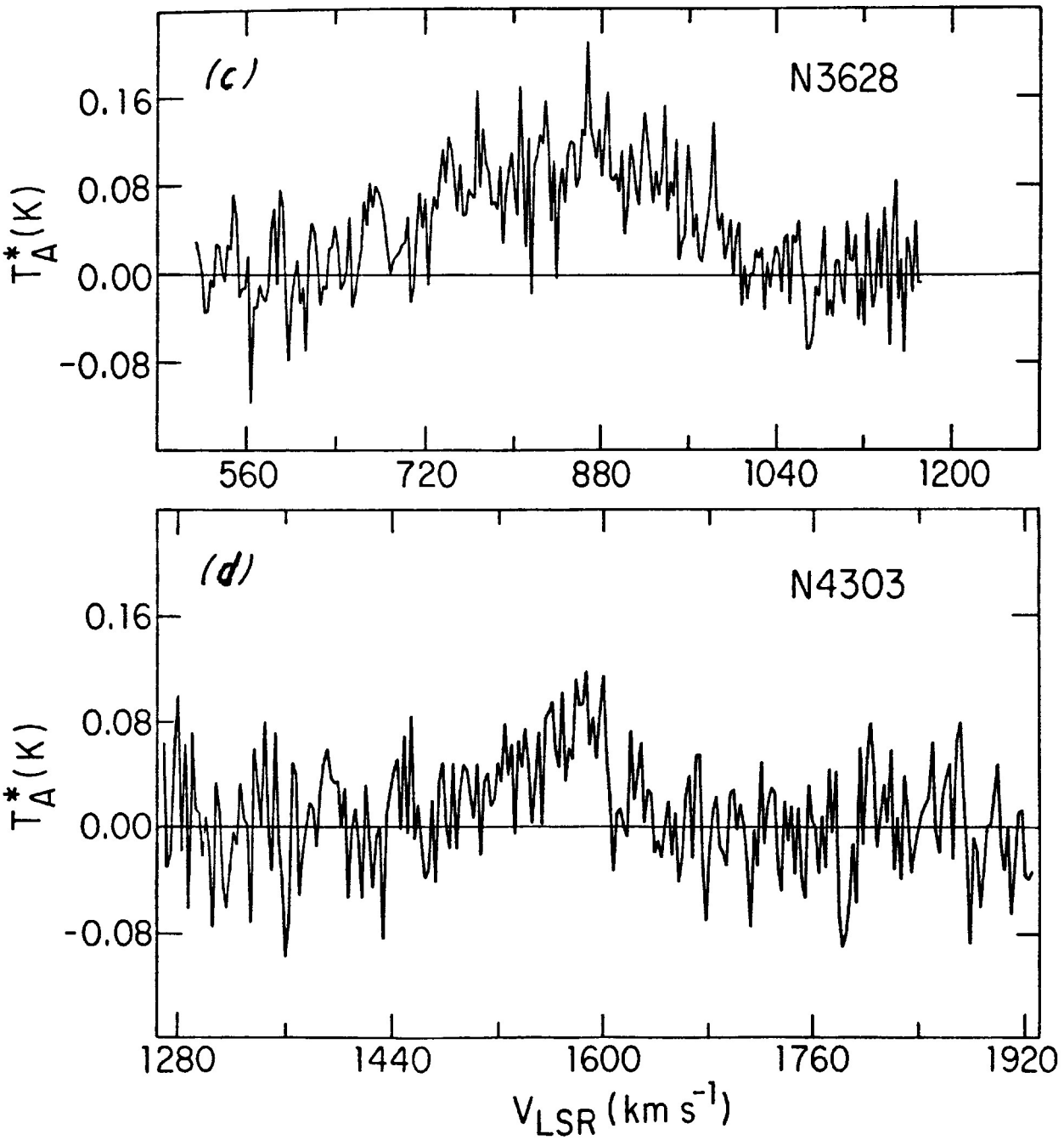

Figure 1 - Continued

Peculiarities of the CO Emission from M82

A. A. Stark
Bell Laboratories
Crawford Hill Laboratory
Holmdel, N.J. 07733

The galaxy M82 has been known to be anomalous in its CO emission ever since the first observations (Rickard et al. 1975; Solomon and deZafra 1975) showed a line of unusual strength. The initial interpretation was that the molecular material in M82 is organized into giant molecular clouds like those in the Galaxy - only there were an enormous number of them, resulting in a very large molecular mass ($\gtrsim 10^{9.5} M_\odot$). This idea seemed to be borne out by the detection of HCN and HCO^+ (Rickard et al. 1977b; Stark and Wolff 1979) in proportions similar to Galactic molecular clouds. Observations of the CO 2->1 line (Knapp et al. 1980; Lo, this symposium) were discrepant, however; M82 was found to be optically thin in CO at the systemic velocity. This suggests the possibility that the bright line originates in a relatively small amount of material arranged in small clumps or in a thin shell, so that the mean column density in molecules is small, while the beam filling factor is fairly large (Knapp et al. 1980). Observations presented here will support this picture: ^{12}CO

J=2->1 and J=1->0 lines which are consistent with previous observations, CO isotope lines which are also consistent with optical thinness, and mapping data which suggests that molecular emission is not confined to the stellar disk of M82 but is associated with the dusty filaments which lie above and below it.

These observations were made in the winter of 1978-79, using the Bell Laboratories 7-meter antenna. Some of the data have been published previously in Stark and Wolff (1979). The observing method and equipment was the same as reported therein, except the front ends used were Richard Linke's cooled WR-8 receiver and Eric Carlson's WR-4 receiver. The J=2→1 observations were made in collaboration with Eric Carlson.

Figures 1, 2, 3, and 4 are spectra at the central position ($\alpha_{1950} = 9^n51^m42^s$, $\delta_{1950} = 69^o\ 54'\ 56''$) of ^{12}CO J=1→0, ^{12}CO J=2→1, ^{13}CO J=1→0 and $C^{18}O$ J=1→0, respectively. These spectra are uncorrected for beam efficiency, which is $\gtrsim$ 90% for the J=1→0 transitions and ~ 45% for the J=2→1 transition. Comparison of the ^{12}CO J=2→1 and J=1→0 spectra shows that at the line peak, the uncorrected J=2→1 line is considerably brighter than the J=1→0 spectrum. The relative beam efficiency corrects the J=2→1 line up by about a factor of 2, while the beam dilution effects (estimated from a small J=2→1 map which

covers the J=1→0 beam) should correct the J=1->0 spectrum upward by a similar factor, yielding a line ratio within a 50" beam of about 2:1. This is consistent with a low optical depth.

The strengths of the isotopic lines of CO are also consistent with a fairly thin ^{12}CO line. The ratio of integrated line strengths $^{13}CO/C^{18}O$ is 4.5 ± 1, roughly the terrestrial value, implying that the ^{12}CO column density should be about 90 times the ^{13}CO column density. At the systemic velocity, the ^{12}CO line is 30 ± 8 times brighter than the ^{13}CO line which, if not precisely the optically thin case, would seem to indicate that the ^{12}CO line is, on average, not too terribly thick.

Figures 5 are position-position maps at various velocities, sampled on a 0.5' grid. The contours are spaced at 2 K km s^{-1} intervals. These maps are similar to those of Rickard et al. 1977a, except for higher sensitivity and lower spatial resolution. The rotation of the galaxy is apparent. One peculiarity of these data is that the emission at the systemic velocity seems to be extended beyond the stellar disk. Figure 6 shows a strip map of the minor axis at the systemic velocity, superposed on a convolution of the stellar disk with the beam shape. There seems to be a considerable amount of emission from points outside the stellar disk. This effect could, of course, be

due to pointing errors (the pointing corrections have not been measured exactly in the direction of M82), so this observation should be checked by an antenna with a smaller beam. It is not impossible that this observation is correct: there are dusty filaments in the direction of the excess CO emission, and dust is an excellent tracer of molecular clouds. If these filaments are in fact molecular objects hanging above the plane of the galaxy, then they are quite dissimilar from all the molecular clouds we know, and it is not too surprising that the CO emission from them is peculiar.

REFERENCES

[1] Knapp, G. R., Phillips, T. G., Huggins, P. J., Leighton, R. B. and Wannier, P. G. 1980, Ap. J., 240, 60.

[2] Lo, K-Y 1981, Greenbank workshop on "Extragalactic Molecules".

[3] Rickard, L. J, Palmer, P., Morris, M., Zuckerman, B. and Turner, B. E. 1975, Ap. J. (Letters), 199, L75.

[4] Rickard, L. J, Palmer, P., Turner, B. E., Morris, M., and Zuckerman, B. 1977a, Ap. J., 213, 673.

[5] Rickard, L. J, Palmer, P., Turner, B. E., Morris, M., and Zuckerman, B. 1977b, Ap. J. 214, 390.

[6] Solomon, P. M., and de Zafra, P. 1975, Ap. J. (Letters), 199, L79

[7] Stark, A. A., and Wolff, R. S. 1979, Ap. J. 229, 118.

Figure 1

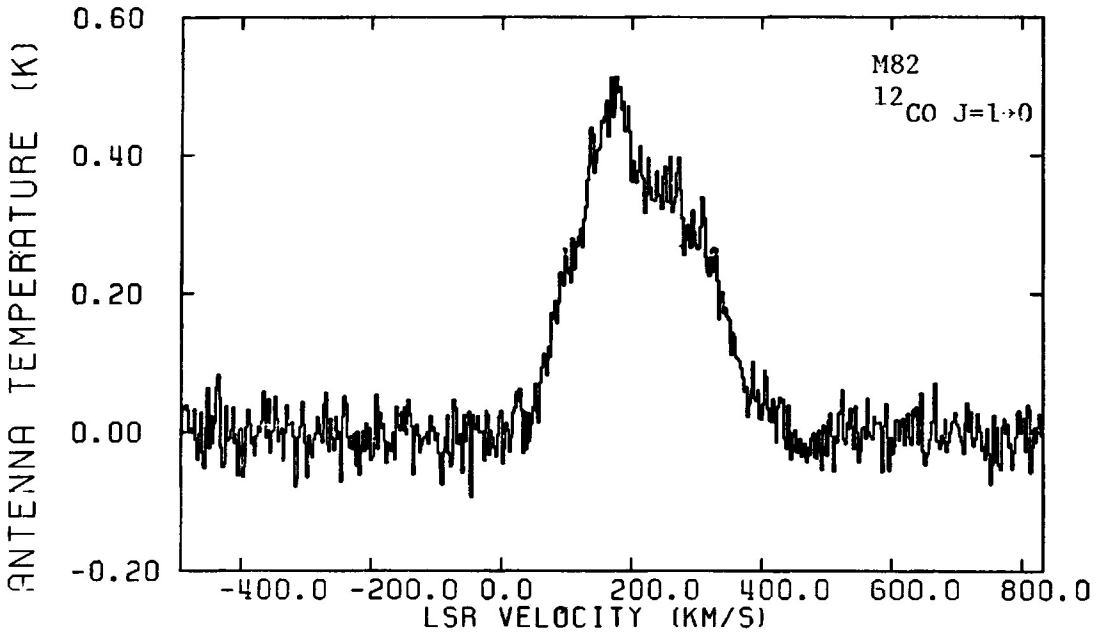

Area = 95.8±0.9 K km/s peak = 0.51 K rms = 29 mK in 1 MHz filters

Figure 2

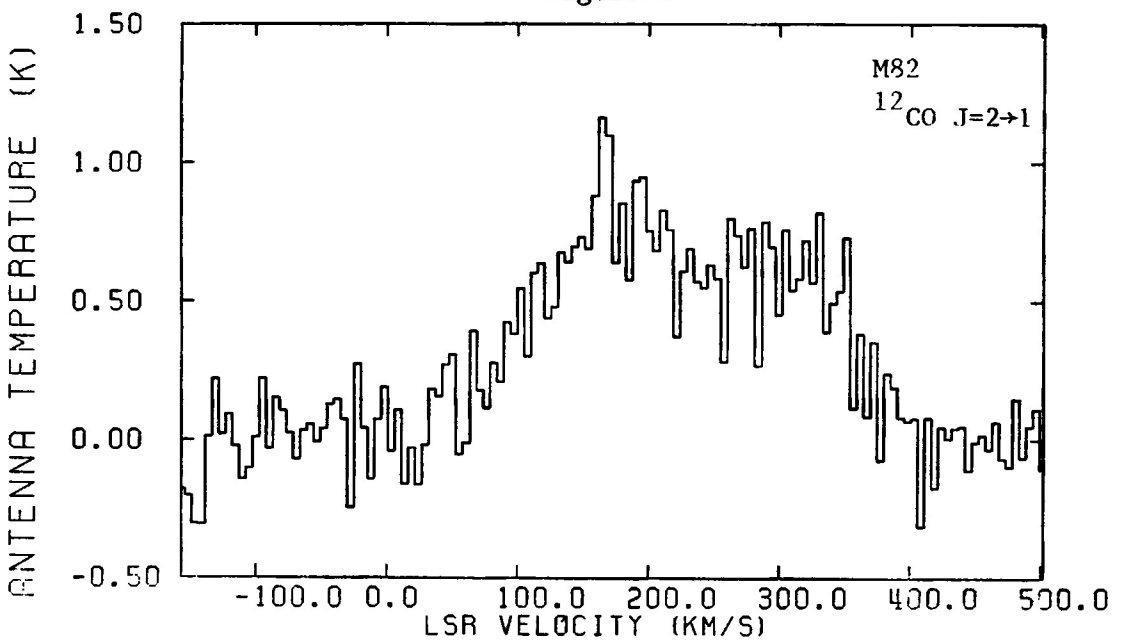

Area = 188±6 K km/s peak = 1.16 K rms = 0.13 in 4 MHz filters

Figure 3

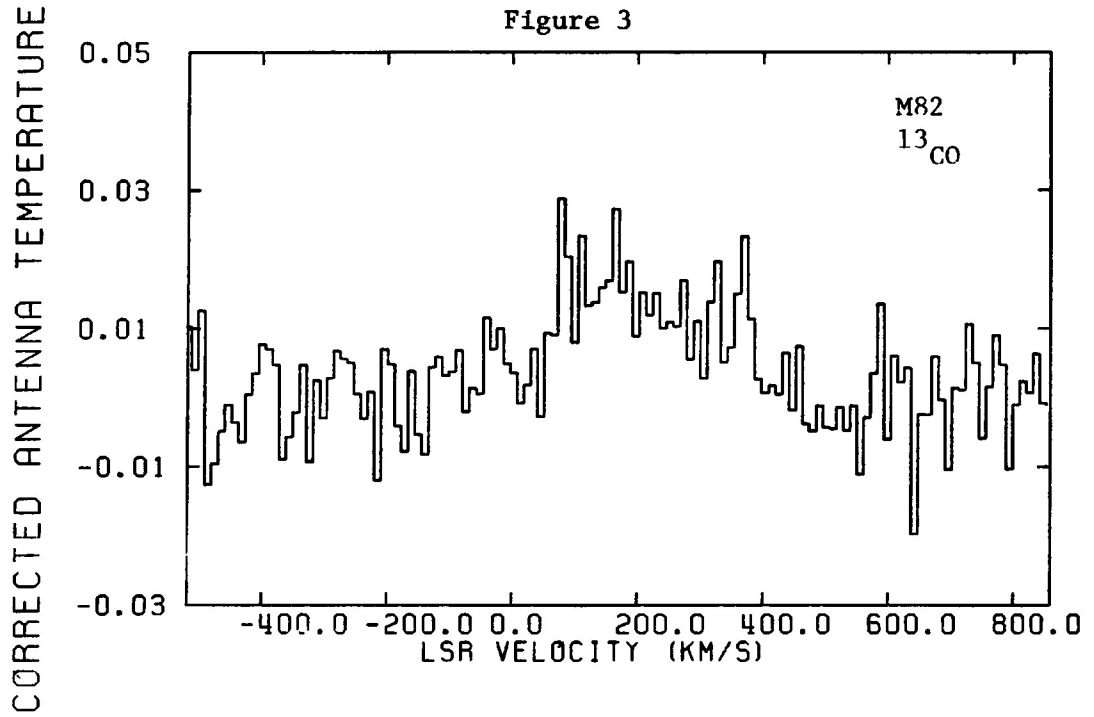

Area = 4.84±0.41 K km/s peak = 29 mK rms = 9.1 mK in 4 MHz filters

Figure 4

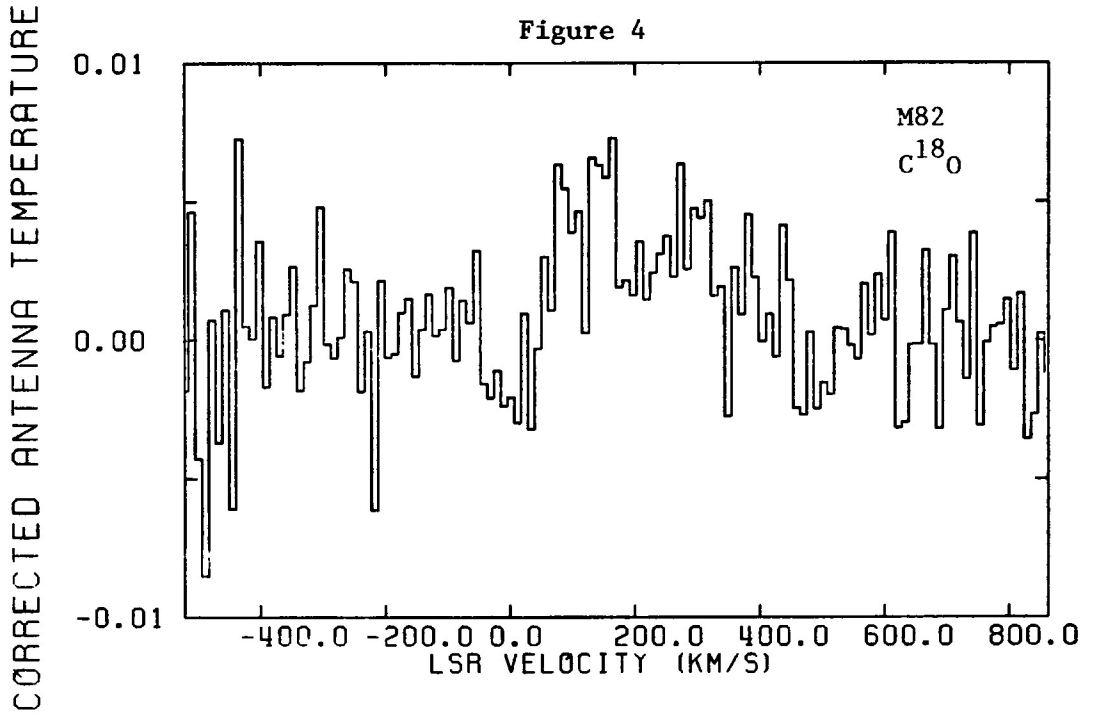

Area = 1.09±0.17 K km/s peak = 7.3 mK rms = 2.5 mK in 4 MHz filters

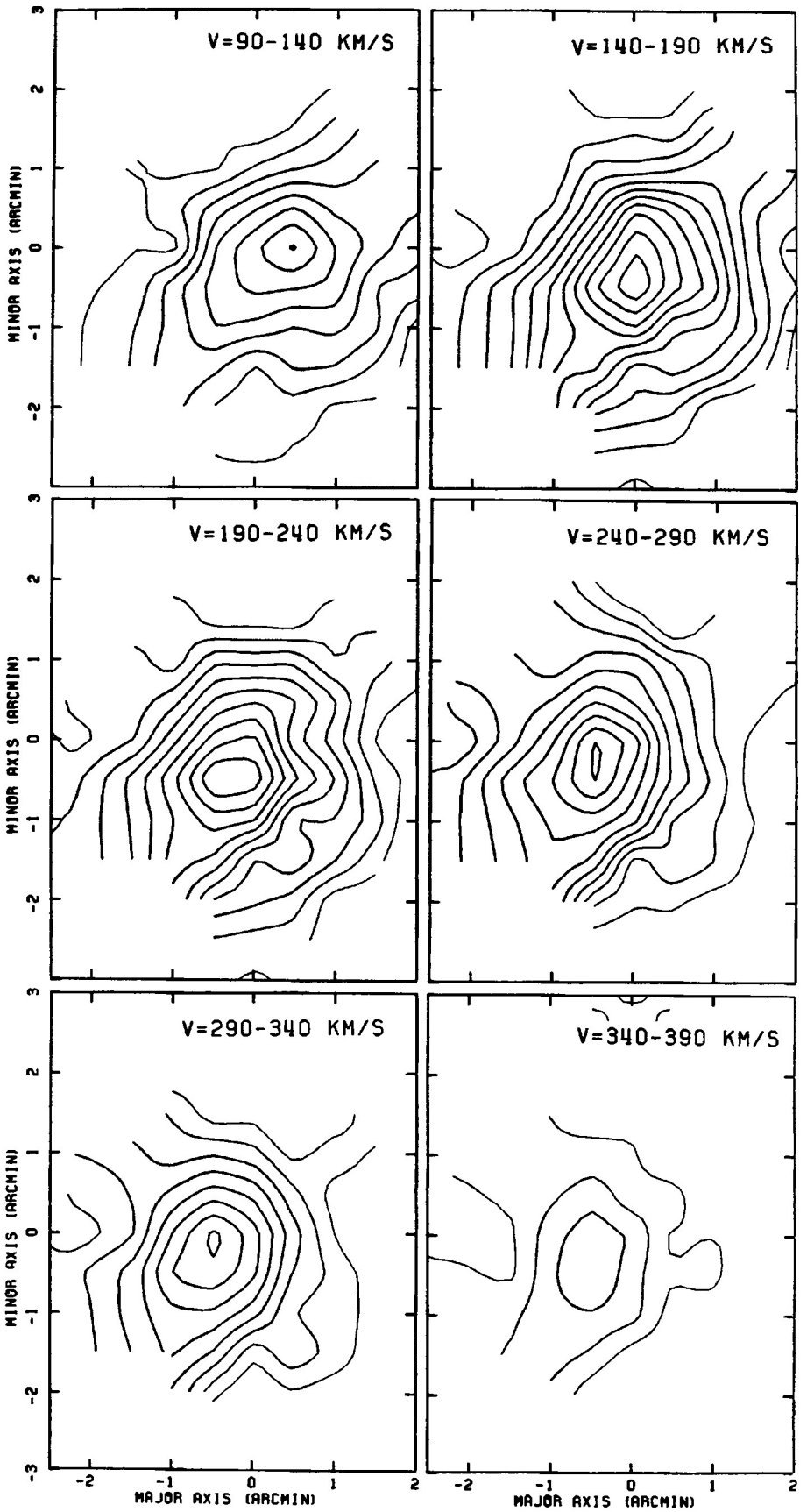
V=90-140 KM/S
V=140-190 KM/S
V=190-240 KM/S
V=240-290 KM/S
V=290-340 KM/S
V=340-390 KM/S
MINOR AXIS (ARCMIN)
MAJOR AXIS (ARCMIN)

Figure 5

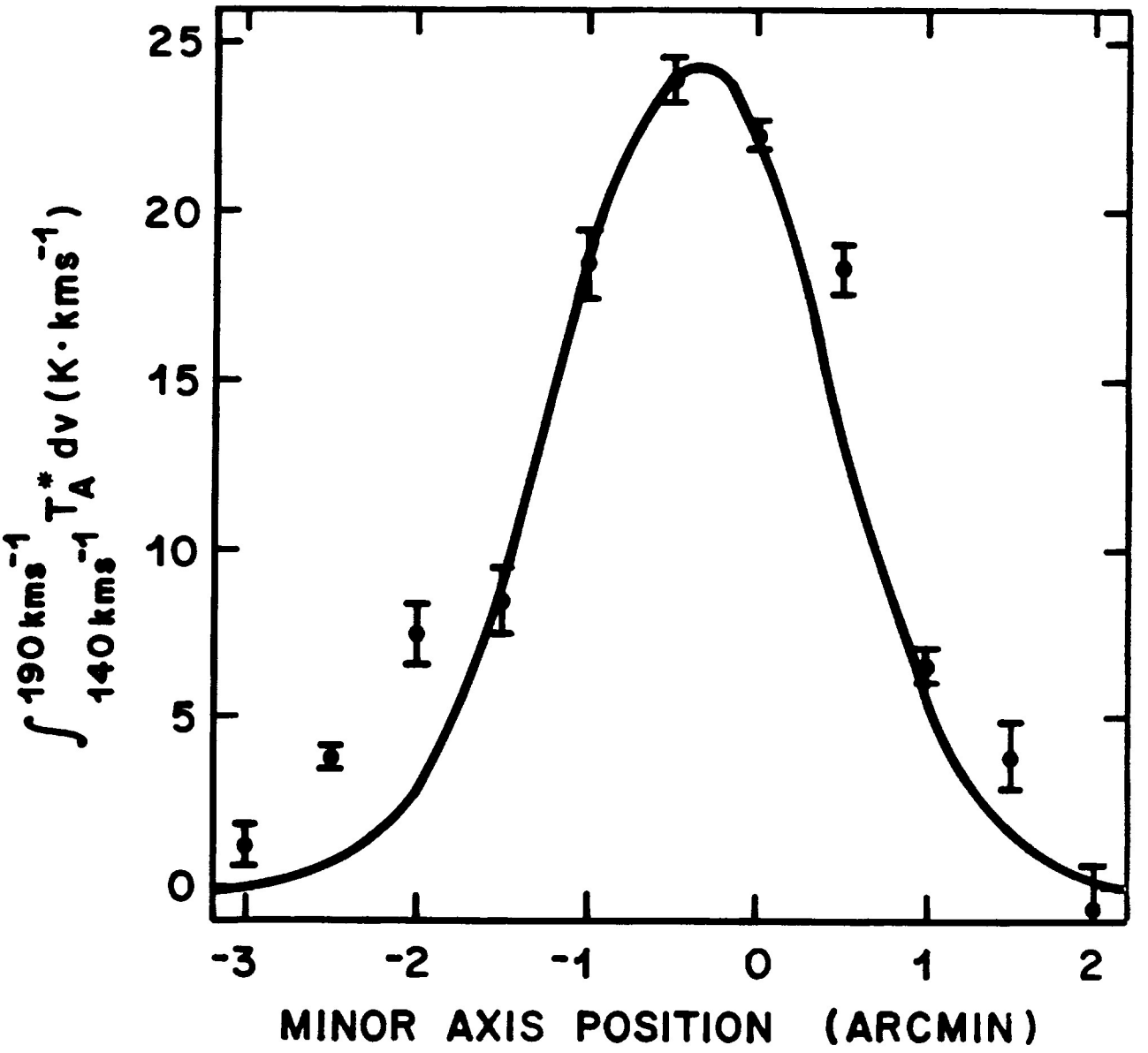
25
20
15
10
5
0
-3
-2
-1
0
1
2
MINOR AXIS POSITION (ARCMIN)
$\int_{140\,kms^{-1}}^{190\,kms^{-1}} T_A^* dv\ (K \cdot kms^{-1})$

Figure 6

CO IN THE ARMS OF ANDROMEDA

Richard A. Linke

Bell Telephone Laboratories, Incorporated
Crawford Hill
Holmdel, New Jersey 07733

The question of whether CO is an accurate tracer of spiral arms* in galaxies has fundamental implications for the very nature of these arms to the extent that CO column density reflects H_2 density. In spite of extensive observations of our own galaxy the answer to this question remains unsettled - partly because of our poor vantage point for observing spiral arms in our galaxy. The obvious way to settle the question is to map another spiral galaxy in CO. Fortunately, M31 with its large angular size gives us thousands of resolution elements even with the rather large beams presently available at CO (1-2 arc min).

Resolution, however, is not the only problem since a "typical" molecular cloud in our galaxy is only 10-20 pc across and has about a 10K surface brightness. Such a cloud at the distance of M31 would give us only 20 mk of antenna temperature with the BTL 1.7' beam. However, there are usually many such clouds in one beam - one BTL beam at M31 corresponds to about one square degree at the distance of the Galactic center.

Observations

With the instrumentation available 3 years ago it was just feasible to consider mapping M31 in CO. The work presented here consists of observations made with A. Stark and M. Frerking on the BTL 7 meter antenna over the 1979-80 and 1980-81 observing years. The data consist of 143 spectra obtained at 1.5 arc minute spacing on a square grid aligned with the major and minor axes of M31. Twenty of the 143 map points were obtained (also at Bell

* In the context of this paper we refer to large scale arm like features as "spiral arms" though they may in fact be rings; the high inclination angle at M31 makes it very difficult to resolve this question.

Labs) by F. Combes and are reported and discussed by Boulanger, Stark and Combes (1981). For further discussions of the present work see Stark, Linke, Frerking (1982). A strip map obtained along the minor axis of M31 clearly shows the ring nature of this galaxy in CO. This ring is not the subject of the present work and the interested reader is referred to Stark (1979) for a discussion of these data.

The 1.7' beam of the BTL 7 meter antenna provides a resolution of 340 pc at M31 for directions parallel to the major axis taking the distance to be 690 kpc. Because of the steep inclination angle of M31 (77.5°) our beam gives a resolution of 1.5 kpc along the minor axis.

The spectrometer used consists of 512 channels of 1 MHz filters which provide a velocity resolution of 2.6 kms^{-1} and more than adequate velocity coverage. The center velocity was -550 kms^{-1} (all velocities are heliocentric) to account for the systemic velocity of -300 kms^{-1} as well as the rotation curve velocity of approximately -250 kms^{-1} at our field. All data were obtained at a uniform noise level of $\sim$ 30 mk RMS which required 1.3 hours of integration in good weather. The observing mode was position switching against two reference positions away from CO emission.

The location of our 15X18 arc minute map is shown on the optical image of M31 on the cover of these Proceedings. The region was selected to show good brightness contrast.

Results

A map of integrated CO intensity (-580 to -420 kms) is shown in Fig. 1 alongside a (negative) optical image of our field in M31. The lowest contour and the contour interval are both 0.5K kms^{-1} or about equal to the statistical noise for the velocity interval used. *It is clear that the CO integrated emission fairly accurately traces out the optical obscuration in this region of M31.* A chain of emission maxima occurs within the dark obscuration band evident in the

photograph.* The most intense of these reaches 5.5K kms^{-1} while a typical value for emission in the dark band is $\sim$ 2K kms^{-1}. By comparison, many spectra obtained away from this band showed no emission consistent with the noise limit of $<$ 0.5K kms^{-1}. We note that our typical integrated intensity of 2K kms^{-1} is only about 1/10 of what we would expect if M31 had the same volume emissivity as the molecular ring of our galaxy assuming 200 pc for the full thickness of the molecular disc in M31 and a value of 20K kms^{-1} kpc^{-1} for our galaxy (Soloman et al. 1979). We also note that our non-detection limit of $<$ 0.5K kms^{-1} is sufficient to rule out the presence of even one giant molecular cloud (GMC) of a few $X10^5 M_\odot$. One such cloud in the beam would produce $\sim$ 2K kms^{-1} of emission. Thus we can rule out the presence of GMC's over large regions of M31 which lie between the obscuration arms. By averaging spectra of 12 contiguous points away from the optical obscuration we obtain an integrated intensity of 0.12 $\pm$0.16K kms^{-1}. Thus we can set a 2σ upper limit of 0.44K kms^{-1} on the emission from this region. This gives a typical arm-inter-arm CO intensity contrast of $>$ 4.5:1 and a peak contrast of $>$ 12.5:1. These values are comparable to contrast ratios obtained for HI gas by Unwin (1980) with a similar angular resolution. The positions and widths of the arms in CO are shown by Boulanger et al. (1981) to agree quite well with the HI arms.

We can estimate H_2 column densities if we take the intensity ratio for ^{13}CO to be 1/10 that of ^{12}CO as the sparse ^{13}CO data seem to indicate (Boulanger et al. 1981). If we also take $^{13}CO/H_2 = 10^{-6}$ we find H_2 column densities which range from our detection limit of $< 2X10^{16}$ cm^{-2} to a maximum of $20X10^{16}$ cm^{-2}. Boulanger et al. (1981) compared these H_2 column densities with atomic hydrogen densities obtained by Unwin (1980) at the same positions and found $N(H_2)/N(H) \sim 0.1 - 0.2$. This is comparable with the outer portions of the Milky way's molecular ring but not with the inner material where $M(H_2) > M(H)$

* The dust lane in question lies along the inner edge of arm S4 (Baade 1963).

(Solomon et al. 1979).

Conclusions

We have obtained a filled CO map of a 15×18 arc minute field in M31 selected to show a distinct dust lane. The integrated CO emission map shows a clear correlation with the optical obscuration. There is also an excellent correlation between CO and HI gas and therefore also with the distribution of HII regions and OB associations as discussed by Unwin (1980). Thus it appears that all available tracers of the interstellar medium are strongly concentrated in the same regions: those of the optical spiral arms.

References

[1] W. Baade 1963, *Evolution of Stars & Galaxies,* ed. Payne-Gaposchkin, Harvard University Press, Cambridge, Mass.

[2] F. Boulanger, A. A. Stark and F. Combes 1981, *Astron. Astrophys.,* 93, L1.

[3] P. M. Solomon, D. B. Sanders, and N. Z. Scoville, 1979 IAU Symposium No. 84, ed. B. Burton, (Dordrecht: D. Reidel).

[4] A. A. Stark, 1979, Thesis, Princeton University.

[5] A. A. Stark, R. A. Linke and M. A. Frerking 1982 (in preparation).

[6] S. C. Unwin 1980, *Mon. Not. R. ast. Soc.,* 190, 575.

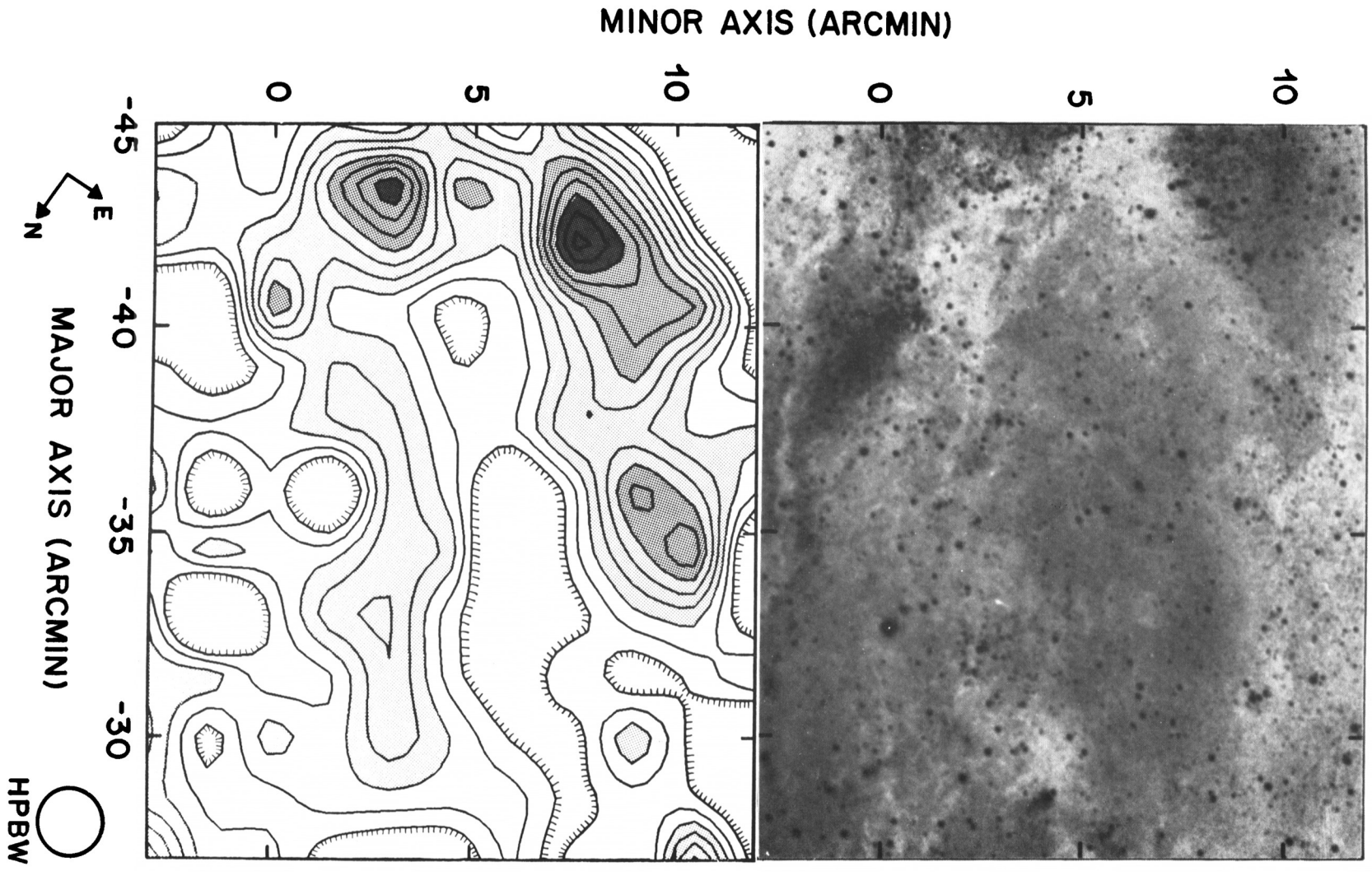

Figure 1 - Integrated CO emission compared against the (negative) optical image of our field in M31. The contour interval and lowest contour are both 0.5K km s^{-1}.

GMCs IN M31

Leo Blitz

University of Maryland

In an attempt to compare properties of Giant Molecular Clouds (GMCs) in M31 with those in the Milky Way, I have made CO observations of 54 HII regions from the Baade and Arp catalogue of HII regions with the 11m telescope at NRAO. To minimize the likelihood of getting more than one GMC in the beam at a time, observations were made in directions where only a single HII region would fall in the beam (except in two cases). CO was detected toward 20 HII regions at an average line strength of 2.3 K km s^{-1}, and a mean line width of 14.5 km s^{-1}. The line parameters were determined by fitting gaussians to the observed spectra.

Figure 1 is a histogram of the number distribution as a function of integrated line profile. The fall off in number towards low values of $\Sigma T_R^* \Delta V$ is probably due to the sensitivity limits of these observations. However, the sharp cutoff in integrated line strength above 3 K km s^{-1} is real and indicates a sharp cutoff in the properties of GMCs in M31. The object with the highest line strength is BA 108, one of the two positions where more than one HII region was in the beam. The emission from this object may therefore represent more than one GMC. The most sensitive factor in the observed line strength is almost surely the beam filling; the cutoff in integrated antenna temperature is therefore probably indicative of a cutoff in the size of GMCs. A similar effect has been established for GMCs in the Milky Way (Blitz 1978, Stark and Blitz 1978, Stark 1979, Solomon, Sanders and Scoville 1980).

Figure 2 is a histogram of the observed and detected GMCs. The unshaded portion represents no detection, the shaded portion is probable detections, and the dark portion is definite detections. The largest fraction of detections occurred between 8 and 10 kpc from the center, but it is not clear whether this is significant.

Figure 3 shows the line widths as a function of radius; the dashed line is a least squares fit to the data. The line width appears to be roughly constant with radius, a result which cannot as yet be compared with the Milky Way because of the unknown degree to which blending affects the line width determinations in the inner Galaxy.

Figure 4 shows the distribution of peak antenna temperature as a function of radius; again, the dashed line is the least squares fit to the data. The CO lines seem to get weaker as a function of radius, a result which implies that either GMCs get smaller and less massive with increasing radius in M31, or that excitation effects cause GMCs at increasing distances from the galactic center to be cooler. If the latter is true (and there seems to be some evidence for this in the Milky Way from comparisons of local observations by Blitz (1978) and the observations of Kutner and Mead (1981)), then ^{12}CO line strength is not a reliable tracer of H_2 mass.

One can compare the expected line strengths of GMCs in M31 by comparing them to observations of local GMC's in the Milky Way. Using Blitz's (1978) Milky values,

$$< \text{peak } T_A^* > = 1.9 \text{ K}$$

$$< \Sigma \, T_A \, \Delta V > = 9 \text{ K km s}^{-1}$$

$$< \Delta V > = 4.7 \text{ km s}^{-1}$$

$$< \text{projected area} > = 2.1 \times 10^3 \text{ pc}^2$$

At the distance of M31 the beam filling for local GMCs is 5.5×10^{-2} and the following values are expected and observed:

	expected	observed	
$< \text{peak } T_A^* >$	0.10	0.16	K
$<\Sigma T_A \Delta V >$	0.46	2.3	K km s^{-1}
$< \Delta V >$	4.7	14.5	km s^{-1}

The difference between the expected and observed antenna temperatures is probably insignificant and may be due to a combination of calibration uncertainties and selection effects (in M31 only the very largest clouds in the sample are detected). The difference in line width is real, however, and may result from one or more of the following:

(1) GMCs in M31 are different from the local sample -- Although this cannot be ruled out, it is hard to understand why only the line widths are different.

(2) Differential rotation from many small clouds in the beam -- This is probably not important since the differential projected velocities in a 1.1′ beam in M31 are much less than 15 km s^{-1}.

(3) Rotation of the complexes. -- An unresolved rotating cloud will give a line significantly broader than that for a resolved cloud, and line widths approaching 15 km s^{-1} can be achieved. However, the integrated line strength is conserved and the peak line intensities would be anomalously small.

(4) Random velocities of many small clouds in the beam -- Observations by Stark (1979) and Blitz (1978) suggest that the cloud-to-cloud velocity disperion of all molecular clouds in the solar vicinity is 7 km s^{-1}. A collection of such clouds in M31 would give a FWHM of 16.5 km s^{-1}, close to the observed value.

The solution to the discrepancy may be some combination of these four points, but the fourth seems to me to be the most plausible.

References

Blitz, L., 1978, Ph.D. Dissertation, Columbia University.

Kutner, M.L. and Mead, K., 1981, in preparation.

Solomon, P.M. and Sanders, D., 1980, in Giant Molecular Clouds in the Galaxy, (Oxford: Pergammon Press), p. 41.

Stark, A.A., 1979, Ph.D. Dissertation, Princeton University.

Stark A.A. and Blitz, L., 1978, Ap.J., (Letters), 225, L15.

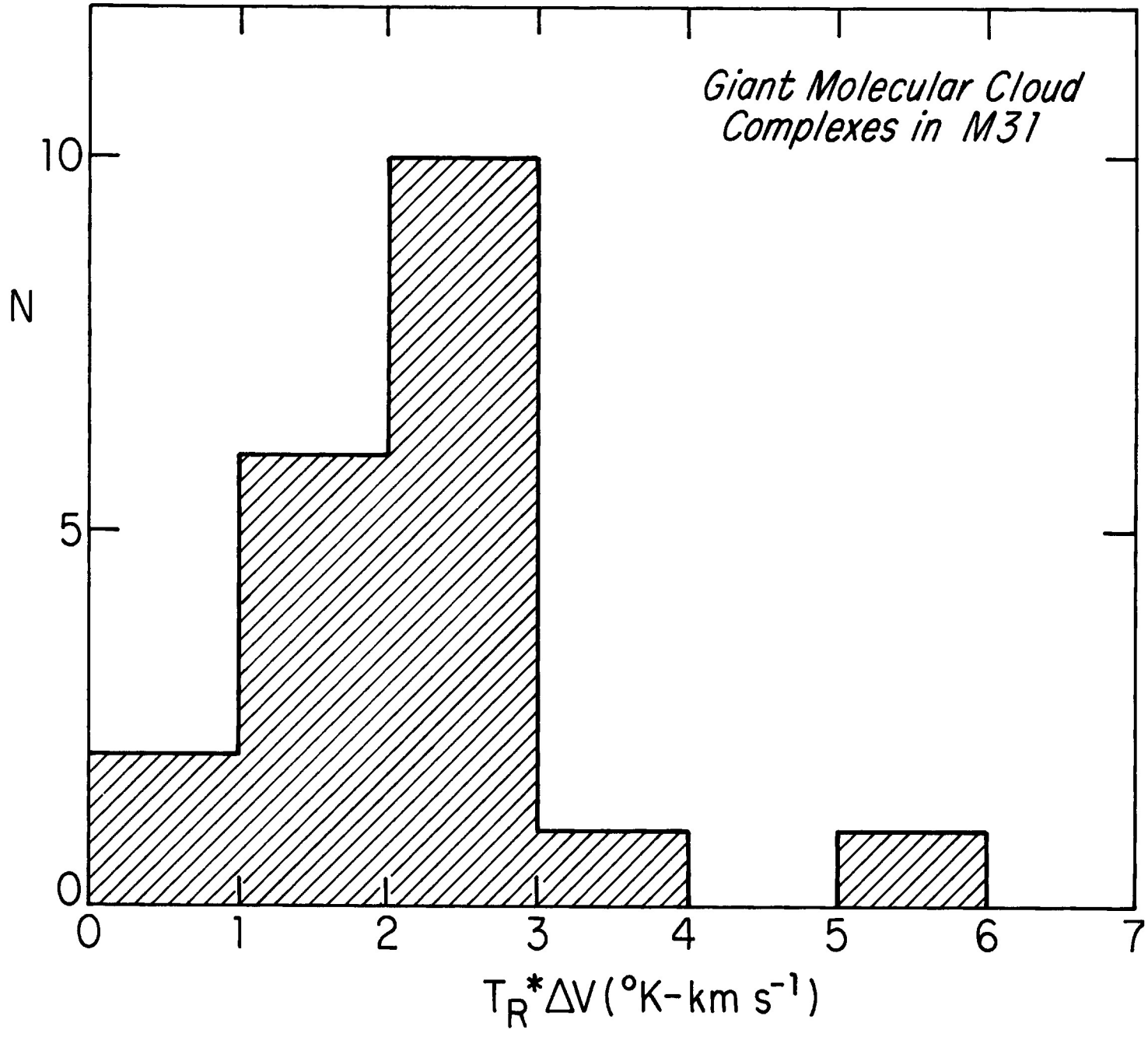

FIGURE 1 Giant molecular cloud complexes in M31.

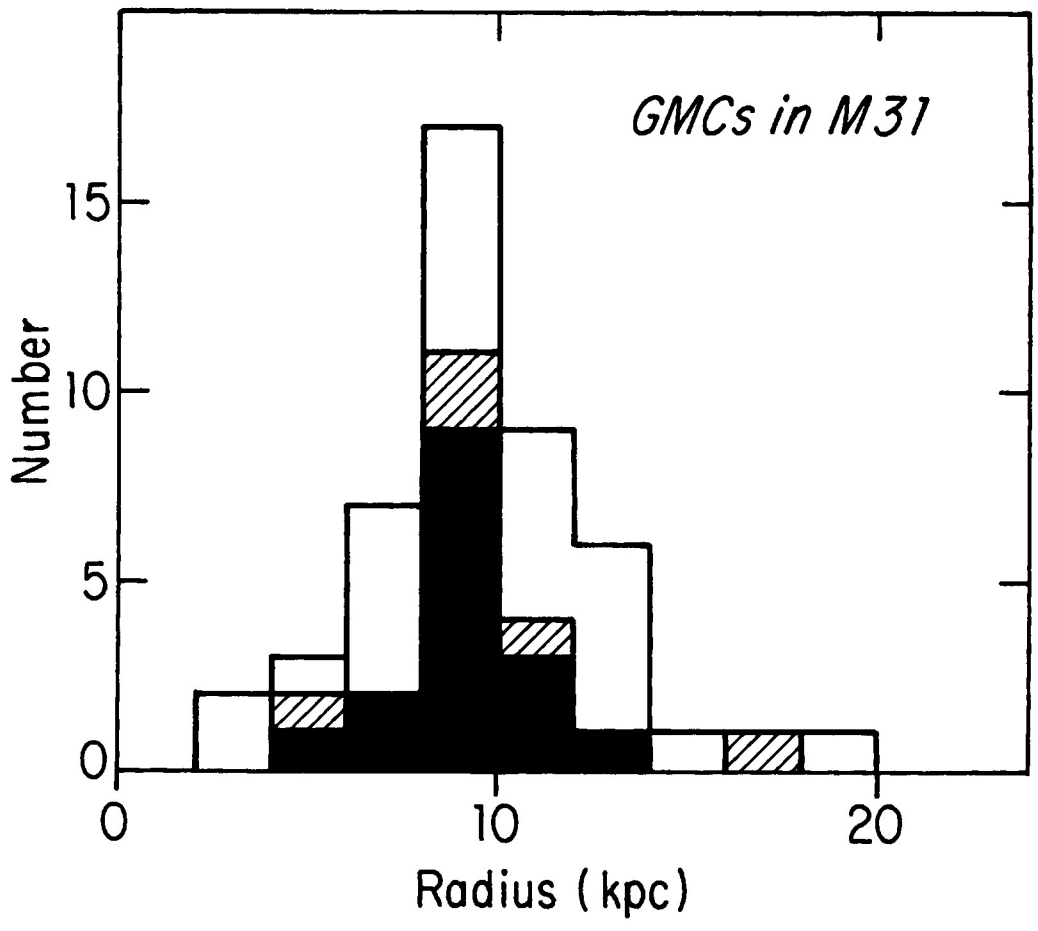

FIGURE 2 CO detections toward HII regions in M31.

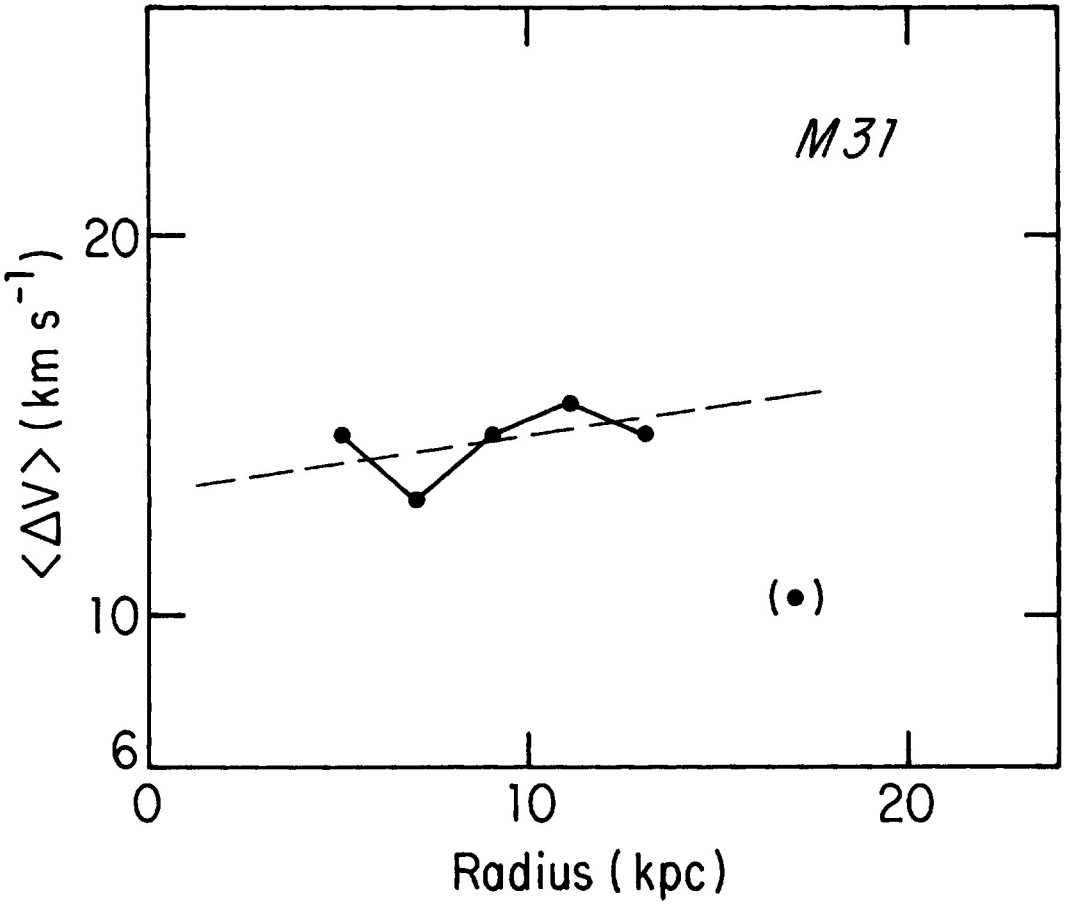

FIGURE 3 Comparison of mean CO linewidth with radius.

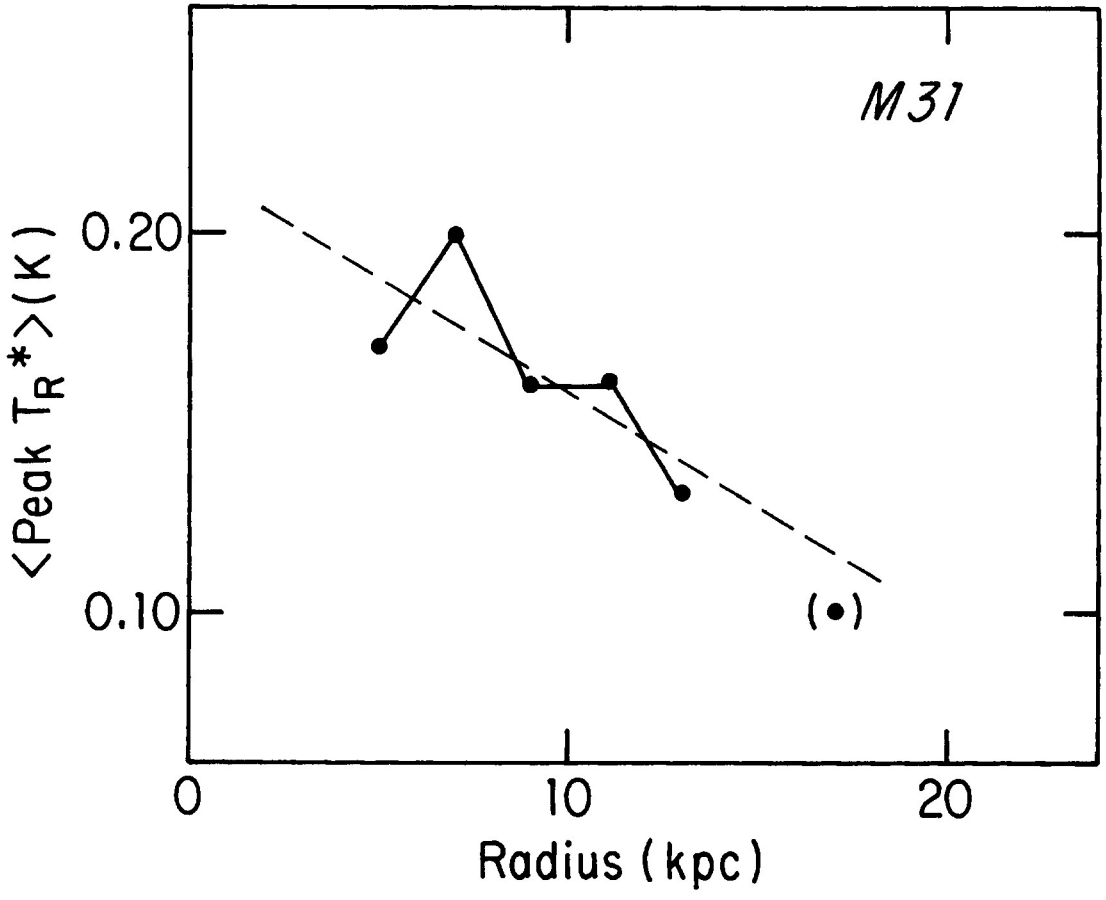

FIGURE 4 Comparison of peak T_R^* with radius.

CO SURVEY: COMPARISON WITH MORPHOLOGICAL TYPE

Fran Verter

Princeton University Observatory

The observational goal of my thesis is to establish the relationship between total galactic molecular gas content and morphological type. To do this, I am using the Bell Labs 7m telescope to conduct a survey of galaxies in the ^{12}CO $J = 1 \rightarrow 0$ line. Most of the observations will consist of a single measurement per galaxy, with the beam positioned on the galactic center. In order to obtain an accurate estimate of the total gas content in this manner, it will be necessary to select galaxies at large enough distances so that the telescope's 1.5 beam covers most of the galactic disk.

I am particularly interested in determining what effect the addition of molecular gas will have on the ratio of HI mass to optical luminosity, as a function of morphological type. Therefore, I will only use galaxies whose HI content is known. Based on the accuracy attained in previous studies of M(HI)/L(opt), (Roberts, 1969; Roberts, 1975; Shostak, 1978), I expect that a statistically significant deviation of the ratio observed in a typical bright Sc would require the detection of about 10^9 $M_\odot$ of H_2, which at the galactic distances considered corresponds to a sensitivity on the order of 10 mK in antenna temperature. Because there is much evidence that integral properties of galaxies scale with their optical luminosity, my galaxy sample will cover a wide luminosity range.

CALIBRATING THE RELATION BETWEEN CO FLUX AND H_2 MASS

In order to convert observations of integrated CO flux into measurements of molecular hydrogen mass, I have written a program which uses a set of model cloud parameters to determine the amount of gas a galaxy needs to reproduce a given observed flux. Each model contains a number of optically thick cloud

populations which are uniformly distributed in the nucleus and/or disk of the galaxy. The spatial distributions of the various cloud populations can be adjusted separately, but their relative filling factors are fixed. Given the galaxy's distance, the FWHM of the telescope beam, and the observed flux, the cloud abundance is adjusted to match this flux and the corresponding total mass is computed.

The result of this modelling program is equivalent to the popular method of multiplying the CO flux by a constant factor which converts it into H_2 mass. In that case, the cloud parameters enter implicitly when the conversion factor is calibrated by observing selected cloud populations within our own galaxy. However, the use of a single conversion factor derived from a single cloud type is an oversimplification which ignores the facts that the observed galaxy most likely contains several cloud populations which are making significant contributions to the total flux, and that the nature of these clouds may differ between the inner and outer parts of the galaxy. Both of these effects can be easily and explicitly incorporated in the modelling program when setting the input parameters.

As a test of the sensitivity of the calculated mass to the assumed cloud parameters, I have compared the results obtained by running the program for several different cloud models, keeping the cloud distribution and the observing conditions fixed. The cloud parameters were taken from descriptions which have appeared in the literature as models of various aspects of the galactic molecular cloud ensemble. These include the "standard" cloud parameters Spitzer (1978) uses to fit the selective extinction distribution; the cloud model which Bieging et al. (1981) derived from Blitz's thesis observations (Blitz, 1978); the clouds which Morris and Lo (1978) used to fit their CO observations of two Scd galaxies, and which were originally derived

from stochastic cloud distribution models of the galaxy (Burton and Gordon, 1976; Baker and Burton, 1975); two of the models which Liszt and Burton (1981) use to simulate the l-v diagram produced by galactic plane survey observations; and the morphological cloud types summarized by Turner (Turner, 1979; Turner, 1981). In those cases where the models did not provide enough information to evaluate all the input parameters required by the program, I referred to Myers' (1978) compilation of cloud properties, applied Larson's (1981) relations to predict velocity dispersions, and constrained the cloud filling factors to be within the limit suggested by the McKee-Ostriker (1977) model of the interstellar medium.

Table 1 lists the input parameters and the resulting mass predictions of the models. Most of the masses agree reasonably well, the two exceptions being Spitzer's standard clouds and the Bieging et al./Blitz clouds. Spitzer's clouds are hotter than the others, and consequently it takes fewer of them to reproduce a given flux, so the molecular mass they predict is an order of magnitude below the other models. However, since these diffuse clouds are not sources of observed CO emission in our galaxy, they may be poor models of the emitting regions in other galaxies. By contrast, the Bieging et al./Blitz clouds give a mass prediction an order of magnitude above the other models. This is due to the low temperature and high mass ascribed to these giant molecular clouds. In general, it is reassuring to see that the results of simple standard cloud models do not differ very much from the prediction of an elaborate description of the interstellar medium such as Turner's cloud types.

This work was supported in part by NSF grant AST-8009252 to Princeton University.

MODELS OF EXTRAGALACTIC MOLECULAR CLOUD ENSEMBLES

main assumptions: optical depth >>1 for all clouds

clouds in annulus between galactocentric radii 4-8 kpc

galaxy distance 30 Mpc

telescope beam 1.5

observed flux 10 K km/s

Model Components	Temperature (K)	Spectral Profile FWHM (km/s)	Area Filling Factor*	Mass Density ($M_\odot/pc^2$)	Calculated Molecular Mass (10^9 $M_\odot$)
Spitzer standard	80.	4.0	1.0	20.	0.23
Morris & Lo	14.	6.0	1.0	100.	4.3
Bieging et al./Blitz	2.	4.2	1.0	94.	40.0
Liszt & Burton	12.	3.1	1.0	51.	5.0
Liszt & Burton fig. 4f					5.3
medium-sized	14.	3.1	1.0	63.	
giant	14.	3.1	.36	63.	
Turner cloud types					1.3
isolated dark clouds	10.	2.5	1.0	410.	
large globules	10.	1.7	1.0	280.	
dark clouds + AB *	25.	2.5	25.	200.	
dark clouds + 0 *	50.	8.3	42.	28.	
giant molecular clouds	15.	12.	37.	71.	

*with respect to component #1

REFERENCES

Baker, P. L. and Burton, W. B. (1975) Ap. J. 198, 281.

Bieging, J. H., Blitz, L., Lada, C. J. and Stark, A. A. (1981) Ap. J. 247, 443

Blitz, L. (1978) Ph.D. thesis, Columbia U.

Burton, W. B. and Gordon, M. A. (1976) Ap. J. 207, L189.

Larson, R. B. (1981) Ap. J. 194, 809.

Liszt, H. S. and Burton, W. B. (1981) Ap. J. 243, 778

McKee, C. F. and Ostriker, J. P. (1977) Ap. J. 218, 148.

Morris, M. and Lo, K. Y. (1978) Ap. J. 223, 803.

Myers, P. C. (1978) Ap. J. 225, 380.

Roberts, M. S. (1969) A. J. 74, 859.

Roberts, M. S. (1975) Stars and Stellar Systems vol. IX p. 309.

Shostak, G. S. (1978) A. Ap. 68, 321.

Spitzer, L. (1978) Physical Processes in the Interstellar Medium

Turner, B. E. (1979) IAU Symp. #84 p. 257.

Turner, B. E. (1981) Morphology and Evolution of Molecular Clouds: A Brief Review text of a talk delivered at a Green Bank workshop, May 1981.

SUMMARY OF ^{12}CO (2 → 1) OBSERVATIONS OF THE MAGELLANIC CLOUDS

Th. de Graauw[1,3], F.P. Israel[1,3], and H. van de Stadt[2,3]

During two observing runs in 1980 and 1981 we have made observations of $^{12}CO(2 \rightarrow 1)$ emission in the direction of the Large and Small Magellanic clouds, the two nearest external galaxies. Motivation of the programme and a discussion of the first results will be given elsewhere (Israel et al., 1982). In this contribution we present a summary of the results to date.

The observations were made with the ESTEC/Utrecht submillimeter receiver. This receiver uses backward-wave oscillators (carcinotrons) as local oscillators and room temperature Schottky barrier diode waveguide mixers. It has been described elsewhere (Lidholm and de Graauw, 1979). During the observations system noise temperatures were between 3200 K and 4500 K. For a backend we used two 256 channel filterbanks with 1 MHz and .25 MHz channels corresponding to 1.3 and .325 km/sec resolution.

System calibration was done with two loads; beam shape and efficiency were determined by observations of Orion and the Moon; atmospheric attenuation was measured with antenna dipping. The observations were made with the 3.6 m telescope at ESO; La Silla (Chile) in May 1980 and October 1981. The resulting overall telescope efficiency was 45%, the beam (HPBW) was about 2 arcmin. Atmospheric opacities during the observations were between 0.1 and 0.25. Pointing and tracking were not very good and had to be checked frequently on the position of nearby field stars.

---

1. Astronomy Division, Space Science Dept., ESA, Noordwijk, NL

2. Sterrewacht of the University of Utrecht, NL

3. Based on observations collected at the European Southern Observatory, La Silla, Chile

All scans taken on the Large Magellanic cloud cover a velocity range from 136 to 468 km s^{-1} (V_{LSR}) in the first filterbank, and one from 260 to 344 km s^{-1} in the second filterbank. The exception is the scan centered on N159 that was taken with velocity ranges of 69 to 401 km s^{-1} and 193 to 277 km s^{-1} respectively. The velocity range covered on the Small Magellanic cloud was 36 to 368 km s^{-1} and 160 to 244 km s^{-1} respectively, escept in the case of N76 that was observed with -28 to 305 and 97 to 180 km s^{-1}.

A summary of the results is given in table I and Table II. The observations of CO(2-1) in the SMC are the first detections of CO in that galaxy.

Table I . Summary of $^{12}CO(2-1)$ Results on SMC

SOURCE	(1950) α	(1950) δ	T_A^* K	ΔV km s^{-1}	V_{LSR}	REMARKS
57	00 44 48	-73 57	1.2	18	118	H_2O maser
			1.3	9	160	near HII
58	00 45 42	-73 24.7	2.3	7	123	near HII
N 30	00 47 12	-73 24	1	6		HII
N 37	00 50 00	-73 00	$\leq$ 1.5			near HII
N 66	00 57 30	-72 30	$\leq$ .7			near HII
N66	01 01 00	-72 30	.7	12	110	near HII
			2.0	8	194	
N 76	01 02 30	-72 15	$\leq$ .9			near HII

Table II. Summary of $^{12}CO(2-1)$ Results on LMC

SOURCE	(1950) α	(1950) δ	T_A^* K	ΔV nm s^{-1}	V_{LSR}	REMARKS
N 105	05 10 12.7	-68 57.1	1.4 ± .3	15.6	238	HII, OH maser
			.9 ± .3	5.2	312	
	05 11 55	-68 57.1	≤ 1.2			
H 21	05 22 00	-69 48	.9 ± .3	6.5	258	Dark Cloud
N 59	05 35 30	-67 36	.8 ± .25	7	267	HII
H 47	05 57 00	-69 45	.7 ± .25	5	258	Dark Cloud
	05 40 00	-70 10	1.0 ± .25	6	237	
H 51	05 38 45	-68 59.5	≤ 1.6			Dark Cloud
30 Dor	05 38 50	-69 07	.8 ± .25	7	245 (310)	HII
30 Dor	05 38 50	-69 17	< .9			HII
30 Dor	05 39 10	-69 05	< .6			HII
N158C	05 39 10	-69 27	< .9			HII
N160A	05 39 30	-69 37	1.1 ± .3	7	240	Near HII
			1.0 ± .3	6	304	
N160A	05 40 12	-69 39.7	< 1.2			Near HII
N159	05 40 30	-69 46	2.5 ± .2	6	235	HII, OH maser
			1.1 ± .3	8	292	

REFERENCES

F.P. Israel, Th. de Graauw, S. Lidholm, H. van der Stadt and C. de Vries, to be published in Ap. J.

S. Lidholm and Th. de Graauw, Fourth International Conference on Infrared and Millimeter Waves and Their Applications. Florida 1979, p. App. 38.

AMMONIA IN THE SPIRAL GALAXY IC342

Paul T.P. Ho

Department of Astronomy
University of California, Berkeley

Robert N. Martin

Max Planck Institut fur Radioastronomie

Using the MPI 100m telescope, the (J,K) = (1,1) and (2,2) lines of NH_3 have been detected toward the spiral galaxy IC342[1,2]. Their nearly equal intensities imply the existence of warm (~ 50K) gas. The mere fact that these lines were detected imply a lower limit to the sizescale of the emission complex (> 25pc). Based on excitation arguments, we find that the NH_3 observations imply density $n(H_2) > 10^2$ cm^{-3} and mass $M > 10^8$ $M_\odot$. If the emission complex consists of many clouds, the total mass estimate will be lowered. These results, when combined with the infrared, radio continuum and CO observations, yield a consistent picture on star formation in the nucleus.

We have attempted to use our current understanding of Galactic molecular complexes as a framework in which to interpret these extragalactic observations. We conclude that gas-dust collisions are the only viable means to heat the gas. Since the total dust luminosity has been measured, we argue that the dust responsible for heating the gas cannot be much warmer than the gas itself. This implies that the gas densities must be high [$n(H_2) > 10^5$ cm^{-3}] so that an upper limit (< 30pc) on the size of the emission complex can be established. By comparing with the sizescale and mass of molecular complexes in the Galaxy, we further conclude that the NH_3 emission region in IC342 must be highly fragmented. The most likely model would be 10^2 giant molecular clouds each with an embedded OB cluster. This appears to be consistent with the CO

observations in the sense that if we modelled the CO emission to arise from 10^2 clouds, the deduced sizescale (30pc) and temperature (10K) of the individual clouds would be in good agreement with typical values for giant molecular clouds. The deduced large number of OB stars is in fact also consistent with the total dust luminosity and the radio continuum emission. In particular, for 10^3 early O stars or 10^5 early B stars we expect on the order of 10^{52} Lyman continuum photons. This should yield a 6cm continuum flux on the order of few x 10mJy. This is in fact what has been observed using the WSRT. If our estimates of the number of OB stars associated with the NH_3 emission region is correct, we then find that the OB star formation rate in the nucleus of IC342 appears to be an order of magnitude higher than that found for the Galaxy. Such a high rate of star formation can be understood in terms of the evolution of molecular gas in the nucleus. We argue that with the large number of clouds, collisions between clouds will play an important role in supporting these clouds against further collapse toward the nucleus. At the same time, the collisions may serve to initiate star formation at a rate consistent with the observations.

More recent VLA observations of IC342 in the NH_3 lines support the interpretation that there are probably many clouds rather than a single giant emission complex (see the discussion by Bob Martin in this volume).

P.T.P.H. acknowledges support from the Miller Institute for Basic Research, and NSF Grant AST 78-21037 to the Radio Astronomy Laboratory.

References

[1]Martin, R.N., Ho, P.T.P., and Ruf, K. 1981, Nature, submitted.

[2]Ho, P.T.P., Martin, R.N., and Ruf, K. 1981, Ap. J., submitted.

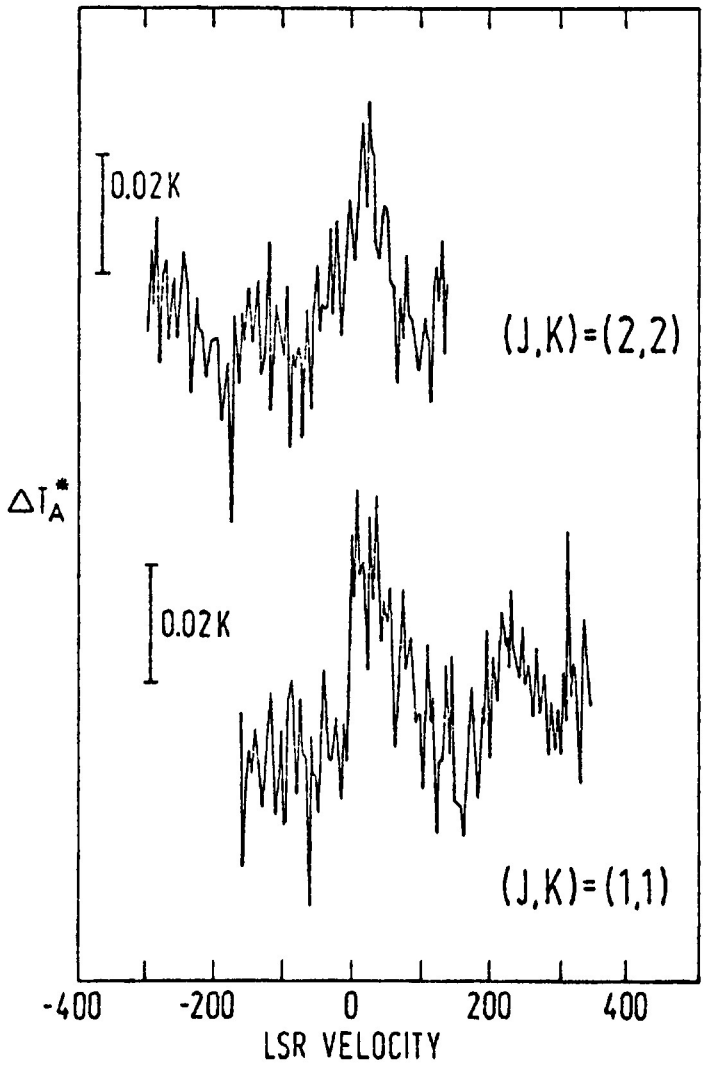

Figure 1. Detected NH_3 lines toward the spiral galaxy IC342.

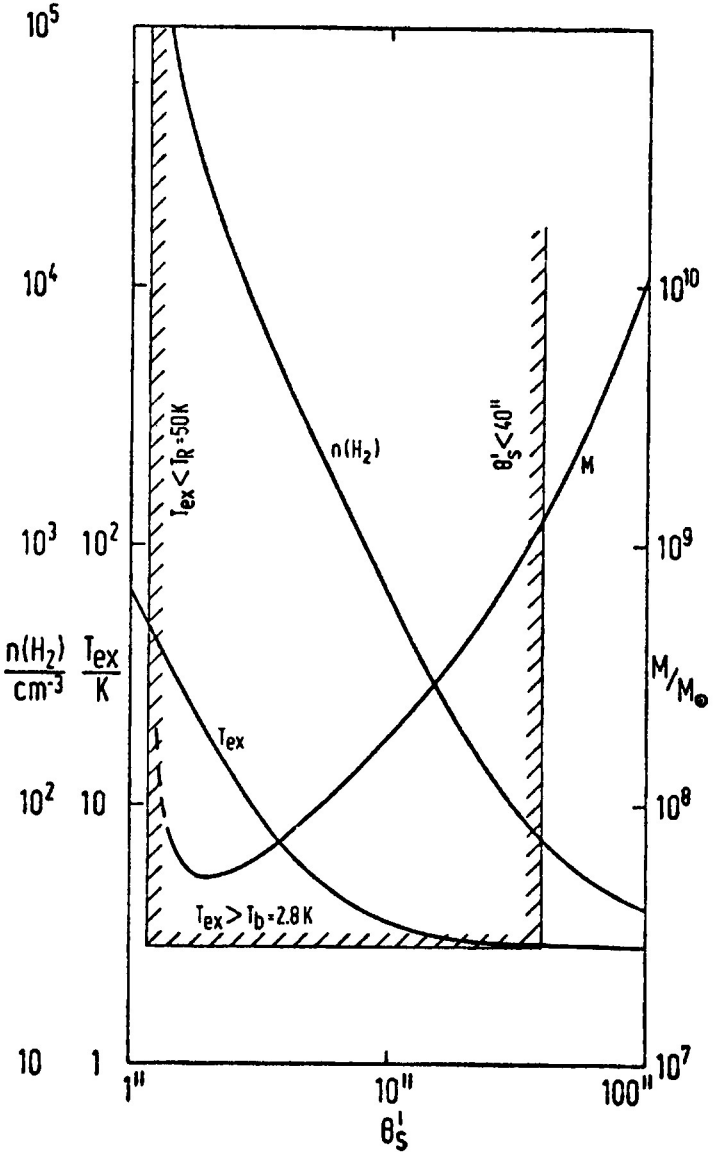

Figure 2. Deduced density, excitation temperature and mass for a single emission complex.

VLA OBSERVATIONS OF EXTRAGALACTIC AMMONIA

Robert N. Martin

Max Planck Institut fur Radioastronomie

Paul T.P. Ho

Department of Astronomy
University of California, Berkeley

Aperture synthesis observations were made of IC342 in the (J,K) = (1,1) and (2,2) lines of NH_3. With the VLA in the D configuration, the synthesized beamwidth was on the order of 5". We had a total of 18 antennas working on the average. Although the system performance at 23.7 GHz is a factor of 2 worse than at the center of the band of the receivers, we achieved a 3σ sensitivity on the order of 10mJy per beam, or ~1K in brightness temperature over a 5" beam. We detected the continuum source associated with the nucleus of IC342. However, after removal of this source, we did not detect any positive signal in the line. This upper limit which is achieved is of interest since if the NH_3 emission region consists of a single complex (see discussion by Paul Ho in this volume), we should have detected it at the VLA at the 10σ level. The failure to detect these lines at the VLA therefore implies that the NH_3 emission detected in IC342 must be extended over at least 3 of the synthesized beams. This supports the conclusion that the NH_3 emission is in fact made up of a large number of hot molecular cores.

P.T.P.H. acknowledges support from the Miller Institute for Basic Research and also NSF Grant AST78-21037 to the Radio Astronomy Laboratory.

OBSERVATIONS OF FAR-INFRARED EMISSION FROM LATE-TYPE GALAXIES

L. J Rickard (Howard University) and P. M. Harvey (University of Texas)

We have been observing the central regions of spiral and Irr II galaxies from the Kuiper Airborne Observatory, using a GaAs bolometer with effective wavelengths of 40, 50, 100, and 160μ. Although originally begun to investigate the properties of molecular clouds in galactic centers, we have extended our study to galaxies of similar types hitherto undetected at 2.6-mm. Of 25 galaxies observed, 3 are well-known IR sources and 18 are new detections at 100μ. The fluxes range from 3 Jy for M81 and M101 (our detection limit) to 97 Jy for NGC 2146.

Figure 1a shows the corresponding luminosity distribution; the luminosities corresponding to our detection limit for distances of 10 and 20 Mpc are marked. Fits to the spectra yield the dust temperatures in figure 1b. NGC 4303 is quite cool, resembling Smith's values for the disk of M51; the CO data also indicate a predominance of disk-type clouds in the inner 1'. The associated dust masses have been converted to surface mass densities, displayed in figure 1c.

Figure 2a shows the excellent correlation of the CO flux and 100μ flux. Presumably, more molecular clouds means greater numbers of massive stars, whose luminosity is efficiently converted to far-IR emission by the associated dust. It does not seem to be the case that the brightness of the CO line is being enhanced by the presence of hotter dust; there is no correlation of the CO luminosity with the

fitted dust temperatures.

Figure 2b shows the good correlation of the 100-μ luminosity with the ratio of radio flux to optical flux (Hummel's R parameter). The far-infrared luminosity is also correlated with the concentration of the radio emission to the center and with the integrated J-K colors. It does not correlate with the total mass, with the hydrogen mass, or with Hubble type.

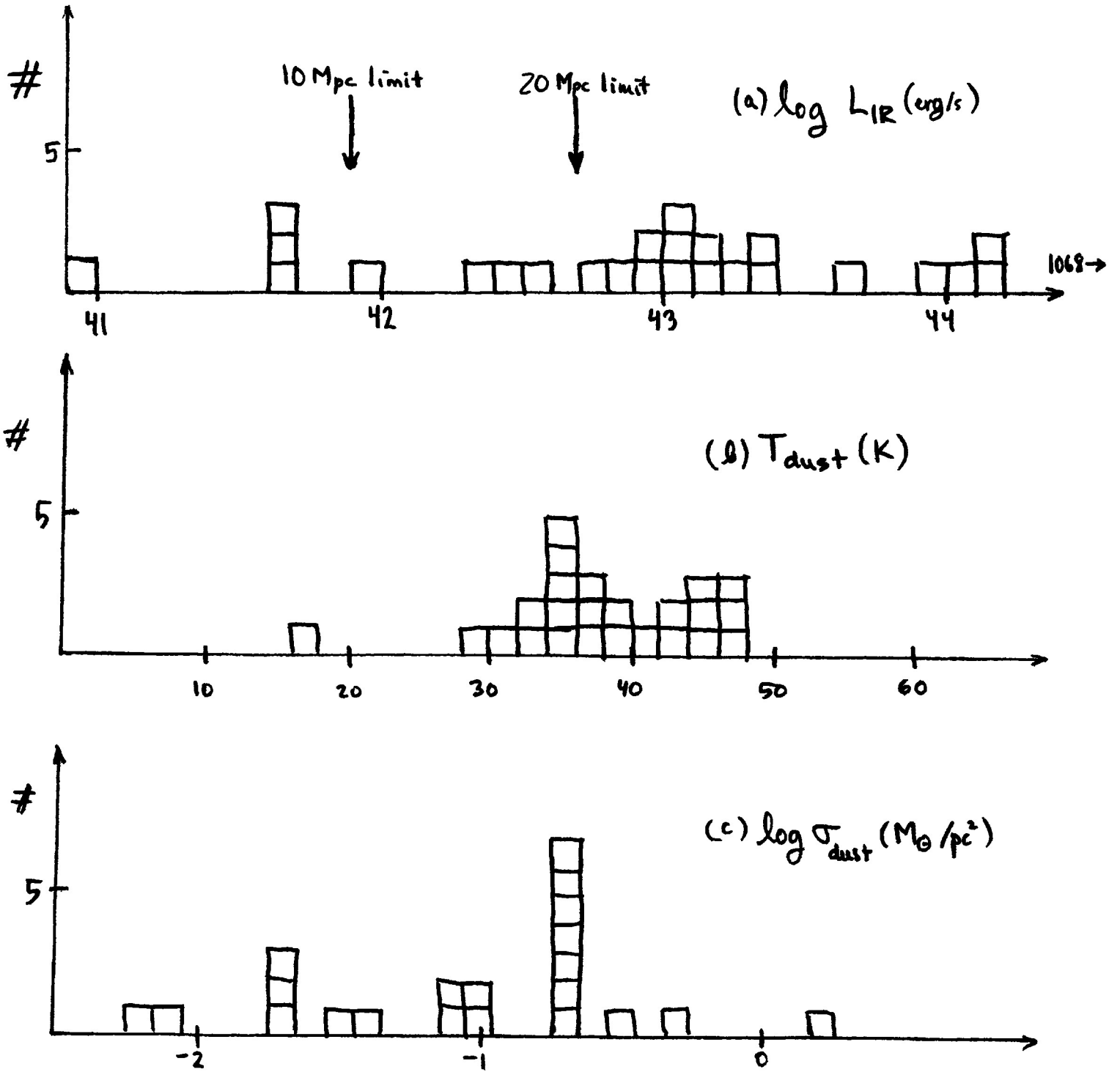
#
5
10 Mpc limit
20 Mpc limit
(a) log L_{IR} (erg/s)
41
42
43
44
10^{x}→
#
5
(b) T_{dust} (K)
10
20
30
40
50
60
#
5
(c) log σ_{dust} ($M_\odot$/pc^2)
-2
-1
0

Figure 1

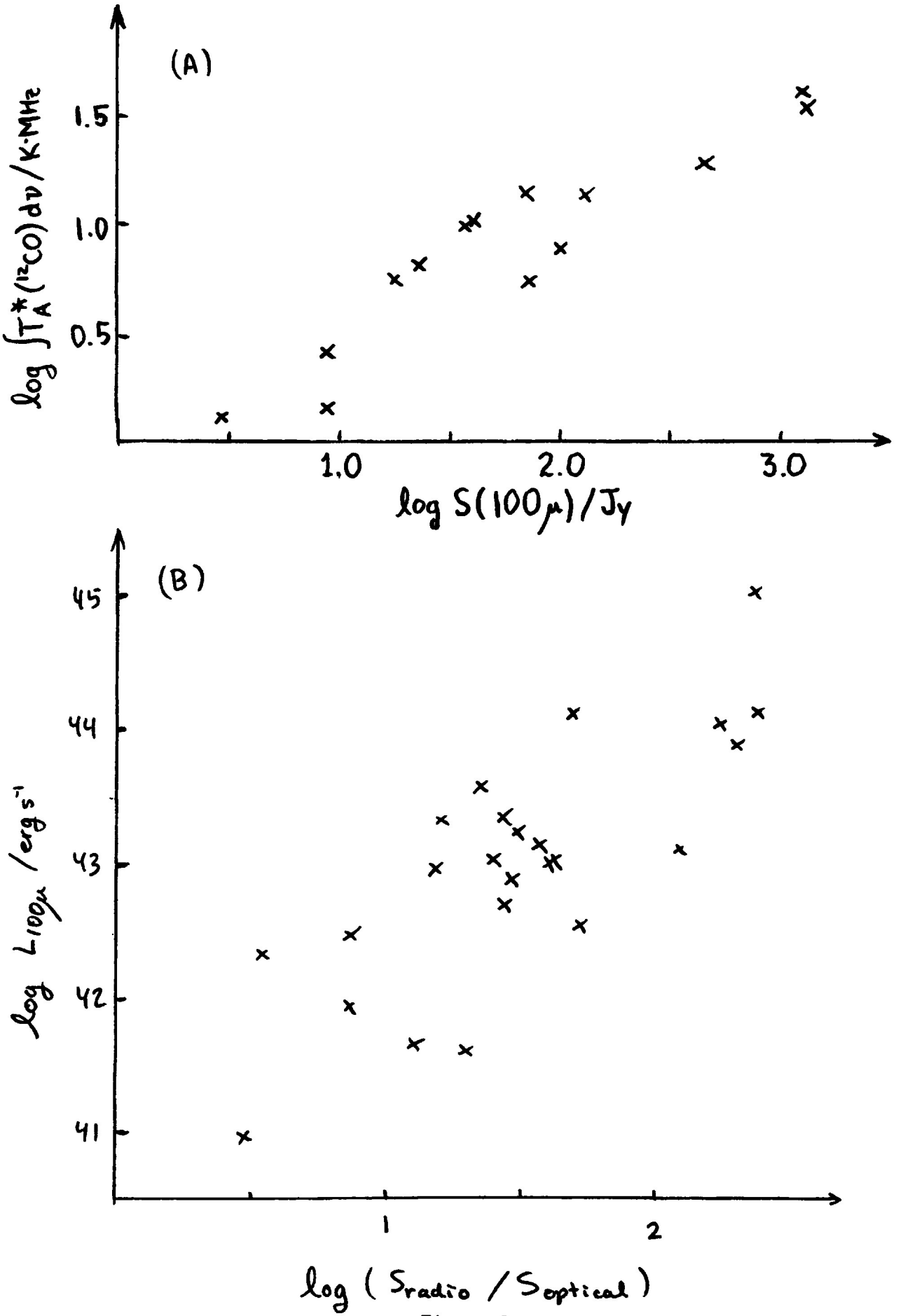
(A)
1.5
1.0
0.5
log ∫T*A(12CO)dv/K·MHz
1.0
2.0
3.0
log S(100μ)/Jy
(B)
45
44
43
42
41
log L100μ /erg s-1
1
2
log (Sradio / Soptical)

Figure 2

THE FAR INFRARED DISK OF M51

J. Smith

Yerkes Observatory, The University of Chicago

ABSTRACT

Far infrared maps and multifrequency photometry are presented for M51 and its companion galaxy NGC 5195. Dust reradiates about half the starlight of the M51 + NGC 5195 system to produce the observed far infrared (80-200 μm) luminosity of 3×10^{10} $L_{\odot}$. Observed with 49" resolution and covering 37 square arc minutes, the maps show that roughly 70% of this luminosity is produced by the 5' (~15 kpc) wide far infrared disk of M51. The photometry shows a difference in energetics at the galactic scale; dust within the central 49" of NGC 5195 [Ip-Ep, Irr II or SBa(r)] is much less abundant and considerably warmer than the ~20 K dust observed throughout the far infrared features of M51 (Sc1). Far infrared properties are given for several galactic-scale complexes of star formation in M51. Relationships are discussed for selected maps of optical starlight and emissions from these components of M51's interstellar medium: dust grains, CO molecules, hydrogen atoms, electrons and H II regions.

TABLE 1

Multiaperture Photometry

Position	Photometer	Aperture (arcsecond)	λ (μm)	F_ν (Jy)	Date
		a) M51			
0,0	A (85-200)	49	130	52 ± 3	3
0,0	A (135-200)	49	170	50 ± 3	3
0,0	SC (85-265)	73	135	82 ± 10	1
0,0	SC (135-265)	73	180	82 ± 4	1
0,0	SM (130-155)	126	140	106 ± 32	1
0,0	SM (160-460)	126	210	126 ± 4	1
0,0	SM (255-460)	126	320	55 ± 8	1
0,0	SC (45- 80)	49	55	*24 ± 4	2
0,0	SC (45- 80)	17 × 55	55	13 ± 2.6	2
15"E,0	SC (45- 80)	17 × 55	55	12 ± 4.1	2
15"W,0	SC (45- 80)	17 × 55	55	11 ± 5.4	2
0,120"N	SC (85-265)	73	135	10 ± 3	1
0,120"N	SC (135-265)	73	180	12 ± 2	1
		b) NGC 5195			
0,0	A (85-200)	49	110	12.4 ± 1.6	3
0,0	A (135-200)	49	170	6.1 ± 1.2	3
0,0	SC (45-120)	33	70	24 ± 3	1

*This 49" photometry, also plotted at 55 μm in Figure 1, is the weighted mean of the three observations made with the 17" × 55" aperture.

Notes. - Positions are relative to the centers of the respective galaxies. The format used for describing the photometers is "x(Δλ)" where Δλ is the half-power bandpass in μm and the codes for x are: A = the array photometer, SC = single channel photometer, SM = submillimeter photometer. F_ν is the flux density (1 Jy = 10^{-26} $Wm^{-2}Hz^{-1}$) observed at the effective wavelength λ and for the indicated aperture diameter or dimensions. The statistical uncertainties are one standard deviation of the mean F_ν. Codes for the dates are: 1 = May, 1980; 2 = August, 1980; 3 = January, 1981.

TABLE 2

Dust Properties for Features and Selected Regions

of M51 and NGC 5195

Location	Size	F (Jy)	T_d (K)	τ	τ_v	Flux (Wm^{-2})	L_d ($L_\odot$)	σ_L ($L_\odot$ pc^{-2})	M_d ($M_\odot$)
M51-Center	0.75	50	20	7×10^{-3}	8	2×10^{-12}	6×10^{9}	1000	7×10^{6}
M51-Bar	6.2	181	20	3×10^{-3}	3	4×10^{-12}	1×10^{10}	230	3×10^{7}
M51-SW	2.5	38	20	1.5×10^{-3}	2	8×10^{-13}	2×10^{9}	120	5×10^{6}
M51-NW	1.3	21	20	1.5×10^{-3}	2	4×10^{-13}	1×10^{9}	120	3×10^{6}
M51	30	387	20	1.3×10^{-3}	1.5	8×10^{-12}	2×10^{10}	100	6×10^{7}
NGC 5195	0.75	6	65	3×10^{-5}	0.04	1×10^{-12}	3×10^{9}	560	3×10^{4}
Map	37	393	20	1×10^{-3}	1	9×10^{-12}	3×10^{10}	90	6×10^{7}

Notes. - The regions of column 1 are also shown in Figure 2. 'M51' refers to the optically bright portion of M51 mapped at 170 μm and also containing much of the two spiral arms (see dashed line in Figure 2b). Each feature's size is in square arc minute. F is the 170 μm flux density (1 Jy = 10^{-26} Wm^{-2} Hz^{-1}) computed from the contour map in Figure 2. For each optically thin region in M51, dust temperatures (T_d) are computed from 130 and 170 μm flux densities (also see Table 1 and Figure 2c) and Q = constant × ν^2 for the absorption efficiency of the dust. For the warmer dust of NGC 5195, T_d is computed from the 70 and 110 μm flux densities (see Table 1) and Q = constant × ν. τ is the mean optical depth in dust at 170 μm computed from F, T_d and Size. $\tau_v \sim 10^3 \times \tau$ is the mean optical depth near 1/2 μm (see Smith et al. 1979). The flux refers to the 80-200 μm interval except that 45-400 and 45-200 μm apply to M51-Center and NGC 5195, resp. L_d is dust luminosity computed from the flux and 9.6 Mpc for the distance between M51 and earth. σ_L is the mean surface brightness for L_d. M_d is the dust mass evaluated from F, T_d and G=0.03 g cm^{-2} for the dust grains at 170 μm (see Smith et al. 1979).

TABLE 3

Decomposition of Mass and Luminosity

for the Central Regions of M51 and NGC 5195

Galaxy	M_T	$\frac{100\ M_d}{M_T}$	L_*	$\frac{L_d}{L_d + L_*}$	$\frac{M_T}{L_*}$	$\frac{M_T}{L_d + L_*}$
M51	5×10^9	0.2	3×10^9	0.7	1.6	0.6
NGC 5195			3×10^9	0.6		

Notes. - Values refer to the central regions of diameter = 49" (2.3 kpc). Units for masses and luminosities are $M_\odot$ and $L_\odot$. Corrected to the 9.6 Mpc distance, the rotation curve analysis of Tully (1974) would give $\sigma = 6.7 \times 10^5\ r^{-1}\ M_\odot\ pc^{-2}$ which was integrated to produce the total mass M_T. 100 M_d is the interstellar mass (atomic + molecular) inferred from the dust mass of Table 2. L_* is the stellar luminosity (not corrected for extinction in M51) produced by integrating the 0.36 - 2.3 μm photometry (aperture = 40-50 for M51 and = 30-40" for NGC 5195) of Penston (1973). Table 2 gives the dust luminosity (L_d) used to compute the total amount of starlight, $L_d + L_*$.

TABLE 4

Some Quantities Relevant to Studies of the

Interstellar Hydrogen in M51 and NGC 5195

Feature	a) Energetics			b) Masses and Densities				
		5 GHz Flux Densities						
	N_c(IR) 10^{52} photons s^{-1}	F(IR) (mJy)	F(OBS) (mJy)	100 M_d ($M_\odot$)	N(H) (atom cm^{-2})	σ_M ($M_\odot pc^{-2}$)	σ_M/σ_H	$M(H_2)$ ($M_\odot$)
M51-Center	30	31	0.6	7×10^8	1.5×10^{22}	120	>50	2×10^8
M51-Bar	55	60	13.9	3×10^9	7×10^{21}	55	10	
M51-SW	12	13	2.3	5×10^8	4×10^{21}	30	5	
M51-NW	6	7	4.3	3×10^8	4×10^{21}	30	3	
M51	120	130	31.7	6×10^9	3×10^{21}	25	3	
NGC 5195	16	17	—	3×10^6	7×10^{19}	0.6	>0.3	
Map	135	145	{33.1 / 110}	6×10^9	2×10^{21}	20	3	

Notes—$N_c(IR) \equiv \langle N_c/L_* \rangle \times L_d$ where L_d is the dust luminosity (see Table 2), N_c is the Lyman continuum luminosity, L_* is stellar luminosity and $\langle N_c/L_* \rangle = 5 \times 10^{43}$ photons s^{-1} $L_\odot^{-1}$ applies to an ensemble of OB stars distributed according to the Salpeter-Sandage initial luminosity function. F(IR) is the expected H II emission inferred from the far infrared flux (see Table 2) and the mean ratio (6×10^{15} Hz) of infrared flux to radio flux density observed for galactic H II regions (e.g., in Harper and Low 1973). F(OBS) are the 5 GHz flux densities (in Israel 1980) contributed by discrete, visible H II regions except for

Notes (cont.)—the 110 mJy given for the Map entry; Israel inferred this value from the radio spectrum of M51 and arguments involving its spectral index near 5 GHz. $100 \times M_d$ is the total (molecule + atom) interstellar mass. See Table 2 for the dust mass M_d. N_H and σ_M are column densities inferred from 100 M_d. σ_M/σ_H is the total/atomic ratio of column densities. σ_H was found by integrating the density map of Weliachew and Gottesman (1973). Rickard et al. (1977) gives the molecular hydrogen mass $M(H_2)$ which refers to the central 65" of M51.

TABLE 5

Comparison of Galaxies

a) Central Regions

Galaxy	L_d ($L_\odot$)	$M(H+H_2)$ ($M_\odot$)	T_d (K)
M51	6×10^9	7×10^8	20
NGC 5195	3×10^9	3×10^6	65
The Galaxy	10^9	$3\text{-}7 \times 10^8$	25-30

b) Disks

Galaxy	σ_L ($L_\odot$ pc^{-2})	σ_M ($M_\odot$ pc^{-2})	T_d (K)
M51	100-200	25-55	20
The Galaxy	20-85	5-10	<25-40

Notes—"Central Regions" and "Disks" refer to the galactocentric radii $\leq$1 and 2-7 kpc, resp. Entries for M51 and NGC 5195 are based on Tables 2 and 4. For the Galaxy, values were taken from the indicated literature: Dust luminosity density (σ_L) from Boisse *et al.* (1981), dust luminosity (L_d) from Low *et al.* (1977), dust temperature (T_d) from Boisse *et al.* and Serra *et al.* (1978), interstellar mass density (σ_M) from Gordon and Burton (1976) and interstellar mass [$M(H+H_2)$] from Bania (1977).

Figure Captions

Fig. 1 — Far infrared spectra of the central 49" of M51 and NGC 5195. See Table 2 except for the 400 μm photometry from Harper (1981). Informative dust continuum spectra (Smith 1982) are also shown for two galactic objects. Statistical uncertainties (one standard deviation of the mean) are shown where they are larger than the symbols. a) Both smooth curves are F_ν = constant × ν^2 B_ν (T_d = 20 K) for $\lambda \geq 100$ μm. Similarities may therefore be drawn between the excitations of the cold dust in the CO galaxy M51 and the optically opaque Orion Molecular Cloud-2. b) The shorter peak wavelength shows that dust in NGC 5195 is much warmer than in the central 49" of M51. Comparable 70-170 μm spectra (T_d = 55-65 K) are observed for NGC 5195 and the center of the low excitation H II region M43.

Fig. 2. — Map of 170 μm dust emission from M51 and NGC 5195 (1' = 2.8 kpc). The major discovery is the far infrared disk of M51 (contours = 9-70, I = 7-40 × 10^{-19} W m^{-2} Hz^{-1} sr^{-1}, diameter ∿15 kpc) which has been emphasized by the choice of logarithmic contours spaced by $\sqrt{2}$. The optical center of M51 ('+') is the brightest measured position with F = 50 Jy/beam and I = 7.8 × 10^{-18} W m^{-2} Hz^{-1} sr^{-1}. The dashed line shows the mapped region; 1 σ level ∿ 2 Jy/beam, faintest contour of 9 corresponds to 2 σ and sampling interval = beam diameter = 49" (see also Figure 2c). b) A blue-sensitive photograph of M51 (from Yerkes Observatory) with the contours of dust emission superposed.

c) Dust features and their temperatures (T_d). Boundaries for the features approximate selected contours of 170 μm surface brightness except for the 49" diameter regions centered on M51 and NGC 5195. The ratio of flux densities, F(130)/F(170 μm), indicates relative T_d; values less than 1 correspond to T_d < 20 K, the dust temperature of M51-Center. Typical uncertainties (one standard deviation of the mean ratio) are ±0.15 except for the ±0.4 applicable to NGC 5195. The 49" diameter beam used for the mapping is shown.

Fig. 3. — Comparison of selected observations of the dust and interstellar gas in M51 and NGC 5195. a) Map of 170 μm dust emission also shown in Figure 2. b) Map of atomic hydrogen column densities after Weliachew and Gottesman (1973, beam diameter = 2'). $N_H < 4.2 \times 10^{20}$ atoms cm^{-2} at the center of M51 ('+'). The linear contour interval is 1.4×10^{20} cm^{-2}. The continuous rim of peak atomic density surrounding the far infrared disk of M51 is marked roughly by '●'. c) Map of integrated CO (J = 1-0) line emission (K kms^{-1}) from Rickard et al. (1981, beam diameter = 65"). Contours are spaced by 2 K kms^{-1} ∿ 1 σ. d) Map of 170 μm dust emission superposed on a map of the most intense H II regions observed in H_α light (intensity = 3 and 4 in Carranza et al. 1969). e) Selected contours (4, 6, 8, 11, 15, 25, 30 and 40) from the map of 21 cm nonthermal emission given by Mathewson et al. (1972, beam = 24" × 32"). Contour = 1 corresponds to 0.8 K in 21 cm brightness temperature.

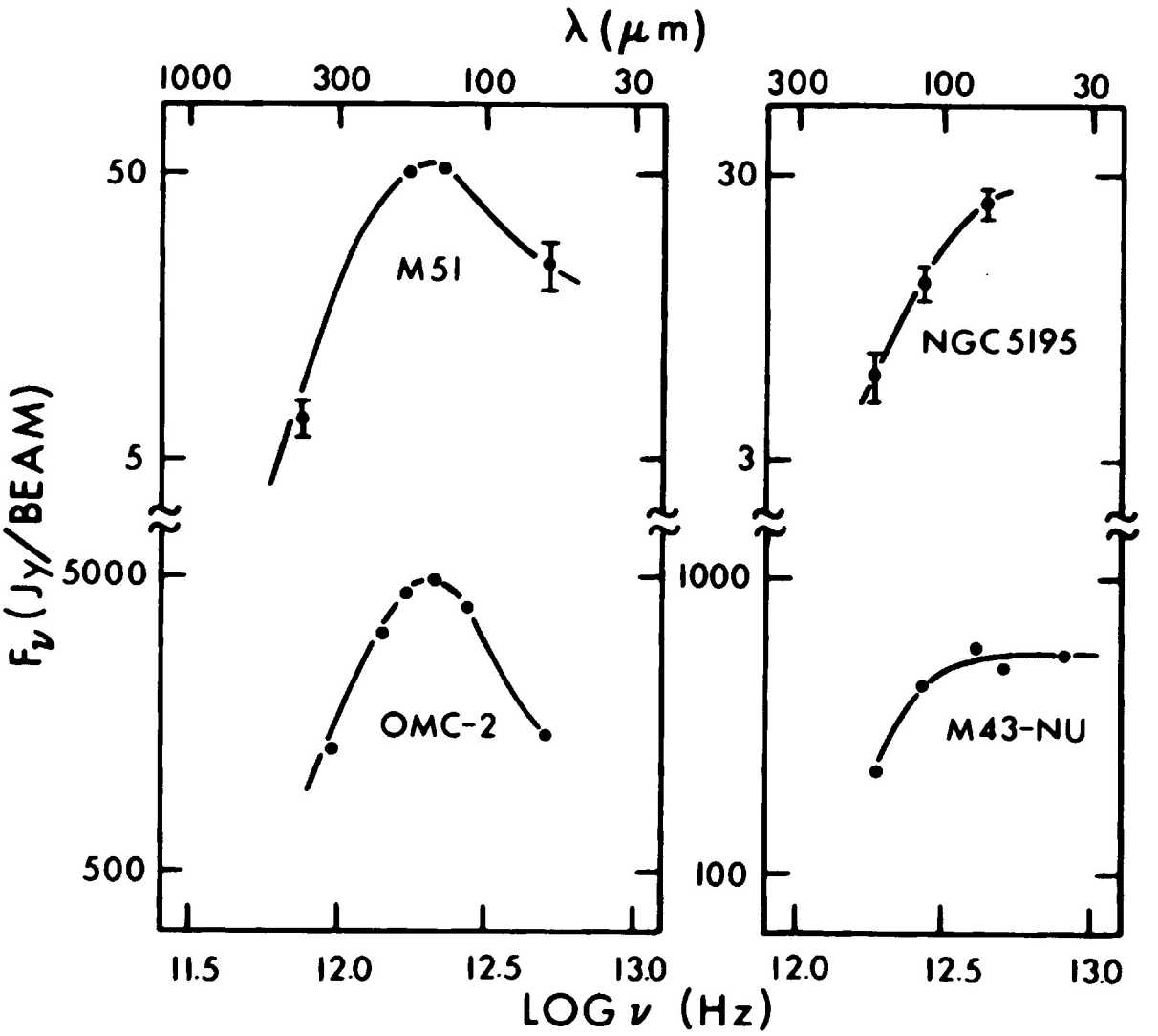
λ (μm)
1000
300
100
30
300
100
30
50
5
30
3
5000
500
1000
100
M51
NGC5195
OMC-2
M43-NU
F_ν (Jy/BEAM)
11.5
12.0
12.5
13.0
12.0
12.5
13.0
LOG ν (Hz)

FIGURE 1

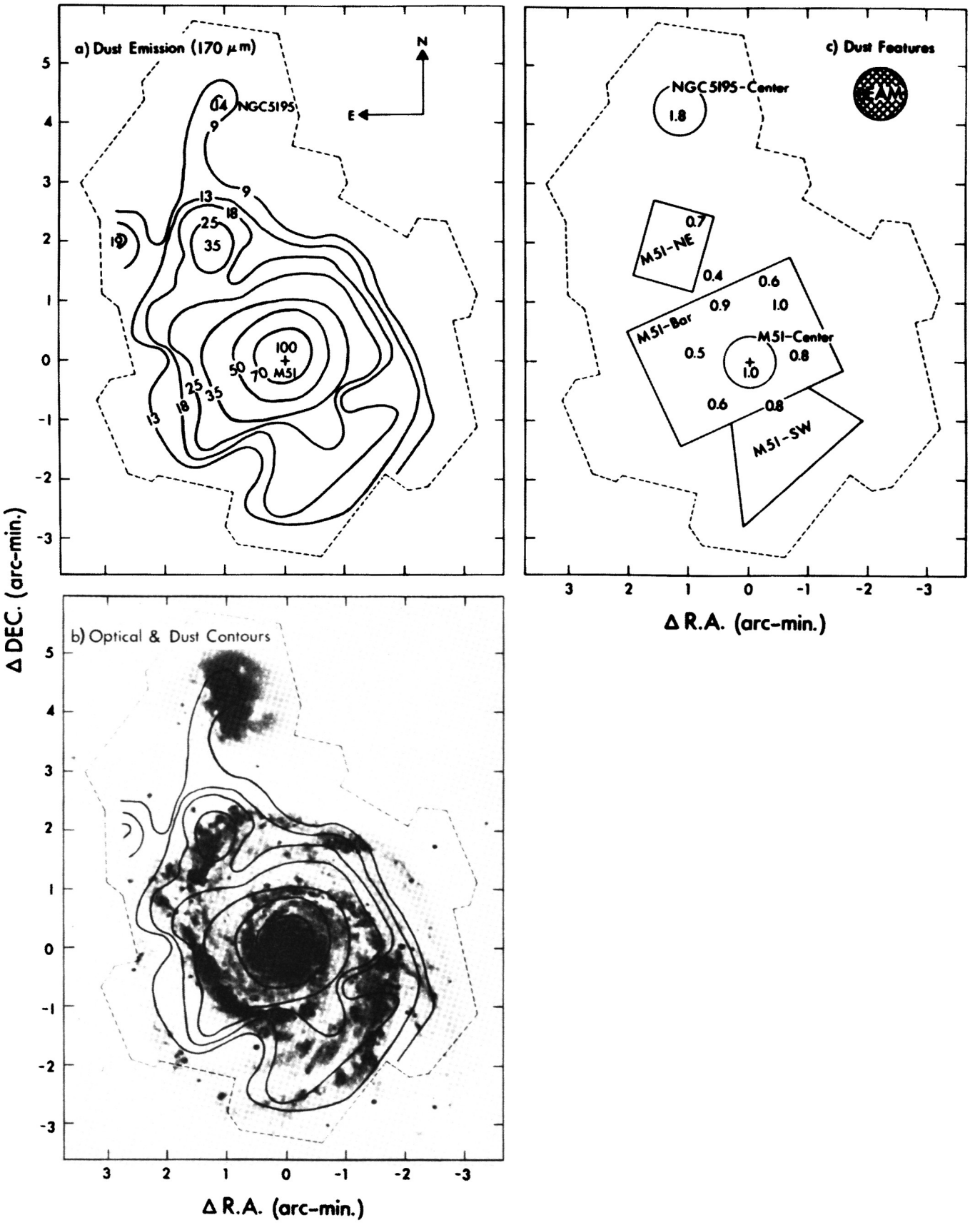
a) Dust Emission (170 μm)
N
E
NGC5195
M51
b) Optical & Dust Contours
c) Dust Features
NGC5195-Center
1.8
M51-NE
0.7
0.4
0.6
0.9
1.0
M51-Bar
M51-Center
0.5
0.8
1.0
0.6
0.8
M51-SW
Δ DEC. (arc-min.)
Δ R.A. (arc-min.)

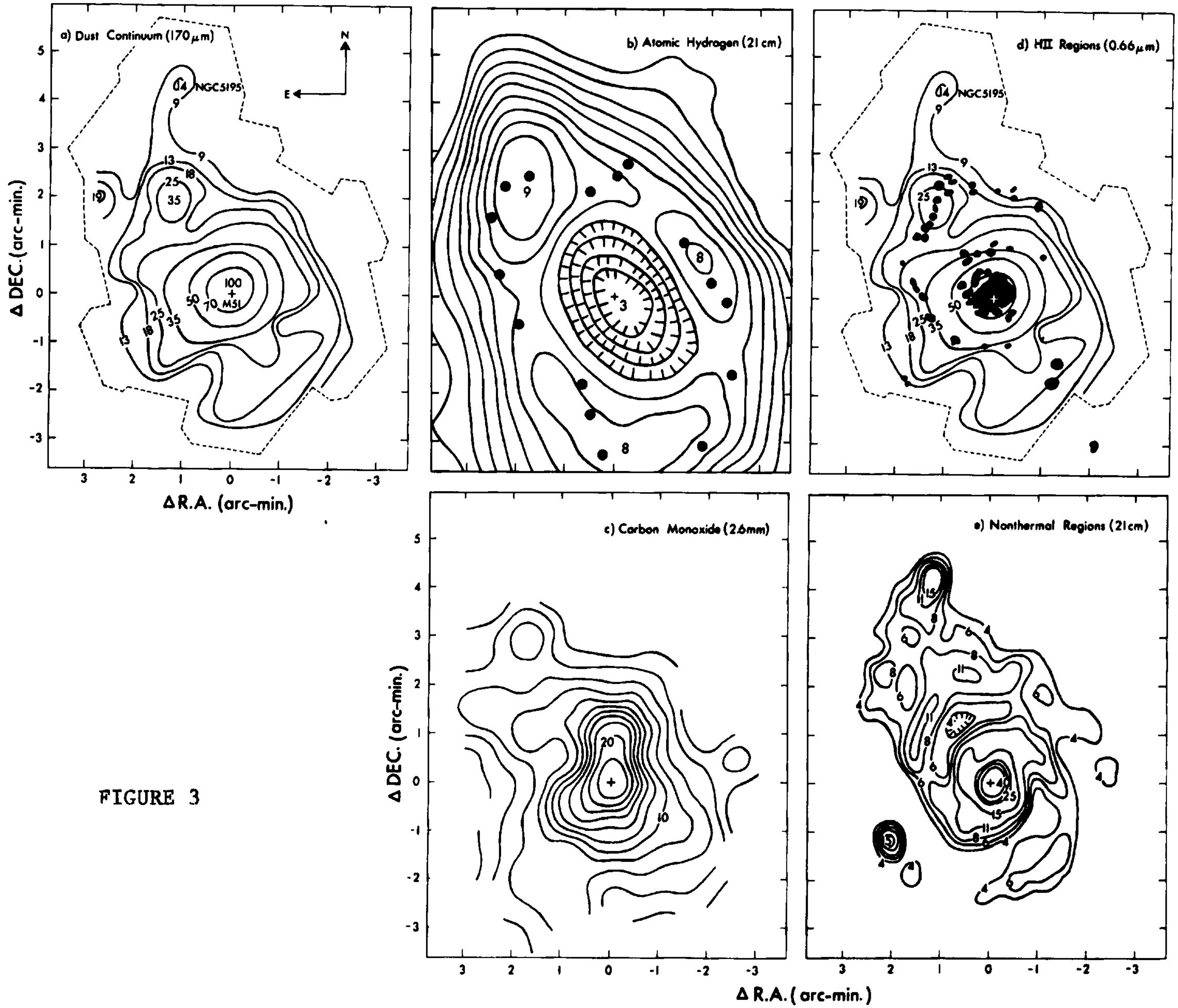
a) Dust Continuum (170 μm)
N
E
NGC5195
M51
Δ DEC. (arc-min.)
Δ R.A. (arc-min.)
b) Atomic Hydrogen (21 cm)
d) HII Regions (0.66 μm)
c) Carbon Monoxide (2.6mm)
e) Nonthermal Regions (21cm)

FIGURE 3

VLA DECTECTION OF H110α in M82

E. R. Seaquist - University of Toronto
M. B. Bell - Herzberg Institute of Astrophysics
R. C. Bignell - National Radio Astronomy Observatory

Our purpose here is to report the detection, with the VLA, of the H110α line (4.8GHz) in the gas rich galaxy M82. The radio recombination line work in external galaxies to date has been done almost exclusively with single dishes (of Bell, 1980). The detected recombination lines in M82 arise by stimulated emission in the presence of nonthermal radio radiation behind ionized hydrogen.

The present work in collaboration with M.B. Bell of the Herzberg Institute of Astrophysics, Ottawa, and R. C. Bignell of the NRAO (VLA) employed the B configuration of the VLA. The bandwidth was 25 MHz with 16 channels, providing a velocity resolution of 96 kms^{-1}. The maps which show the line emission are heavily tapered to produce a synthesized beam of ~4". The integration time is about 4 hours.

The line emission is strongest at $V_{LSR} \cong 163$ kms^{-1}, which is the velocity of peak emission seen with single dishes. This peak (4.4 mJy $beam^{-1}$) occurs about 8" SW of the IR nucleus of the galaxy. Figure 1 shows a continuum map and a line map with 3 channels averaged & centered on $V_{LSR}=163kms^{-1}$. The cross marks the IR nucleus. The peak emission is coincident with emission at similar velocity in NeII at λ12.8μ (Beck et al 1978) and with a general region of intense emission in Bα (Simon and Joyce, 1979). It also coincides with the continuum radio source labelled 42.5 + 59 in the M82 map by Kronberg and Wilkinson (1975).

More recently, Kronberg et al (1981) have identified this area as having a flat continuum spectral index (~-0.2) between 1.4 and 4.8GHz compared to the rest of the galaxy (~-0.7). It is now clear that this flattening is produced by free-free absorption at the lower frequency in the same gas that produces the line emission.

The potential of the recombination line maps is that they may be compared with the continuum maps and IR recombination line maps to infer something about the physical state of the gas and the relative positions of thermal and nonthermal components. Our present plan is to improve the S/N ratio on the maps by using C configuration at H110α and B configuration at H166α (1.4GHz) and by doubling the integration time. We propose also to observe NGC 253 for which radio recombination lines have been detected with a single dish.

REFERENCES:

Beck, S. C. et al. ApJ 226, 545.

Bell, M. B. (1980) in Radio Recombination Lines, P. A. Shaver (ed.) p. 259.

Kronberg, P. P. et al. (1981) ApJ 246, 751.

Kronberg, P. P., and Wilkinson (1975) ApJ 200, 430.

Simon, M. and Joyce, R. R. (1979) ApJ 227, 64.

ERS/cbm

CONTINUUM (CLEAN)

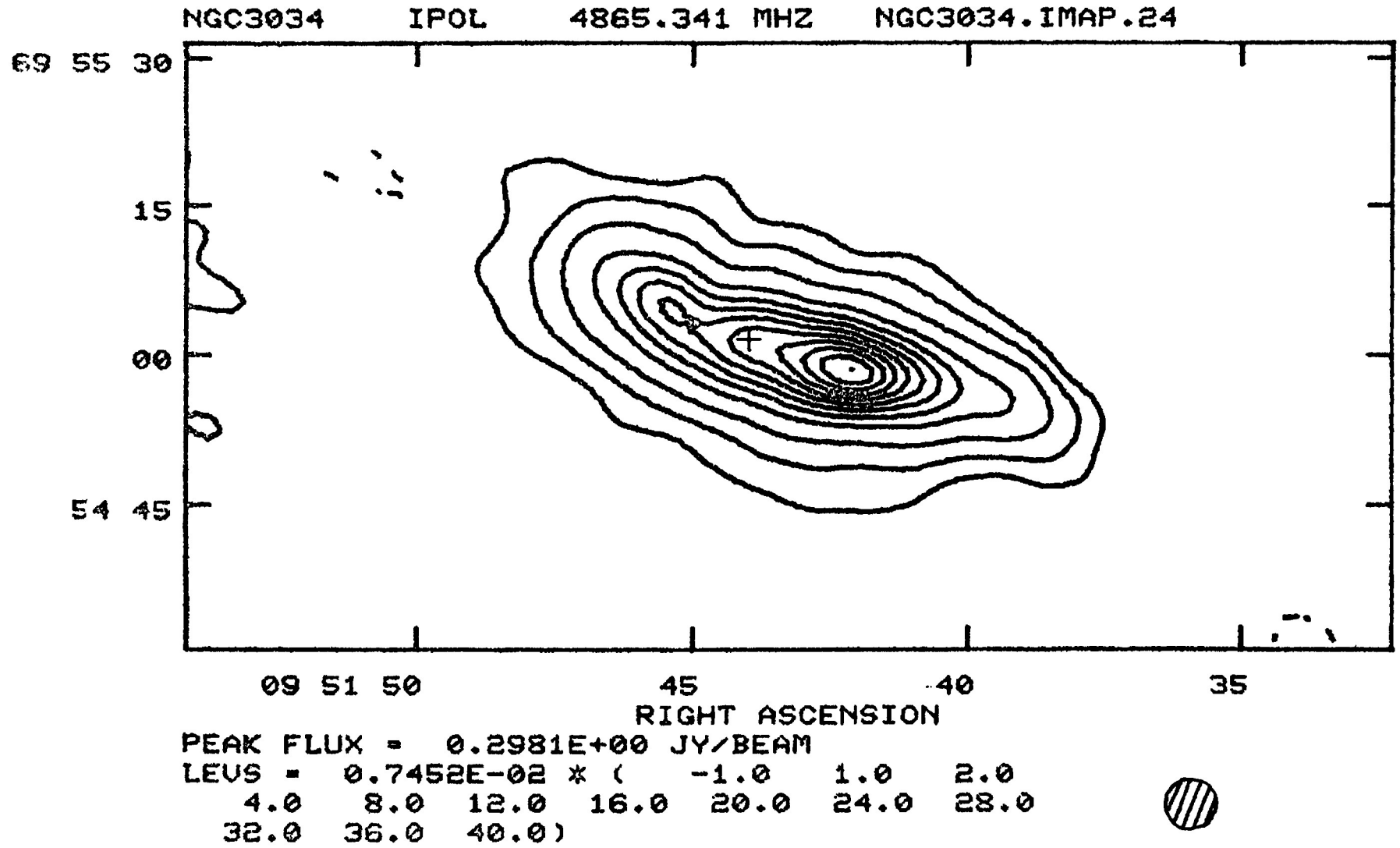

FIGURE 1(a)

Channels 7, 8, 9 (Hanning) $19\ kms^{-1} \leq V \leq 307\ kms^{-1}$

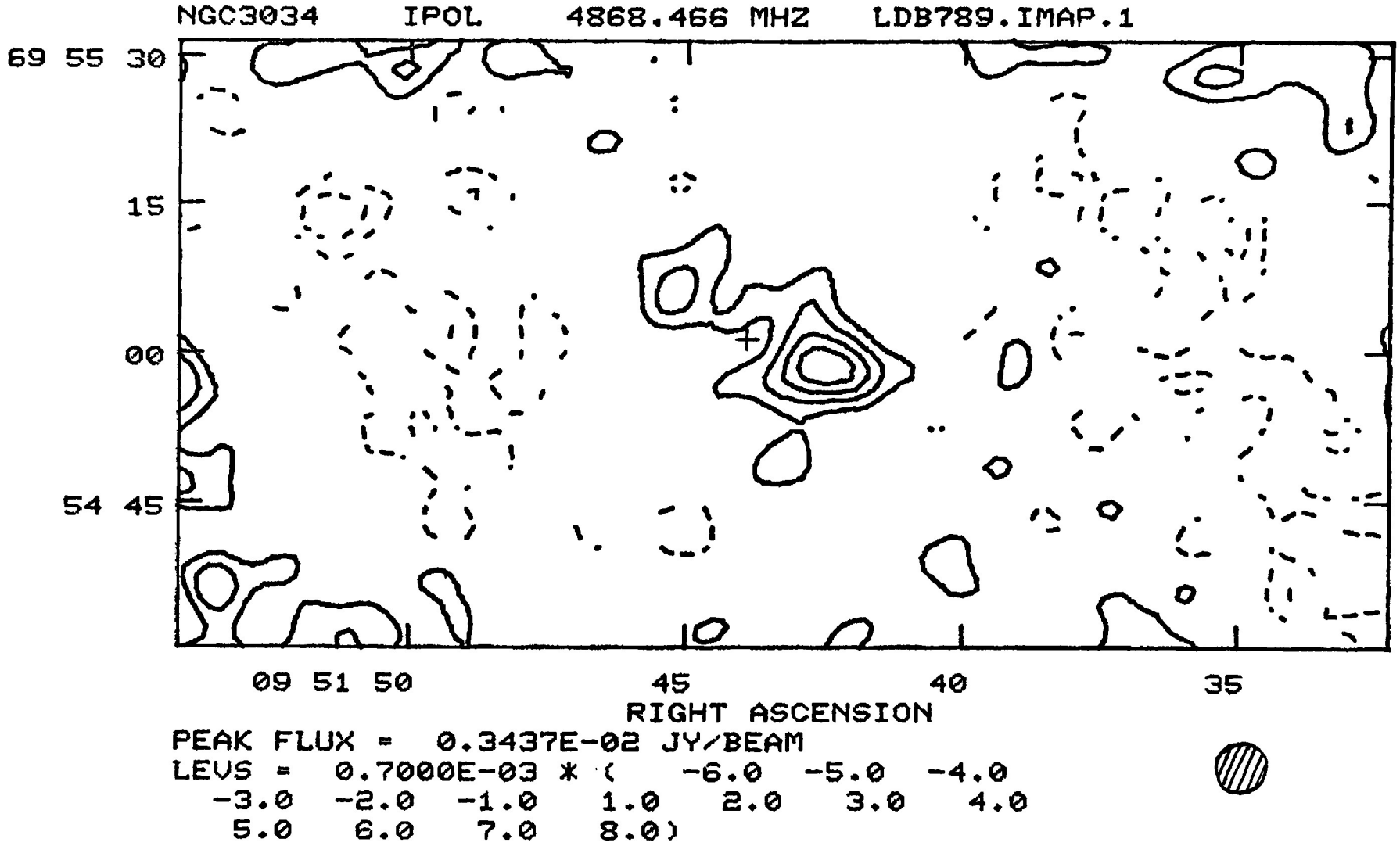

FIGURE 1(b)

HI KINEMATICS OF SPIRAL GALAXIES

Albert Bosma

Columbia University

In this contribution I would like to emphasize a few points about HI studies and their relevance for the interpretation of the new CO observations of nearby spirals.

1°. HI global profiles are available for all the galaxies sofar detected in CO. A comparison of the recently observed CO profile of NGC 4303 and the HI profiles published in the literature (Davies and Lewis, 1973; Huchtmeier et al., 1976; Dickel and Rood, 1978 and Shostak, 1978) shows that while the CO profile is flattopped the HI profile has two "horns" characteristic for a flat rotation curve and an extended HI distribution. This implies that the CO-distribution is more peaked towards the centre, as is the case in other Sc's like NGC 6946 and IC 342.

2°. Our Galaxy and M31 have a radial distribution in CO which differs from the CO distribution in M51, NGC 6946, IC342 and M101. In the latter 4 galaxies the CO follows the light distribution, in our Galaxy and in M31 there is a "ring" type distribution. There are several galaxies studied in HI which have a radial distribution in HI gas with a hole or a depression in the centre. It seems that the depression in Sc-galaxies is now compensated by abundance in H_2. In earlier type spirals, however, the hole remains there. In general I would ascribe this to 2 causes: a) the presence of a bulge and b) the presence of a bar.

There are several cases where the HI hole more or less coincides with the bulge: NGC 2841, M81 and M31 are good examples. In our Galaxy there is, however, a lot of gas (CO and HI) in the central 1 kpc, so the analog with the other galaxies with bulges does not hold. However there are several early type barred spirals where the bar seems to be clear of gas. Current models

of barred spirals, in particular those of Schwarz (1981), indicate that the gas can be easily moved away from a smooth distribution into rings and onto the centre by the continuing presence of a bar. My new VLA 21 cm line observations of the early type barred spiral NGC 1398 clearly shows the presence of a hole which is probably larger than the size of the bulge. For our own Galaxy, which is of a later type than NGC 1398, I would like to revive interest in the suggestion that there is a central bar which causes the dip in the radial distribution of gas around 2-4 kpc and the concentration of gas in the centre.

3°. The new CO observations indicate that the ratio of surface densities of light and molecular gas is constant as function of radius in at least 4 Sc galaxies. Since the mass-to-light ratio in the inner parts of these galaxies probably does not vary all that much, and since most of the gas is in molecular form, it appears that the ratio of total mass to gas is constant. This is interesting in view of the now well established abundance gradients in these galaxies (see Pagel and Edmunds, 1981 for a review). In a simple model of galactic evolution we have

$$\log \frac{\text{total mass}}{\text{gas mass}} * \text{yield} = \text{abundance of element i}$$

where the yield is the ratio of the rate at which heavy elements are produced by nucleosynthesis and ejected into the interstellar gas to the net rate at which hydrogen is removed from the interstellar gas by star formation. If this simple model holds, which may not be the case, then the yield must vary as function of radius in order to produce an abundance gradient. Since now

the data are available both on the abundances and on the gas-to-mass ratio, at least as good as we can get them, more work should be done to study this problem.

References:

Davies, R. D. and Lewis, B. M. (1973). Mon. Not. R. Astron. Soc. *165*, 231.

Dickel, F. R. and Rood, H. J. (1978) Astrophys. J. *223*, 391.

Huchtmeier, W. K., Tammann, G. A., Wendker, H. J. (1976) Astron. Astrophys. *46*, 381.

Pagel, B. E. J. and Edmunds, M. G. (1981) Ann. Rev. of Astron. Astrophys. *19*, 77.

Schwarz, M. P. (1981), Astrophys. J. *247*, 77.

Shostak, G. S. (1978), Astron. Astrophys. *68*, 321.

On the HI Content and Size of Galaxies

Riccardo Giovanelli, NRAO

The HI content of galaxies has traditionally been expressed by using the ratio M_H/L, between HI mass and blue luminosity. One of the main virtues of that ratio is its distance independence. For many years M_H/L has been known to be a function of morphological type, in the sense that the average value of M_H/L for galaxies of a given classification is a fairly well defined function of type itself. However, the range of values of M_H/L observed within a given type (a real spread, not due to uncertainties in the data) may be as large as the range of values of $\langle M_H/L \rangle$ over all morphological classifications. Hence we ask: which other parameter is important in predicting the HI content of a galaxy, besides type?, or, can we find a better one?

A statistically homogeneous sample of 324 "isolated" galaxies, observed in collaboration with Martha Haynes at Arecibo, was used to approach that question. The sample covers a wide range of luminosities, redshifts, types and sizes; its main virtue consists in being comprised by galaxies as little affected by environmental effects (such as tidal interactions with neighbors, sweeping or evaporation due to a conspicuous intergalactic medium, other consequences of high galaxian densities) as possible; i.e. it constitutes as "clean" a sample as one can possibly define.

Bottinelli and Gouguenheim (1974) suggested that, besides on type, there is a residual dependence of M_H/L on luminosity. The dependence is confirmed by the isolated galaxy data, being stronger for earlier types. However, a better correlation is found between M_H/L and optical surface brightness (SB). In fact, the dependence of M_H/L on SB is more than residual in character: the

average difference in log (M_H/L) between two galaxies of different type (say an S0 and an Sc) but same SB, say 16.5, is much smaller ($\sim$ 0.2) than the difference between two galaxies of the same type, say Sc, but different surface brightness, say 15 and 18 ($\sim$ 0.9), as illustrated by comparing figures 1a and 1b.

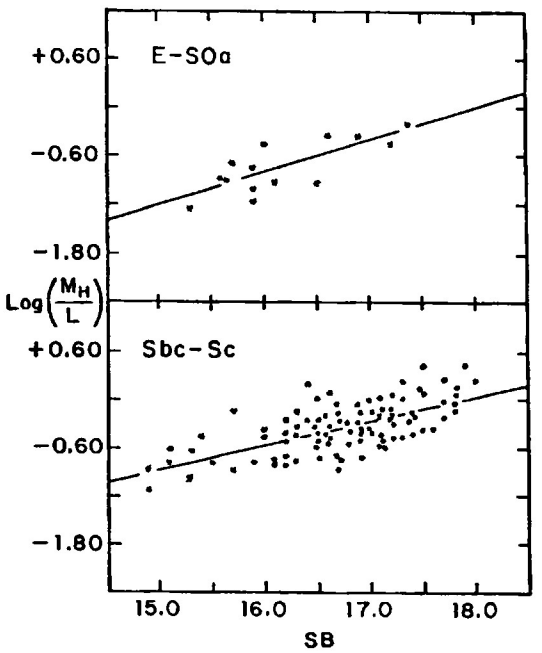

Figure 1.

In addition, there is a good deal of similarity between the lines that describe the relationship between log (M_H/L) and SB for different types. This similarity can be enhanced by subtracting the bulge luminosity from the total luminosity in the expression of M_H/L and SB; in other words, if we compare the properties of the disks of galaxies.

Disk-to-bulge ratios are only available for few galaxies, but the average disk to bulge ratio is known to depend on the morphological type (the situation is somewhat similar to the dependence of M_H/L: average values vary monotonically with type, but the scatter within a type is very large, and real). Average values of the disk to bulge ratio for each type were drawn from the work of Boroson (1981), de Vaucouleurs (1977) and Burstein (1980), and the luminosity of each galaxy in the sample was reduced by a factor indicated by the average disk-to-bulge ratio corresponding to its type. This conversion to a set of "statistical" disk luminosities produces a convergence of the lines best fitting the log (M_H/L) vs. SB plots of various morphological types. Although the difference between fits corresponding to different types is not completely eliminated, it is substantially reduced.

It appears clear that the disk SB, a distance independent parameter, may be the best optical parameter to diagnose the HI content of a galaxy of any morphological type; however, disk luminosities are not readily available. Total surface brightness, i.e. including both disk and bulge, is an acceptable tool if one keeps in mind the morphological bias. But a parameter more tightly associated with disk properties is desirable. Such may be the diameter. In fact, the slope of the log (M_H/L) vs. SB fits is not far from 0.4; such a slope implies a very tight correlation between M_H and the diameter D. Figure 2 illustrates such correlation separately for all morphological types. D in

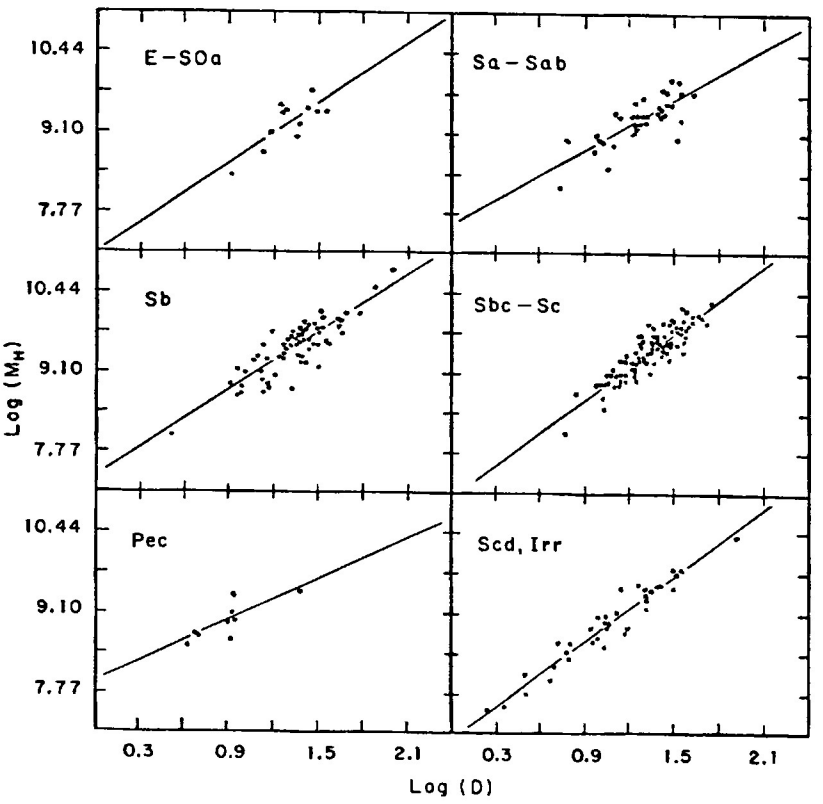

Figure 2.

fig. 2 is an optical diameter (the blue one in the UGC). About 40 of our sample galaxies were large enough to be mapped. For those we obtained HI diameters. The correlation between M_H and D_H is excellent, and no noticeable

differences were found over the range of morphological types of the galaxies mapped, Sa to Scd, as shown in fig. 3. The correlations between M_H and diameter are all of rather high quality, and slopes, rather similar and close to a $M_H \propto D^2$ law. Such a law would imply that the HI surface brightness, averaged over the whole optical disk, is constant. The best fit for figure 3 is of the type $M_H \propto D^{1.85}$.

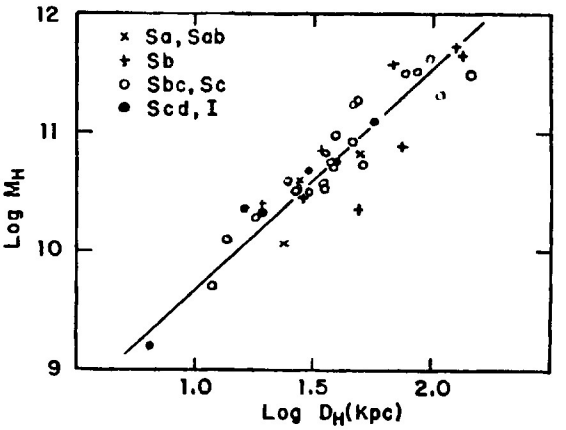

Figure 3.

These results, although still preliminary, allow the tentative conclusion that surface brightness, or even better, disk surface brightness, is the best distance-independent diagnostic optical tool for the HI content, expressed as M_H/L ratio, of galaxies of any morphological type. The optical diameter, which for most galaxies is a relatively clean disk property, correlates with HI mass best than any other parameter; it is unfortunately dependent on the assumed distance scale. However, because of the closeness of the relation between M_H and D to an $M_H \propto D^2$ law, the error introduced by the uncertainty on the distance scale is small, and the residual dependence of M_H on morphological type is a mere perturbation, described in the following paragraph.

If $f(D) = a + b \log D$ is the best fit line to a $\log M_H$ vs. $\log D$ plot, the residuals $\log M_H - f(D)$ show a weak correlation with luminosity and type, in the sense that galaxies of type earlier than Sb and high luminosity tend to show negative residuals, i.e. low HI mass for their size. Now, the luminous galaxies of early type that have been synthesized in HI tend to show very deep central "holes" in their radial distribution of HI surface density. They also tend to be objects of higher bulge-to-disk luminosity ratio. Are these central holes

as void of interstellar material as the HI maps suggest? The evidence collected via CO observations seems to point in that direction. Galaxies that show an exponential disk of molecular gas tend to be objects of low disk-to-bulge ratios and shallow central holes in their HI distribution. On the other hand, objects that have not been detected, usually after observations of their centers, have large disk to bulge ratios or prominent holes in their HI distribution. While M51 is a good prototype of the first class, M31 is a suggestive example of what most galaxies of the second type may be like: while largely swept of gas in the central regions, molecular and neutral gas disks appear outside of the bulge-dominated regions. I conclude proposing that disk-to-bulge ratios and shape of the HI radial distribution may be attractive diagnostic tools of the characteristics of the molecular content of galaxies.

References

Boroson, T. 1981, Ap. J. Suppl. Ser. 46, 177.

Bottinelli, L. and Gouguenheim, L. 1974, Astr. Ap. 36, 461.

Burstein, D. 1979, Ap. J. 234, 435.

de Vaucouleurs, G. 1977, in "The Evolution of Galaxies and Stellar Populations", ed. by B. M. Tinsley and R. B. Larson (New Haven: Yale Univ. Press), p. 43.

SYSTEMATIC DYNAMICAL PROPERTIES OF SPIRAL GALAXIES

Norbert Thonnard
Department of Terrestrial Magnetism
Carnegie Institution of Washington

We now have high resolution long slit spectra in the Hα region for 60 spiral galaxies of Hubble types Sa, Sb and Sc, and high signal to noise global 21-cm neutral hydrogen profiles for approximately 3/4 of these galaxies. The sample was chosen carefully to be well classified by Hubble type, to have a large spread in luminosity at each Hubble type, not to be strongly barred, and to be of high enough inclination to minimize deprojection errors. We discuss below some of the salient characteristics and systematic properties of spiral galaxies that can be inferred from the data. Distances are derived from the redshift using H = 50 km s^{-1} Mpc^{-1}.

I. Observed Dynamical Properties

In Figure 1 we show an image tube photograph (of moderate exposure in blue, which emphasizes inner structure) and a spectrum along the major axis for NGC 1035, a typical low luminosity Sc, and NGC 753, a typical high luminosity Sc. Note the characteristic features of the low luminosity galaxy: small radius, knotty, ill-defined arms, weak continuum in the nucleus, gentle velocity gradient through the nucleus with rotational velocities increasing to the outer extremes, and no significant differences in emission line characteristics between the nuclear region and the outer regions of the galaxy. The high luminosity galaxy, instead, has a large radius, well-defined spiral arms, strong, stellar nucleus, most of the rotational velocity gradient occurring in the nucleus with essentially constant rotational velocity elsewhere, and a definite break in emission line characteristics at the nucleus with [NII] stronger than very weak or absent Hα.

Rotation curves derived from spectra for 21 Sc galaxies are shown in the next figure (Rubin, Ford and Thonnard, 1980, Ap.J., 238, 471).

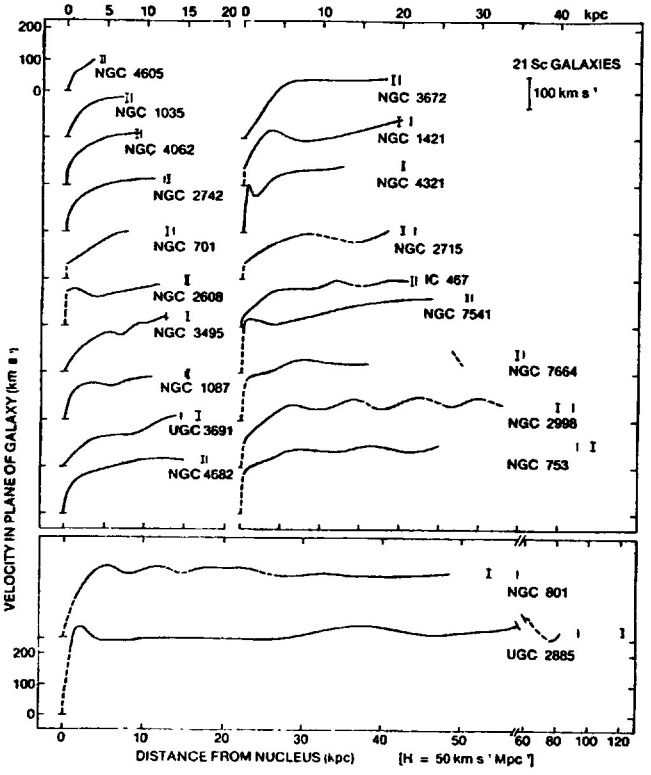

The galaxies are arranged in order of increasing radius; ordering by increasing luminosity would be essentially the same. Note that the small galaxies have rotation curves that predominantly rise slowly at the center and continue rising to the outer edge of the galaxy, reaching rotational velocities not much greater than 100 km s^{-1}, whereas for the large galaxies, the rotation curve rises steeply at the center and then remains essentially constant or only slightly rising to a maximum that is higher than 200 km s^{-1}. The same general features are seen in the Sb galaxies (Rubin, Ford, Thonnard and Burstein, 1982, in preparation), with the exception that all rotational velocities are higher at equivalent luminosity.

II. Effects of Dynamics on Global 21-cm Profiles

The observed global neutral hydrogen velocity profile results from the convolution of the hydrogen distribution and velocity field of the galaxy. Knowing the rotation curve eliminates one of the variables, making interpretation of profile shapes simpler. The following illustration indicates the principal variables governing the profile shape:

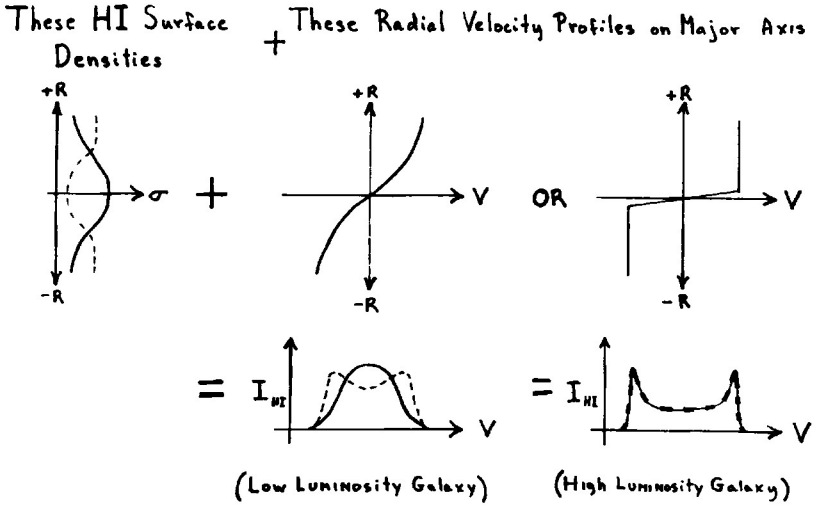

Note that for a rotation curve that is rising over most of the galaxy radius, the global profile shape is quite sensitive to the hydrogen distribution; a centrally peaked HI distribution will produce a profile with a single peak, whereas a flat HI distribution with a central depression produces the characteristic "rabbit ear" profile. But for the high luminosity galaxy with rotational velocities that are constant over most of its radius, as long as the HI extent is greater than 1 kpc, the profile shape is independent of the HI distribution. The following four 21-cm profiles will illustrate this.

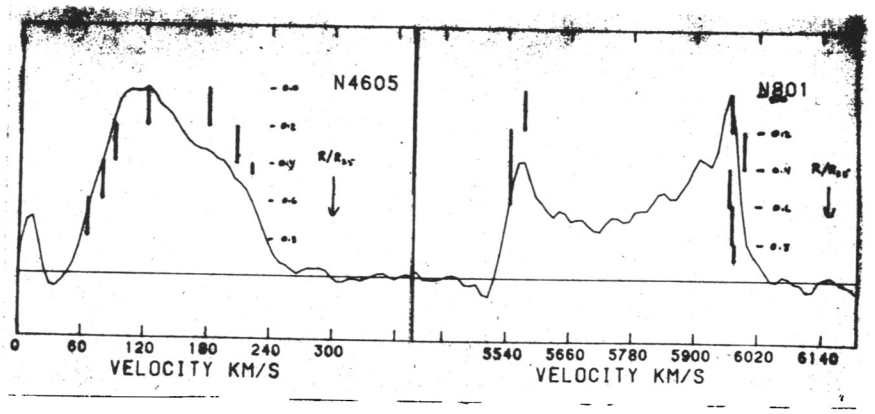

Superimposed on the global HI velocity profiles (light line) are the observed optical velocities (heavy vertical lines) averaged over 20% intervals of the isophotal (R_{25}) radius. On the left we show NGC 4605, M_B = -18.6, the faintest Sc galaxy in the sample. Note that the rotational velocities increase over the entire radius of the galaxy and that the profile is single peaked. In addition, we note that on the low velocity side, Hα emission was measurable to 80% of the radius, while on the high velocity side, the emission was measurable only to 45% of the radius. The 21-cm profile shows a lack of HI on the same side. NGC 801 (right), a high luminosity galaxy, M_B = -23.3, has optical velocities that are essentially constant over the entire radius of the galaxy and a 21-cm profile with steep edges, sharp peaks and a deep central dip in intensity. Interestingly, the side of the galaxy with less Hα extent also shows less HI emission. The next two galaxies, both of intermediate luminosity and similar velocity gradients in their rotation curves, show remarkably different profiles.

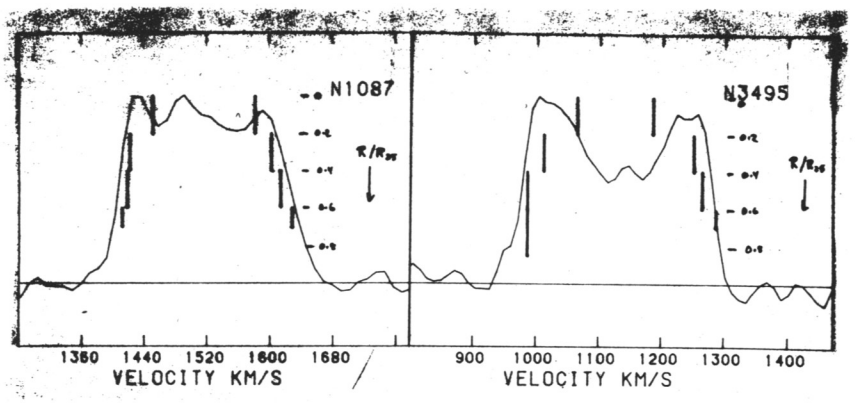

Even though NGC 1087 has rotational velocities that are more constant with radius than NGC 3495, its profile has no central minimum, whereas NGC 3495 has a deep minimum. This implies that NGC 1087 has a centrally peaked HI distribution, while NGC 3495 has little HI in the center. The above examples show that knowing the rotation curve can give some information on the HI distribution and that there is good correlation between the Hα emission and the global 21-cm properties of the galaxies.

We raise a caution in interpreting some of the new extragalactic CO observations. In comparing global HI profiles with CO profiles, one must remember that the telescope beam often intercepts only the central kpc or

so of the galaxy. Therefore, the observed profile shape will be a strong function of the rotation curve shape and the fraction of the galaxy intercepted by the beam. The CO profile shapes will be even more difficult to interpret if strong central sources are present.

III. Systematics of Luminosity and Mass

Rotational velocities are a function of both luminosity and Hubble type. In the next figure we have averaged together several rotation curves to generate mean rotation curves at three different luminosity levels for Sc and Sa galaxies. The radius of each galaxy has been normalized to its own isophotal radius.

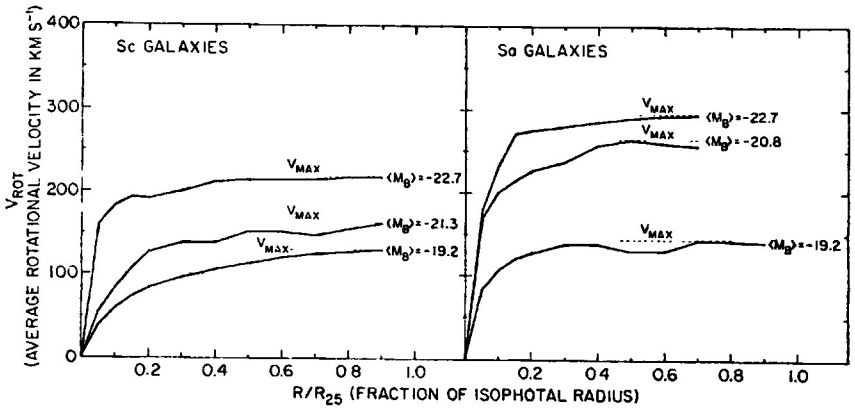

It is clear from these plots that at any radius, an Sa galaxy has a considerably higher rotational velocity than an Sc of the same blue luminosity. The Tully-Fisher relation is also clear; V_{max} increases with luminosity both for the Sc's and the Sa's, but the functional form is obviously different. It is also clear that a Tully-Fisher like relation could be determined at any fraction of the radius, as illustrated below.

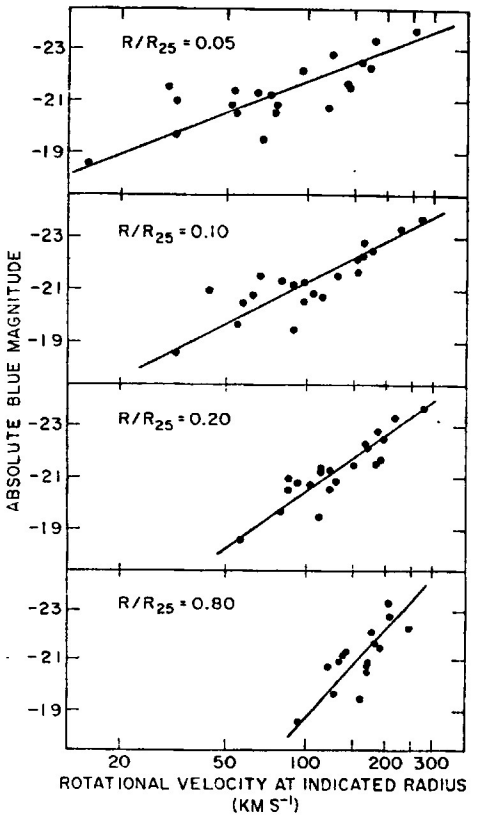

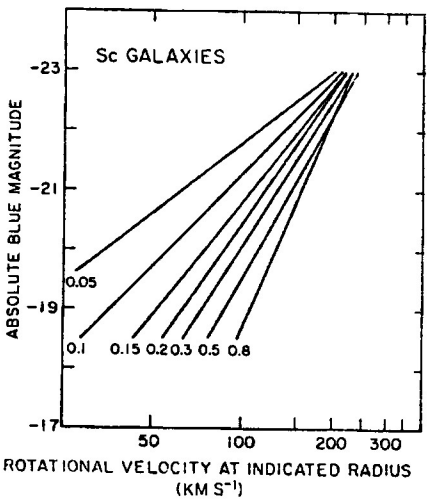

On the left, we plot absolute magnitude for the 21 Sc galaxies as a function of the rotational velocity determined at 5, 10, 20 and 80% of the isophotal radius. On the right we show the superimposed regression lines for a whole family of Tully-Fisher relations determined at various fractions of the isophotal radius to indicate the very regular form of this relationship. The above figures suggest that the entire rotation curve is systematically related to luminosity and other global properties of the galaxy.

The systematic nature of the rotational velocities is clearly illustrated if we study the properties of the Sc galaxies in the integral mass-log R plane (Burstein, Rubin, Thonnard and Ford, Feb. 1, 1982, Ap.J.).

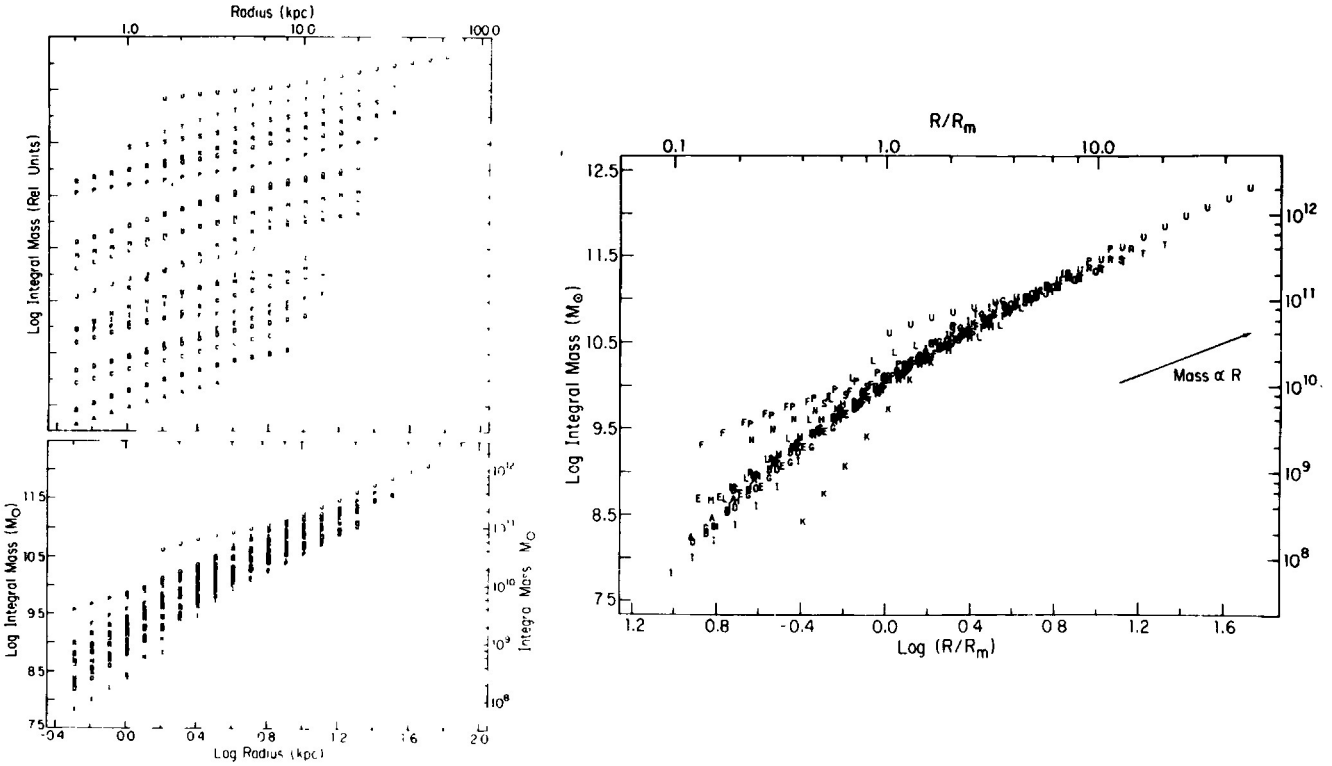

(© 1982, The Astrophysical Journal)

On the left (upper) are plotted the integral masses, offset by 0.5 in the log, of each of the 21 Sc galaxies as a function of the radius. In the lower panel, they have been plotted together, showing the general shape of the relationship and the systematic mass differences. If each galaxy in the lower left is slid in the log R direction (which is equivalent to scaling by some mass scale length, R_m) to minimize the scatter in the log Mass direction, we get the plot on the right. The low scatter in this plot tells us that the mass distribution in an Sc galaxy can be characterized by a single universal mass distribution and a mass scale length of order 1 to 4 kpc. The small galaxies will then have few mass scale lengths within their isophotal radius, defining only the lower part of the plot, while the large galaxies include many mass scale lengths within their radius, defining the entire plot.

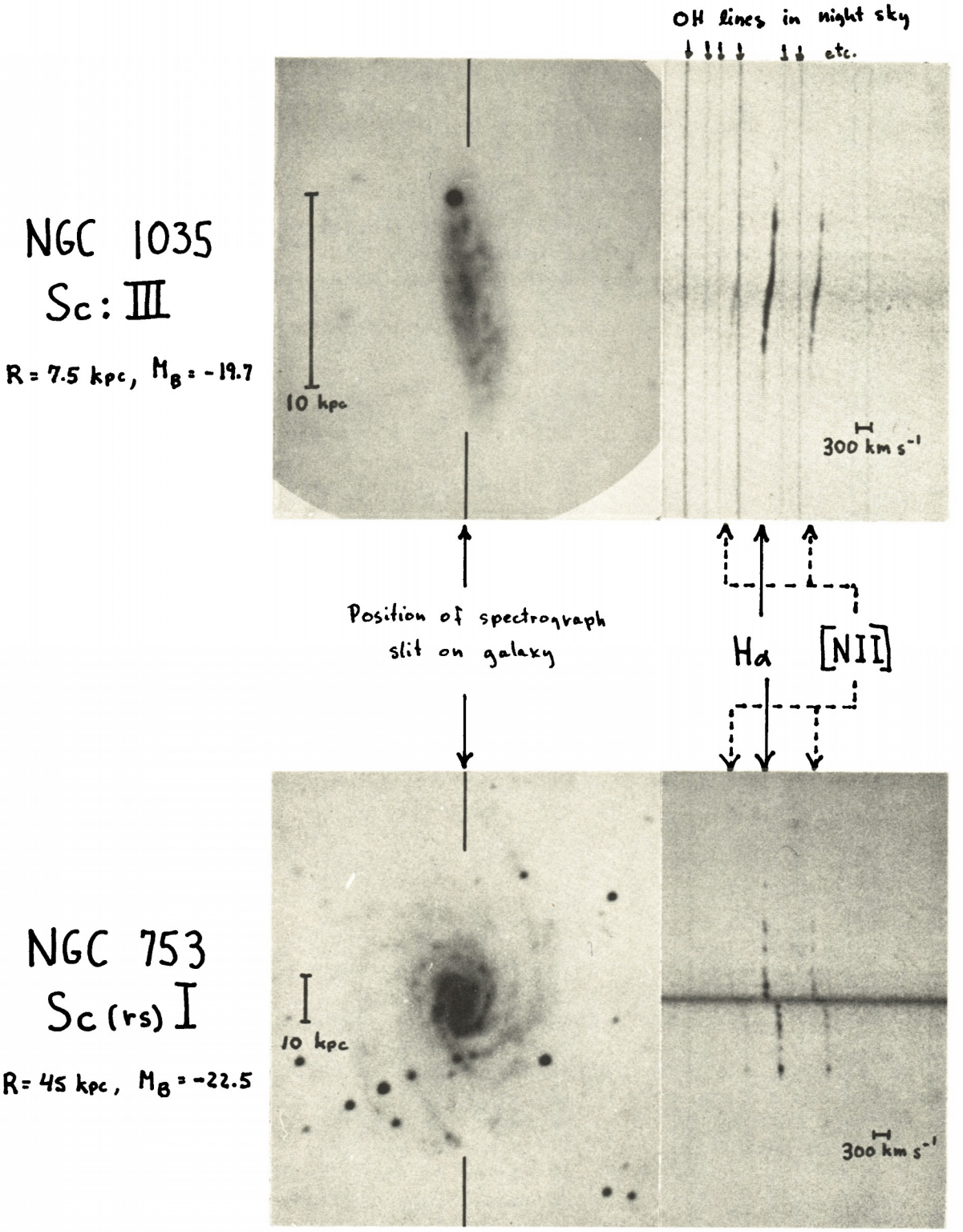

Figure 1. Image tube photograph and spectrum of typical low luminosity (upper) and high luminosity (lower) Sc galaxies. The spectrograph slit in NGC 1035 was rotated slightly from the major axis to avoid the bright star. The spectrum of NGC 753 was exposed half as long as that of NGC 1035.

ONE PERSPECTIVE ON THE WORKSHOP

By F. J. Kerr

The presentation of the many interesting results on extragalactic molecules has reminded me of two historical episodes that seem strange now. Around 1950, the great astronomer Walter Baade is reported to have said that he could not support the building of more equipment for radio astronomy, because the essential discoveries had been made and only details remained. Also in the 1950's, it was generally held that interstellar densities were too low for many atoms to combine into molecules, and the few molecules that had formed could only be in the ground state. How far we have come since then!

The title of this workshop is "Extragalactic molecules", but in fact the subject matter was mainly concerned with distribution, structure and kinematics, with nothing on the astrophysics or the formation of molecules, and little about relationships to the rest of extragalactic astronomy.

Some of the main problem areas that are being addressed are as follows: (i) Is spiral structure evident in the distribution of molecules in galaxies? (ii) How long do giant molecular clouds last? (iii) How accurately can CO column densities be converted to H_2 values?, and (iv) What are the important parameters in comparing one galaxy with another?

In considering the spiral structure question, we should remember that in our Galaxy the spiral structure is complex, with different pattern parameters in different parts of the Galaxy. In particular, spiral arms appear to differ in their characteristics along their length. We can therefore expect very complex patterns in other galaxies also. Comparisons between HI and CO exist in our Galaxy and in external systems, but they are incomplete.

Evidence in support of the density-wave theory of spiral structure is easier to find in other galaxies than in our own. We can expect extragalactic CO observations to contribute to this problem.

There is an unfortunate tendency to take the ratio of H_2 to CO as constant over a galaxy, but in fact the CO excitation is likely to vary over the disk of a galaxy, and formation processes can be different in different regions, as indicated by the way that the density ratio of different types of molecules is known to vary with location. In this connection, differences in cosmic-ray heating and variations in isotope ratios were also discussed by earlier speakers.

A number of comparisons were made between the distributions of molecules in other galaxies and in our own. Some surprise was expressed at the way a central hole was found in some galaxies, but not in others. More attention needs to be given to careful comparisons with Hubble types of galaxies. Some recent discussions of the collapse of protogalaxies have focused on the way that the final arrangement depends very much on the degree to which the protogalactic gas is cleaned up in the central region during the collapse. In some cases, additional gas comes into the central region from outside at a later stage, but in all cases the amount of gas in the center is certainly important for an understanding of the behavior of a galaxy.

The volume and range of new results discussed at the workshop led to a very interesting and stimulating meeting. I have two final thoughts. It was clear many times that advances were seriously limited by lack of resolution, and therefore extragalactic studies point strongly to the need for the proposed 25-meter millimeter-wave telescope. Throughout the workshop, it was pleasing to see the strong role that women are playing in this branch of astronomy.

The Large Scale Distribution of Molecular Clouds in the Outer Galaxy

Kathryn N. Mead
Physics Department, Rensselaer Polytechnic Institute

We have used the NRAO[1] 36-ft telescope to survey the first quadrant of the galaxy for CO emission from molecular clouds outside the solar circle. Three strips, at b = 1.3, 1.5 and 1.7° were observed in the longitude range 55° to 95° in 0.1° steps. The latitude range corresponds to the centroid latitude of negative velocity HI.

The large scale CO distribution is shown in an l-v diagram in Fig. 1, and in a galactic projection in Fig. 2. Most of the emission is at a low level, with T_R^* in the 1 - 2 K range. There is evidence for two major arm-like concentrations, one at about -35 km/s and the other at about -75 km/s. The former is about 12 kpc from the galactic center, and appears to be an extension of the Perseus arm into the first quadrant. The latter appears to be an arm about 15 kpc from the galactic center.

A crude estimate of the H_2 mass in the outer galaxy can be made from our data. In order to make a direct comparison of our data with data in the inner galaxy, we use the conversion factor, $N(H_2) = 4 \times 10^{20}\ cm^{-2} \int T_R^*(^{12}CO)dv$. (As will be pointed out by Kutner, in the next paper, there is some question about the general validity of this number.) We have corrected for unsampled galactic azimuth, but not for unsampled galactic latitudes. Because of this last point, we would expect our estimate to be a lower limit, especially since more recent observations have shown us that the scale height for molecular material (just as for HI) is greater in the outer galaxy than in the inner galaxy. With these assumptions, we find an H_2 mass of $6 \times 10^8\ M_\odot$ between 10 and 16 kpc, about half that in the inner galaxy, and a surface density of $10^6\ M_\odot/kpc^2$, about one quarter that in the inner galaxy. Recent estimates of the HI distribution place about $10^9\ M_\odot$ inside the solar circle and twice that between 10 and 16 kpc.

[1]The NRAO is operated by Associated Universities, Inc. under contract to the National Science Foundation.

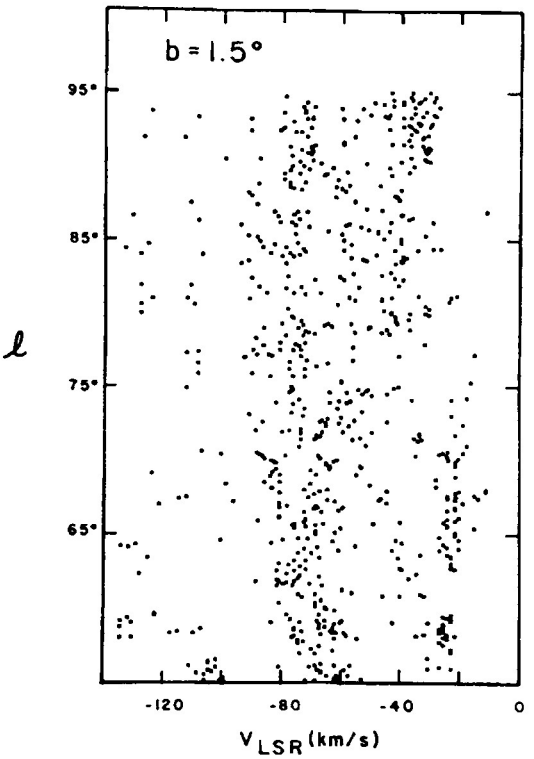

FIG. 1.—A representation of the survey in a longitude-velocity diagram. Data were taken in 0°.1 intervals of l. Each data point represents a detected spectral line. Almost all lines have T_R^* in the range of 1–2 K. The rms noise levels in the spectra were typically less than 0.3 K. Not all spectra were usable in the -90 to -135 km s^{-1} range.

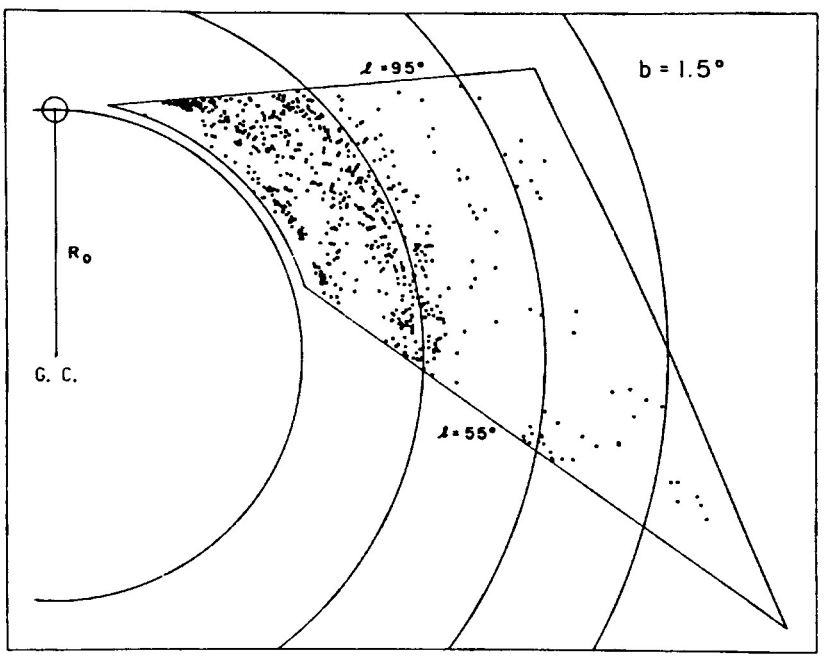

FIG. 2.—The data shown in Fig. 1, plotted to show location of the points in the Galaxy. Kinematic distances were found by assuming a flat rotation curve with $v_0 = 250$ km s^{-1}, and $R_0 = 10$ kpc. The limits of the survey are indicated by the lines at $l = 55°$ and 95° and by the curves corresponding to LSR velocities of -10 and -135 km s^{-1}.

Physical Properties of Molecular Clouds in the Outer Galaxy

Marc L. Kutner
Physics Department, Rensselaer Polytechnic Institute

In the previous paper, Mead presented the results of a large-scale survey of CO emission from clouds outside the solar circle. We now present the results of detailed maps of some of these clouds. We have used the NRAO[1] 36-ft telescope to make one-beamwidth maps of about two dozen clouds. Five of these maps are shown in Fig. 1. We see what appear to be giant molecular cloud (GMC) complexes, some 50 - 80 pc long, like those in the solar neighborhood. However, we see that the CO temperatures, in both the envelopes and at the peaks appear lower than in the local clouds.

We have compared our maps with those of local GMCs (with the local maps having an appropriate degradation in resolution). For the most part, it appears that the outer galaxy clouds we have mapped do not contain giant HII regions. However, there are signs of star-formation "activity" around the peaks, such as the CO lines getting broader (in one case as broad as 20 km/s). In addition, we have used the 36-ft telescope to detect 2-mm H_2CO emission from five of these peaks. Comparisons with local clouds suggest that most of these peaks resemble those associated with reflection nebulae, and probably contain one or more B stars.

We have mapped these 5 clouds in CO and ^{13}CO using the 45-ft telescope of the FCRAO, and find that the ^{13}CO column densities appear to be comparable to those in the local clouds. We have also mapped the clouds in the CO $2\rightarrow1$ line, using the U. Tx. MWO 16-ft telescope, and over most of the clouds, the $2\rightarrow1$ and $1\rightarrow0$ lines have the same strength, indicating that the CO is thermalized. All of this indicates that the clouds have masses that are typical for local GMCs ($\sim10^5$ $M_\odot$), but kinetic temperatures that are about half those in the local clouds. We have calculated that such a lower envelope kinetic temperature can be explained by a factor of 3 - 10 drop in the cosmic ray flux from the inner to the outer galaxy, consistent with the falloff derived from gamma ray observations.

These results have important consequences for the use of ^{12}CO data to directly determine molecular masses. At some point the integrated intensity of ^{12}CO no longer serves as a direct tracer, since the excitation is changing from the inner parts to the outer parts of galaxies. The "mass-to-CO-luminosity ratio" should be a function of cosmic ray flux, heating from local O stars and metallicity. Therefore, we must be careful in exporting any conversion factor from our galaxy to others, or in applying a single conversion factor over a whole galaxy.

[1]The NRAO is operated by Associated Universities, Inc. under contract with the National Science Foundation.

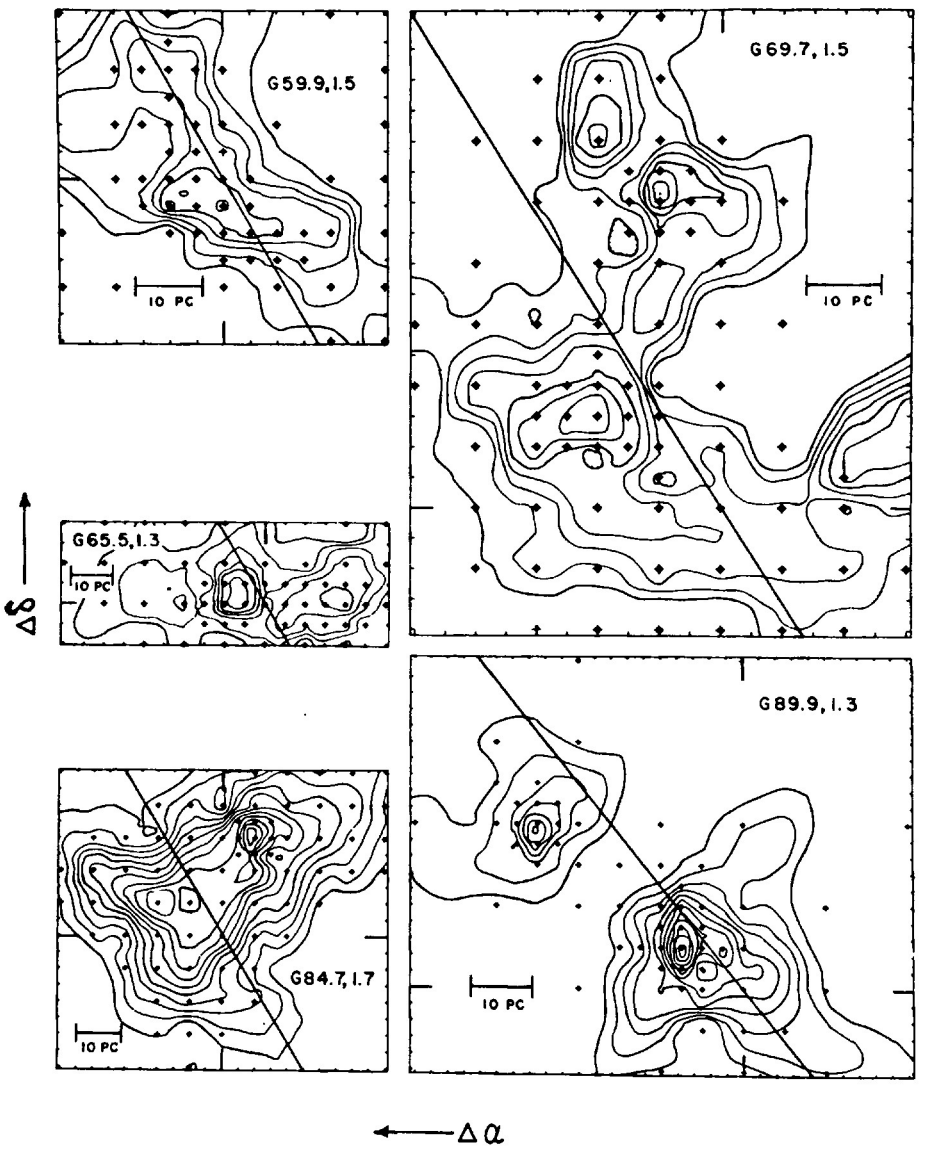

FIG. 1.—Contour maps of five clouds from the survey. Dots mark the observed positions. In all maps each fiducial mark represents 1′ offset from the reference position (indicated by the longer fiducial marks). The diagonal line in each map is parallel to the galactic equator at the latitude given in the source name. Linear scales were established by assuming kinematic distances, as in Fig. 2. The lowest contour in each map is $T_R^* = 1.0$ K, and contours go up in 0.5 K intervals. Typical rms noise levels are 0.3 K. The HPBW is 70″.

CAN SPIRAL ARMS FORM GIANT MOLECULAR CLOUDS?

F. COMBES

Observatoire de Meudon

and

Ecole Normale Superieure

If the interstellar medium is pervaded by a very hot gas at 10^6K (x-ray observations), which filling factor can be as high as 80% (e.g. Mc KEE and OSTRIKER 1977), then the interstellar medium cannot be shocked in the crossing of a spiral arm potential well. Molecular clouds (and we know now that they can be giant) have to be formed by an other processus. Collisions have been proposed as a mechanism and indeed, collisions are very inelastic between molecular clouds and coalescence is likely. Previous estimations, from a mean molecular gas density in the Galaxy, concluded that the growth time of a GMC is quite long and, to maintain the observed giant molecular cloud abundance, their lifetime should be superior to 2.10^8 years (cf. KWAN 1979). Here we build a collisional model to show that, if the gas density is enhanced in spiral arms, giant molecular clouds have time to be formed substantially in the arms, even if their lifetime is as short as 4.10^7 years. A collisional steady-state is not reached either in arms nor in interarms for molecular clouds, but giant clouds are much more concentrated in spiral arms than the whole interstellar matter.

Our model takes into account coalescence of molecular clouds, fragmentation, and disruption of giant clouds after star formation. Velocity dispersion of clouds are computed self-consistently and their values depend on two processus : the energy dissipation by collisions and the energy input in clouds reinjected after the disruption of a giant molecular cloud. Of course with collisions alone, all cloud velocities would come to zero very quickly, and the clouds need to be accelerated between collisions. This acceleration is provided by stellar winds, supernovae explosions, etc... following star formation bursts in GMC . On this energy input depends the

velocity spectrum of clouds, which therefore has not to be in kinetic energy equipartition. Indeed if the reinjected velocity spectrum is flat, the resulting velocity spectrum would be very flat, of power lawbetween -0.1 and -0.2 , very consistent with observations of molecular clouds.

The details of our collision model is inspired from Taff and Savedoff (1973) and from the computer modelisation of BOULANGER (1981 in preparation). The method is a Monte-Carlo simulation. About $1-2.10^4$ clouds are simulated, a number of the same order of magnitude as the total number of clouds in a region of our Galaxy. Masses of molecular clouds range from $10^{2.7}$ to $10^{5.7}$ $M_\odot$. The internal density of clouds is assumed to be 40 H_2 cm^{-3} (cf. STARK and BLITZ 1978) and the clouds diameters range from 8 to 80 pc. The collisional cross-sections are geometrical. Statistically, one standard run ends up with 47% of coalescence, 52% of fragmentation of clouds (2 fragments).

RESULTS.

When the mean molecular density is held fixed, simulating an infinite time spent in arm (or interarm) regions, we obtain a mass fraction in GMC (f_{GMC}) of 48% in arms and 15% in interarms. Times to reach steady-state equilibrium are 5.10^8 years for a density of $\bar{\rho} = 0.9$ H_2 cm^{-3} (interarm) and 4.10^8 years for a density ten times as large (a very contrasted spiral arm region).

The ensemble of molecular clouds cannot be considered as a fluid on dynamical time-scales shorter than these. We have computed the equivalent sound speed of the fluid when T is larger than 5.10^8 years. This sound speed is the same for both high and low density regions, and this comes from the different velocity spectrum of clouds in the two regions * . The result of the simulation of the ensemble of clouds along their circular trajectory around the galactic center is shown in figure 1 . Here we have taken 2 arms of width 0.9Kpc each, of pitch angle 20° (in the middle of the molecular ring at 6Kpc). The arm contrast is assumed to be 10 in the underlying gas density (density waves generated for instance by a central bar

* in contradiction with COWIE (1980)

distortion). It can be seen in figure I that the contrast in GMC is larger than the underlying gas density contrast. GMC can be substantially formed in spiral arms. The contrast diminishes when the rotation period shortens (it is lower at 4Kpc than at 8Kpc) since the time spent in spiral arms is reduced. When the density contrast is 5, the GMC contrast is 10, (when the density contrast is 10, the GMC one is 25) cf. figure 2.

To compare with the observations, we mention that the observations of SOLOMON et al. (1979) imply a mass spectrum of clouds of -1.43 and those of STARK (1979) of -1.53, which both are very consistent with the value of -1.5 found in this model. The velocity dispersions are very difficult to infer from observations, but the work of STARK (1979) is consistent with an almost flat velocity spectrum of molecular clouds (slopes between -0.1 and -0.2).

In conclusion, collisions are efficient enough to form the Giant Molecular Clouds even assuming for them a short lifetime of 4.10^7 years. The ensemble of clouds is always very far from a steady-state equilibrium when in rotation around the galactic center and cannot be considered as a fluid.

FIGURE 1 : Evolution of the ensemble of molecular clouds in rotation around the Galactic Center at a radius of 8 Kpc (corresponding period 2 10^8 years). The gas density is assumed to increase by a factor 10 in the arms. The average density is 2 H_2 cm^{-3}. L is the index of the velocity spectrum, $\bar{m}$ is the mean mass per cloud, f_{GMC} is the fraction of total mass contained in GMC, c^2 is the mass-averaged square of velocity dispersions.

FIGURE 2 : Fraction of the total mass contained in GMC at different radii in the Galaxy, and for two different values of the underlying gas contrast : 5 ($\langle \bar{\rho} \rangle$ = 1.4 H_2 cm^{-3}) and 10 ($\langle \bar{\rho} \rangle$ = 2 H_2 cm^{-3}).

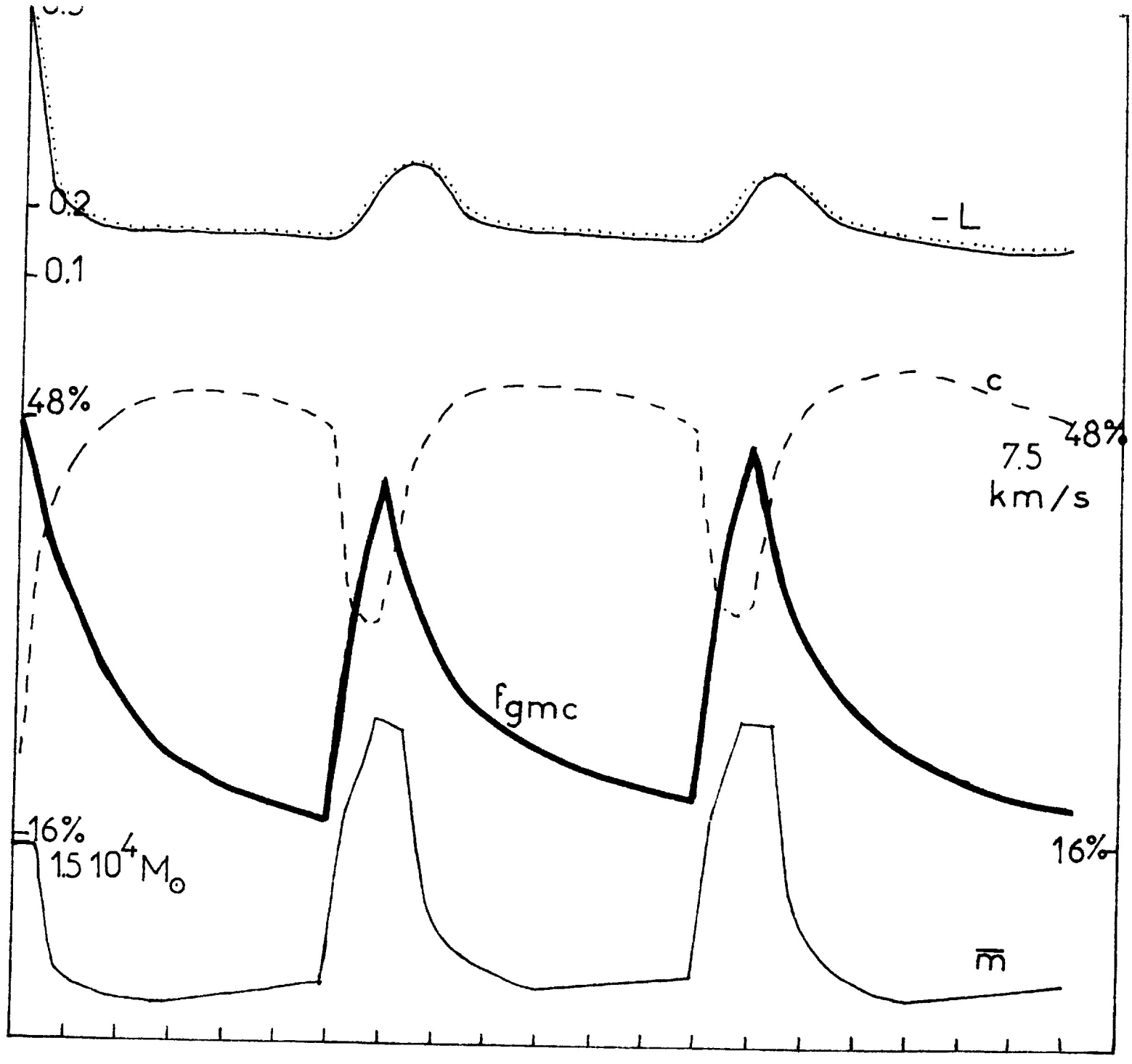

Figure 1

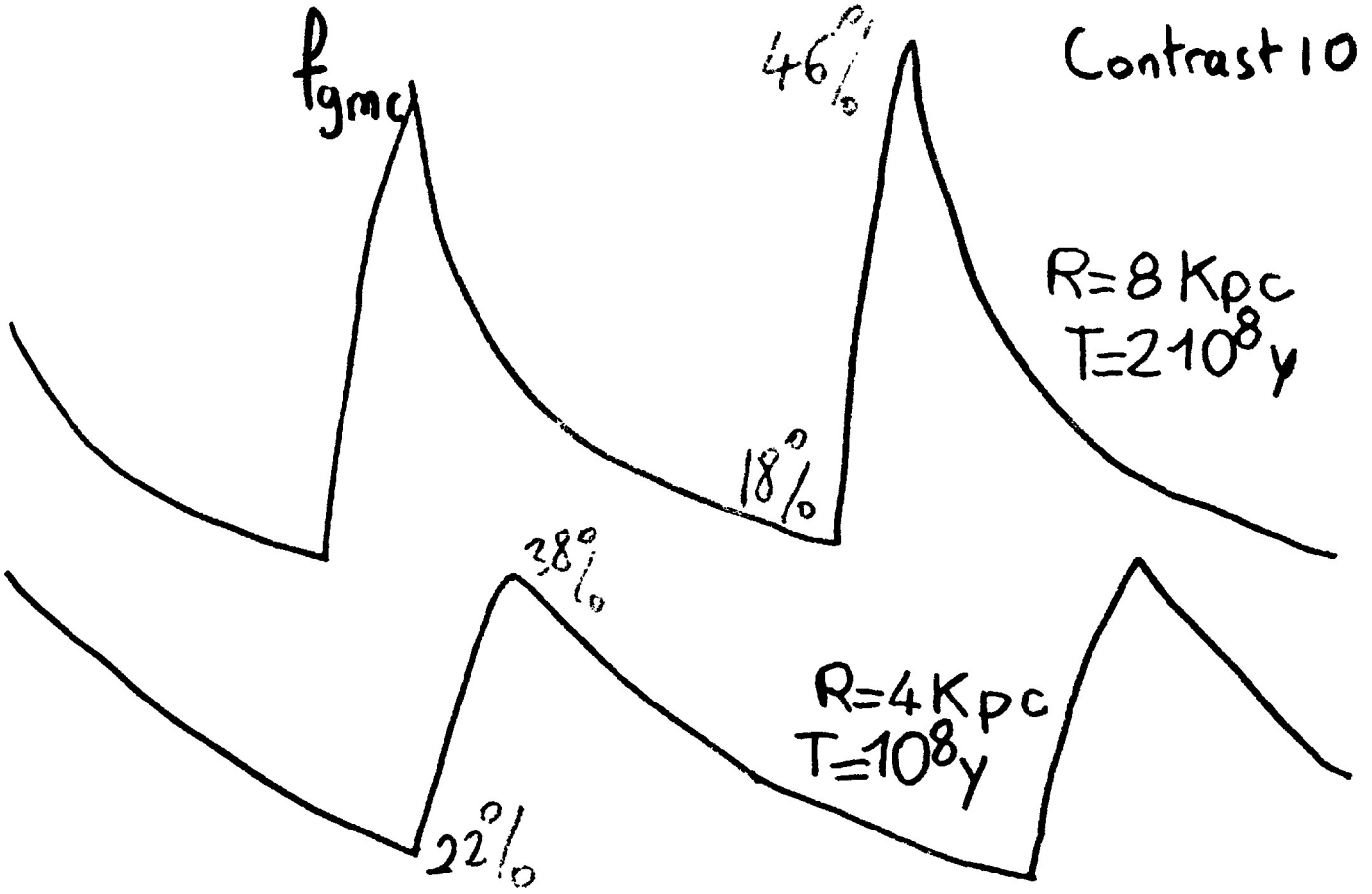
Contrast 10
f_{gmc}
46%
18%
R=8 Kpc
T=2 10^8 y
38%
22%
R=4 Kpc
T=10^8 y

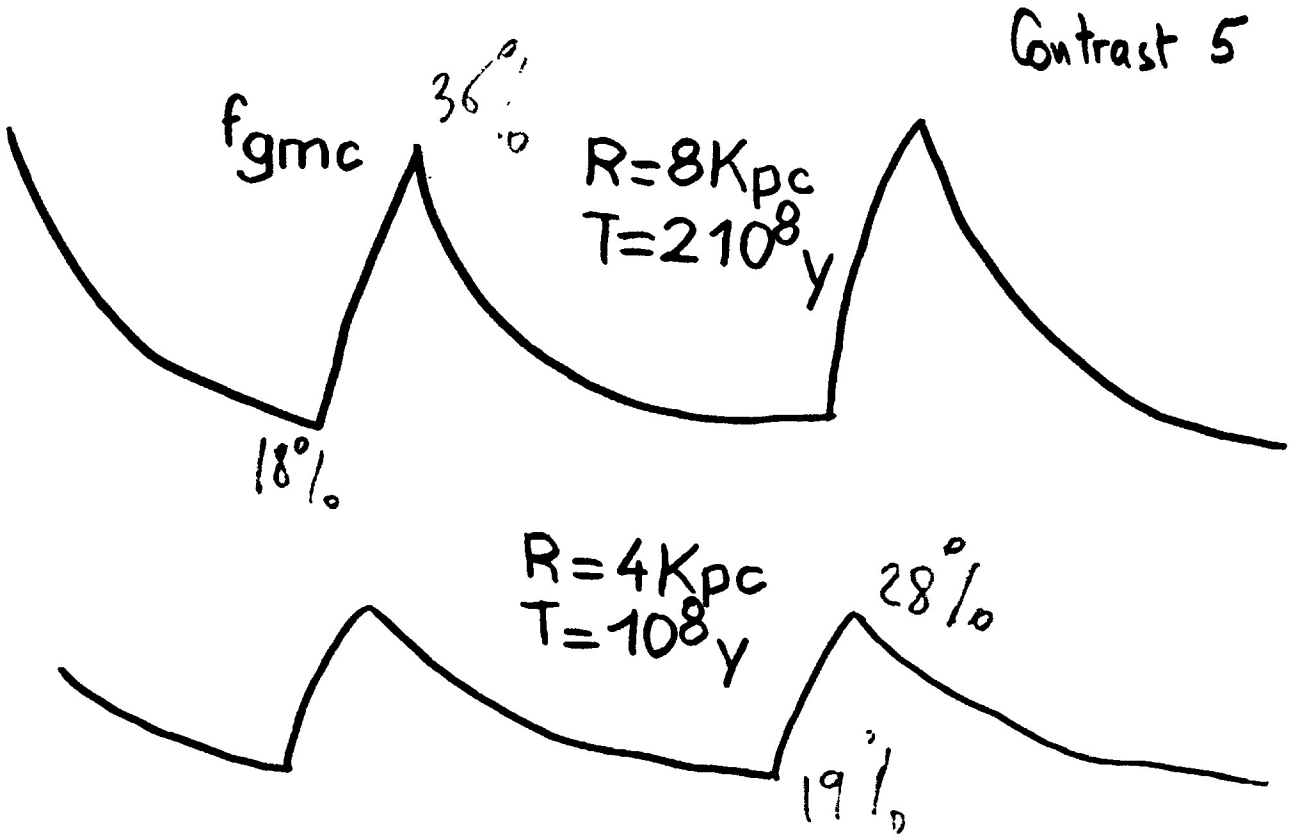
Contrast 5
f_{gmc}
36%
18%
R=8Kpc
T=2 10^8 y
R=4Kpc
T=10^8 y
28%
19%

Figure 2

WIDESPREAD GALACTIC OH EMISSION AT 1720 MHz: A NEW TRACER OF SPIRAL ARMS

B. E. Turner

National Radio Astronomy Observatory
Charlottesville, Virginia

Although not as spectacular as the anomalous main-line OH masers which often occur in star forming regions, nor the 1612 MHz OH masers associated with evolved stellar envelopes, anomalous OH emission in the 1720 MHz transition has nevertheless long been recognized in our galaxy, most commonly as a weak variety arising in cold, dark dust clouds of modest mass (Turner and Heiles 1971). This emission is spatially extended (within the confines of the dark clouds), a not-surprising property given that the excitation anomaly is weak and that the corresponding emission is not of the maser type. The first indication that the weak, extended 1720 type of anomaly might not be confined just to small dark clouds was its observation by Haynes and Caswell (1977) in the direction of 7 of 19 continuum sources searched in the region $326° \leq \ell \leq 340°$, $b = 0°$. For the first time, the anomaly was seen at non-local velocities, implying in two or three cases objects larger than the usual small dark clouds.

These results inspired a search of the Green Bank OH survey results (Turner 1979) for more cases of the weak ($T_A < 2K$) extended 1720 MHz emission. In the region $337° \leq \ell \leq 50°$, $-1° \leq b \leq 1°$, there were found at least 53 highly spatially extended 1720 MHz OH clouds, the majority of which exhibit main-line absorption or at least no detectable main-line emission to a level at least 3 times less than the 1720 MHz brightness. Thus the relative 1720 anomaly in these cases is considerably stronger than in the usual dark cloud cases. Velocities range up to tangential values, implying very large linear

sizes for some of these clouds. Yet the linewidths are surprisingly small (1 - 3 km/s) and the velocities surprisingly constant over each of these highly extended regions (up to 2° or more).

Figure 1 is a position diagram of all 1720 MHz emission found in the Green Bank survey which is not accompanyed by emission in any of the other 18 cm cm OH lines and which has non-maser characteristics ($T_B < 2K$). The dots represent observed positions, while the contours around the dots take into account the 18' beamwidth of the 140 foot telescope. Fifty-three of the contours contain more than one observed point (all at the same velocity) and therefore represent regions of extended emission. Another 42 regions contain a single observed point.

In a subsequent observing session in 1981 October, all 42 of the single-point regions were in fact found to be extended, and many (~30) new extended regions of 1720 MHz emission were found. Many of the regions in Figure 1 were found to be much larger than shown.

All of the original Green Bank survey data, and some data from the subsequent observing run are plotted in an ℓ, v diagram in Figure 2. This diagram is the crux of the 1720 emission so far as galactic structure is concerned, for it suggests that the anomalous 1720 OH clouds are confined to spiral arms. The ℓ, v distribution is very similar to that of HII regions (Lockman 1979; Downes et al. 1980) in that there is less of a dispersion in the velocities than is the case for CO or H_2CO. Both CO (Cohen et al. 1980) and H_2CO (Downes et al. 1980) show a wide distribution of cloud velocities, and no clearly defined (ℓ, v) structures which can be associated with spiral arms. By contrast, the anomalous 1720 OH clouds, like the HII regions, show a run of points from v = 0 to 60 km/s from ℓ = 10° to 55° which marks the Sagittarius arm, and a run of points from v = 0 to 100 km/s from ℓ = 5° to 32°

which can be assigned to an inner Scutum arm. (Three points near ℓ = 38° and v = 80 km/s mar this otherwise clear picture (they lie in the expected interarm gap along the terminal velocity line which should comprise the interval 32° $\leq \ell$ 48°). However there is a known large HII region at ℓ = 37°7, v = 86 km/s (Downes et al. 1980) which can account for these points.) We may conclude, therefore, that insofar as HII regions trace spiral arms, so do the anomalous 1720 OH clouds, the first molecular tracers found which clearly do so.

What type of clouds are these 1720 OH objects? If we adopt near-kinematic distances for just the original 53 extended regions in the Green Bank survey (the more recent data haven't been included yet), we get a size distribution (measured along directions of maximum extent) shown in Figure 3. The shaded areas represent objects with "local" (v < 10 km/s) velocities and are probably just nearby small dark clouds. The remainder of the distribution looks very much like what we would attribute to giant molecular clouds as observed in CO (Solomon and Sanders 1980; Liszt and Burton 1981). The median size is ~40 pc and there is a long tail in the distribution toward very large objects. When the 1981 October data are incorporated, they will shift many of the intermediate-sized clouds to larger sizes, but they will also add many new extended regions of modest size. Thus the overall distribution is not expected to change much.

Perhaps the hardest question to answer is whether we have actually shown that GMCs lie only in spiral arms, or whether it is merely the particular anomalous excitation mechanism that is confined to spiral arms. The answer requires knowledge of the excitation mechanism. Whatever the pump is, it must be very non-specific in nature, because the 1720 OH emission is not generally related to the positions of HII regions, IR sources, or any other identifiable

pumping agents. Also, the widespread nature of the emission suggests a very general pump mechanism. These arguments suggest collisional pumping, and indeed a model of this type, aimed at the dark dust cloud form of 1720 anomaly, already exists (Guibert et al. 1978) and appears readily applicable to the similar type of emission discussed here. Briefly, collisional excitation to the lowest, $\pi_{3/2}$, J = 5/2 rotational state, and to none other, will enhance the excitation temperature of the 1720 MHz transition and not the other 18 cm transitions, so long as the radiative decay (at 120 μm) to the ground rotational state is optically thick ($N_{OH} \geq 5 \times 10^{14}$ cm^{-2} for zero velocity gradient). If $T_k < 15$K this state will not be adequately excited, while $T_k > 50$K will excite higher rotational states as well, and these lead to other types of ground state anomalies. Required densities appear to be in the range 200 to 600 cm^{-3}. These densities and temperatures seem perfectly consistent with our current understanding of the properties of GMCs.

From the foregoing, it is certainly clear that our "spiral arm distribution" of GMCs could well be just a spiral arm distribution of temperature. The clouds in the spiral arms are the hotter ones, exceeding the 15K pumping threshold. Some evidence for this already exists for CO: the brightest (hottest) CO clouds seem in ℓ, v diagrams to resemble the HII region/1720 MHz OH distributions even though the overall CO does not. In addition, we failed to detect 1720-anomalous OH in the outer spiral arms recently elucidated by Kutner and Mead (1981). This failure is consistent with the common belief that average cloud temperatures decrease with increasing galactocentric radius.

On the other hand, we performed highly sensitive searches in 1981 October for anomalous 1720 OH in many positions in the interarm gap and found none to a level 20 times lower than the typical emission seen in the arms. The pumping

threshold temperature, if that is indeed the effect, must therefore be very abrupt, as must be the difference in gas temperature in and between the arms. Perhaps even more intriguing is the prevalence of the similar 1720 OH anomaly in "cold" dark dust clouds, whose CO-derived temperatures are $\lesssim$ 10K, and which are in many nearby cases known to lie between spiral arms. (Distant dark dust clouds are not detectable in 1720 OH owing to excessive beam dilution). Cold dark clouds are probably both colder and denser than most of the gas in GMCs, so the pumping could be different. But if the pumping mechanism is the same, then the conclusion would seem to be that the GMCs themselves, not just their excitation, are confined to spiral arms.

Like so many other problems of galactic structure, the question whether GMCs as seen in anomalous 1720 MHz OH are really confined to spiral arms will probably be answered only by looking at other galaxies. The large angular size of M31 and the CO results reported for that galaxy by Linke in this volume make M31 a good first candidate.

REFERENCES

Cohen, R. S., Cong, H., Dame, T. H., and Thaddeus, P. 1980, Ap. J. (Letters) 239, L53.

Downes, D., Wilson, T. L., Bieging, J., and Wink, J. 1980, Astr. Ap. Suppl. 40, 379.

Guibert, J., Elitzur, M., and Rieu, N-Q. 1978, Astr. Ap. 66, 395.

Haynes, R. F., and Caswell, J. L. 1977, M.N.R.A.S. 178, 219.

Kutner, M. L., and Mead, K. N. 1981, Ap. J. (Letters) 249, L15.

Liszt, H. S., and Burton, W. B. 1981, Ap. J. 243, 778.

Lockman, F. J. 1979, Ap. J. 232, 761.

Solomon, P. M., and Sanders, D. B. 1980 in Giant Molecular Clouds in the Galaxy, ed. P. M. Solomon (Oxford, Pergamon)

Turner, B. E. 1979, Astr. Ap. Suppl. 37, 1.

Turner, B. E., and Heiles, C. E. 1971, Ap. J. 170, 453.

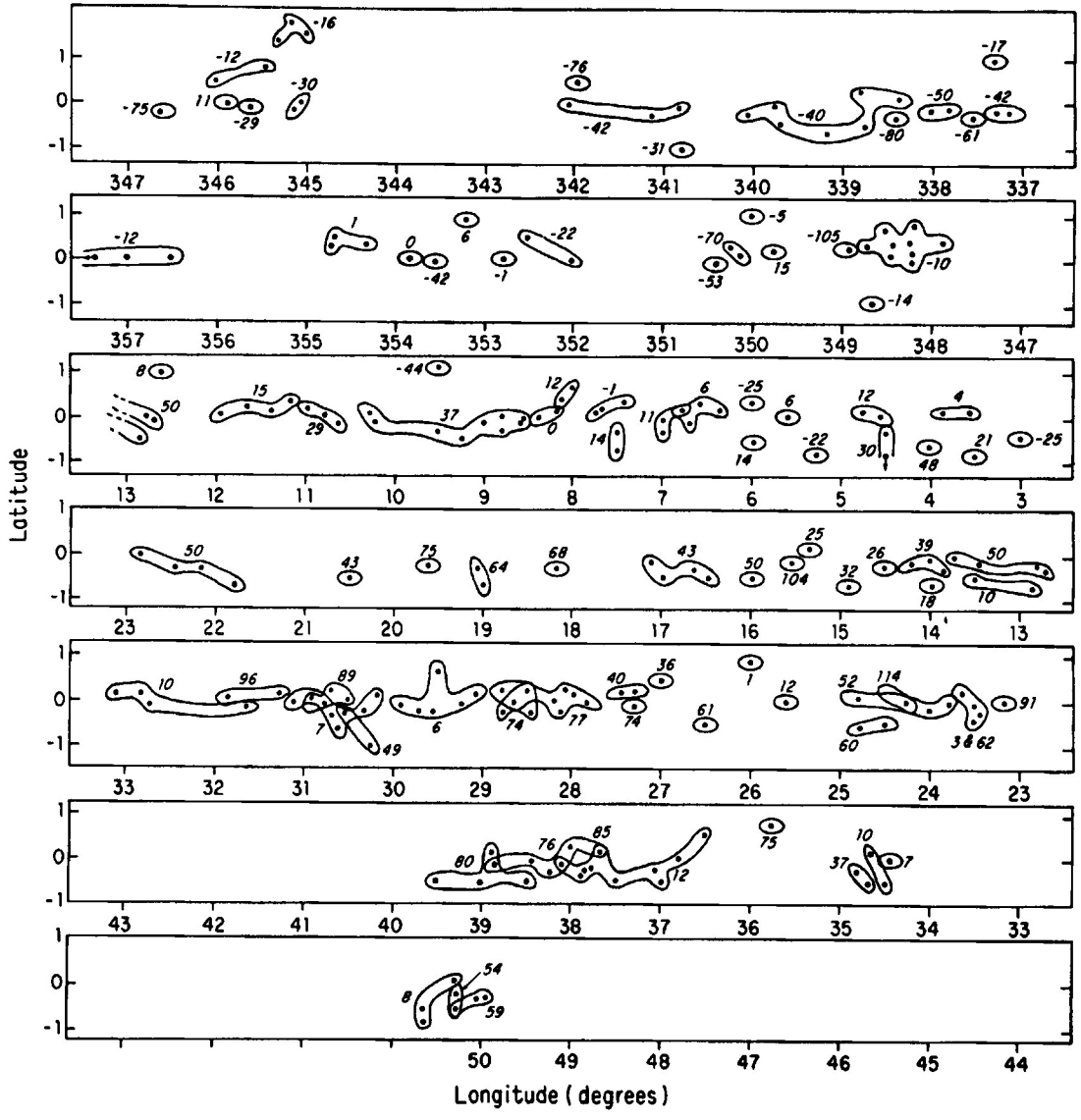

Figure 1. Position Diagram of Extended 1720 MHz OH Clouds in the Galaxy (partial data).

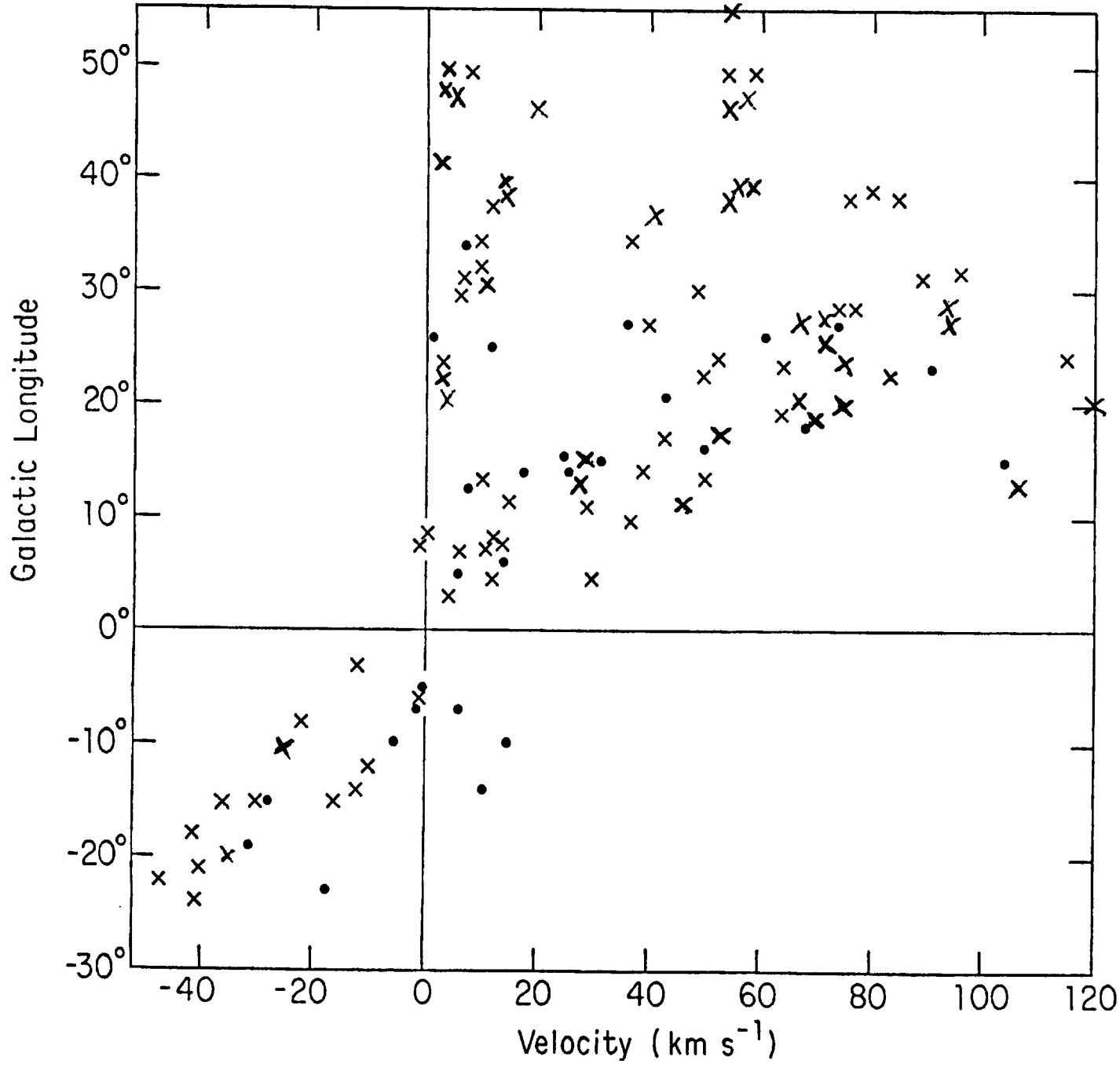

Figure 2. ℓ, v Diagram of Extended 1720 MHz OH Clouds in the Galaxy

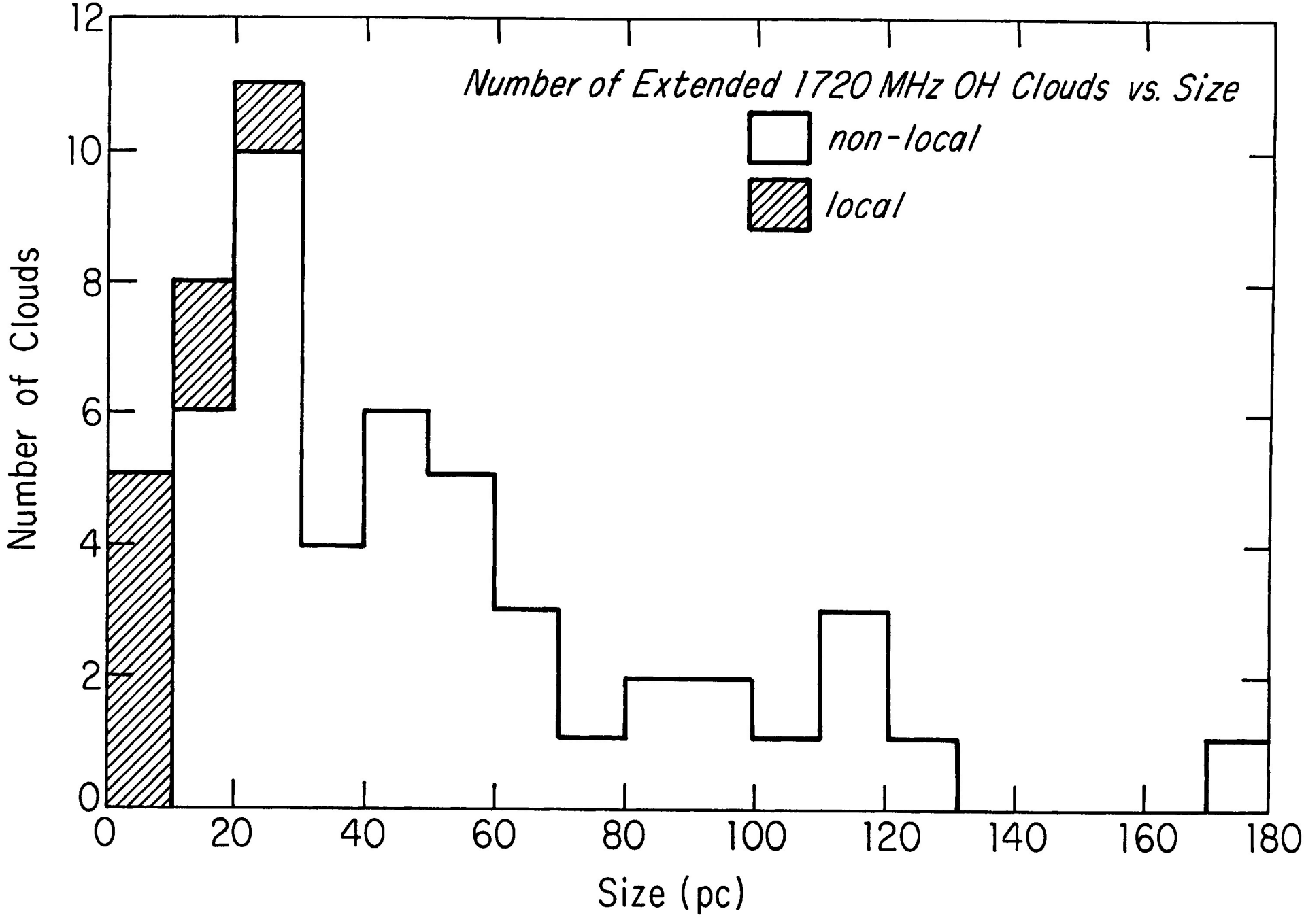
Number of Extended 1720 MHz OH Clouds vs. Size
non-local
local
Number of Clouds
Size (pc)
0
2
4
6
8
10
12
0
20
40
60
80
100
120
140
160
180

Figure 3

Comparison of J=2-1 vs. J=1-0 CO Emission in the Galactic Plane

Preliminary Results

by William L. Peters

Astronomy Department

University of Texas

Frank Bash and I have observed the 230 GHz line of ^{12}CO in the Galactic plane in the longitude range 20 to 35° at a spacing of 0°.2 in longitude. The observations were made with the University of Texas 4.9 m antenna (beam size = 1'.3 at 230 GHz). The spectra were compared with the Burton and Gordon (1976) J=1-0 CO survey which was made at the same positions and velocity resolution as our data and at nearly the same angular resolution (NRAO 11 m beam = 1'.1 at 115 GHz). The conversion of the J=2-1 antenna temperatures to $T_R^*(2-1)$ was based on chopper wheel calibration method supplemented by observations Jupiter (for beam shape) and of the moon through several lunations (for the absolute temperature scale).

We compared the J=2-1 line profiles with the corresponding J=1-0 line profiles channel by channel for all channels with $T_R^* \geq 0.5$ K in both lines. We found that most of the ratios, $T_R^*(2-1)/T_R^*(1-0)$, to be in the range of 0.5 to 1.0. We used the "large velocity gradient" (LVG) model, which solves simultaneously for the statistical equilibrium of the rotational level populations and the radiative transfer, to derive the physical conditions required by the observations. In about 30% of the channels, we found combinations of $T_R^*(2-1)$ and $T_R^*(1-0)$ that could not be explained by any proposed physical conditions. The number of these unphysical combinations could be reduced to <10% if we arbitrarily scaled up the $T_R^*(2-1)$ by 3/2 or scaled down the $T_R^*(1-0)$ by 2/3. It is hard to justify either of these. Scaling up all of the Texas J=2-1 data would yield unreasonably large T_R^*'s for Orion A, etc. Scaling up only the survey data would require an η_p corresponding to a typical angular scale of $\lesssim 1'$ for the "clouds" in the beam which in turn would imply a linear scale of <2 pc at these longitudes. Gordon (private communication) could account for at most only a 15% revision in the $T_R^*(1-0)$ survey data due to problems caused by the "error beam" of the NRAO 11 m. Other possible explanations are that the two sets of data were taken at slightly different positions in the sky or that the LVG code is inappropriate for these observations.

Assuming that the J=1-0 data should be rescaled, we found that most of the data required a kinetic temperature of about 15 K and a hydrogen volume density of about 3000 cm^{-3}. We found no patterns of T_K or $n(H_2)$ in the velocity-longitude diagram other than those seen when $T_R^*(1-0)$ is plotted. Comparing the CO column density obtained from the LVG model with that implied by $\int T_R^*(1-0)dv$ we find that the LVG model gives about 14 times less (16 times less if no rescaling of T_R^* is done). This is probably caused by the LVG code requiring only enough opacity in the ^{12}CO lines to reproduce the line profiles as opposed to the large opacities required when ^{12}CO and ^{13}CO observations are compared. (This will be checked by rerunning the LVG calculations on which the above was based).

Reference:

Gordon, M. A., and Burton, W. B.: Ap. J., 208, 346 (1976)

Relating CO Line Flux to Molecular Column Density

Judy Young and Nick Scoville
Five College Radio Astronomy Observatory
University of Massachustts, Amherst

One aim of extragalactic CO observations is to determine the amount of molecular hydrogen which is present in external galaxies. To obtain an H_2 mass estimate from the observed CO emission, we rely upon results from analysis of the CO emission in the Milky Way and assume a linear relationship between CO line flux and H_2 column density. Most previous analysis of extragalactic CO emission has relied upon the same assumption of linearity at least in regions outside the nucleus (e.g. Rickard et al. 1977 and Morris and Lo 1978) and an adopted constant of proportionality based on a single "standard" cloud which is thought to produce most of the emission. Rather than assume such a single standard cloud, we choose here to adopt a constant of proportionality based on samples of molecular clouds observed in our Galaxy.

In this paper we examine observational data for various clouds observed in the Milky Way to derive an empirical relationship between the observed CO intensity integrals and the H_2 column density obtained from either extinction estimates, ^{13}CO measurements, or Virial theorem analysis. We consider as a representative range of CO emission regions: (1) the hot core regions observed in a few clouds such as Orion; (2) nearby dark nebulae (observed by Dickman 1978 and Frerking et al. 1981); and (3) a sample of giant molecular clouds sampled from a survey of the inner galactic plane (Solomon, Sanders, and Scoville 1981). In Table I we have tabulated the CO intensities I_{CO}[K km s^{-1}], the intensity ratio $I_{CO}/I_{^{13}CO}$, H_2 column densities, and lastly the ratio N_{H_2}/I_{CO} for these sources. All CO intensities were reduced to a common brightness temperature scale adopted by Ulich and Haas (1976) at NRAO.

The H_2 column densities used in this analysis are from numerous sources. For the dark nebulae the H_2 column densities were determined from visual and

IR extinction estimates assuming a standard gas-to-dust ratio $N_{H_2}/A_V = 0.94 \times 10^{21}$ cm^{-2} mag^{-1} (Bohlin et al. 1978). In the cloud cores N_{H_2} was derived from LTE analysis of ^{13}CO and CO data and an abundance ratio $[H_2/^{13}CO] = 10^6$ appropriate to $A_V > 4$ mag (Frerking, Langer, and Wilson 1981). In the galactic plane sample of Solomon, Scoville, and Sanders (1981), column densities in 25 clouds were estimated from the line widths and sizes using the Virial theorem, and a more limited sample of 15 was also measured in ^{13}CO. The two methods agree within 30% for a fixed abundance ratio $[H_2/^{13}CO] = 10^6$.

From the last column of Table I it is evident that both the dark cloud and giant cloud samples yield similar empirical values for the ratio $\langle N_{H_2}/I_{CO} \rangle$ although the mean column densities in the two samples vary by a factor of ten. Excepting the positions of hot cores in molecular clouds we find an approximately constant value for the ratio N_{H_2}/I_{CO} of 2 to 4 x 10^{20} H_2 cm^{-2} (K km s^{-1})$^{-1}$. The giant cloud sample is probably most applicable to analysis of the CO emission in external galaxies since the 25 clouds came from an unbiased survey of the galactic plane at ℓ = 15-35° with no preference to locate and observe either a particular cloud type or the centers of clouds. Based on this work, the empirical relations between the intensity integral and the inferred face-on surface density of H_2 are

$$N_{H_2} \simeq 4 \times 10^{20} I_{CO} \cos i \quad H_2 \text{ cm}^{-2} \tag{1a}$$

or

$$\sigma_{H_2} \simeq 6 I_{CO} \cos i \quad M_\odot \text{ pc}^{-2} \tag{1b}$$

where I_{CO} is the intensity integral [K km s^{-1}] and i is the galaxy inclination. The factor cos i corrects the column density to that which would be observed for a "face-on" galaxy.

Thus, over a set of regions which includes dark nebulae with $\langle A_V \rangle \simeq 2$ mag and giant clouds with $\langle A_V \rangle \simeq 22$ mag the range in the ratio N_{H_2}/I_{CO} is only ~ 40%, which is within the dispersion found for the points in each individual sample. It is unlikely that this constancy is fortuitous since the H_2 column

densities in the different samples were obtained by independent techniques (extinction, Virial theorem, and ^{13}CO analysis) and invloved three different observing groups. The fact that similar N_{H_2}/I_{CO} ratios were obtained in the different regions suggests that when one observes an ensemble of molecular clouds, the mean CO emission is related to the H_2 column density through equation (1). In external galaxies we are observing such ensembles of molecular clouds. The correlated increase in I_{CO} with column density may be due to an increase in the line width (ΔV) for more massive clouds even if the cloud temperatures are relatively constant from one cloud to next.

If we take the variation in the empirical ratio N_{H_2}/I_{CO} from one sample to another (or the dispersion within each sample) as indictive of the uncertainties in the derived N_{H_2} we must conservatively take the mass estimates in the external galaxies to be uncertain by at least a factor of two. There may of course be additional uncertainty in the assumption of similar gas-to-dust and C/H ratios in the external galaxies as in the Milky Way. However, lowering the abundance of a species does <u>not</u> reduce its observed intensity by a similar amount, as is obvious comparing ^{13}CO and CO observations in the Galaxy (Solomon, Scoville and Sanders 1979). The ^{13}C abundance is $\sim 1/89^{th}$ of the ^{12}C abundance (Wilson et al. 1981) and yet the observed ^{13}CO emission is 1/5th of ^{12}CO emission. Thus even if C/H ratios change by an order of magnitude the H_2 mass derived from <u>observed</u> CO emission will change by a much smaller factor.

The only area of disagreement with a constant value of 4×10^{20} for the ratio is in the cloud cores where the mean ratio is a factor of five larger. We do not believe such regions are at all representative of the areas producing detectable CO emission in external galaxies (due to their small cross section); they are included here simply for comparison. Adoption of the cloud core ratio for application in the galaxies would <u>raise</u> the derived masses by a factor of five!

Table I
CO Emission and H_2 Column Densities for Milky Way Sources

Cloud Sample	No. in Sample	$\langle I_{CO} \rangle^a$ [K km s^{-1}]	$\langle I_{CO}/I_{^{13}CO} \rangle$	$\langle N_{H_2} \rangle^b$ [cm^{-2}]	$\langle N_{H_2}/I_{CO} \rangle^c$ [cm^{-2}(K km s^{-1})$^{-1}$]
Cloud Core Regions					
Orion KL	1	200	5.3	3×10^{23}	1.5×10^{21}
M175W	1	331	5.9	9×10^{23}	2.7×10^{21}
W30H	1	109	2.4	2×10^{23}	1.8×10^{21}
Dark Nebulae					
Lynds	68	7.9	4.0	1.7×10^{21}	$2.5 \pm 2 \times 10^{20}$
Taurus	14	11.7	5.4	5.8×10^{21}	$3.2 \pm 2 \times 10^{20}$
Ophiucus	12	23.4	14.4	5.7×10^{21}	$2.5 \pm 2 \times 10^{20}$
Giant Molecular Clouds					
ℓ = 24 - 30°	25	59.0	5.7[d]	2.2×10^{22}	$4.2 \pm 2 \times 10^{20}$

Notes to Table

Data are from Ulich and Haas (1976) for the cloud cores; from Dickman (1978) for the Lynds clouds; from Frerking, Langer, and Wilson (1981) for the Taurus and Ophiucus clouds; and from Solomon, Sanders, and Scoville (1981) for the sample of giant molecular clouds at ℓ = 24-30°. The last two samples are likely to be most representative of the regions producing most of the observed emission in the external galaxies since the core regions take up a relatively small area in each cloud and in the Dickman sample we have included only positions where actual extinction estimates are given (as opposed to limits). Thus this sample is biased towards clouds of low extinction.

a) All ^{12}CO integrated intensities were converted to the Kitt Peak scale T_A^* (Ulich and Haas 1976). The radiation temperatures given by Dickman (1978) and the T_A^* at Bell Labs given by Frerking, Langer, and Wilson (1981) were therefore multiplied by factors of 0.65 and 0.85 respectively which are the ratios of the Orion A CO radiation temperature to T_A^* (see Ulich and Haas 1976), and the ratio of T_A^* measured at Bell Labs on Orion to that measured by Ulich and Haas on the NRAO 11-m antenna.

b) H_2 column densities were derived from visual and IR extinction estimates in the dark clouds (given by Dickman 1978 and Frerking, Langer, and Wilson 1981) and from LTE analysis of ^{13}CO and CO measurements in the cloud cores assuming an abundance ratio $[H_2/^{13}CO] = 10^6$ as obtained by Frerking, Langer, and Wilson (1981) in Taurus at $A_V > 4$ mag. To convert from extinction to column density we adopt a constant gas-to-dust ratio of $N_{H_2}/A_V = 0.94 \times 10^{21}$ cm^{-2} mag^{-1} (Bohlin et al. 1978). The column densities in the giant cloud sample were derived from application of the Virial theorem to the measured line widths and sizes (Solomon, Scoville, and Sanders 1981). These Virial theorem estimates are within 30% of estimates based on ^{13}CO column densities assuming $[N_{H_2}/^{13}CO] = 10^6$.
c) Empirical ratio of derived $\langle N_{H_2}/I_{CO} \rangle$ for the sample. The errors given are the 1σ dispersion of the sample points about the mean.
d) Only 14 of the 25 clouds were measured in ^{13}CO.

References

Bohlin, R.C., Savage, B.D., and Drake, J.F. 1978, Ap.J., 224, 132.

Dickman, R.L. 1978, Ap.J.Suppl, 37, 407.

Frerking, M., Langer, W.D., and Wilson, R.W. 1981, Ap.J., in press.

Morris, M., and Lo, K.Y. 1978, Ap.J., 223, 803.

Rickard, L.J., Palmer, P., Morris, M., Turner, B.E., and Zuckerman, B. 1977, Ap.J., 213, 673.

Solomon, P.M., Scoville, N.Z., and Sanders, D.B. 1979, Ap.J.(Letters), 232, L89.

_____ 1981, in preparation.

Ulich, B.L., and Haas, R.W. 1976, Ap.J.Suppl., 30, 247.

Wilson, R.W., Langer, W.D., and Goldsmith, P.F. 1981, Ap.J.(Letters), 243, L47.

Correcting HI Surveys for Self-Absorption

John Dickey

The determination of the ratio of molecular to atomic surface densities as a function of galactocentric distance requires not only sensitive measurements of CO column densities and a good estimate of the H_2/CO ratio, but also accurate estimates of the atomic hydrogen column density. This is not given automatically by 21 cm emission surveys at low latitudes because the optical depth is often high, i.e., the emission is saturated. The original technique for optical depth correction (Kerr and Westerhout 1965) assumed uniform excitation temperature of 125 K and derived optical depths from the observed antenna temperatures (always less than 100 K). These optical depths were not large so the self absorption correction was always small. This method is incorrect since the interstellar H I must have a broad range of excitation temperatures from ~25 K to several thousand K (e.g. Dickey et al. 1977). A more realistic approach by Burton and Gordon (1978) uses a Monte Carlo simulation to model the self-absorption expected from an ideal two-phase medium (Baker and Burton 1975). If the interstellar medium is more complex, in particular if a considerable amount of H I were present in cold clouds ($T_{ex} < 20$ K) it is hard to know how to adjust the results of the simulation.

In an attempt to measure directly the effect of self-absorption on estimates of the HI column density from emission surveys we have developed an interferometer system using the 300 foot and the 140 foot telescopes together (Dickey and Benson 1982). This system has resolution ≅15", gain ≅0.5 K/Jy and primary HPBW ≅ 14', so it is particularly insensitive to small scale emission fluctuations which cause errors in low latitude absorption measurements by

other telescopes. A typical low latitude spectrum (toward W3) is shown on Figure 1. The upper profile shows the emission measured by the 300 foot telescope, the lower profile shows the absorption (inverted). This spectrum is taken toward the western continuum peak (G133.7+1.2). The H I absorption stops at -51 km/s, which would be 4 kpc distant if the radial velocity were due to Schmidt rotation, as shown by the rotation curve drawn at the bottom of the figure. The saturated line ($-35 > v > -51$ km/s) corresponds to a similarly broad, saturated CO line (Wilson et al. 1974). It is clear in this case that the molecular cloud associated with the H II region has abundant atomic hydrogen as well as molecular hydrogen. The 21 cm optical depth is greater than four over a spread of more than 10 km/s.

We can estimate how much H I is concealed inside the optically thick gas assuming a single temperature for the HI at each velocity:

$$(1) \qquad \frac{N_c}{N_{em}} = \frac{\int T_{em}(v) \frac{\tau(v)}{1-e^{-\tau(v)}} dv}{\int T_{em}(v)\, dv}$$

where $T_{em}(v)$ is the H I emission brightness temperature, N_{em} is the column density estimate of an emission survey, and N_c is the corrected column density. Relaxing the single temperature assumption leads to a spread of N_c values, centered around the result of equation 1 (Dickey and Benson 1982). Figure 2 shows the measured values of the ratio N_c/N_{em} for the 45 directions observed in the Green Bank experiment, plotted against galactic latitude (log of the path length through a plane parallel galaxy). In most cases at high and intermediate latitudes not much correction needs to be made: $N_c/N_{em} \sim 1.1$ to 1.2. In directions below $|b| = 3°$, however, there are cases where the correction factor approaches 2. These (like W3) are toward background sources behind optically thick clouds which often correspond to

molecular emission regions. The correction factors at high and intermediate latitudes are similar to the predictions of Burton and Gordon (1978), so the molecular to atomic ratios derived by them are in many cases appropriate. In giant molecular clouds, however, there may be more atomic gas concealed than was expected before. The ring of high molecular abundance at $4 < \pi < 6$ kpc may be a region of high atomic surface density as well, although this is not indicated by H I emission surveys. A more extensive survey of low latitude 21 cm absorption is clearly needed.

Baker, P. L. and Burton, W. B. (1975) Astrophys. J. 198, 281.

Burton, W. B. and Gordon, M. A. (1978) Astron. Astrophys. 63, 7.

Dickey, J. M. and Benson, J. M. (1982) Astronomical Journal, February, in press.

Dickey, J. M., Salpeter, E. E., and Terzian, Y. (1979) Astrophys. J. 228, 465.

Kerr, F. J. and Westerhout, G. (1965) in Stars and Stellar Systems, Vol. V: Galactic Structure, eds: A. Blaauw and M. Schmidt (Chicago: University of Chicago Press).

Wilson, W. J., Schwartz, P. R., Epstein, E. E., Johnson, W. A., Etcheverry, R. D., Mori, T. T., Berry, G. G., and Dyson, H. B. (1974) Astrophys. J. 191, 357.

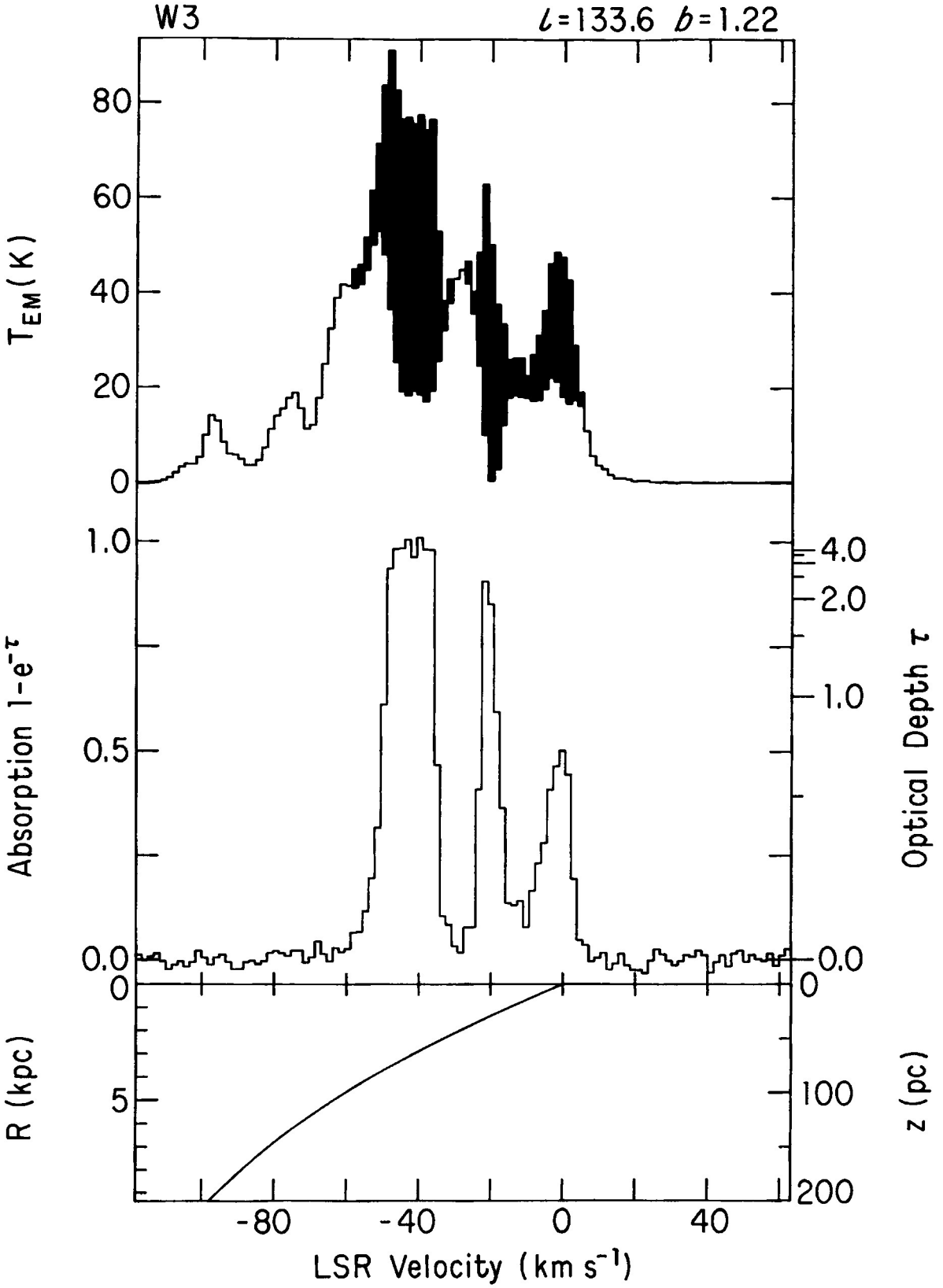
W3
ℓ=133.6 b=1.22
T_{EM}(K)
80
60
40
20
0
Absorption 1-e$^{-\tau}$
1.0
0.5
0.0
Optical Depth τ
4.0
2.0
1.0
0.0
R (kpc)
0
5
z (pc)
0
100
200
-80
-40
0
40
LSR Velocity (km s^{-1})

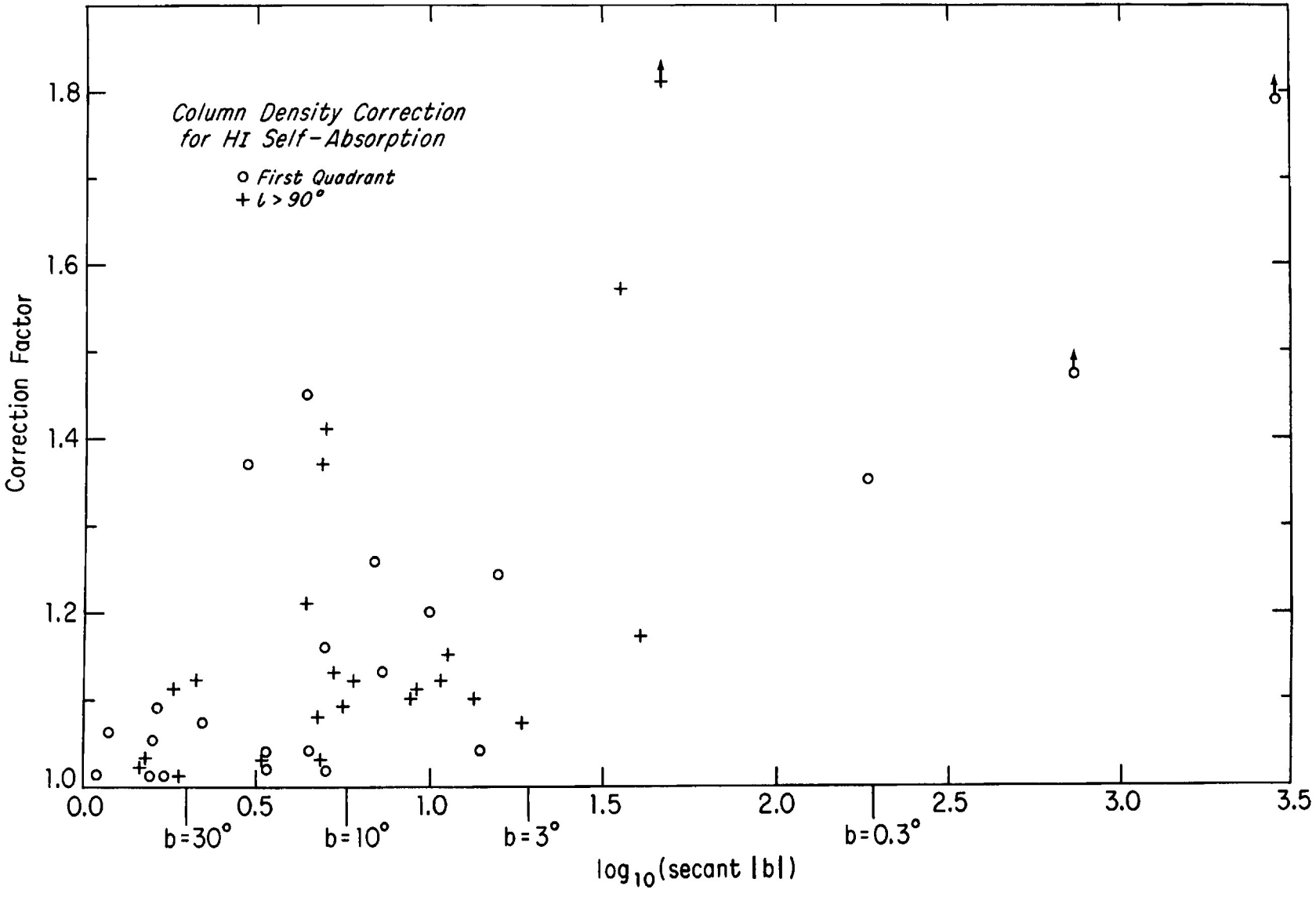
Column Density Correction
for HI Self-Absorption
o First Quadrant
+ l > 90°
Correction Factor
1.0
1.2
1.4
1.6
1.8
0.0
0.5
1.0
1.5
2.0
2.5
3.0
3.5
b=30°
b=10°
b=3°
b=0.3°
log10(secant |b|)

FORMATION OF OB CLUSTERS

Paul T.P. Ho

Department of Astronomy
University of California, Berkeley

Aubrey D. Haschick

Haystack Observatory
Massachusetts Institute of Technology

Continuum aperture synthesis observatons of compact HII regions at 20, 6 and 2cm were made using the VLA[1,2]. Four regions W33, G10.6-0.4, G19.6-0.2, and G20.1-0.1 were chosen for study since previous interferometric studies indicated that small scale structures may exist. In all cases, we find that the morphology consists of multiple structures on the scale of $\lesssim$ 0.1pc which can be interpreted as the Stromgren spheres of a cluster of OB stars.

If this cluster interpretation is correct, we find that the similar size scales of the HII regions and their close spatial distribution imply star formation that is well confined in space and time. Differences in formation time scales can only be on the order of 10^3-10^4 yr, so that the entire cluster of stars have formed essentially at the same time. Calculation of the formation time scale indicates that the final collapse toward stellar densities must have occurred at fairly high densities. Furthermore, the close proximity of the stars implies that collisions between cloud fragments must have been important until $n(H_2) > 10^5$ cm^{-3}. Hence fragment coagulation processes must have been important in building massive stars in these cases.

The radio continuum measurements also allow us to identify the spectral type of the exciting stars of the individual knots of ionized gas. We compare the distribution of spectral types in the cases of W33 and G10.6-0.4 with the

IMF of field stars[3]. The good agreement which is found supports the cluster interpretation since a priori there is no reason why knots of ionized gas should follow any kind of distribution. The good agreement with the IMF also suggests that lower mass stars may be present in the region although they are undetected in the present experiments. We calculate the intrinsic luminosity of a cluster of stars which followsthe IMF of field stars, and compare that to the observed far-infrared luminosity. Since the far-infrared should give a good estimate of the total luminosity of the region, we were able to set lower mass cutoffs for the clusters. In the case of G10.6-0.4, the maximum and minimum spectral types are probably O6 and B3. For W33, the maximum and minimum spectral types are probably O5 and O8. This supports directly the notion that the more massive stars and the less massive stars are in fact formed via different processes.

In the case of W33, we also compare the spatial distribution of the extended and compact HII regions with that of the molecular gas. We find that first of all the most massive stars tend to be collected into the most compact structures, and second the most compact continuum structures tend to be directly aligned with the molecular peaks. The implication seems to be that star formation proceeds by the more traditional route of a slow collection of the gas, followed by fragmentation, collisions and subsequent coagulations.

P.T.P.H. acknowledges support from the Miller Institute for Basic Research, and also NSF Grant AST78-21037 to the Radio Astronomy Laboratory.

References

[1]Ho, P.T.P., and Haschick, A.D. 1981, Ap. J., 248, 622.

[2]Haschick, A.D., and Ho, P.T.P. 1981, Ap. J., submitted.

[3]Miller, G.M., and Scalo, J.M. 1979, Ap. J. Suppl., 41, 513.

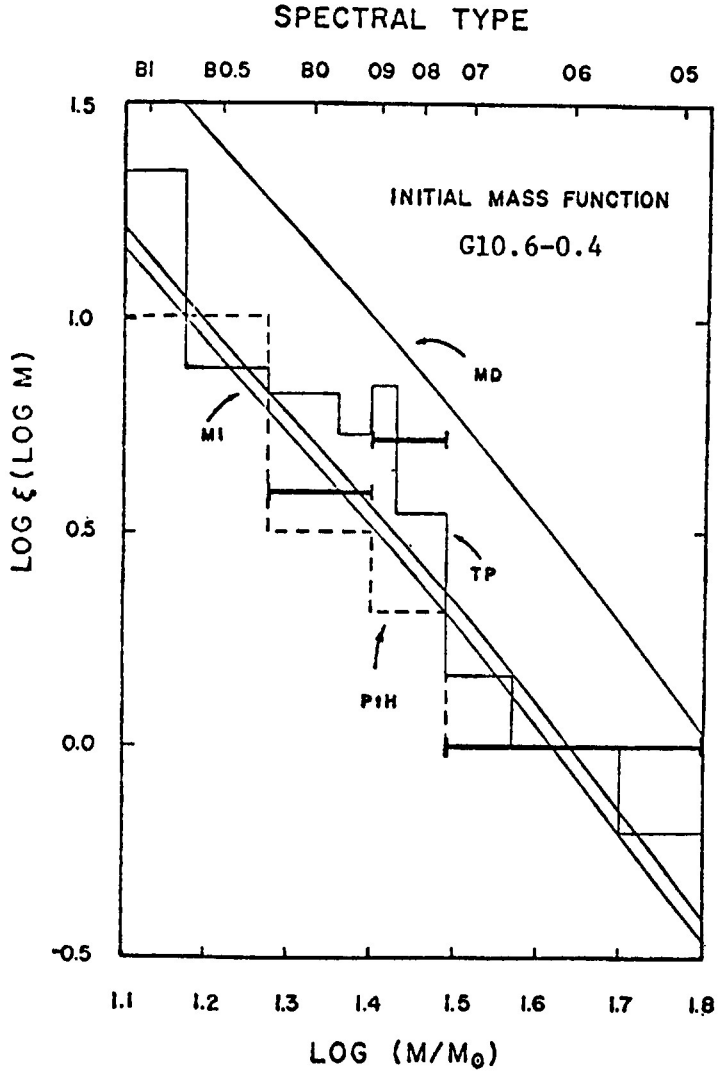

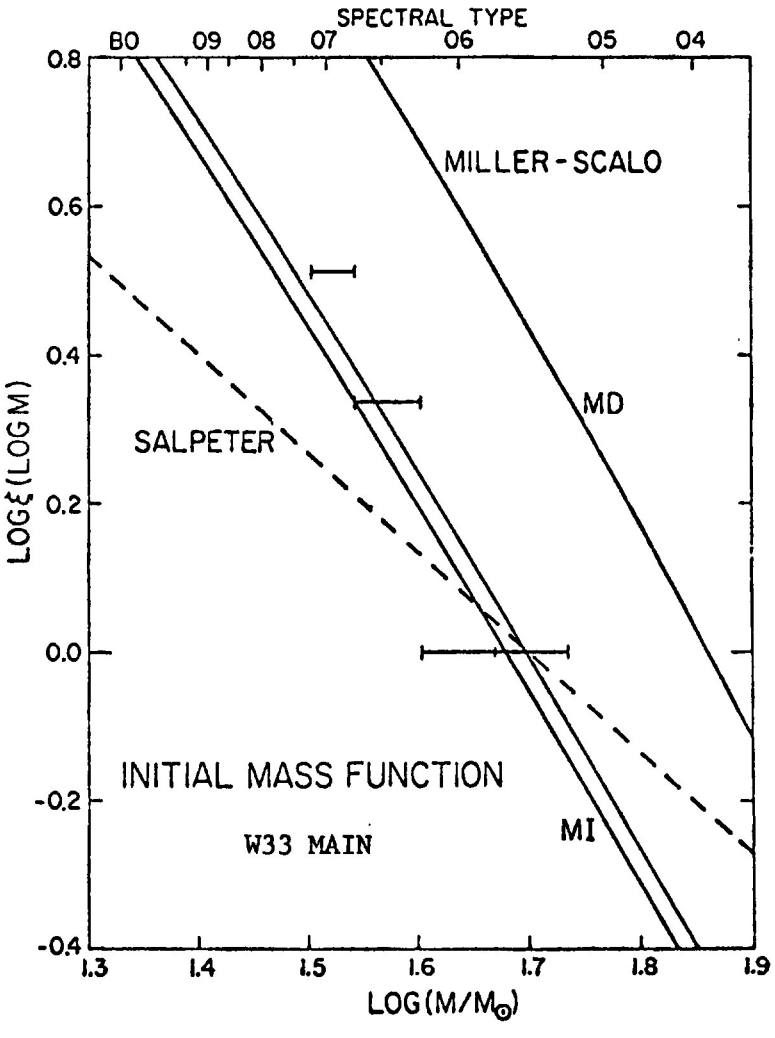

Figure 1 (a) and (b). The distribution of spectral types in G10.6 and W33 (error bars), plotted against the initial mass function of field stars (solid curves).

A Two-Fluid Model for Population I

Kevin H. Prendergast
Columbia University, Department of Astronomy

We consider a strongly interacting system of gas and stars, under the assumptions that (i) stars form spontaneously wherever gas is present, (ii) stars lose mass, (iii) stars provide energy to the gas, and (iv) the gas cools spontaneously. The behavior of this system will be studied by solving the following two sets of coupled hydrodynamic equations: let ρ, U_i and P_{ik} be the density, velocity and pressure tensor for the gas, and let ν, W_i and π_{ik} be the same quantities for the stars. Then the system of equations to be solved is

$$\rho_{,t} + (\rho U_i)_{,i} = -\alpha\rho + \beta\nu \quad , \tag{1}$$

$$\rho U_{k,t} + \rho U_i U_{k,i} + P_{ik,i} + \rho\psi_{,k} = \beta\nu(W_k - U_k) \quad , \tag{2}$$

$$P_{k\ell,t} + U_i P_{k\ell,i} + U_{i,i} P_{k\ell} + U_{k,i} P_{\ell i} + U_{\ell,i} P_{ik} =$$

$$- \alpha P_{k\ell} + \beta\pi_{k\ell} + \beta\nu(W_k - U_k)(W_\ell - U_\ell) - \kappa P_{k\ell} + \frac{1}{3} a^2 \beta\nu\delta_{k\ell} \tag{3}$$

$$\nu_{,t} + (\nu W_i)_{,i} = -\beta\nu + \alpha\rho \quad , \tag{4}$$

$$\nu W_{i,t} + \nu W_j W_{i,j} + \pi_{ij,j} + \nu\psi_{,i} = \alpha\rho(U_i - W_i) \quad , \tag{5}$$

and

$$\pi_{ij,t} + W_\ell \pi_{ij,\ell} + W_{\ell,\ell} \pi_{ij} + W_{i,\ell} \pi_{j\ell} + W_{j,\ell} \pi_{i\ell}$$

$$= -\beta \pi_{ij} + \alpha P_{ij} + \alpha \rho (U_i - W_i)(U_j - W_j) \quad . \qquad (6$$

In the right sides of these equations, α is the star creation rate, β is the mass loss rate, κ is the gas cooling rate and a, the "equivalent wind speed," is a parameter which measures the rate of energy transport from stars to gas. The detailed nature of this transport (via supernovae, stellar winds or other mechanisms) need not be specified at this point. As Larson has shown, all of the terms in equations 1) through 6), with the exception of the heating and cooling terms in equation 3), can be derived by taking moments of coupled Boltzmann equations for the velocity distribution functions of the stars and the gas. The system of moment equations is closed by dropping the third order central moments.

The main difference between our equations and Larson's is the heating term, which he did not have. When heating is taken into account a uniform mixture of stars and gas can reach a state of mechanical, thermal and chemical equilibrium, meaning that there is no net tendency to change the star-to-gas ratio. The conditions for equilibrium are easily seen to be

$$\alpha \rho = \beta \nu \quad ,$$

$$\alpha P_{k\ell} = \beta \pi_{k\ell} \quad ,$$

and

$$\kappa P_{k\ell} = \frac{1}{3} a^2 \beta \nu \delta_{k\ell} \quad .$$

A particular equilibrium state is specified (up to scale factors) by assigning values to two dimensionless parameters which we can choose to be (β/α) and (κ/α).

We have made a start on the study of this model by examing the stability of the equilibrium states. For the special case when α and κ are independent of gas density and pressure it was found that significant instabilities exist only if the time scale for cooling is less than the time scale for star formation by a factor of 100 or more. For $(\kappa/\alpha) \approx 100$ only those systems having comparable gas and star densities are unstable, but for larger values the range of unstable equilibrium states is broader; at $\kappa/\alpha \approx 10^3$ all systems with star-to-gas ratios between 0.3 and 30 are unstable. The growth rate of the instability depends on the wavelength of the perturbation. Very long and very short wavelengths are always stable; the maximum growth rate may be as much as 10 times the star formation rate at intermediate wavelengths.

The surprising thing about these unstable modes is that they are travelling waves. An observer at rest with respect to the unperturbed medium would experience a maximum gas density, then a velocity maximum, then a pressure maximum and finally a maximum star density as the wave moves past him. This is just the order of events we could expect for propagating star formation. That this is indeed the correct interpretation was proved by omitting the term in the perturbation equations which increases the gas pressure when the star density

is increased - the travelling wave instability disappeared.

To see if this result is sensitive to the assumption of constant star formation and cooling rates, we tried ten different power laws for κ and α as functions of P and ρ. Propagating star formation was found in every case. Moreover, the set of unstable equilibrium states was shown to be sensitive only to the density dependence of the cooling rate. If κ increases with ρ, a wider range of equilibrium states is unstable than if κ is constant, and the growth rates are substantially higher - up to 100 times the star formation rate. It was also found that if κ is a strongly increasing function of gas density the most unstable modes may be stationary for certain star-to-gas density ratios. Systems in this region of parameter space are unstable to star formation, but the phenomenon does not propagate because the energy input from the stars formed in the dense regions is insufficient to halt the compression of the gas.

Implications of Collisionally-Supported Giant Molecular Clouds for Spiral Galactic Structure and Massive Star Formation

David Leisawitz and Frank Bash

Department of Astronomy

The University of Texas at Austin

A study has been made of the environment experienced by ballistically-moving giant molecular clouds (GMCs) as they encounter a hydrodynamically-flowing interstellar medium. The hydrodynamically-flowing gas is assumed to consist of an ensemble of discrete small clouds. GMCs are assumed to be born in spiral galactic shock fronts from which they are ejected at post-shock velocities. The mechanism for the support of GMCs suggested by Bash, Hausman, and Papaloizou is invoked to determine the fate of these clouds (i.e. lifetime and star-forming capability). According to that model, support occurs when the energy loss through decay of turbulence in the clouds is balanced by energy input via collisions with smaller clouds. Additionally, we assume that an excessive energy input will destroy a GMC and that an unsupported cloud will collapse to form massive stars and H II regions. If the galactic distributions of small colliding clouds are like those observed for H I, the model predictions are in agreement with several observational characteristics of the Galaxy and M81. Radial rates of star formation (the H II region distributions) are reproduced for both galaxies as are the H II region locations relative to the spiral shocks in M81. We also predict CO and H II region velocity-longitude diagrams for the Galaxy. No such agreement with observations is seen when the small clouds are assumed to be distributed in a "molecular ring".

TWO-FLUID GRAVITATIONAL INSTABILITIES IN THE GALAXY

Chanda J. Jog

Department of Physics
S.U.N.Y. at Stony Brook

Here I will briefly describe the theoretical work on two-fluid gravitational instabilities in the galaxy that is currently in progress as a part of my doctoral thesis work and will soon be published in detail elsewhere (see Jog and Solomon 1981).

I. INTRODUCTION

The observations of the millimeter line emission from the tracer ^{12}CO (Scoville and Solomon 1975, Gordon and Burton 1976) and ^{13}CO (Solomon et al. 1979a, 1979b, Liszt and Burton 1981) molecules in the galactic disk show that the average gas density in the inner galaxy ($R < R_\odot$) is large (n_{H_2} = 1-3 cm^{-3}); the surface density of interstellar matter is much higher than previously realized from HI observations. The gas exhibits a wide-spread clumpy distribution in the disk and most of the gas resides in molecular form in Giant Clouds with mass$>10^5 M_\odot$ and density $n_{H_2} \sim 300$ cm^{-3} (Solomon and Sanders 1980, Solomon, Sanders and Scoville 1979b, Liszt and Burton 1981). These observations suggest that the self-gravitational forces in the interstellar gas may be significant. Yet, when one applies the necessary criterion for the growth of gravitational instabilities in a fluid that is uniformly distributed in a flattened but finite height disk which is supported by rotation and random motion (Goldreich and Lynden-Bell 1965, Toomre 1964), one finds that the gas, at the average spread out density and observed velocity dispersion, would be stable. The gas density however needs to be increased by only a small factor ($\sim$ 2) before the gas becomes susceptible to the formation of instabilities in it.

II. TWO-FLUID GRAVITATIONAL INSTABILITIES

We note that the stars constitute the largest mass component of the galactic disk and therefore it is compelling to study what effect the stellar gravitational potential, associated with the stars in the disk, has on the behaviour of the gas in the disk. For this purpose we have formulated a two-fluid scheme wherein the stars in the galactic disk are represented as an isothermal fluid and the interstellar gas in the disk is represented as another isothermal fluid and the two fluids interact gravitationally with each other. The disk is supported by rotation and random motion. Here, we investigate the formation and the properties of two-fluid gravitational instabilities in the galactic disk and study their implications for the disk stability and their effect on the interstellar gas.

We derive the hydrodynamic equations describing the above two-fluid system and solve the local, linearized perturbation equations by the method of modes, (for details, see Jog and Solomon 1981); and thus obtain the dispersion relation and hence an instability criterion for the two-fluid system.

The dispersion relation for the above two-fluid system is:

$$(\omega^2 - \alpha_s) (\omega^2 - \alpha_g) - \beta_s \beta_g = 0$$

where,

$$\alpha_s = \kappa^2 + k^2 c_s^2 - 2\pi G k \mu_s$$

$$\alpha_g = \kappa^2 + k^2 c_g^2 - 2\pi G k \mu_g$$

$$\beta_s = 2\pi G k \mu_s$$

$$\beta_g = 2\pi G k \mu_g$$

κ is the epicyclic frequency; μ_s and μ_g represent the surface densities of the stellar fluid and of the gas respectively; c_s and c_g denote the velocity dispersion in the stellar fluid and in the gas respectively. The perturbation mode is characterized by k, the wavenumber and ω, the angular frequency. The corresponding wavelength, λ, is equal to $(2\pi/k)$.

The above dispersion relation is solved to obtain an expression for $\omega^2(k)$:

$$\omega^2(k) = \tfrac{1}{2} \{ (\alpha_s + \alpha_g) - [(\alpha_s + \alpha_g)^2 - 4 (\alpha_s \alpha_g - \beta_s \beta_g)]^{\frac{1}{2}} \}$$

Whenever $\omega^2(k) < 0$, the two-fluid system is unstable to the growth of the perturbation (k,ω) in it. Thus, we obtain the instability criterion for the two-fluid system from the derived expression for $\omega^2(k)$. When $\omega^2(k) < 0$, $\sqrt{-\omega^2(k)}$ gives the rate of growth of the mode (k,ω).

III. APPLICATIONS TO THE GALAXY OF THE TWO-FLUID ANALYSIS

The gravitational interaction between the two fluids is a crucial feature of our analysis, as it turns out that, it is this additional gravitational self-energy in the two-fluid system that enables the formation of the joint two-fluid instabilities, even when neither fluid may be unstable individually.

On applying the criterion for the onset of two-fluid instabilities to the solar neighborhood, we find that the contribution to the formation of two-fluid instabilities by interstellar gas is as high as 25 - 35 % even when the gas surface density is only about 10% of the total surface

density of the disk. The importance of the gas contribution is attributed to the lower velocity dispersion and the lower scale-height of the gas as compared respectively to the velocity dispersion and the scale-height of the stars.

It is instructive to plot $\omega^2(k)$ vs. k (or, $\omega^2(k)$ vs. λ^{-1}) for different input parameters in order to study the properties of the resulting two-fluid instabilities. For the purpose of demonstrating the effect of the two fluid instability on the galactic disk we have assumed in presenting Figures 1 and 2 ,that the average gas surface density (H_2 + HI) in the disk is 10% of the total surface density at all R > 5 kpc. This is very close to that found by Solomon et al. (1979a) and Liszt and Burton (1981) from ^{13}CO observations if the measured scale height (HWHM = 60 pc) (Solomon et al. 1979b) is combined with the determination of mid plane H_2 density. It is a factor of between 1.5 and 2 less than the gas surface density of Solomon and Sanders (1980) and Solomon et al. (1979b). At R = 10 kpc, we assume $\mu_g = 8\ M_\odot/pc^2$ and at 6 kpc , $\mu_g = 19\ M_\odot/pc^2$. (A full discussion of observed surface densities can be found in D. Sanders' thesis(1981).) For the total surface density we adopt the model of Ostriker and Caldwell (1981).

In Figure 1, the curves labeled S, G and S + G represent the function $\omega^2(k)$ vs. λ^{-1}, calculated at the solar neighbourhood (R = 10 kpc), for the stellar fluid and the gas and the joint two-fluid system respectively. Note that even when the stellar fluid is neutrally stable and the gas is stable; the joint two-fluid system, because of the gravitational interaction

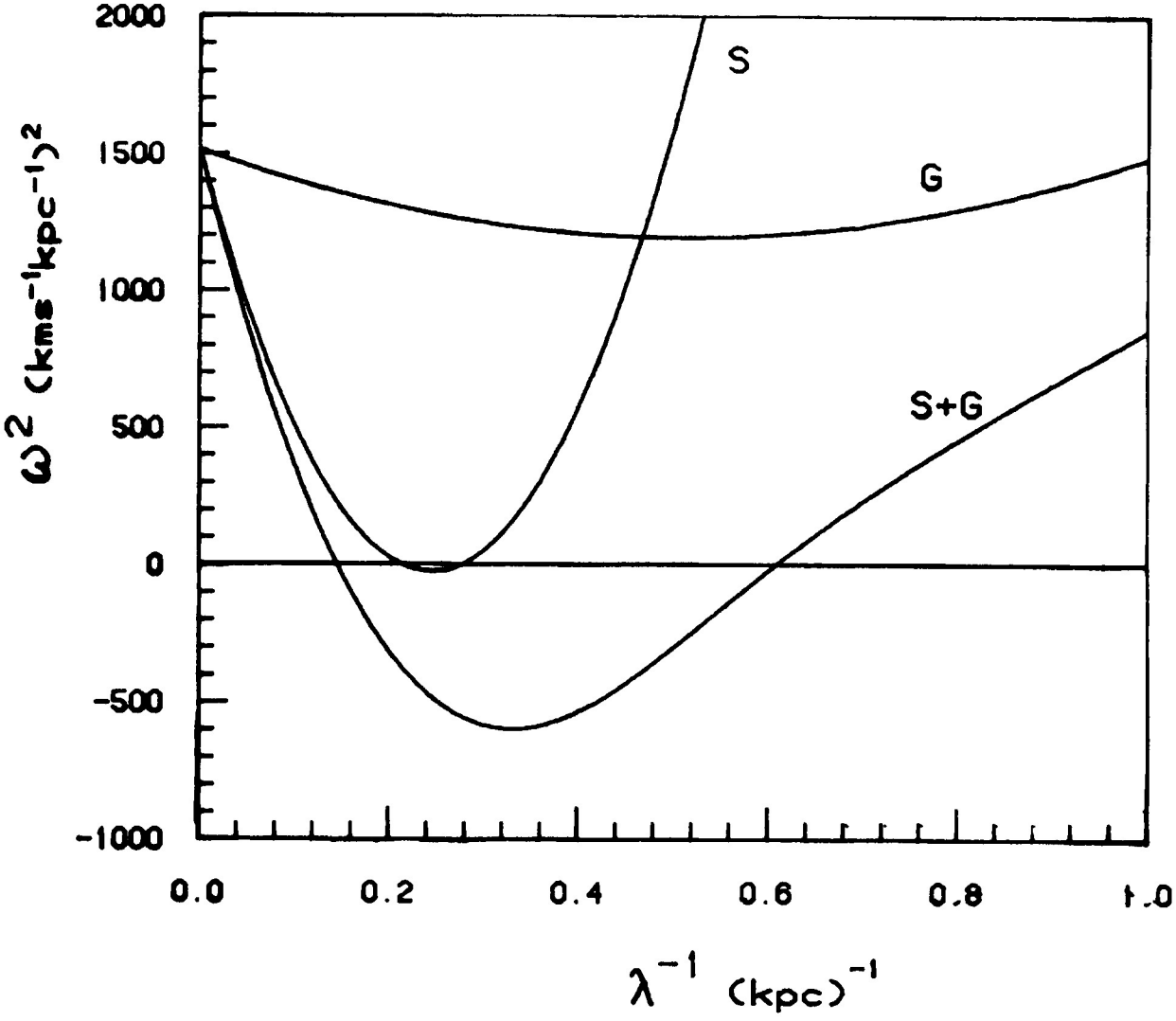

FIGURE 1 : Plots of $\omega^2(\text{kms}^{-1}\text{kpc}^{-1})2$ versus $\lambda^{-1}(\text{kpc})^{-1}$, drawn at R = 10 kpc, for stars-alone,gas-alone,two-fluid system respectively.The above plots are drawn for μ_{total}= 82 $M_\odot pc^{-2}$ and μ_g/μ_s= 0.10

between the two fluids, does exhibit instabilities. The fastest growing mode is described by (k_{peak}, ω_{peak}) where k_{peak} is the wavenumber corresponding to the fastest growing mode and ω_{peak} is the rate of fastest growth. From Figure 1, k_{peak} ($= 2\pi/\lambda_{peak}$)$=2.39 kpc^{-1}$ and ω_{peak} = 24.3 kms^{-1} kpc^{-1} = 2.43 x 10^{-8} yrs^{-1}.

In Figure 2, curves similar to those in Figure 1 are drawn for R = 6 kpc. Note that ω_{peak} (R = 6 kpc) = 40.3 kms^{-1} kpc^{-1} (= 4.03 x 10^{-8} yrs^{-1}) is greater than ω_{peak} (R = 10 kpc). This is so because the growth rate depends on the absolute surface densities of the gas and the stellar fluid.

The ratio (μ_g/μ_s) is a very important parameter in this scheme as can be seen from Figure 3. The three curves in Figure 3 represent $\omega^2(k)$ vs. λ^{-1}, calculated at the solar neighbourhood with μ_g/μ_s = 0.1, 0.15, 0.2 respectively; while keeping $\mu_{total} = \mu_g + \mu_s$ = constant at 82 $M_\odot$ pc^{-2}. From Figure 3, we can see that the maximum growth rate of the resulting two-fluid instability is a strong function of μ_g/μ_s. Also, $\Delta\lambda$, the range of wavelengths over which two-fluid instabilities can occur, increases dramatically as μ_g/μ_s is increased from 0.1 to 0.2.

Figures 1 - 3 illustrate the basic features of the two-fluid instabilities in the galaxy. In the real galaxy, however, one expects (extending to the two-fluid case, the argument of self-regulation that Toomre (1964) applied for the stars-alone case) the joint two-fluid system to be on average neutrally stable.

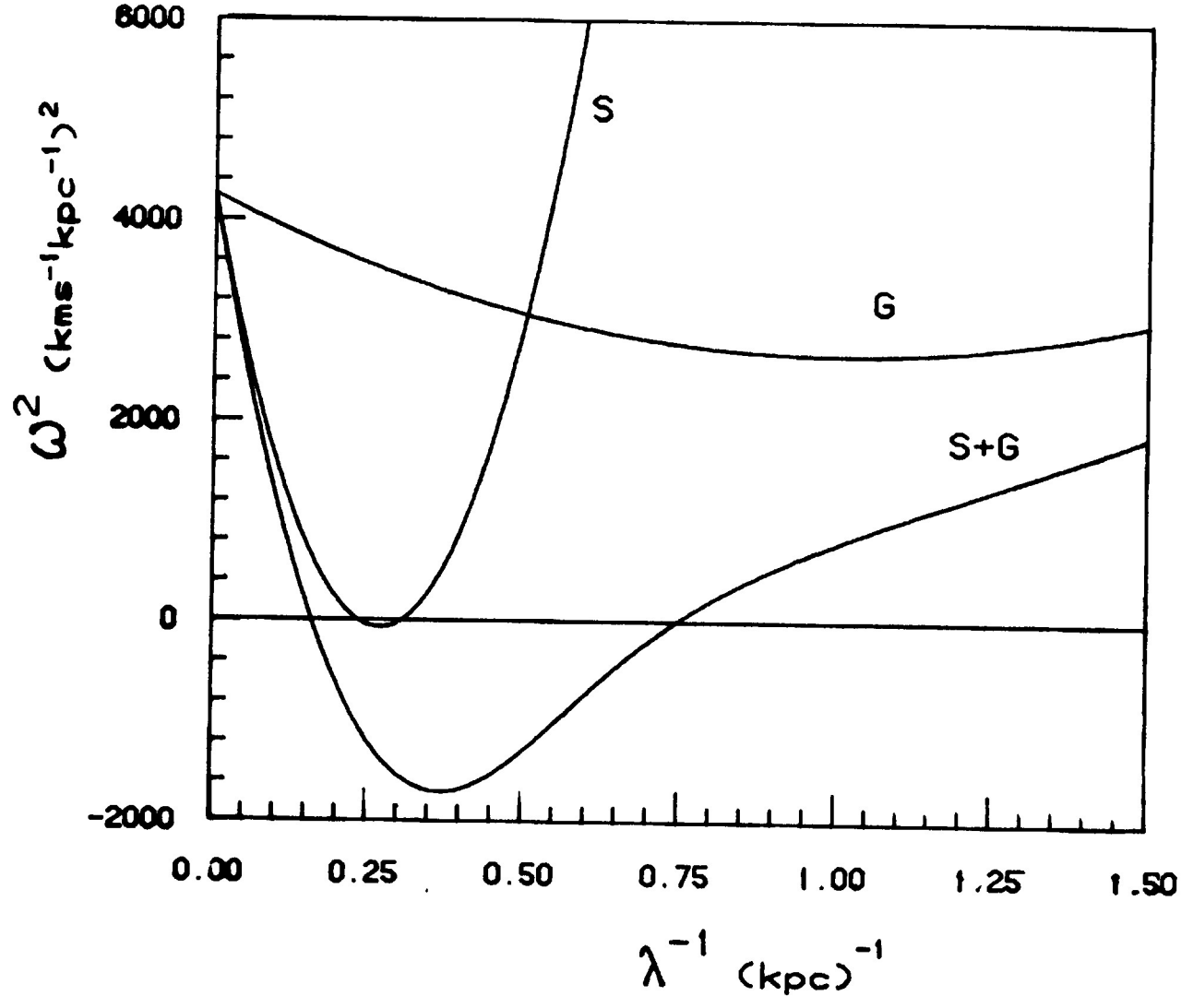

FIGURE 2 : Plots of $\omega^2(\text{kms}^{-1}\text{kpc}^{-1})^2$ versus $\lambda^{-1}(\text{kpc})^{-1}$, drawn at R = 6 kpc, for stars-alone, gas-alone, two-fluid system respectively. The above plots are drawn for μ_{total} = 190 $M_\odot pc^{-2}$ and μ_g/μ_s=0.10

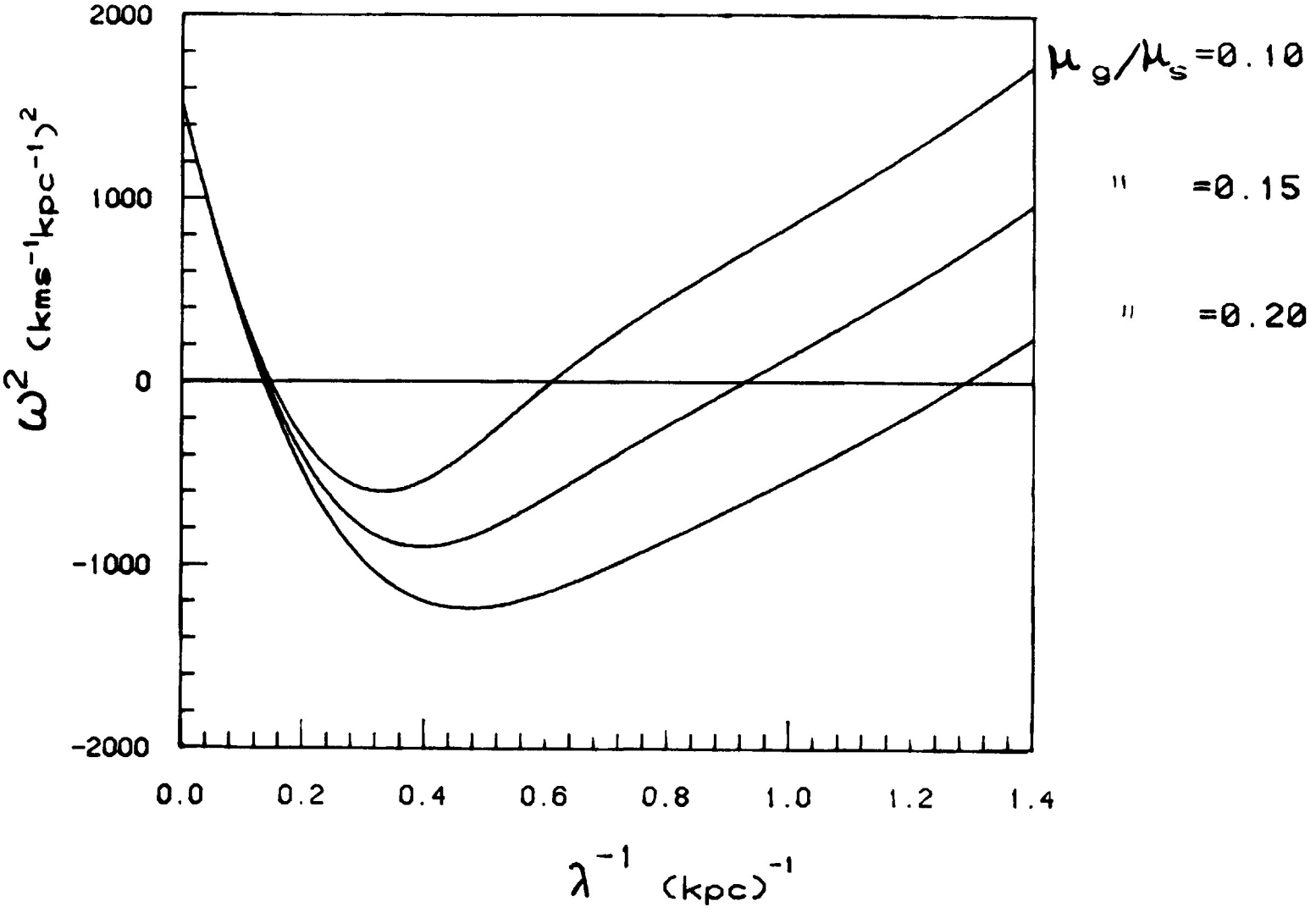

FIGURE 3 : Plots of $\omega^2(\text{kms}^{-1}\text{kpc}^{-1})^2$ versus $\lambda^{-1}(\text{kpc})^{-1}$, drawn at R = 10 kpc, for the two-fluid system, for μ_g/μ_s= 0.10, 0.15, 0.20 respectively. Each of the above plots is drawn for μ_{total}= 82 $M_\odot pc^{-2}$ and at a stellar velocity corresponding to the stellar neutral equilibrium in each case.

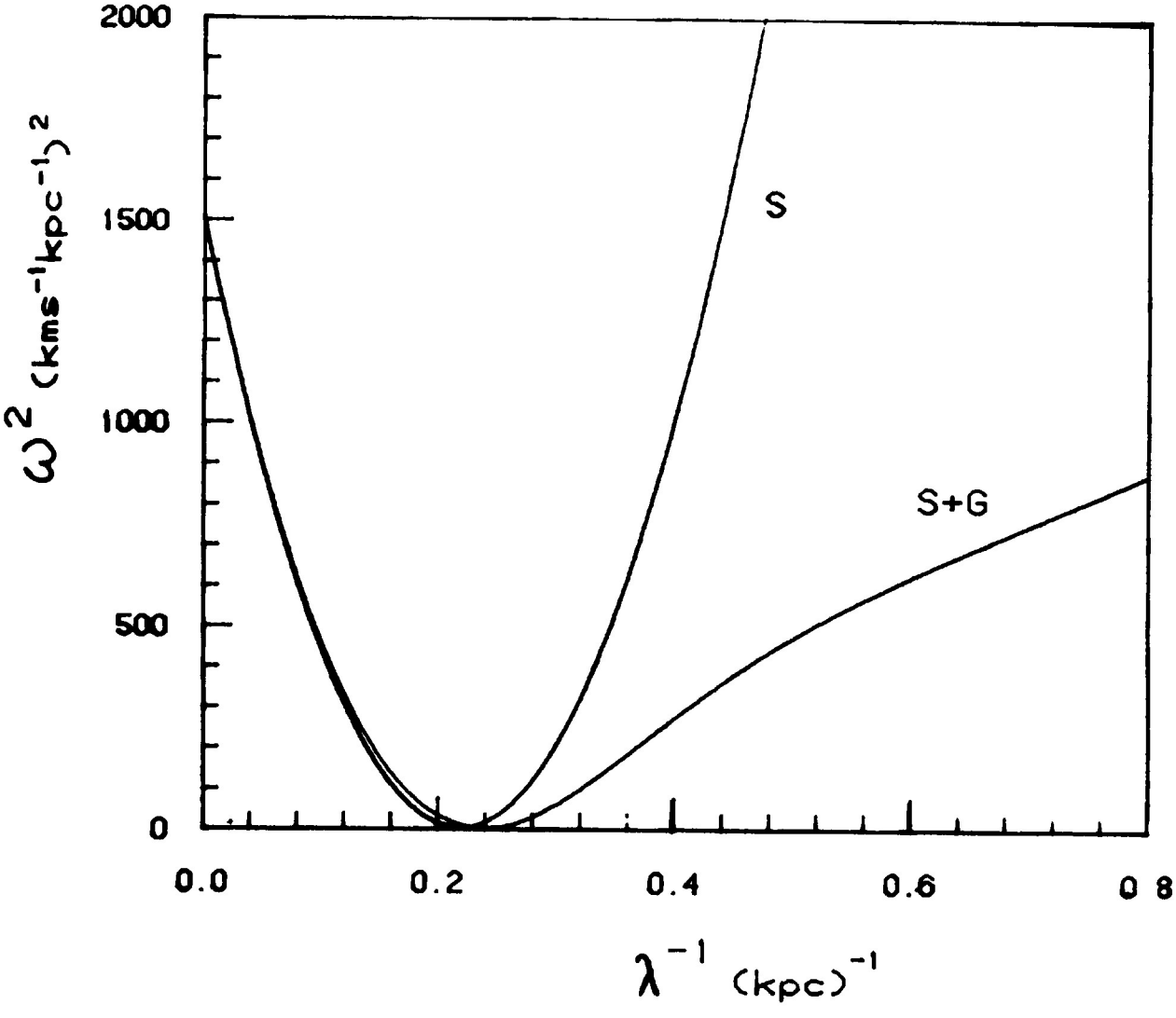

FIGURE 4 : Plots of $\omega^2(\text{kms}^{-1}\text{kpc}^{-1})^2$ versus $\lambda^{-1}(\text{kpc})^{-1}$, drawn at R = 10 kpc, for μ_g/μ_s= 0.10,for stellar neutral equilibrium(curve S) at stellar velocity dispersion = 25.1 kms^{-1} and for two-fluid neutral equilibrium (curve S+G) at stellar velocity dispersion = 27.7 kms^{-1}.In each case, μ_{total}= 82 $M_\odot pc^{-2}$.

In fact, from our analysis we can calculate the critical stellar velocity dispersion that is needed to keep the two-fluid system in neutral equilibrium. We find that the ratio of the critical stellar velocity dispersion for two-fluid neutral stability, $(C_s, \text{min})_{2\text{-f}}$, to the critical stellar velocity dispersion for one-fluid (stars-alone) neutral stability, $(C_s, \text{min})_{1\text{-f}}$, (with μ_{total} in the two-fluid case = μ_s in the one-fluid case) is = 1.10 for $\mu_g/\mu_s = 0.1$ (see Figure 4). This ratio increases substantially as μ_g/μ_s increases. Therefore, we have, via above two-fluid analysis, redefined the criterion of disk stability for a disk consisting of gas and stars.

IV. EFFECTS OF THE TWO-FLUID GRAVITATIONAL INSTABILITIES ON GAS

We find that, as a result of formation of a two-fluid instability, the gas density in the instability increases (by a factor which we call the amplification factor) and at this higher gas density, the gas itself may become unstable to the formation of instabilities even if the gas is stable by itself.

If gas-alone instabilities occur at this higher effective gas density, then we call them induced gas instabilities; so called, because they are possible solely as a result of the help from the two-fluid instabilities. The typical wavelength of an induced gas instability is $\lesssim$(300 - 800) pc, the range represents the possible range of values for the gas velocity dispersion from 5 to 8 kms^{-1} and the possible range of values for the

epicyclic frequency corresponding to the galactocentric distance range of R = 6 to 10 kpc. The wavelength will be larger for R > 10 kpc; however, we do not present this case here.

We expect the galaxy to contain gaseous features with lengthscale in the above range. Presumably, each of these features appears as a cluster of Giant Molecular Clouds.

V. CONCLUSIONS

1. For a disk galaxy consisting of stars and gas, the gas cannot be ignored when the dynamic stability of the entire disk is under consideration; the stability criterion should be derived for the two-fluid system.

The critical velocity dispersion of stars for disk stability is significantly larger for the two-fluid case than it is for the one-fluid case, especially when μ_g/μ_s is high. For example, as μ_g/μ_s increases from 0.1 to 0.2, the ratio of the critical velocity dispersion of stars for disk stability for two-fluid case as compared to the same for one-fluid case increases from 1.10 to 1.23.

2. When the observed stellar velocity dispersion is less than the critical velocity dispersion for two-fluid disk stability, then localized two-fluid instabilities occur; which have (for input parameters similar to those in the galaxy from R = 6 to 10 kpc) typical wavelength of 2-3 kpc and $\omega_{peak}/\Omega \gtrsim 1$. The wavelength will be longer for R > 10 kpc, however, we do not present this case here.

3. As a result of the existence of two-fluid instabilities, the gas density is amplified and induced gas instabilities may be feasible at this higher density (even when gas alone is stable).

For parameters typifying the galactic region from R = 6 to 10 kpc, the typical wavelength of induced gas instabilities is $\lesssim$ (300 - 800) pc. We expect the galaxy to contain concentrations of interstellar matter with lengthscale in this range. Each of these features, presumably, appears as a cluster of several GMCs.

4. Induced gas instabilities seem more feasible at high μ_g; hence $\mu_g(H_2)/\mu_g(HI)$ is expected to increase with the total surface density of gas, μ_g. We thus expect to find strong molecular emission in those galaxies with high total gas surface density.

REFERENCES

Goldreich, P. and Lynden-Bell D. 1965, M.N.R.A.S., 130, 125.

Gordon, M. A. and Burton, W. B. 1976, Ap. J., 208, 346.

Jog, C. J. and Solomon, P. M. 1981, in preparation.

Liszt, H. S. and Burton, W. B. 1981, preprint.

Ostriker, J. P. and Caldwell, J. A. R. 1981, preprint.

Sanders, D. B. 1981, Ph. D. Thesis, SUNY Stony Brook.

Scoville, N. Z. and Solomon, P. M. 1975, Ap. J. (Letters), 199, L105.

Solomon, P. M. and Sanders, D. B. 1980, in "Proceedings of Gregynog Conference on Giant Molecular Clouds", eds. M. Edmunds and P. M. Solomon, Pergamon Press, Oxford, England, pg. 41.

Solomon, P. M., Scoville, N. Z. and Sanders, D. B. 1979a, Ap. J. (Letters), 232, L89.

Solomon, P. M., Sanders, D. B. and Scoville, N. Z. 1979b, in IAU Symposium No. 84, The Large Scale Characteristics of the Galaxy, ed. W. B. Burton (Dordrecht: Reidel), p. 35.

Toomre, A. 1964, Ap. J., 139, 1217.

A BIBLIOGRAPHY OF OBSERVATIONS OF MOLECULAR CLOUDS IN GALAXIES

- L. J Rickard, Howard University

OH

Radhakrishnan, V. 1967, Austr. J. Phys., 20, 203. - neg. results in LMC, SMC

Roberts, M. S. 1967, Ap. J., 148, 931. - neg. results

Weliachew, L. 1971, Ap. J. (Letters), 167, L47. - discovery - M82, NGC 253

Whiteoak, J. B., and Gardner, F. F. 1973, Ap. Letters, 15, 211. - NGC 4945, 253

Gardner, F. F., and Whiteoak, J. B. 1975, M. N. R. A. S., 173, 77P. - NGC 253

Whiteoak, J. B., and Gardner, F. F. 1975, Ap. J. (Letters), 195, L81. - NGC 4945

Nguyen-Q-Rieu, Mebold, U., Winnberg, A., Guibert, J., and Booth, R. 1976, Astr. Ap., 52, 467. - M82

Whiteoak, J. B., and Gardner, F. F. 1976, M. N. R. A. S., 176, 25P. - LMC (N159)

Gardner, F. F., and Whiteoak, J. B. 1976, Proc. Astr. Soc. Australia, 3, 63. - NGC 5128

Caswell, J. L., and Haynes, R. F. 1981, M. N. R. A. S., 194, 33P. - LMC

Rickard, L. J, Bania, T. M., and Turner, B. E. 1982, Ap. J., in press. - NGC 660, 3227, 3504, 3628, 5363, plus neg. results

Turner, B. E., Kazes, I., Rickard, L. J, and Gerard, E. 1982, in preparation. - NGC 3079, 7469

Weliachew, L., Greisen, E., and Fomalont, E. 1982, in preparation. - M82

H_2O

Johnston, K. J., Knowles, S. H., Sullivan, W. T., 1971, Ap. J. (Letters), 167, L93. - neg. results (LMC)

Dickinson, D. F., and Chaisson, E. J. 1971, Ap. J., 169, 207. - neg. results (M33)

Sullivan, W. T. 1973, Ap. J. Suppl., 25, 393. - neg. results

Andrew, B. H., Bell, M. B., Broten, N. W., and Mac Leod, J. M. 1975, Astr. Ap., 39, 421. - neg. results, poss. det. in M82?

Kaufmann, P., Zisk, S., Scalise, E., Schaal, R. E., and Gammon, R. H. 1977, Astr. J., 82, 577. - neg. results (LMC)

Churchwell, E., Witzel, A., Huchtmeier, W., Pauliny-Toth, I., Roland, J., and Sieber, W. 1977, Astr. Ap., 54, 969. - discovery, M33

Lepine, J. R. D., and Dos Santos, P. M. 1977, Nature, 270, 501. - NGC 253

Huchtmeier, W. K., Witzel, A., Kuhr, H., Pauliny-Toth, I. I., and Roland, J. 1978, Astr. Ap., 64, L21. - M33, IC 342

Dos Santos, P. M., and Lepine, J. R. D. 1979, Nature, 278, 34. - NGC 4945

Huchtmeier, W. K., Richter, O.-G., Witzel, A., and Pauliny-Toth, I. 1980, Astr. Ap., 91, 259. - M33, negative results

Lepine, J. R. D., and Dos Santos, P. M. 1980, in Interstellar Molecules (IAU Symposium No. 87), ed. B. H. Andrew (Dordrecht: D. Reidel), p. 599 - NGC 4945

Scalise, E., and Braz, M. A. 1981, Nature, 290, 36. - LMC

Scalise, E., and Braz, M. A. 1982, in preparation (for Astr. J.) - LMC, SMC

H_2CO

Gardner, F. F., and Whiteoak, J. B. 1974, Nature, 247, 526. - discovery, NGC 253, 4945

Whiteoak, J. B., and Gardner, F. F. 1976, M. N. R. A. S., 174, 51P. - LMC

Gardner, F. F., and Whiteoak, J. B. 1976, M. N. R. A. S., 175, 9P. - NGC 5128

Graham, D. A., Emerson, D. T., Weiler, K. W., Wielebinski, R., and de Jager, G. 1978, Astr. Ap., 70, L69 - M82

Cohen, R. J., Few, R. W., and Booth, R. S. 1979, M. N. R. A. S., 187, 35P. - M31

Gardner, F. F., and Whiteoak, J. B. 1979, M. N. R. A. S., 189, 51P. - 2cm, NGC 5128

CO

Penzias, A. A., Jefferts, K. B., and Wilson, R. W. 1971, Ap. J., 165, 229. - neg. res.

Rickard, L. J, Palmer, P., Morris, M., Zuckerman, B., and Turner, B. E. 1975, Ap. J. (Letters), 199, L75. - discovery - M82, NGC 253, M51, M83

Solomon, P. M., and de Zafra, R. 1975, Ap. J. (Letters), 199, L79. - M82, NGC 253, M51

Huggins, P. J., Gillespie, A. R., Phillips, T. G., Gardner, F., and Knowles, S. 1975, M. N. R. A. S., 173, 69P. - LMC

Rickard, L. J, Palmer, P., Morris, M., Turner, B. E., and Zuckerman, B. 1977, Ap. J., 213, 673. - M82, NGC 253, M51, M83, NGC 1068

Rickard, L. J, Turner, B. E., and Palmer, P. 1977, Ap. J. (Letters), 218, L51. - Maffei 2

Combes, F., Encrenaz, P. J., Lucas, R., and Weliachew, L. 1977, Astr. Ap., 55, 311. - M3

Combes, F., Encrenaz, P. J., Lucas, R., and Weliachew, L. 1977, Astr. Ap., 61, L7. - M31

Emerson, D. T. 1978, Astr. Ap., 63, L29. - HI vs. CO (M31)

Morris, M., and Lo, K. Y. 1978, Ap. J., 223, 803. - NGC 6946, IC 342

Combes, F., Encrenaz, P. J., Lucas, R., and Weliachew, L. 1978, Astr. Ap., 63, 303. - neg. results

Combes, F., Encrenaz, P. J., Lucas, R., and Weliachew, L. 1978, Astr. Ap., 67, L13. - M83

Encrenaz, P. J., Stark, A. A., Combes, F., and Wilson, R. W. 1979, Astr. Ap., 78, L1. - ^{13}CO

Wilson, T. L., Fricke, K. J., and Biermann, P. 1979, Astr. Ap., 79, 245. - neg. results

Knapp, G. R., Phillips, T. G., Huggins, P. J., Leighton, R. B., and Wannier, P. G. 1980, Ap. J., 240, 60. - 2-1 (M82)

Elmegreen, B. G., Elmegreen, D. M., and Morris, M. 1980, Ap. J., 240, 455. - NGC 7793

Johnson, D. W., and Gottesman, S. T. 1980, in Photometry, Kinematics, and Dynamics of Galaxies, ed. D. S. Evans (Austin: U. Texas), p. 57. - NGC 185

Rowan-Robinson, M., Phillips, T. G., and White, G. 1980, Astr. Ap., 82, 381. - survey

De Graauw, T., Lidholm, S., Fitton, B., Israel, F. P., Beckmann, J., Nieuwenhuyzen, H., and Vermuc, J. 1980, in Interstellar Molecules (IAU Symposium No. 87), ed. B. H. Andrew (Dordrecht: D. Reidel), p. 125. - LMC, SMC (2-1)

Lo, K. Y., Phillips, T. G., Knapp, G. R., Wootten, H. A., and Huggins, P. 1980, B. A. A. S., 12, 859. - NGC 253 (2-1)

Boulanger, F., Stark, A. A., and Combes, F. 1981, Astr. Ap., 93, L1. - M31

Bieging, J. H., Blitz, L., Lada, C. J., and Stark, A. A. 1981, Ap. J., 247, 443 - NGC 3227, 4051

Blitz, L., Israel, F. P., Neugebauer, G., Gatley, I., Lee, T. J., and Beattie, D. H. 1981, Ap. J., 249, 76. - M101

Rickard, L. J, and Palmer, P. 1981, Astr. Ap., in press. - M51, NGC 6946, IC 342.

Lord, S., Young, J. S., and Scoville, N. Z. 1981, B. A. A. S., 13, 535. - M51

Tacconi, L. J., Young, J. S., and Scoville, N. Z. 1981, B. A. A. S., 13, 535. - NGC 3628

Stark, A. A., Linke, R. A., and Frerking, M. A. 1981, B. A. A. S., 13, 535. - M31.

Young, J. S., and Scoville, N. Z. 1981, B. A. A. S., 13, 538. - NGC 6946, IC 342.

Rickard, L. J, Palmer, P., and Turner, B. E. 1982, in preparation. - NGC 660, 3504, 3628, and 4303.

Rickard, L. J, Palmer, P., and Turner, B. E. 1982, in preparation. - M51, Maffei 2

Israel, F. P., De Graauw, T., Lidholm, S., van de Stadt, H., and De Vries, C. 1982, in preparation. - LMC, SMC (2-1)

Johnson, D. W., and Gottesman, S. T. 1982, Astr. J., submitted. - NGC 185

Israel, F. P., and Rowan-Robinson, M. 1982, Ap. J., submitted. - CO and nonthermal em.

Other

HCN - Rickard, L. J, Palmer, P., Turner, B. E., Morris, M., and Zuckerman, B. 1977, Ap. J., 214, 390. - discovery (M82, NGC 253)

H_2 - Thompson, R. I., Lebofsky, M. J., and Rieke, G. H. 1978, Ap. J. (Letters), 222, L49. - discovery (NGC 1068)

HCO^+, HCN - Stark, A. A., and Woolf, R. S. 1979, Ap. J., 229, 118. - HCO^+ discovery (M82

NH_3 - Martin, R. N., and Ho, P. T. P. 1979, Astr. Ap., 74, L7. - discovery (NGC 253, IC 342)

CH - Whiteoak, J. B., Gardner, F. F., and Hoglund, B. 1980, M. N. R. A. S., 190, 17P. - discovery (LMC, NGC 4945, 5128, 253?)

H_2 - Carlson, W. J., and Foltz, C. B. 1979, Ap. J., 233, 39. - NGC 1068

NH_3 - Ho, P. T. P., Martin, R. N., and Ruf, K. 1980, B. A. A. S., 12, 845. - IC 342

HCO^+ - Rickard, L. J, and Palmer, P. 1981, Ap. J., 243, 765. - NGC 253

HCO^+ - Batchelor, R. A., McCulloch, M. G., and Whiteoak, J. B. 1981, M. N. R. A. S., 194, 911. - LMC, NGC 5128?

H_2 - Hall, D. N. B., Kleinmann, S. G., Scoville, N. A., and Ridgeway, S. T. 1981, Ap. J., 248, 898. - NGC 1068